Investigation of physiological roles of AMP-activated protein kinase γ3

Philipp Jurijvic RHEIN

EPFL

École
polytechnique
fédérale
de Lausanne

2021

"If you don't look back at yourself and think, *'Wow, how stupid I was a year ago'*, then you must not have learned much in the last year."

(Raymond Dalio)

Acknowledgements

What people generally strive for are achievements, which are portrayed, sold and written about by researchers and journalists in pieces that resemble snapshots of history. They aim to provide an image of noble characteristics and success with an assertion to follow those if one desires to reach that very same achievement. As with social media in the 21st century, snapshots of single moments of time may provide a certain comfort, but wonderfully fail to provide any information of the development prior to that moment or of the potential future development. While people may see completed work at the end of more than four years' time, it is well worth taking a step back to appreciate that the work in front of you is a shared success in many layers. It comprises fruitful collaborations across multiple labs and institutes and even more commitment from individuals whose contributions should not be undervalued.

First and foremost, I would like to thank my (two) supervisors Kei and Patrick for the support and guidance throughout the entire time. I am extremely grateful to Kei for creating this opportunity, being unbelievably resourceful and hard working. Despite me being far from a model student, you managed to strive for perfection and inspire me to do the same. The care for detail and quality is unmatched in the field and will continue to shape my thoughts. Thank you also for your help with the student association, which we inherited and continued with Christopher and Margherita. I am sure we worked quite orthogonal to common expectation, but you managed to accommodate and support even unusual ideas. Thank you very much to Patrick, who took me into his group and elegantly managed to keep a smooth transition and united front for the project. In difficult and uncertain times, you managed to navigate unknown waters for the team and provided unconditional support. Thanks for letting me be part of the team and thank you very much indeed to the entire genomics team. I would like to extent my gratitude also to Etienne, whose understanding and challenging discussions were valuable input for the work.

As mentioned above, this work is the result of many collaborators sacrificing their time to create a common success. Thank you very much to Nicolas, who regardless of some faint memories of the summer of 2018 which I am sure you won't be tired reminding me of, provided such valuable results of *ex vivo* muscle work and set-up together with Mathieu. Of course, José cannot be missed with his unrivalled skills in animal handling for all *in vivo* experiments. Your deep care for good quality science is of great value and hotline to your broker of great memory. Thank you also to Jens for teaching me how a qPCR works and your analysis of mitochondrial DNA. My qPCR experiments would not have worked without the help of

Sylviane either, so thank you very much for your help with the RNA extraction and coping with my constant orders of exotic reagents. Thank you also to Alix for statistical expertise and Guillaume for your help with muscle fibre analysis. I know the value of QC now and won't forget how muscle fibres look up closely. Thank you also to our collaborators at McMaster University, where Eric Desjardins did an outstanding job in BAT analysis under the guidance of Prof Gregory Steinberg. Many thanks to Shuai Chen and his group at Nanjing university and their help with all the additional AMPK mouse models.

We also had the great pleasure to work with Eric and Christoph on the future and development of the student association which evolved over time thanks to your support after Kei's departure. I would like to extend my sincere thanks to the extraordinary work done by the initiators Caterina, Isabelle and Omid as well as to my fellows in the continuation with Christopher and Margherita and later also Mel and Aidan. Thank you for your continuous efforts and great teamwork on display in so many events. I strongly believe that our different yet compatible skill sets were vital for this success and am I am very glad indeed to see the current and future development. Thank you for great memories within and beyond NR. Thank you Christopher, for your rule challenging appetite and laughs. Great achievements in pizza delivery and energy storage remain legendary and I am sure many more legends remain to be created. Thank you Mel, for your continuous efforts in organising and keeping the ship afloat, the YSN would not be where it is without you. Thank you for your thoughtful challenges throughout the time and bringing such a great attitude to work. Thank you to Mary, I cannot describe how much I enjoyed setting up the new testing system and improving every week. It was the best possible distraction from thesis writing within the institute on Tuesdays. I always had a great time on testing days and really appreciate your support, advice, chats and laughs we had.

I would also like to thank Carles' team who accommodated in their office in my starting days at NIHS with Carles, Joanna, Miriam, Magali and later Angelique and Eleonora. Thank you for welcoming me with open arms and your advice on how to get along in the institute. As part of the early days of the institute, I also thank Sebastian, Laura, Romy and Phung for making this place pleasant and joyful. It's great to keep in touch with you and remember the times together.

Despite only a short overlap that we shared in my early days, I am thankful to Serge and Saif who were crucial in setting up the lab as such and so many techniques/protocols. Thank you for your insights and advice from a detached standpoint, which oftentimes helped me to put things into perspective.

Many thanks to all the other members of the open office which became my second home and you guys made such a great place to be in. Thanks to Steve and Jonathan for keeping up with me. Thanks also to great discussions and laughs shared with Arianna (I hope some of our ideas will bear fruits one day), Virginie and Maria who were part of this little group of people on site every day in early 2021 and provided support in this time. Special thanks to Judith, you challenge me nonstop and impress me at the same time. It is scary at times how accurately you read and interpret situations, but I am thankful for your help to make me more considerate in my thoughts. As I don't believe in metal borders or separating buildings, my deep gratitude extends to Vincenzo for your curiosity in new technologies and applications in companies. Your foresight and judgements made many ideas pop and helped cope on bad afternoons after the bell. Thank you to Lucie, Anna, Mapi and Christopher for lots of those happy hours on Tuesdays. Thanks also to the countless discussions about football (among others) with Gabriele D, Gabriele C, Joris, Jérôme and Omid. The Champions League anthem unites us, and I hope there will always be a meeting room booked for this purpose. Thank you also to Sonia for all your help with muscle fibres and generally just knowing everything about reagents, samples and locations in this institute. Special thanks to Sara and your crucial role in fixing last-minute emergencies before FIR2020 and being part of the team to make this event reality. I always knew I could count on you and it really means a lot to me. I think we share and understand many experiences along our PhD journeys, and I am very thankful for your genuine support and honesty, the rant sessions and finding most appropriate smileys for every situation on Skype. (I wish I could insert one here) Many thanks also to Isabelle, who is the owner of the most adorable cats and beautiful orchids and whose thoughtful and calm decision-making I admire a lot. Thanks for so many memories in and outside the institute and hope there will be more of them with you and Seb across the 'Röstigraben'.

Prior to my arrival at the institute and in fact many months and years into it, I could always count on my London family. Despite our living conditions at the time, we managed to make the best out of it and make it a unifying experience. Many thanks to Raph on teaching us how to use Swiss army knives and enabling Chelsea roof experiences. Thank you, Mathilde for getting me into running and your can-do attitude to overcome any problem. Thanks to Shayne for making me think beyond myself and reaching out in difficult situations. Thank you to Desmond, our gold journeys and shared passion for flights, miles and finding the true value behind a locksmith's shop. Thank you also to Redwan, the joie de vivre across the world that you perhaps embrace as much as I do. Thank you to the great friends I made at Imperial, thank you Tycho for being such an honest and competitive opponent in squash to keep me sane, to Fran and Michael and the study sessions, to Jas for your feedback and support in preparing presentations, to Frederik, Sourojeet,

Rob, Julia and the class of 2016 for making this time unforgettable. The time in the UK would not be complete without thanking Moritz, for understanding the value of meal deals by the pitch, your incredible attention to details and pivoting the way to Switzerland.

I also wish to thank the friends I made at EPFL, who were not part of NIHS, but almost felt like they were. Thanks to Maria & Jake for my first thanksgiving dinner(s) which hopefully won't be the last. I am surprised we never actually crossed in GVA airport, but this should happen soon. Thanks for being such an inspiration for resilience and strength. Thank you also to Radek, Steph, Patrick who never stop believing in their dreams and goals. I had the enormous privilege to join shARE EPFL where I learned so much and whose members will always remain in my heart. We started out as a small group with Alex, Natalia, Leo, David, Lukas, Mikhail and Michael. I am humbled to have taken over as president from Alex who was instrumental in coaching me and whose pragmatism and analytics will take him to the moon one way or the other. ($GME may not have been the one) Thanks to Leo for your tremendous support and leadership during your time as VP and project lead. I am amazed by your determination and maturity and thankful to have worked with you. I could not be prouder of the new generation taking over a growing association and Mikhail, Melanie and Rachel already showing such strength and leadership in what are perhaps some of the most uncertain and challenging periods in a student's generation. Thanks to Apsara for all your background work and keeping things together, to Elena for your immensely valuable coaching and Seb for the very stimulating discussions you initiated in the summer of 2020. I can't forget and thank José, Rayan and Tijana enough for all the successful collaborations with TCS and the great fun in the challenges we faced and overcame. Thank you also to very successful collaborations with André, David and Alexandre with a project that remains to date one of the greatest experiences of my time in shARE.

Many thanks to the BioScience Network Lausanne (BSNL) for the opportunities and lessons I could share with you. Special thanks to Marija, your creativity and problem-solving during our FIR project played a monumental role in its success. I am proud of the team with Sara and Christopher and excited to see the FIR journey continuing with Katia onboard. Many thanks to the senior members Norine, Flo, Marilena and Julie for helping me to find ground in BSNL and get started.

Outside of the professional environment, I am extremely privileged to have so many people support me in any activity or idea I have. Thank you for adding life to years instead of just years to life. I think connected minds overcome any separation or distance and the shared experiences in Hong Kong make up so many joyful memories in my heart. I think of this time being unique in my life and cherish every single memory made in that time. It is hard to express all the feelings towards you guys and many of the

details may not be suitable for this audience. More than 7 years later, the spirit that made up Tat Chee Ave and Cornwall St remains unchanged in every single meet-up I was fortunate to have. Many thanks to my B**** Brothers Agustin and David, I won't forget the most expensive drink in my life and our time in Europe and CDMX with Sergio, Carlos and Ricardo, filled with great memories and … tacos. Both of you are beyond limits in hospitality and generosity. #LowingAndL best describes our trips with Agustin, Christian and Luis. Thank you to the group of people who share and create a sense of home in the weirdest places the European map can offer. Thank you, Lukas, Markus, Gautier, Alex, Margaux, Eric, Winnie, Rish, Mike, Victor, Isabel for laughs, debates, celebrations and all your support over all those years. I cannot appreciate all the friends I made across the world who welcome me with open arms wherever I go. Thank you to the MTL team Nic, Etienne, Xavier, Virginie and Olivier making my trip so memorable and marathon possible. Thank you also to the extended MTL team with Sam L and Tove in Europe and Sam in Sydney. Thanks to Denym across the Tasman Sea, your entrepreneurial spirit mixed with those midnight and beach snags are unforgettable. Thanks to Marta, Aleks, Laurenz and Richard for our Swiss adventures, your support and advice. Thank you to David in ZG, you are a true role model realising your dreams and visions starting from 2015 with my first visit and the ones that followed. Thank you to AJ for chasing your aspirations and goals in such an inspiring way. Thanks for showing me around in the Americas, Francisco, Santi, Tomas, Lynn and making ORD way less boring Joseph. Thanks to so many other travel experiences made by so many special people, thank you to the Iranian ***** Amir, Sattar, Navid, Mehdi for exploring Swiss mountains and enjoying Interlaken. Thanks to Teodora, Dan, Nika, Verche for all my Balkan ventures, the ajvar and cevapi.

I would like to express my deepest appreciation to the AMPK group with all its early members Serge, Saif, Maria, Matthew, Caterina, Eva, Nicolas, Sonia and later Mayuko, Katya and Robin. Thank you for all your efforts, discussions and support. Since I spent a majority of my time here, I can't value your presence enough. None of this work would have been possible without you and I will be forever thankful for that. Special thanks to Maria, thank you so much for all your efforts in the recombinant protein phase of my project, all the preps that were highly anticipated and evaluated, all the tweaks made and achieved to improve yield. All the sacrifices you made for your family and strength you showed continue to impress me. We all miss you a lot in the lab and I hope we will visit Dundee very soon. Many thanks also to Robin, your honest criticism and judgement are institutional pillars of my work. Thank you very much for picking me up from my favourite chalet in Verbier, cycling along with me in my foolish attempts to break running times, trying to introduce me to the odd game of cricket and birdwatching on the Sea Eagle.

I'm deeply indebted to Matt who accompanied me from day 1 when starting at the institute. It is hard to fit all of the lessons I learned into a space-limited paragraph. What started out as "Matt's book of wisdom" should correctly be referred to as learning journey across fields of life, bearing its own hashtag (#WWMD). Indeed, you served as sort of a moral compass and continue to do so with or without your presence. Whether putting me in place when I crossed a line or taking nuanced approaches in judgement over a sledgehammer approach, you always provided reasonable counterarguments which made my life harder but showed me the need for learning and improvement. Thank you for caring in some of my most difficult times, which seemed obviously clear to you but remained oddly opaque to me. I cannot appreciate this enough, being brutally honest and having good interests at heart. Thank you for your help in the last metres of my marathon, the physical one and the mental one.

When it comes to role models and inspiration possibly throughout NR, it is impossible to miss Omid. His open-mindedness and persistence cannot truly be reflected by words. Luckily, nobody needs words to sense this in person. I am truly grateful for the discussions we have, the outlook on the world of science, business and humanity. You are such a strong character and it is my sole honour to have crossed paths with you. So many memories come to mind since I first entered the doors of this institute and yet many more are to be created. Thank you for your kindness, generosity, human brilliance and sheer joy. If not biologically (but who knows), we remain brothers in spirit.

I would not be at the stage where I am, if it was not for Caterina. Despite no confirmed biological relation either, you are way more than just a colleague or friend. To me, you are like a sister. Through all the blood, sweat and tears we invested, you have seen me at my worst but never hesitated to offer your full support and energy to overcome any issue. No obstacle, border or distance would result in diminished support from your side and there won't ever be enough space and time to express my gratitude for this appropriately. If hardship or #meripenopi moments create something, it may well be this unique bond. Thank you for your support during weeks and months of home-office, thank you for your radical honesty, all the fun conversations, #ItalianNews and relevant scientific discoveries outside our field of expertise. I continue to be impressed by your willingness and ability to learn and improve and I am incredibly happy to share some of those paths.

I am extremely grateful for the help and support of my brother who is the harshest critic of my actions while understanding my rationale. This constant cycle of improvement needs balance occasionally, but broadly led to so many good decisions. (#DiamondHands) We understood this from early on and motivated each other constantly. If anyone would have told us at a young age, we would do even half of

what we do now, we would not have been able to imagine it. Thank you also to my mother for her early investment and belief in me. This laid the foundation of where I am today.

Unfortunately, we cannot control all aspects of life. Not everything we hope for plays out the way we want. Sadly, my grandmother cannot witness this moment in person anymore. A moment she would have been proud of and a moment that was enabled by her continuous and never-ending curiosity and encouragement. I dedicate this work to her.

Resumée

Des études cliniques ont démontré que les activateurs directs de la protéine kinase activée par l'AMP (AMPK), un capteur métabolique conservé au cours de l'évolution, peuvent prévenir, et même guérir, efficacement certaines maladies métaboliques, à l'instar du diabète de type 2. Ces activateurs, comme par exemple le 991/MK-8722, peuvent se lier à un site de régulation appelé "allosteric drug and metabolite" (site ADaM), situé à l'interface entre la sous-unité catalytique α et la sous-unité régulatrice β. Une autre approche directe d'activation de l'AMPK consiste à imiter l'AMP/ADP, ses ligands naturels, en se liant au site nucléotidique de la sous-unité γ, comme c'est le cas pour le 5-aminoimidazole-4-carboxamide ribonucléotide (AICAR). Leur capacité à influencer l'homéostasie du glucose serait due à l'activation des complexes AMPK trouvés dans le muscle squelettique. L'AMPKγ3 est unique en tant qu'isoforme de sous-unité AMPK car elle est exprimée sélectivement dans les fibres musculaires glycolytiques.

Pour comprendre l'impact de la régulation spécifique de l'isoforme γ3 sur le métabolisme du glucose, nous avons utilisé un modèle de souris knock-out de γ3 (γ3$^{-/-}$) afin d'étudier les effets de l'AICAR et du 991/MK-8722. Nous avons constaté que l'expression et l'activité de l'isoforme γ3 sont élevées dans les muscles glycolytiques comme l'extensor digitorum longus (EDL) mais peu détectées dans le muscle oxydatif soleus (SOL). Nous avons également démontré que l'AICAR et le 991/MK-8722 stimulent tous deux l'absorption du glucose dans les muscles EDL et SOL. En revanche, seule la capacité d'absorption du glucose induite par l'AICAR est diminuée dans l'EDL γ3$^{-/-}$. La clairance du glucose est également affectée dans les muscles γ3$^{-/-}$ en réponse à l'AICAR, tandis que MK-8722 abaisse la glycémie de façon similaire chez les souris WT et γ3$^{-/-}$, et ce, malgré la présence de complexes contenant γ1, qui prédominent dans les muscles EDL et SOL. Cela suggère que différentes isoformes d'AMPK γ jouent un rôle différent dans l'homéostasie du glucose en réponse à l'AICAR.

Nous avons également examiné la synthèse *de novo* du glycogène et l'utilisation du glucose dans le muscle. Malgré une absorption de glucose basal similaire entre les muscles de WT et γ3$^{-/-}$, la perte de γ3 diminue le niveau basal du glycogène spécifiquement dans les muscles glycolytiques. Nous démontrons que cela ne peut pas être dû à une incapacité à synthétiser le glycogène, puisque MK-8722 augmente bien les niveaux de glycogène dans l'EDL, mais que la diminution du glycogène basal dans l'EDL γ3$^{-/-}$ pourrait

être liée à une expression plus faible de l'UDP-glucose pyrophosphorylase 2 (UGP2). Cela suggère que l'AMPKγ3 pourrait jouer un rôle dans le devenir moléculaire du glucose.

Pour résumer, nous avons démontré que la sous-unité γ3 est facultative pour le transport du glucose *ex vivo* et l'homéostasie du glucose *in vivo* en réponse aux activateurs AMPK du site ADaM, mais que l'activation à médiation nucléotidique de γ3 par AICAR est altérée dans les muscles $\gamma3^{-/-}$. Des recherches supplémentaires seront nécessaires pour comprendre la régulation nucléotidique de différents complexes AMPK contenant des sous-unités γ. Ce mécanisme d'activation différentiel pourrait être exploité pour cibler spécifiquement les complexes AMPKγ3 dans le muscle, afin d'éviter les effets délétères de l'activation des complexes AMPK dans d'autres tissus.

Mots-clés :

Abstract

Clinical trials have shown that direct activators of an evolutionary-conserved metabolic sensor, AMP-activated protein kinase (AMPK), are beneficial in preventing/treating a range of metabolic disorders, including type 2 diabetes. These activators, including 991/MK-8722, bind at regulatory site, termed the allosteric drug and metabolite (ADaM-site) at the interface between the catalytic α subunit and regulatory β subunit. In addition, another approach for direct activation of AMPK is through mimicking its natural ligands, AMP/ADP, by binding to the nucleotide site in the γ subunit, e.g. 5-aminoimidazole-4-carboxamide ribonucleotide (AICAR). Interestingly, their ability to influence glucose homeostasis is reported to be through activation of AMPK complexes found within the skeletal muscle. The AMPKγ3 is unique as an AMPK subunit isoform since it is selectively expressed in glycolytic skeletal muscle fibres.

To gain more insight into the γ3 isoform-specific regulation of glucose metabolism, we used a γ3 knock-out ($γ3^{-/-}$) mouse model to investigate the effects of the AICAR and 991/MK-8722. We confirm that γ3 isoform expression and activity is high glycolytic muscles, including extensor digitorum longus (EDL), whereas there is very little detected in oxidative soleus (SOL) muscle. We show that AICAR and 991/MK-8722 stimulated glucose uptake in both EDL and SOL muscles. Interestingly, only the ability of AICAR to induce glucose uptake was blunted in EDL muscle taken from $γ3^{-/-}$ mice. Consistent with this, whole-body glucose clearance was also impaired in $γ3^{-/-}$ mice in response to an AICAR, whilst MK-8722 lowered blood glucose similarly between WT and $γ3^{-/-}$ mice. Despite the presence of γ1-containing complexes, which are the most predominant complexes in both EDL and SOL muscles, this suggests that different AMPK γ isoforms play different roles in glucose homeostasis in response to AICAR.

We further looked at de novo glycogen synthesis and glucose utilisation in skeletal muscle. Despite similar basal glucose uptake between muscles from WT and $γ3^{-/-}$, γ3-deficiency results in lower basal glycogen content only in glycolytic muscles. We show that this is not due to an inability to synthesise glycogen de novo, since MK-8722 was able to increase glycogen levels in EDL. Instead, we show that the decrease in basal glycogen in $γ3^{-/-}$ EDL, may be linked lower expression of UDP-glucose pyrophosphorylase 2 (UGP2). This suggests that AMPKγ3 may play a role in steering the molecular fate of glucose inside the cell.

Taken together, whilst we show that AMPKγ3 is dispensable for *ex vivo* glucose transport and *in vivo* glucose homeostasis in response to ADaM-site AMPK activators, nucleotide-mediated activation of γ3 by AICAR is impaired. Further research is required to understand the nucleotide regulation of different γ-

containing AMPK complexes. This differential activation mechanism could be exploited to specifically target AMPKγ3 complexes in the muscle, and potentially avoid deleterious effects of activation of AMPK complexes in other tissues.

Table of Contents

List of Figures

List of Tables

Abbreviations

2-DG	2-deoxyglucose
ACC	Acetyl-CoA carboxylase
ADaM-site	Allosteric drug and metabolite binding site
ADP	Adenosine diphosphate
ATP	Adenosine triphosphate
AICAR	5-aminoimidazole-4-carboxamide ribonucleoside
AID	Auto-inhibitory domain
AMPK	AMP-activated protein kinase
ANOVA	Analysis of variance
α-RIM	α-subunit regulatory interacting motif
ATP	Adenosine triphosphate
BAT	Brown adipose tissue
β-CBM	β-subunit carbohydrate-binding module
β-CTD	β-C-terminal domain
Ca^{2+}	Calcium
CAMKKβ	Ca^{2+}-/calmodulin-dependent protein kinase kinase β
CBS	Cystathionine β-synthase
CTD	C-terminal domain
EDL	Exterior degitorum longus
GAP	GTPase-activating protein
GAS	Gastrocnemius
GLP-1	Glucagon-like peptide 1
GLUT4	Glucose transporter 4
GP	Glycogen phosphorylase
GS	Glycogen synthase
GusB	β-glucuronidase

HKII	Hexokinase II
HMG-CoA	3-hydroxy-3-methylglutaryl-CoA
Hprt1	Hypoxanthine ribosyltransferase
IP	Immunoprecipitated
KD	Kinase domain
K_d	Dissociation constant
KO	Knockout
LKB1	Liver kinase B1
MO25α/β	Mouse protein 25 α and β
MyHC	Myosin heavy chain
PCR	Polymerase chain reaction
P_i	Inorganic phosphate
Pgk1	Phosphoglycerate kinase 1
PPP	Pentose phosphate pathway
PKB	Protein kinase B
SGLT	Sodium-glucose co-transporter
SOL	Soleus
STBD1	Starch Binding Domain 1
T2DM	Type 2 diabetes mellitus
TBC1D1	TBC1 (Tre-2/USP6, BUB2, Cdc16) domain family, member 1
UDP-glucose	Uridine diphosphate glucose
UGP2	UDP-glucose pyrophosphorylase 2
WAT	White adipose tissue
WB	Western blot
WT	Wild-type
ZMP	AICAR monophosphate

List of Appendix Figures

1 Introduction

1.1 Significance and Relevance of Research on AMP-activated Protein Kinase (AMPK) in Health and Disease

Across the world, obesity and being overweight is becoming a prevalent problem with wide implications. Since the year 2000, the number of obese adults increased by a factor of 1.5 to 13.1% in 2016 and is projected to further increase dramatically [1]. Combined with increasing sedentary lifestyle choices, these problems can lead to an increased risk of developing type 2 diabetes mellitus (T2DM), imposing a growing burden on global healthcare systems and global economic growth. Diabetes alone caused 1.5 million deaths in 2012 and is estimated to cost over 800 billion USD annually leading up to 1.7 trillion USD of global GDP loss by 2030 [2]. Diabetes and its underlying health conditions increase the chance of other chronic or acute complications like cardiovascular diseases, kidney problems and others [3].

As for generations, lifestyle changes and physical exercise remain some of the best strategies in prevention and management of obesity and the associated health and metabolic dysfunctions [4]. However, these strategies may fail to achieve their goal due to medical reasons or the lack of patient compliance [5]. Traditional pharmacological approaches of T2DM management focus on and around decreasing hyperglycaemia. Well known drugs like sulphonylureas, metformin or insulin itself can have undesirable side effects such as weight gain or gastrointestinal upset and limitations in efficacy or patient tolerance [6]. Other interesting drug classes include glucagon-like peptide 1 (GLP-1) receptor agonists [7] and sodium-glucose co-transporter (SGLT) inhibitors, more specifically SGLT2 inhibitors [8]. GLP-1 receptor agonists act by activating GLP-1 receptors in the pancreas, improving insulin sensitivity and inhibiting glucagon secretion which in turn decreases hepatic glucose production [9]. Despite multiple drugs being approved and clinically effective, their short half-life remains a major drawback and research currently focuses improving the degradation resistance of this drug class [7]. SGLT inhibitors follow a rather orthogonal approach by targeting glucose reabsorption in the kidney. Under healthy conditions glucose is excreted through the urine which would lead to dramatic loss of a major body fuel. To prevent a constant glucose drain, the kidney works to take up glucose from the urine through SGLTs [8]. In an effort to decrease excess levels of glucose in the body, inhibitors of this reabsorption process were identified and studied in rodents in the 1980s and their development gained traction with the recent approval of a number of drugs [10]. Importantly, traditional pharmacological diabetes treatments often

fall short of addressing the problem of insulin resistance, which affects many T2DM patients and obese pre-diabetic patients with other predispositions [11].

To possibly overcome this, biochemical research started to uncover signalling and regulatory mechanisms of key metabolic functions and gained interest in the idea of mimicking or augmenting beneficial effects of physical exercise to improve metabolic health. Among other identified targets, the description of AMP-activated protein kinase (AMPK) as master regulator of metabolism and cellular energy sensor drew particular attention to it as potentially attractive therapeutic target [12].

AMPK is an evolutionary conserved Ser/Thr protein kinase and acts as a key energy-sensing enzyme, expressed in almost all eukaryotic cells [13, 14]. It balances cellular energy in the form of adenosine 5'-triphosphate (ATP), which is seen as the essential molecular energy carrier molecule [15]. ATP exists in an equilibrium between differently phosphorylated adenosine nucleotides counterparts such as adenosine nucleotide 5'-monophosphate (AMP) or adenosine nucleotide diphosphate (ADP) as shown below with P_i representing the free phosphate group as a result of ATP hydrolysis.

$$ATP + H_2O \rightleftharpoons ADP + P_i \quad (1)$$

$$ADP + H_2O \rightleftharpoons AMP + P_i \quad (2)$$

$$2\,ADP \rightleftharpoons AMP + ATP \quad (3)$$
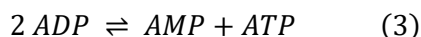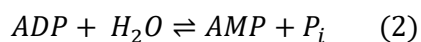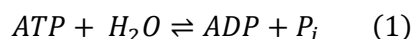
From a pure chemical perspective, the equilibrium of reaction (1) would lie heavily on the right towards ATP hydrolysis and release a part of the free energy as heat to the environment [16]. This would represent a depreciation of cellular energy and lead to an inert steady state. Falling ATP not only causes a rise in ADP levels, but consequently also AMP levels through hydrolysis in reaction (2) and reaction (3) catalysed by adenylate kinase. Given that reaction (3) usually occurring near the equilibrium, AMP levels rise relatively higher than ADP upon ATP hydrolysis [17]. To counteract equilibrium (1) and maintain a high charge of cellular energy, cells act to restore a high ATP to ADP/AMP ratio by a process called catabolism. It is exactly this process of carefully monitoring and balancing those levels of cellular energy where AMPK has been a major player over an evolutionary period and is therefore described as the "guardian of cellular energy" [13].

AMPK is activated under conditions of any metabolic stress which depletes the cell of its ATP and in return increases AMP/ADP:ATP ratios. Activated AMPK will then act as a switch to activate catabolic or ATP producing pathways, while inhibiting anabolic or ATP consuming pathways leading to a net gain in ATP

[18]. The pathways involved in this energy level adaptation include glycolysis, glucose uptake and beta oxidation of fatty acids representing the catabolic side of the balance and protein as well as fatty acid synthesis the anabolic side. Activation of AMPK was shown to counteract hyperglycaemia through increased glucose uptake into skeletal muscle in contexts of metabolic diseases linked to T2DM or the presence of insulin resistance [19, 20]. The latter raised the hope of an alternative treatment for patients suffering from insulin resistance and suggested that AMPK activation may have beneficial effects similar to physical exercise, making it an exciting potential drug target for new diabetes therapies [21, 22].

Since then, significant effort was put into unveiling molecular mechanisms of AMPK regulation and downstream effects to develop and improve AMPK activating compounds. Numerous drugs are known to activate AMPK either indirectly by altering the ratio of adenine nucleotides or directly by binding to the protein itself. Recently, a systemic pan-AMPK activator was shown to treat key components of T2DM in several diabetic animal models. Interestingly, these effects were shown to be mediated by activation of AMPK in skeletal muscle [23]. This opens the door for thoughts on targeting muscle-specific AMPK populations as a strategy for treatment of T2DM. In the future, this approach could have the intriguing benefit of avoiding any unwanted off-target effects of AMPK activation in other tissues [24].

1.2 Structure and Expression of AMPK

1.2.1   AMPK Subunits & Isoforms

Since first rat liver purifications in 1987 of an at the time unknown protein kinase phosphorylating acetyl-CoA carboxylase (ACC) and 3-hydroxy-3-methylglutaryl-CoA (HMG-CoA) reductase [25], later to be known as AMPK [26, 27], tremendous progress in understanding this enzyme has been made in the last few decades.

Now it is known that AMPK expressed in mammalian cells occurs as a heterotrimeric complex denoted as αβγ complex. It comprises the catalytically active α subunit and the two regulatory subunits, namely the β and γ subunits. The subunits themselves may individually occur in up to 7 different isoforms and some splice variants thereof. All isoforms are encoded by different genes denoted by the prefix "*prka*" and a suffix of the respective isoform (α1, α2, β1, β2, γ1, γ2 and γ3) as seen in Figure 1, which allows a total number of 12 unique combinations to form a heterotrimer [19].

Depending on the nature of the isoforms, AMPK shows differences in expression and regulation [28, 29] throughout an organism, which allows unique metabolic regulation and may in turn be utilised for isoform- or complex-specific drug development [14]. However, precise roles of those isoform combinations *in vivo* and in individual tissues remain largely unknown.

The following sections will focus in more detail on structural and regulatory features of AMPK to understand molecular mechanisms and effects of its activation.
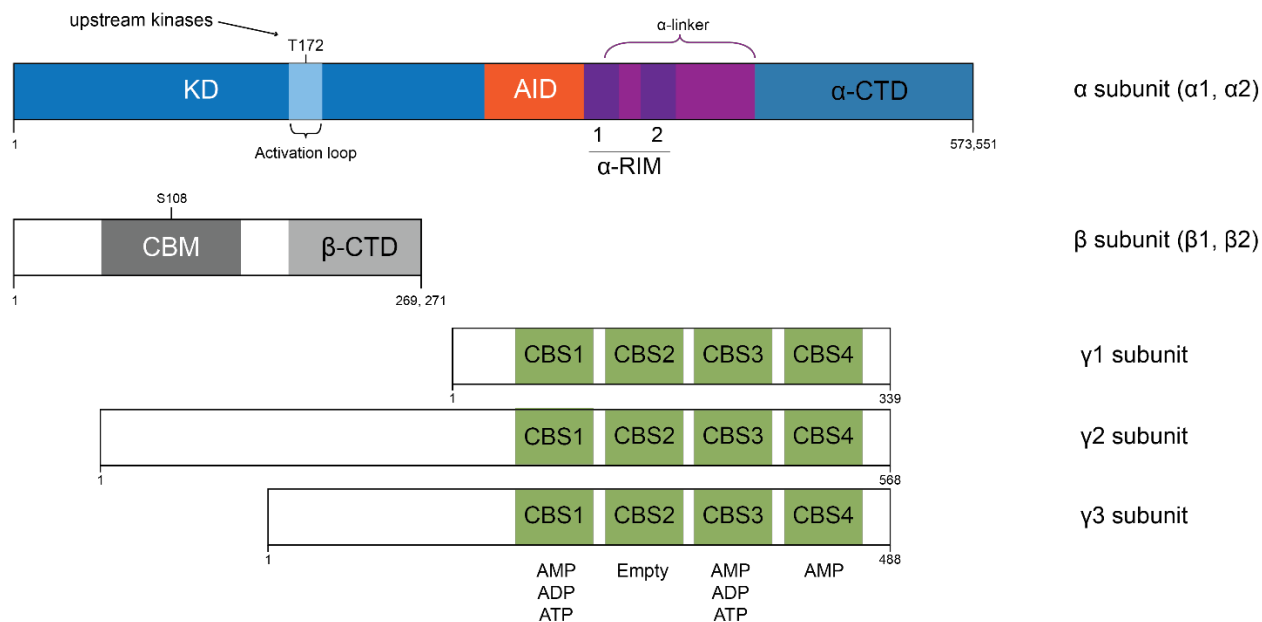
Figure 1 Scheme of the isoforms and domain structure of the AMPK subunits.
The individual sequences are shown with the N-terminus on the left (labelled 1) and the C-terminus on the right (labelled according to the length of the subunit). The shown subunit isoforms are encoded by the following human genes in accessed in UniGene (NCBI, US National Library of Medicine) with the numbers NP_996790.3 (*PRKAA1*, AMPKα1), NP_006243.2 (*PRKAA2*, AMPKα2), NP_006244.2 (*PRKAB1*, AMPKβ1), XP_003960220.1 (*PRKAB2*, AMPKβ2), NP_001193638.1 (*PRKAG1*, AMPKγ1), NP_057287.2 (PRKAG2, AMPKγ2) and NP_059127.2 (*PRKAG3*, AMPKγ3).
α subunit: KD, kinase domain with activation loop and residue T172; AID, auto-inhibitory domain; α-RIMs, regulatory element interacting motifs within a linker region between the N-terminal kinase domain and the C-terminus; α-CTD, α C-terminal domain interacting with the β subunit. β subunit: CBM, carbohydrate binding module with S108 autophosphorylation site; β-CTD, β C-terminal domain interacting with the α/γ subunits. γ subunits: three subunits with distinctly different N-termini; CBS, four repeats of cystathione β-synthase motifs, responsible for nucleotide binding.

1.2.2 AMPK Structure & Function

The α subunit contains the canonical N-terminal Ser/Thr kinase domain (KD) with its conserved activation loop around the Thr172 (T172) phosphorylation site [30]. The activation site lies encompassed between the smaller N-lobe and the larger C-lobe and is required to be phosphorylated to achieve maximum kinase activity [31]. Similar to many other kinases, other upstream kinases phosphorylate this main activation

26

site, which leads to activation of the enzyme [32]. In the search of upstream kinases of AMPK, the tumour suppressor liver kinase B1 (LKB1) [33, 34] as well as Ca^{2+}/calmodulin-dependent kinase kinase β (CaMKKβ) [35, 36] were identified and will be discussed in context of AMPK regulation.
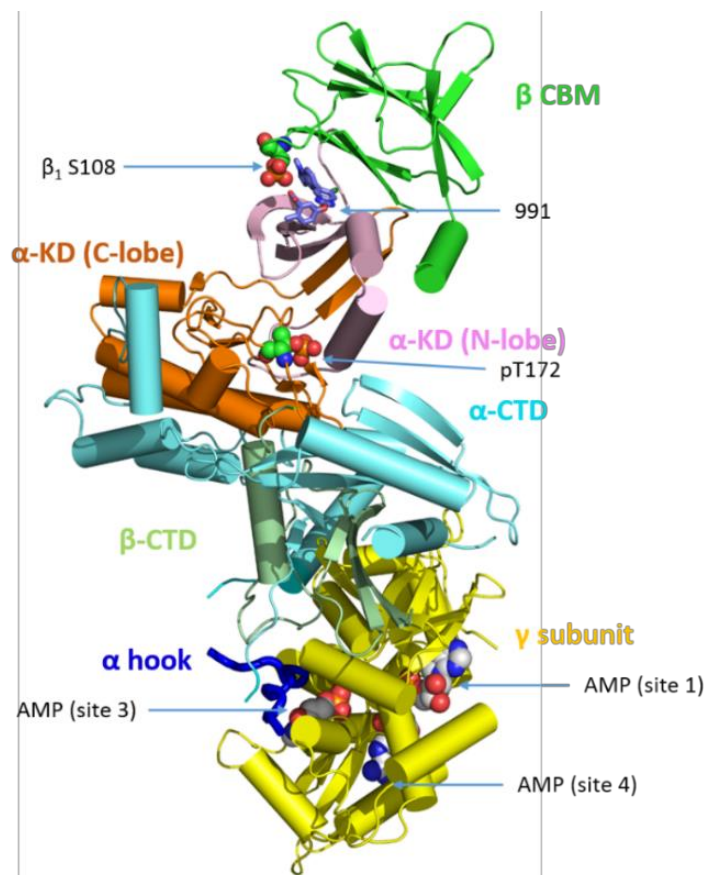
Figure 2 Crystal structure of recombinant full-length human AMPK α2β1γ1 complex, co-crystallised with bound ligands AMP and 991 and published by Xiao *et al.* with the protein data bank (PDB, Research Collaboratory for Structural Bioinformatics) ID **4CFE.pdb** [37].
Crystallography studies of full-length AMPK complexes allowed understandings of the relationship between catalytic and regulatory domains to form. Out of four adenine nucleotide binding sites in the γ1 subunit, only three (sites 1, 3 and 4) appear to be occupied at all, two of which (sites 1 and 3) are exchangeable binding sites and site 4 being permanently bound to AMP. The synthetic activator 991 was shown to bind in a distinct pocket formed between the α2 kinase domain (KD) and the β1 carbohydrate binding module (CBM) [38]. α-KD: kinase domain with activation loop and residue T172 on the C-lobe; α-CTD: α C-terminal domain interacting with the β subunit. β CBM: carbohydrate binding module with β1 S108 autophosphorylation site; β-CTD: β C-terminal domain interacting with the α/γ subunits. The image was created using PyMOL (The PyMOL Molecular Graphics System, Version 1.2r3pre, Schrödinger, LLC) sphere representations of the pT172 site and bound ligands.

The α-KD is followed C-terminally by an auto-inhibitory domain (AID), which bears its name from the fact that it acts as a self-inhibitory sequence for the enzyme when bound to the α-KD and thus keeping it in a basal inactive conformation [39]. On the contrary, it shifts away from the kinase domain upon AMP activation, allowing a catalytically active conformation [40, 41]. C-terminally of the AID lies a so called

"linker" region containing two α-regulatory interacting motifs (α-RIM), connecting the AID to the C-terminal domain (α-CTD) [42].

The regulatory β subunits carry a post-translational myristoylation at the N-terminal Gly2, which is thought to play an important role in subcellular localisation and thus intracellular regulation of AMPK signalling [43]. Additionally, both β subunits contain a sequence that is thought bind to glycogen and therefore named carbohydrate-binding module (CBM) or glycogen-binding domain (GBD). This domain binds to glycogen or other carbohydrate species and is thought to inhibit AMPK activity, providing a link between AMPK signalling and a major carbohydrate storage form of the cell [44, 45]. To investigate the physiological significance of glycogen binding to AMPK, recent studies focused on the molecular mechanism of glycogen/AMPK-interaction using cell-free assays [46, 47] and genetically modified mice [48]. Hardie *et al.* showed the inhibitory effect of glycogen on AMPK activity *in vitro* and identified point mutations in the β1 and β2 CBM enabling the binding. Mutations of β1 W100 and W133 as well as β2 W99 and W133 abolishes the inhibitory effect of glycogen and other branched oligosaccharides leading to the hypothesis that AMPK's role to sense energy status may not be limited to nucleotides [46]. Further insight into AMPK-glycogen-interactions was gained through the discovery of an AMPK autophosphorylation site (β1 T148), which in a phosphorylated state prevents carbohydrate binding to AMPK. Interestingly, subcellular localisation of AMPK was impacted in phospho-mimicking T148D mutants *in vitro* using HepG2 and HEK293T cells. AMPKβ-T148D failed to co-localise with intracellular glycogen while also exhibiting less phosphorylation of Ser7 in Glycogen Synthase (GS) in response to AMPK activators [47]. In a recent study, the previously identified CBM interaction sites β1 W100 and β2 W98 were used in a mouse knock-in (KI) model to disrupt the respective β isoform binding interaction with glycogen on a physiological scale. Since skeletal mouse muscle predominantly expresses the β2 isoform, the β2 W98A KI model was particularly useful for insights into *in vivo* skeletal muscle effects of AMPK and glycogen. While both models showed decreased expression and activity of total AMPK likely due to complex destabilisation as well as increased fat content in liver and muscle respectively, only the latter model showed decreased glucose tolerance on a whole-body-level and decreased exercise ability [48]. These results highlight the importance of glycogen for AMPK activity modulation either allosterically or through subcellular localisation, which impacts metabolic function and energy homeostasis in tissues like skeletal muscle. However, it should be noted that there was no evidence/data shown if the W98A mutant was dissociated from glycogen in skeletal muscle (*in vivo*).

In the folded AMPK complex, the CBM interacts with the N lobe of the α-KD mediated by a helical structure immediately adjacent to the CBM sequence (C-interacting helix) [41]. The formed pocket between the kinase domain and the CBM was found to be the binding site for small allosteric AMPK activators and possibly endogenous metabolites (as suggested by Pinkosky *et al*. [49]), leading to the term Allosteric Drug and Metabolite (ADaM) site [41, 50]. A crucial autophosphorylation site was identified within the β1 CBM, the mutation of which to alanine (S108A) renders complexes less sensitive to allosteric activation by ADaM site binding activators [41]. Recent crystal structures of β2 complexes indicate that a β2-specific D111 residue may mediate ADaM-site binding of direct activators, underlining the importance of isoform-specific drug targeting [51]. The β C-terminal domain (β-CTD) is thought to serve as connecting element between the C-terminal α subunit domain and the nucleotide-binding domain of the γ subunits [37].

The γ subunit isoforms share some highly conserved key domains but are largely speaking the ones that show the most variation from one another. The γ subunits harbour four cystathionine β-synthase (CBS) motifs, which are responsible for binding of the regulatory adenine nucleotides AMP, ADP and ATP [37, 38]. The CBS domains are the conserved elements of the isoforms and they occur in four repeats, forming two tandem pairs [52]. Despite having four possible binding adenine nucleotide binding sites, it appears that only three of them are ever occupied with site 2 being unoccupied [38]. AMP, ADP and Mg^{2+}.ATP were shown to bind to two exchangeable nucleotide binding sites 1 and 3 in the γ1 subunit. Interestingly, these two exchangeable binding sites display different binding affinities (about 30-fold) to nucleotides and are thought to have distinct functions [38, 53, 54]. The main difference between the isoforms lies in their respective N-termini, which vary in both length and sequence. The γ1 subunit is the shortest of all isoforms, while γ2 and γ3 both have long but unrelated N-terminal extensions. The precise role or structure of those extensions remains elusive, although a function in sub-cellular localisation was suggested recently [55]. All published structural studies on AMPK were performed on γ1 containing complexes and until today, no full-length crystal structure for other complexes is available. This leaves a gap in the knowledge of the molecular mechanisms involved in regulation and function of both γ2 and γ3 subunits.

1.2.3   AMPK Expression in Tissues

The expression and distribution of AMPK subunit isoforms varies substantially across tissues as well as species. Importantly, this expression pattern differs from human to rodent models as seen in the opposite β isoform expression in the respective liver tissues. Both mice and rats are thought to express almost exclusively β1 complexes in liver, while humans do so with a similar exclusivity for β2 complexes [56].

Generally speaking, AMPK complexes containing α1, β1 and γ1 complexes are ubiquitously expressed across tissues, while other isoforms such as α2, β2 and γ3 show more restricted expression patterns, which may suggest specific roles of certain isoforms in different tissues [14]. Differences in subunit isoform expressions across species remain a major concern in animal studies and disease modelling as seen in the expression of γ2, which is highly expressed in human heart but shows a more broad and variable expression in mice [57]. AMPK subunit isoform expression was also shown to be dynamic, with a gradual increase of β2 and γ3 expression in differentiating mouse myotubes [58]. While there were attempts of quantification of AMPK subunit expression in human skeletal muscles [59], there is still a lack of adequate measures across tissues which is essential for development of isoform-specific activators for clinical use.

The following sections will highlight the expression and function of AMPK in skeletal muscle as well as brown adipose tissue (BAT), including functional and regulatory aspects.

1.2.3.1 AMPK in Skeletal Muscle

Muscle contraction and physical exercise are unsurprisingly very potent metabolic stressors, linked to enhanced glucose uptake and insulin sensitivity [60-62]. Thus, targeting and enhancing skeletal muscle AMPK signalling could be a reasonable physiological approach to improve metabolic parameters. A link between exercise and AMPK activation was shown in rat [63] and human skeletal muscle [64], with the latter showing a preferential α2 subunit activation [65]. Later studies identified the α2β2γ3 complex as predominantly activated complex in response to exercise [66]. Studies show that only α2β2γ3, α2β2γ1 and α1β2γ1 isoforms are expressed in skeletal muscle [67], with γ3 being selectively expressed in this tissue. Therefore, activation of α2β2γ3 could be a good starting point for the development muscle-specific AMPK activators.

Genetic mouse models were used to assess the role of AMPK in skeletal muscle glucose uptake in response to exercise and drug stimulation. Whole-body knock-outs (KO) of AMPK subunits α2 [68], β2 [69] and γ3 [70] and expression of a kinase-dead α2 isoform (α2-K45R) [71] eradicated 5-aminoimidazole-4-carboxamide ribonucleotide (AICAR)-stimulated *ex vivo* glucose uptake in skeletal muscle. Based on the findings of those genetic models, the α2β2γ3 heterotrimer was suggested to mediate contraction-stimulated glucose uptake. Muscle-specific double knock-out of β1/β2 (mdKO) subunits [72] show an impaired *ex vivo* (electrically-induced contractions) and *in vivo* (treadmill running exercise) glucose uptake in mice. This provides genetic evidence for an essential role of AMPK mediating insulin-independent glucose uptake in skeletal muscle in response to contractions and drug stimulation.

To date, most direct AMPK activators such as A-769662 preferentially activate complexes expressing the β1 subunit, due to tighter binding to the ADaM site. Discoveries of more potent direct activators and dual-drug treatments [73, 74] opened up more possibilities to also target β2 complexes and achieve greater AMPK activation, which is particularly relevant for targeting skeletal muscle where the latter is highly expressed and plays an important role in metabolic regulation [75]. β2 KO mice showed profoundly reduced muscle AMPK activity, AICAR-stimulated glucose uptake and generally lower exercise capacity [69]. Compound 991 (also known as ex229) for instance increases skeletal muscle AMPK activity and glucose uptake *ex vivo* in a dose-dependent manner [76]. A dual treatment approach of A-769662 and the AMP-mimetic AICAR increased AMPK activation in β1 expressing cells [74], whereas a combination of 991 and either AICAR or contraction enhanced AMPK activation in both β1 and β2 in intact cells [73]. Notably, a dual treatment also improved AMPK activation of skeletal muscle-selective γ3 complexes (such as α2β2γ3) *ex vivo*, providing an interesting finding for muscle-specific AMPK activation [73].

Taken together, several studies provided evidence of the involvement of the α2, β2 and γ3 subunits in AMPK activator-induced metabolic processes/improvements in skeletal muscle on a genetic level, indicating an involvement of the α2β2γ3 complex. This complex has also been shown to be significantly activated in response to exercise, making it highly interesting to study AMPK function, with specific emphasis on the α2β2γ3 complex, in skeletal muscle. Therefore, understanding the physiological regulatory mechanisms underlying the glucose metabolism in skeletal muscle as well as the involved AMPK complexes is crucial for the development of tissue and isoform-specific AMPK activators.

1.2.3.2 AMPK in Brown Adipose Tissue (BAT)

Recently, AMPK was shown to be required for the metabolic remodelling of white adipocytes in response to stimulation of β-adrenergic receptors and mitochondrial function, supporting a regulatory role of AMPK in BAT. In line with this discovery, Perdikari *et al*. showed that BAT formation (referred to as browning of adipocytes) may be linked to AMPK both in cells and *in vivo* using both pharmacological inhibitors and short hairpin RNA (shRNA) knock-down to screen for kinases involved in adipocyte browning. ShRNA knock-down of the γ3 isoform encoding gene *Prkag3 in vitro* indicated a reduced brown adipocyte formation, suggesting an additional role of the γ3 subunit outside of skeletal muscle [77]. Chronic oral administration of rats with the AMPK activator C163 (compound number 163 in a patent library from Merck [78]) led to increased UCP1 expression and number of brown adipocytes in their BAT [77], supporting the idea of a role of AMPK in BAT development. Indications of the involvement of AMPKα [79] and AMPKβ [80] in BAT formation and AMPK activation in BAT upon cold exposure in mice [81] provide

interesting findings for further research into AMPK regulation in other metabolic tissues. Cold exposure also improved insulin sensitivity in humans after 10 days of adaptation at 14-15 °C. Although GLUT4 translocation was increased in muscle, AMPK signalling was not affected [82]. This supports the idea of BAT relevance in human physiology and perhaps cold adaptation, but also shows the necessity for further studies into the role of AMPK in this process. Recently, it was suggested that PRDM16 may play an intermediary role in AMPK-mediated brown adipogenesis [83, 84], but little is known about the roles of different subunit isoforms in BAT. The description of the use of immortalised brown pre-adipocytes could offer a useful platform to study the role of different AMPK subunits and activators in BAT formation and differentiation [85].

In summary, further insights into the involvement of AMPK and the γ3 isoform in the development of BAT could be relevant for pharmaceutical and therapeutic targeting of BAT to improve metabolic effects in alternative tissues.

1.3 AMPK Regulation

1.3.1 AMPK Regulation by Adenine Nucleotides

The activation of AMPK can involve three separate effects, also referred to as "tripartite mechanism of activation by AMP" [86], although the activating effects can also be triggered as combinations of the three by different activators [39]. Those effects include allosteric activation, the protection against dephosphorylation by phosphatases and the promotion of phosphorylation of T172 by upstream kinases as seen in Figure 3. The first major upstream kinase identified was a complex of STE20-related kinase adaptor α/β (STRAD α/β), mouse protein 25 α/β (MO25 α/β) and LKB1 as mentioned above. LKB1 was identified to phosphorylate T172 in rat liver [34, 87] and appears to be constitutively active without response to physiological or pharmacological AMPK activators in skeletal muscle [88]. LKB1-deficient cells show majorly impaired AMPK activation, suggesting indeed a role as upstream kinase of AMPK [34, 88]. CaMKKβ is another upstream kinase shown to activate AMPK *in vivo* [35, 36] in absence of LKB1 in cells [89], providing a potential link between AMPK activation and physiological changes in cellular Ca^{2+} levels, which is an important signalling mechanism in skeletal muscle and other tissues [90]. Whether CaMKKβ is a physiologically relevant upstream kinase for AMPK in skeletal muscle has not yet been verified using genetic models.

It is established that AMP acts through allosteric activation as well as protection against dephosphorylation, but whether it does through promotion of T172 phosphorylation is controversial [38,

91]. Some studies found an AMP-stimulated increase in phosphorylation of T172 by CaMKKβ when the β-subunit is N-terminally myristoylated [43], but further investigation is necessary to elucidate the function of this modification. Others suggest an increased phosphorylation of rat liver AMPK mediated exclusively by LKB1 [92], demonstrating remaining controversy on AMP-stimulated AMPK phosphorylation and the involved upstream kinases given that both phosphorylate the same residue in AMPK.
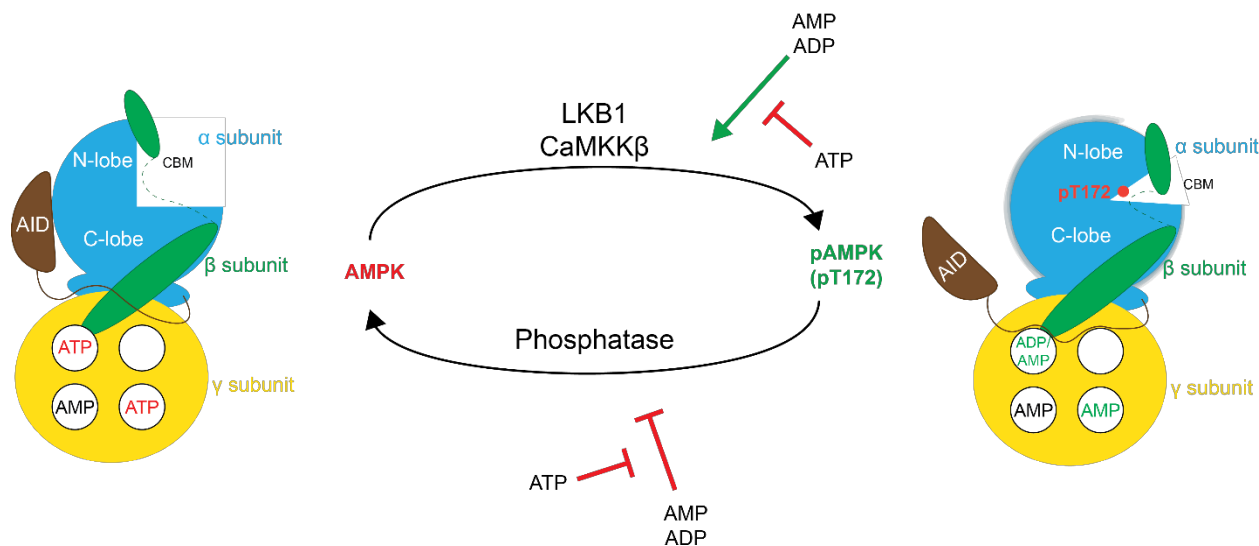
Figure 3 Schematic representation of AMPK regulation by adenine nucleotides.
AMPK complexes as shown with their respective α subunits in blue with N- and C-Lobe labelled, auto-inhibitory domains (AID) in brown), β subunits in green and γ subunits in yellow. The γ subunits contain the four possible nucleotide binding sites with site 2 being unbound and AMP being permanently bound to site 4 (AMP label in black). Site 1 is shown in the bottom right of the sites and site 3 on the top left. The activated AMPK complex contains a marked pT172 in the α subunit, indicated by the red dot and labelled accordingly.

Crystallographic studies of AMPK complexes with full-length γ1 subunit gave an insight into the nucleotide regulation. As mentioned above, all structural knowledge is based on crystal structures of γ1 containing complexes, while structures of full-length γ2 or γ3 complexes have not been published to date, which presents a caveat in regulatory understanding of different AMPK complexes. Nonetheless, the CBS domains are actually the only conserved regions between the γ isoforms [93] and structural analysis shows that only three out of four possible binding sites are occupied with AMP being constitutively bound to site 4 (CBS4 in Figure 1). AMP is competing with other adenine nucleotides for two exchangeable nucleotide binding sites 1 and 3 [38]. While the permanently bound AMP at site 4 might play a role in stabilisation of the AMPK complex, the exchangeable binding sites 1 and 3 show different binding affinities (about 30-fold) to nucleotides and are thought to have distinct functions [53, 54]. The tight binding site 1 was found to be involved in allosteric activation of AMP, whereas the weaker site 3 can bind nucleotides to regulate protection from dephosphorylation [53]. Likewise, ATP and ADP can also bind to the nucleotide binding

sites. While ATP antagonises activation effects, it was shown that ADP binding at the weaker site 3 inhibits dephosphorylation without activating AMPK allosterically [53].

In a physiological context, it is worth mentioning that although the concentration of ATP is generally far higher than ADP and even higher than AMP, ATP is mostly complexed with Mg^{2+} ions (Mg^{2+}-ATP) whereas AMP and ADP are not [94]. This complexation has been shown to decrease its binding affinity by tenfold compared to free ATP, making competition of ADP binding to the exchangeable sites possibly a physiologically relevant factor for protection against dephosphorylation [53].

Further studies have focussed on understanding structural elements linking nucleotide binding to the γ subunit with changes in catalytic activity in the α subunit. The AID was found to contact both N- and C-lobes of the kinase domain involving the KD αC-helix and stabilising an open and inactive kinase conformation [95]. Binding of ATP to the γ subunit maintains those interactions [96], while increasing AMP concentrations and binding to the γ subunit causes conformational changes around site 3 [42]. This allows an α-hook structure (referred to as αRIM [32, 42]) in the α subunit (αRIM-2 in Figure 1) to bind to AMP-bound site 3, leading to a disengagement of the AID from the KD and adaptation of a compact, activated conformation [32, 40, 53]. Recent studies suggest additional interactions between the N-terminus of the αRIM (αRIM-1 in Figure 1) and the adjacent AID with the unoccupied nucleotide binding site 2, reducing the inhibitory effect of the AID towards the KD and thus activating the enzyme [40, 42]. This model provides a mechanistic link between nucleotide binding and change as well as maintenance of the catalytic activity of AMPK and is illustrated as a cartoon structure in Figure 3.

1.3.2 AMPK Regulation by Small Molecule Activators

To assess the importance and potential of AMPK as a therapeutic target for treatment of metabolic disorders, researchers have sought to discover or design effective AMPK activators. An extensive number of AMPK activators have been reported but most appear to act indirectly, by elevating intracellular AMP:ATP and ADP:ATP ratios, for example as a consequence of inhibition of the respiratory chain [42]. Many compounds derived from herbs and plants such as berberine and quercetin, but also synthetic compounds like R419 [97] and PT-1 [98] act broadly by inhibiting mitochondrial function and subsequent changes in AMP/ADP:ATP ratios [99]. R419 was found to activate AMPK, increase muscle glucose uptake and improve insulin sensitivity in HFD-fed mice, but independently of skeletal muscle AMPK [100]. The widely known polyphenol resveratrol which is found in red grapes and thought to act through multiple mechanisms that may alter adenine nucleotide ratios [101] improves metabolic health parameters in mice

[102], but fails to reproducibly translate those benefits to obese patients in clinic [103]. This leaves the field of indirect AMPK activators open for exploration, but subject to the common and likely risk of AMPK-independent side effects.

Another class of AMPK activator is defined as AMP mimetic since the basis of this drug is the binding to the nucleotide regulatory site on the γ subunit. The first compound of this class to be identified was AICAR which has been extensively used for a number of years now [45], since it is metabolised to the AMP-analogue ZMP in the cell, and regulates the enzyme in the same manner as AMP, albeit with weaker affinity. However, due to the nature of activating AMPK through a nucleotide-like mechanism, several of the functions previously associated with AMPK activation by these two classes of AMPK activators, have been challenged with genetic knock-out models of AMPK [43, 104]. This is likely due to binding to other nucleotide-regulated proteins within the cell like fructose 1,6-bisphosphatase (FBP) or glycogen phosphorylase (GP), which may result in adverse off-target effects, making this overall approach less favourable from a therapeutic perspective.

Recently, a novel compound developed by Betagenon AB (O304) passed phase IIa clinical trials, in which an oral dose reduced fasting glucose levels in diabetic patients and showed improved glucose homeostasis in mice. The compound acts by protection against dephosphorylation of AMPK without allosteric activation, which resembles the effect of ADP rather than AMP [105]. To this date, a binding site for this compound has not been identified, but it is one of the few compounds in active clinical trials for diabetes treatment.

In 2006, a study from Abbott Laboratories described the first direct non-nucleotide AMPK activator (A-769662) and demonstrated its beneficial effects on lipid and glucose metabolism *in vivo* in rodents [50]. Soon afterwards it was shown that the compound activates AMPK allosterically and inhibits dephosphorylation (without promoting phosphorylation) independently of AMP [38]. Crystal structures of another small-molecule activator (compound 991) bound to AMPK revealed the binding site to be the ADaM site [53] (shown in α2β1γ1 in Figure 2). A-769662 and 991 were demonstrated to share the same binding site, and these studies revealed for the first time a unique ligand binding pocket for non-nucleotide small molecule activators that is being explored as a potentially druggable site in AMPK ever since [50, 53]. Other natural compounds or close relatives thereof like salicylate were also shown to bind to the that site [106], sparking thoughts of potential endogenous ligands or metabolites to bind there as well.

Mutating the key β1 phosphorylation site (β1-S108A) dramatically reduced binding of A-769662 as well as 991 [41] and salicylate [106], highlighting the importance of that residue in determining the mode of action of AMPK activators. Though β1 and β2 complexes show a great degree of sequence similarity, the Ser108 site is not involved in binding of 991 in β2 complexes [107]. Instead, studies following the development of another activator (SC4) suggest that β2-Asp111 may be a key binding interaction residue in AMPK β2 complexes [51] underlining differences in subunit isoform regulation and showing potential for isoform-specific complex activation. Furthermore, a recent report suggested that the γ subunit isoform composition may also influence 991 activation of AMPK through the ADaM site [55]. These studies reveal the potential to specifically target key AMPK isoform complexes *in vivo*, which may offer therapeutic advantages by tissue-specific AMPK complex activation and reduction of side-effects.

However, most of the currently identified ADaM-site binding activators show a strong isoform-selective activation and binding towards β1 complexes as shown in Table 1, leaving β2 complex activation underdeveloped. A-769662 and 991 have both been demonstrated to bind weaker to β2-containing complexes and thus display a poorer activation of these complexes [50, 95]. In the case of A-769662 and some others, the weaker affinities mean that activation of β2-complexes in some cells/tissues cannot be achieved due to the inability to attain the required doses in these systems. This effectively renders some activators to be β1-specific and therefore limits their use in *in vivo* settings. Despite higher β1 affinities, other recently developed compounds show sufficiently strong binding to β2 complexes to make them useful for *in vivo* studies [23, 24]. MK-8722 (often referred to as Merck compound) in particular was developed based on 991 to improve the bioavailability of the latter and shows the highest potency of activation of β2 complexes until now and allows oral dosage *in vivo* [24, 108]. Pfizer developed another highly potent compound (PF739), which in very similar studies to the Merck compound showed improved glucose uptake and overall homeostasis in mice and non-human primates acting mainly through skeletal muscle [23].

Table 1 Binding affinities towards β subunit isoform of selected ADaM-site binding AMPK activators.
The preference for β1 complexes is calculated by the ratio of the binding affinity of β2/β1 and expressed as fold difference.

Compound	K_d β1	K_d β2	β1 preference (K_d β2/K_d β1)	Reference
Salicylate	1 mM	10 mM	10x	[106]
A-769662 (Abbott)	0.5 µM	15 µM	30x	[50]
991 (Merck)	0.05 µM	0.5 µM	10x	[41]
PF249 (Pfizer)	0.01 µM	40 µM	4,000x	[109]
PF739 (Pfizer)	0.01 µM	0.1 µM	10x	[23]
SC4	0.005 µM	0.02 µM	4x	[51]
MK-8722 (Merck)	0.001 µM	0.05 µM	50x	[24]

These small molecule AMPK activators provide important tools to examine the importance of direct activation of AMPK in a number of metabolic pathways, including its effects on glucose and lipid metabolism. Some of the potentially beneficial effects of AMPK in these two pathways, which were revealed using non-specific AMPK activators, have been challenged, raising the question of the potential importance of AMPK in treatment of various metabolic disorders [39]. Importantly, two breakthrough papers were published recently which identified specific AMPK activators displaying beneficial effects in all the type 2 diabetic models tested, including non-human primate models [23, 24]. Interestingly, it was suggested that the beneficial effects of these AMPK activators, were mediated by activation of AMPK in skeletal muscle and increasing glucose uptake into this tissue. Not only do these studies offer a definitive beneficial role of AMPK activation in glucose metabolism, but they also suggest that targeting skeletal muscle and the AMPK isoform complexes that are expressed (e.g. β2 and γ3), is an important area to extensively explore further.

1.3.3   AMPK Regulation by Physiological and Pathological Stimuli

Broadly speaking, any cellular stress or change in AMP:ATP (and ADP:ATP) ratio would lead to an AMPK activation due to its ability to sense changing levels in adenine nucleotides. Depletion of ATP levels and simultaneous increase of ADP and AMP levels can have various causes such as hypoxia [110], ischemia [111] or low glucose levels [112] all leading to an activation of AMPK. Naturally, physical exercise on a

macro level or muscle contraction on a micro level lead to increased consumption of ATP and therefore cause AMPK activation [63, 113, 114].

Other than acting as cellular energy sensor exclusively regulating anabolic and catabolic reactions, it becomes more evident that AMPK is also involved in global energy homeostasis by reacting to hormonal and nutritional signals [115]. Leptin (derived from the Greek word for "thin") for example acts as anorexigen, thus inhibiting hunger and limiting food intake signals in the brain [116]. It acts similarly to glucose and insulin by decreasing AMPK activity in the hypothalamus [117], while its antagonist hormone in this environment, ghrelin activates AMPK [118] which leads to increased food uptake. However, hormonal regulation of AMPK is more complex and highly dependent on the tissue of interest, since leptin administration for example increases AMPK activation and expression in skeletal muscle [119].

Other studies also linked hormone receptors and second messengers to AMPK regulation. In the case of ghrelin, the binding to growth hormone secretagogue receptor type 1 (GHSR1) was proposed to activate production of inositol phosphate (IP$_3$) and trigger release of intracellular Ca^{2+}. The release of Ca^{2+} in turn increases AMPK activity through its upstream kinase CaMKKβ [120].

Adiponectin is another key antidiabetic adipokine released by adipocytes and demonstrated to activate AMPK *in vitro* and *in vivo* and leading to improved insulin sensitivity and an increase in glucose uptake as well as fatty acid oxidation [121, 122]. Mechanistically, it was shown to increase Ca^{2+} levels *in vitro* through its receptor (adiponectin receptor 1, AdipoR1), which again links Ca^{2+} signalling to increased AMPK activity mediated by CaMKKβ [123]. Interestingly, adiponectin was also shown to have simulative effects on mitochondrial biogenesis in human myotubes [124] and deletion of AdipoR1 in mouse skeletal muscle lead to impaired proliferator-activated receptor γ coactivator-1α (PGC1α) expression and decreased the number of mitochondria [123].

The example of those three hormones underlines the slightly more complex interplay of AMPK activity on the central nervous system (CNS) and hormone signalling and regulation. It also highlights the need of a differentiated and balanced view on AMPK activation in a tissue-specific context since AMPK activation in the CNS and peripheral tissues (e.g. skeletal muscle) can have opposite effects [117, 125].

1.4 Downstream Targets of AMPK

1.4.1 Regulation of Carbohydrate Metabolism

Since the discovery of AMPK orthologs such as (sucrose non-fermenting 1) SNF1 related kinases and their key role in adapting to glucose limitation and switch to other carbon sources for growth in yeast [30], AMPK was thought to play a major role in carbohydrate metabolism is mammalian systems as well. Indeed, AMPK activation impacts carbohydrate metabolism by increasing glucose uptake and glucose utilisation, while inhibiting gluconeogenesis in relevant tissues [13]. On a whole body-level this alleviates the adverse effects of hyperglycaemia without depending on insulin signalling. It was shown that AMPK activation induced glucose uptake into skeletal muscle was not reduced by wortmannin, which inhibits the insulin mediated phosphatidylinositol 3 kinase (PI3K) signalling cascade [126, 127]. This insulin-independent way of increasing glucose uptake through AMPK gained a lot of interest as therapeutic alternative for treatment of metabolic disorders and started a series of studies involving numerous genetically modified mouse models to determine the role and function of AMPK in this process.

1.4.1.1 Glucose Uptake

Skeletal muscle is of particular physiological importance in whole-body glucose clearance since a majority of over 70 % of post prandial glucose is taken up into it [128, 129]. The discovery of the glucose transporter family and in particular the glucose transporter 4 (GLUT4) in muscle enabled studies of molecular mechanisms allowing facilitated diffusion across the cell membrane [130]. It was established that, despite having independent signalling mechanisms, both insulin [131] and AMPK signalling [132, 133] in the end act by increasing GLUT4 translocation from intracellular storage vesicles to the plasma membrane which permits glucose to enter the cell. Indeed, knocking out GLUT4 largely impairs the glucose uptake both in response to insulin and muscle contraction [134]. The translocation of GLUT4 to the plasma membrane together with the extracellular glucose concentration gradient are considered to be main rate-limiting steps in the glucose uptake process in response to either muscle contraction or insulin [14]. Therefore, the finding that pharmacological AMPK activation can lead to an increased glucose uptake into skeletal muscle independently from insulin opened the door for thoughts of therapeutic AMPK activators to overcome insulin resistance and ameliorate metabolic parameters [127, 135].

It was shown that AICAR induced glucose uptake is abolished in AMPKα2 KO [68] and dominant inhibitory AMPKα2 kinase dead (K45R) [71] mice. AMPKβ2 KO mice [69] and AMPKγ3 KO mice [70] also show a decreased response to AICAR-induced glucose uptake into skeletal muscle, highlighting that probably a

subpopulation of AMPK including the subunits α2, β2 and γ3 is mainly involved in skeletal muscle glucose uptake. Interestingly, this exact α2β2γ3 heterotrimer was found to be the predominantly activated AMPK complex in response to exercise in humans, supporting the role of those isoforms in skeletal muscle AMPK signalling [66]. Further, a deletion of the upstream kinase LKB1 in muscle prevented AICAR treatment from increasing glucose uptake or activating AMPK, indicative of a dependence on LKB1 [136].

On the contrary, the role of AMPK in *ex vivo* contraction-mediated glucose uptake remains controversial. While muscle specific β1/β2 double KO mice show severely reduced glucose uptake in response to exercise and contraction [72], muscle specific α1/α2 KO models do not back this up [137, 138]. Recent studies suggest added complexity in this field as AMPK-deficient mice showed normal glucose update during, but not after *in situ* contraction [139]. Further insights into exercise-mediated glucose uptake into skeletal muscle were provided in a recent study linking reactive oxygen species (ROS) and their production by NADPH oxidase (NOX) to increased GLUT4 translocation and glucose uptake. Impairment of the NOX2 regulatory protein p47phox through a genetic loss-of-function mutation decreased ROS production and exercise-induced glucose uptake into isolated skeletal muscle [140]. Similarly, muscle-specific deficiency of Rac1 as well as chemical inhibition thereof also showed defects in contraction- and exercise-stimulated glucose uptake [141]. Rac1 in its GTP-bound form as well as the prior mentioned p47phox both play a role in NOX2 activation and ROS production [142], which supports the additional regulatory layer those secondary messengers add to contraction- and exercise-mediated glucose uptake. Since exercise/contraction affects numerous cellular processes, it is unlikely that there is a single underlying mechanism.

When looking into cellular glucose uptake in more detail, GLUT4 translocation is the last part of a chain of complex interactions and signalling pathways as shown in Figure 4. Insulin acts through its transmembrane insulin receptor (IR) which triggers a cascade involving phosphorylation of insulin-receptor substrate (IRS) proteins and a subsequent activation of phosphoinositide 3-kinase (PI3K). This in turn increases the formation of PI-3,4,5-triphosphate (PIP3), which activates Akt (also known as protein kinase B) by facilitating the phosphorylation of sites Thr308 and Ser473 [131]. Multiple substrates of Akt are thought to be mediating GLUT4 translocation. The so called Akt substrate of 160 kDa (AS160) (also known as TBC1D4) and the paralogue TBC1D1 were identified as Akt targets. Both are members of the tre-2/BUB2/cdc 1 domain family of Rab GTPase-activating proteins (GAP), involved in the regulation of GLUT4 vesicle formation and trafficking [143]. This signalling pathway was first discovered as insulin responding pathway but was soon linked to AMPK-mediated glucose uptake as well [132, 133]. Several residues of

both AS160 and TBC1D1 get phosphorylated by Akt and AMPK with some sites appearing to be pathway specific [144, 145]. Phosphorylation of both targets decreases their Rab-GAP activity through 14-3-3 protein binding which in turn activates target Rab proteins (Rab-GTP) and ultimately leads to GLUT4 vesicle exocytosis [146]. In this context, both TBC1D1 and TBC1D4 could be described act as removable signalling barriers (or "signalling brakes") for GLUT4 vesicles. Despite sharing similarities in signalling pathways and structural features, TBC1D1 and AS160 show some differences in tissue and species expression, notably in the preference of AS160 expression in mouse soleus muscle compared to EDL muscle [147, 148]. This difference in expression depending on the muscle type could not be seen in rats [149] or humans [59] though.
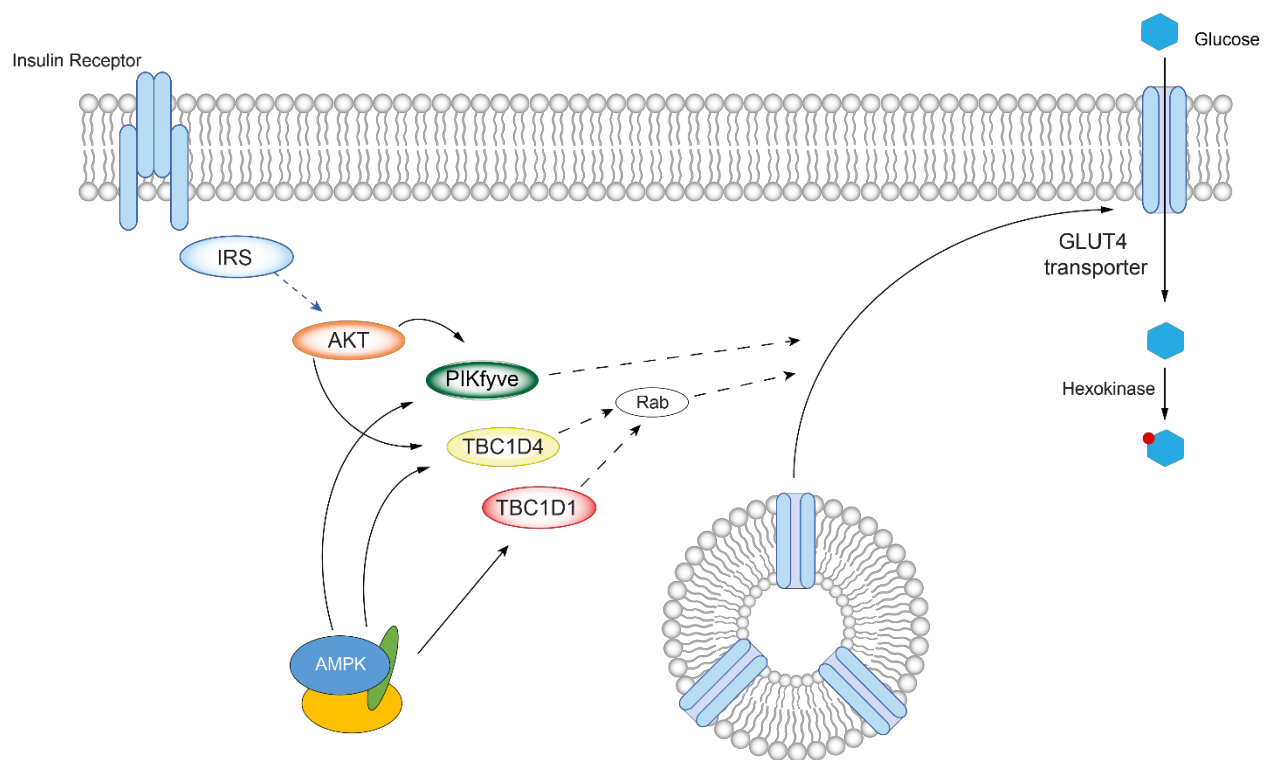
Figure 4 Schematic representation of the signalling pathway underlying insulin- and AMPK-mediated GLUT4 translocation.
Insulin acts through the insulin receptor and its subsequent autophosphorylation initiates a cascade including the insulin receptor substrate (IRS) and ultimately leading to phosphorylation of Akt. Activated AMPK as well as Akt act through downstream targets which include FYVE domain-containing phosphatidylinositol 3-phosphate 5-kinase (PIKfyve) and the two Rab GTPase-activating proteins (GAP) TBC1D1 and TBC1D4. Phosphorylation of the latter two decreases their GAP activity through increased Rab-GTP formation, which in turn facilitates budding and fusion of GLUT4 loaded vesicles to the plasma membrane. In turn, increased GLUT4 translocation promotes glucose transport through the plasma membrane, where it is phosphorylated by hexokinases.

Insulin-induced phosphorylation of AS160 sites Thr642 and Ser588 was shown to be crucial for glucose uptake *in vitro*, indicating the importance of those sites for Akt-regulated GLUT4 translocation [150]. AMPK-regulated GLUT4 translocation however does not seem to rely on the same phosphorylation sites

as shown in a non-phosphorylatable (Thr642Ala in human numbering, corresponding to Thr649 for mouse numbering) KI mouse model. Neither AICAR nor *ex vivo* contraction stimulation showed increased phosphorylation of Thr642 in WT mice or alterations in glucose uptake in the Thr642Ala KI mice [151]. Though, recent studies identified other AMPK-dependent phosphorylation sites such as Ser711 (equivalent to Ser704 in human AS160) [152], the phosphorylation of which was suggested to improve insulin-sensitivity in skeletal muscle [62, 153]. Interestingly, the AICAR-induced insulin-sensitising effect seemed to be accompanied by an activation of the α2β2γ3 complex and dependent on AMPKγ3 [153].

TBC1D1 is the paralogue of the described TBC1D4/AS160, sharing 50% total sequence identity as well as four major domain elements [154]. It was predicted and shown to be an AMPK target with multiple phosphorylation sites, including Ser237 and Ser660 (representing human numbering) [148, 154-156]. TBC1D1 contains only one canonical Akt phosphorylation motif (Thr596-TBC1D1 corresponding to Thr642-AS160), shown to respond to insulin [157] as opposed to five such motifs in AS160 [150]. Early mechanistic studies were performed in adipocytes, but given the higher expression of TBC1D1 in muscle, recent focus shifted towards the latter tissue [148]. The Akt motif site Thr596 was indeed shown to have the strongest effect upon insulin treatment in mouse muscle, while Ser237 remained unaffected [156, 158]. Phosphorylation of TBC1D1 was also investigated in response to AMPK activators, exercise and contraction. *In situ* contraction increased Ser237 and Ser660 phosphorylation without altering Thr596. This was shown to be decreased in an inactive form of α2 (α2i TG), thus indicating distinct insulin and AMPK-related phosphorylation sites [159]. *Ex vivo* contraction data in mouse EDL correlates well with phosphorylation of Ser237, Ser660, but also shows an increased phosphorylation of Thr596 and Ser700, which is markedly reduced in α2 KO muscles [160]. In the same study, exercise effects on human subjects were analysed and revealed similar TBC1D1 phosphorylation patterns, including a correlation of Ser237 and T596 phosphorylation with AMPKα2β2γ3 complex activity [160]. Similar to contraction, AICAR incubation was demonstrated to increase phosphorylation on sites Ser237, Ser660 and Ser700, but not Thr596 [159]. The direct allosteric AMPK activators MK-8722 and PF-739 were shown to phosphorylate at least two sites on TBC1D1 *in vivo* at Ser237 [23] and Ser700 [24]. Sites Ser237 and Ser700 are also direct consensus matches for the AMPK phosphorylation motif (Φ(Xβ)XX[S/T]XXXΦ; Φ (hydrophobic)= Met, Val, Leu, Ile, or Phe, and β (basic) = Arg, Lys, or His) [161], which overall supports the view of at least Ser237 likely to be a major direct AMPK phosphorylation site on TBC1D1. Knock-out models of TBC1D1 were also generated and displayed diminished abilities in contraction- as well as AICAR-induced glucose uptake into EDL muscle [162, 163]. However, a major drawback of the studied model is the reduction of GLUT4 expression in the TBC1D1 deficient animals, which may partly explain the decrease in glucose uptake,

making it a less suitable model to study insulin or AMPK-mediated glucose uptake. Another genetic model investigated the effect of non-phosphorylatable TBC1D1 at site Ser237 (Ser231Ala according to mouse numbering). Interestingly, the KI mice do not show changes in contraction- or exercise-stimulated glucose uptake, while showing partial impairment with AICAR-stimulation [164, 165].

Other converging points for insulin- and AMPK-mediated glucose uptake were suggested with the lipid kinase PIKfyve (FYVE domain-containing phosphatidylinositol 3-phosphate 5-kinase) and the discovery of AMPK-phosphorylation sites [166]. Previously shown to be involved insulin-mediated glucose uptake into adipocytes [167] and skeletal muscle [168], PIKfyve was shown to be phosphorylated by PKB on Ser307 [169]. Later efforts also demonstrated the same site to be phosphorylated by AMPK in C2C12 myotubes as well as in cell-free assays, acknowledging the existence of potential alternative phosphorylation sites on Ser48 [166]. As in the previous muscle-specific KO [168], siRNA knock-down in C2C12 as well as chemical inhibition of PIKfyve *ex vivo* led to decreased glucose uptake in response to insulin and AICAR [166], strengthening its position in the signalling cascade required to promote glucose uptake.

1.4.1.2 Glycogen Metabolism

Carbohydrate metabolism on a whole-body level encompasses also processes happening after glucose has been take up into cells or tissues. An important mechanism of glucose utilisation for storage purposes is glycogen metabolism. After glucose enters the cell, hexokinases act to phosphorylate free glucose to keep it in the cell. After a cascade of reactions, glycogen synthase (GS) is the rate-limiting step in this process, where it elongates the nascent glycogen polymer chain by incorporating glycosyl residues from UDP-glucose and releasing UDP [170]. There are two isoenzymes of GS, encoded by the *GYS1* and *GYS2* genes. GS-2 (encoded by *GYS2*) seems to be liver restricted, while GS-1 (encoded by *GYS1*) is expressed in most cells and tissues including skeletal muscle [170]. Multiple phosphorylation sites were identified on the N- and C-terminus of GS, four of which were found to be particularly important for regulating the enzyme activity. They are oftentimes referred to as sites 2, 2a (N-terminus) and 3a, 3b (C-terminus) although this numbering does not represent the protein sequence [171, 172].

Among other kinases, AMPK was found to phosphorylate and thus inhibit GS directly at site 2 *in vitro* (Ser8 in the mouse sequence) [173]. This discovery was supported by mouse models, showing an α2 dependent inhibitory phosphorylation of GS. AMPKα2 KO mice displayed a lack of pSer8 and thus higher GS activity in response to AICAR, while AMPKα1 KO mice did not [68]. Somewhat paradoxically though, long term exposure to AICAR was found to increase glycogen levels in skeletal muscle *in vivo,* which was thought to be associated with the increased glucose uptake [174]. Indeed, later studies found that increased glucose-

6-phosphate (G6P) as a result of higher glucose uptake can allosterically activate GS and overcome inhibitory phosphorylation (as shown in Figure 5) to restore enzyme activity and increase glycogen synthesis and storage in the muscle [175]. More recently, human studies confirmed the necessity for muscle AMPK for glycogen synthesis after exercise through sustained activation of GS and increased insulin sensitivity. The sustained GS activation was also shown to be dependent on allosteric activation by G6P in mice [176], following the mechanisms indicated above and shown in Figure 5. On the contrary, a genetic deletion of muscle glycogen synthase (*GYS1*) led to markedly lower levels of glycogen and glucose uptake, highlighting the key role of GS for regulating glycogen levels in skeletal muscle [177]. The liver glycogen synthase isoform GS-2 is also phosphorylated and inactivated by AMPK in response to AICAR or A-769662, an effect which is blunted in AMPKα1/2 KO cells [178] and the physiological consequence of which is yet to be identified.
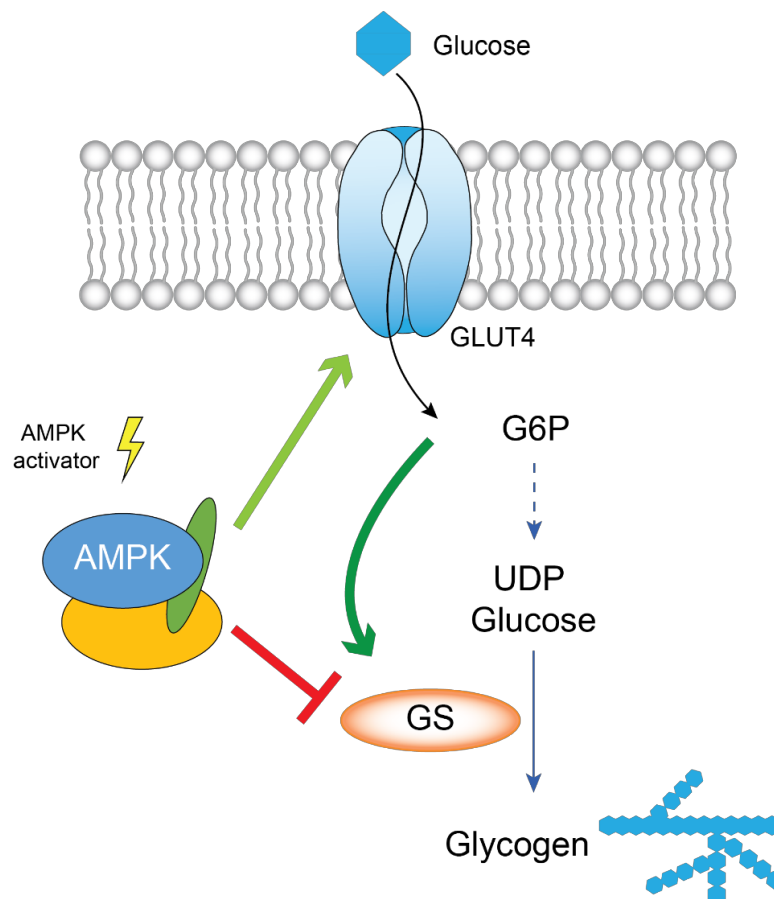
Figure 5 Schematic representation of AMPK-mediated signalling pathway leading to muscle glycogen accumulation.
Activation of AMPK increases GLUT4 translocation to the plasma membrane and in response glucose transport and G6P formation through hexokinases. Concomitantly, AMPK phosphorylates and inactivates glycogen synthase (GS) through phosphorylation at Ser7. Increases of G6P inside the cell allosterically activate GS and thus override the inhibitory effect of AMPK, leading to a net increase of GS activity, glycogen synthesis and storage.

Another enzyme involved in glycogen homeostasis is glycogen phosphorylase (GP), which counteracts GS in breaking down glycogen by liberating glucose-1-phosphate from the glycogen polymer in a process called glycogenolysis. A deficiency or malfunction of GP leads to an accumulation of glycogen in the muscle as seen in McArdle's disease, which is characterised by limited glucose availability through inability of utilisation of glycogen as metabolic fuel [179].

Interestingly, also two naturally occurring point mutations in two γ isoforms of AMPK cause an overaccumulation of glycogen. Mutated γ2 was found to cause increased glycogen levels in human heart, leading to cardiomyopathy and hypertrophy in a disease known as Wolff-Parkinson-White (WPW) syndrome [180]. Quite similarly, a point mutation in γ3 was found to cause excessive glycogen storage in pig (γ3 R225Q mutation) [181], human (γ3 R225W mutation) [182] and mouse (γ3 R225Q mutation) [70] muscle. A genetically modified mouse model aimed to mimic chronic AMPK activation of γ1 complexes (γ1 R70Q mutation) showed increased glycogen accumulation in skeletal muscle [183], supporting the notion that activated AMPK increases glycogen formation despite phosphorylating GS. This further holds up when examining AMPK deficient models, where both β2 KO mice [69] and γ3 KO mice [184] have reduced basal glycogen levels. Those important observations need to be considered for further development of pharmacological activators, as AMPK activation has an impact on glycogen storage and accumulation in physiological settings as well as in pharmacological interventions as seen recently [23, 24]. Further research and risk mitigation are warranted for development of therapeutic applications of AMPK activation in this case.

Taken together, a body of evidence suggests that AMPK has a great amount of influence on the molecular fate of glucose once it enters the cell. One major pathway for glucose utilisation is glycogen synthesis, which can be modulated by primary and secondary effects of AMPK. Further insights into effects of direct glycogen/AMPK interactions and subcellular glycogen localisation as well as potentially AMPK subunit-specific targets would be valuable to understand the molecular details of the regulatory mechanisms of AMPK in glycogen metabolism.

1.4.2   Role of AMPK in Adipose Browning

The traditional understanding defines BAT as a type of fat tissue which, in contrast to energy storing white adipose tissue (WAT), is rich in mitochondria and generates heat through the presence of uncoupling protein 1 (UCP1) [185]. It plays a role in non-shivering thermogenesis [186, 187] and increases energy

expenditure [188], which could be an exciting alternative approach to reverse obesity and its health implications.

Besides regular BAT and WAT, so called beige or "brite" ("brown-like in white") adipocytes exist with a similar morphology as brown adipocytes while also expressing UCP1 protein. Unlike their classical brown adipocyte counterparts (myf5+), reports show beige adipocytes originate from a myf5- progenitor lineage [189]. They were also shown to have thermogenesis pathways depending on calcium and creatine cycling rather than exclusively depending on UCP1 [190]. Additionally, recent reports suggest a more complex array of adipocyte lineages, opening up a field of more functionally distinct types of adipocytes [191]. While non-shivering thermogenesis is primarily regulated through sympathetic nerve activity and release of norepinephrine (Figure 6), which increases lipolysis and mitochondrial biogenesis, chronic cold-exposure was found to activate AMPK in brown adipocytes [81], which may suggest a role in regulation thereof.

Perdikari *et al*. found that also BAT formation may be linked to AMPK both in cells and *in vivo* making use of a kinase screening method based on chemical inhibition as well as shRNA silencing [77]. A genetic deletion of the predominant AMPKα1 isoform in brown progenitor cells [192] showed impaired BAT formation potentially due to decreased α-ketoglutarate and a subsequent decrease in expression of the transcription factor PRDM16 [84], further supporting the role of AMPK in brown adipocyte development. PRDM16 expression and browning of adipocytes was also found to be increased following AMPK activation by the adipokine apelin *in vitro* and *in vivo* [193]. A recent study also linked secretion of apelin as a result of maternal exercise with increased fetal BAT development through increased PRDM16 expression, adding evidence to its involvement brown adipogenesis and a potential link to cytokine signalling [194]. Further, circulation of microRNAs (miRNA) may also have an effect on BAT formation as shown by miRNA-455 and its suppression of hypoxia-inducible factor 1-α inhibitor (HIF1-α1n), which led to increased AMPK activity, UCP1 expression and mitochondrial biogenesis [195]. Similar fates can be achieved by AMPK activation through resveratrol [196], metformin or AICAR [84] in a high-fat diet or obese context, highlighting the therapeutic potential of AMPK activation in brown adipose tissue development.
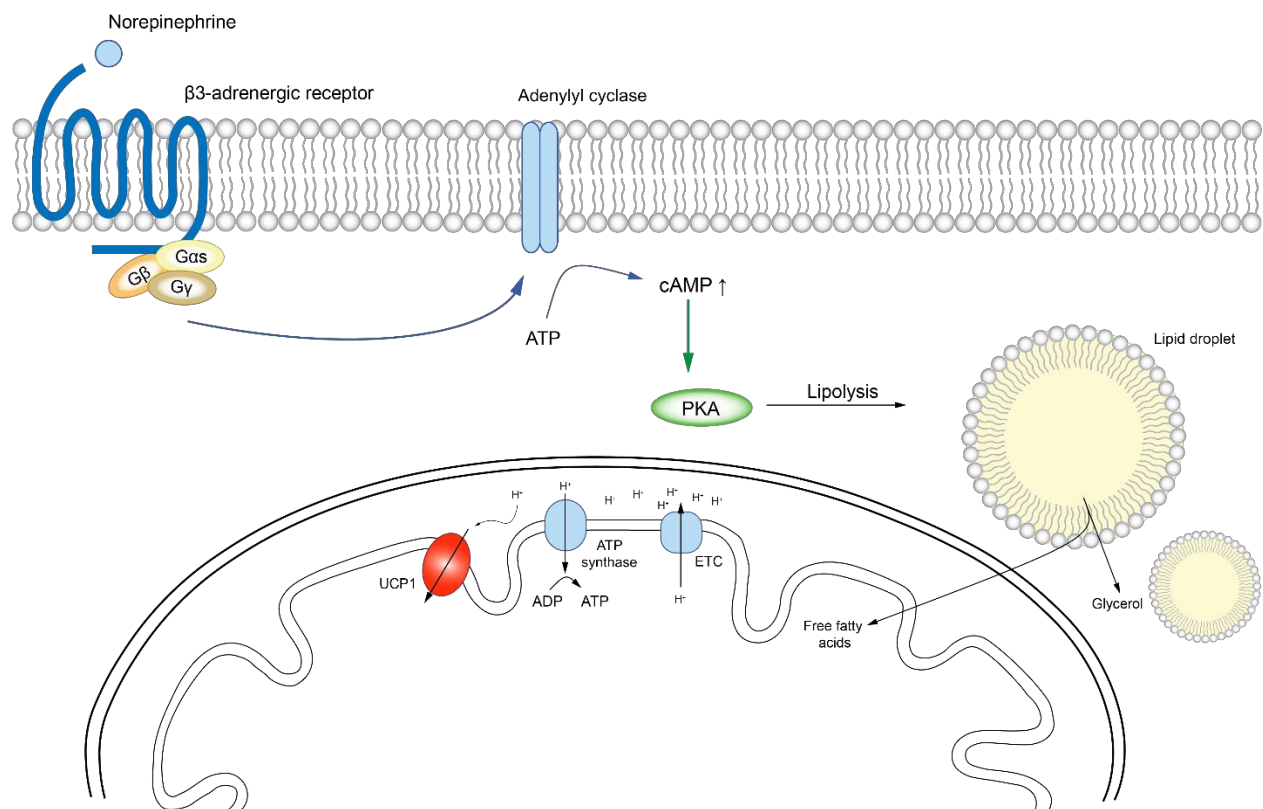
Figure 6 BAT thermogenesis in response to β3-adrenergic activation through UCP1 uncoupling.
External adrenergic stimuli like cold or β3 adrenergic receptor agonists lead to activation of the G-protein coupled receptor. Signal transduction from the receptor happens through guanidine nucleotide exchange and binding of GTP to the Gα subunit (here Gαs indicating the activation of cAMP-dependent pathways). GTP-bound Gαs acts as a second messenger to activate adenylyl cyclase, which leads to an increase in cyclic AMP (cAMP) levels. cAMP then activates protein kinase A (PKA), which acts to phosphorylate various targets among which are lipases which are stimulated and increase lipolysis and therefore the release of free fatty acids used to fuel β oxidation and possibly to participate in UCP1 activation. Inside the mitochondria, the electron transport chain (ETC) acts to create a proton gradient, which ATP synthase uses to synthesise ATP. UCP1 acts to distort this coupled mechanism by proton transmission and heat generation.

The development of adipocyte-specific AMPK KO models allowed for further insight into the role of AMPK in brown adipose tissue function. Adipocyte-specific α1/α2 [79] and β1/β2 [80] KO mice both show impaired cold tolerance β-adrenergic stimulation, further supporting this line of thought. The failure of adequate BAT thermogenesis was associated with defects in maintenance of mitochondrial health as seen by decreased ULK1 phosphorylation and impaired mitophagy overall with an accumulation of damaged mitochondria [80]. These studies suggest the importance of AMPK in maintaining mitochondrial function and health in BAT, which are essential for its thermogenesis function. Other genetic models made use of a gain-of-function mutation in AMPK γ1 (D316A) to mimic chronic AMPK activation genetically rather than usage of pharmacological activators. This model was first used in a liver-specific mutant, which showed decreased hepatic glucose output and protection from liver steatosis on high fructose diet, but had no

effect on mice fed with chow or high fat diet [197]. The same AMPK mutation was then used to generate a whole-body D316A-transgenic model and investigate effects on other tissues including BAT.

On a high-fat diet, D316A mice were less prone to weight gain due to increased energy expenditure and body surface temperature without changes in food intake, resulting in lower fat mass overall and decreased lipid accumulation in liver [198]. Interestingly, a closer look at BAT revealed that β-adrenergic stimulation increases oxygen consumption and *Ucp1* mRNA expression similarly in both D316A mice and their control group, arguing for a dispensable effect of AMPK activation on BAT function *in vivo*. At the same time, thermoneutral conditions preserved the protective effect of D316A against diet-induced weight gain through increased oxygen consumption, indicating that AMPK activation plays a role in protection from obesity, but likely independently of BAT. The protection effect was rather found to be caused by changes in WAT morphology including decrease of lipid droplet size, increased oxygen consumption and mitochondrial markers without the increase of *Ucp1* mRNA or presence of UCP1 protein respectively [198]. Such a UCP1-independent contribution of WAT to energy expenditure was described in other studies [199, 200] in response to cold- or β-adrenergic stimulus, but not in response to chronic AMPK activation. Finally, a transcriptome analysis shed light onto the mechanisms underlying this observation which include the increase of genes typically expressed in skeletal muscle [198] as well as previously identified genes involved in UCP1-independent thermogenesis like *Ckmt2* [199] or proteins like sarco/endoplasmic reticulum Ca^{2+}-ATPase (SERCA) [201]. Taken together, those results suggest a metabolic and phenotypical shift of a WAT subpopulation towards characteristics more similar to skeletal muscle tissue in response to HFD and chronic AMPK activation. This led to the proposal of the term skeletal muscle-like AMPK reprogrammed thermogenic (SMART) adipocytes for this particular subpopulation [198].

In summary, a major role of AMPK in regulating BAT development and maintenance of its function through improved mitochondrial health gained substantial traction in the last years. Especially chronic AMPK activation studies in high-fat diet environment raised hope in therapeutic potential of adipocytes despite being possibly independent of BAT and UCP1. Questions about detailed mechanisms of AMPK activation and increased adipocyte energy expenditure as well as further characterisation of adipocyte subpopulations remain to be answered though. Further insights into the involvement of specific AMPK subunit isoforms or other enzymes involved in UCP1-independent thermogenesis could be relevant for pharmaceutical targeting of adipocytes to improve metabolic effects.

1.5 Investigations of Functions of the AMPKγ Subunit

As previously mentioned, AMPK shows a ubiquitous expression pattern in the body. While this is true for complexes containing the γ1 subunit across species, the other γ subunit isoforms show a more restrictive expression pattern with γ2 showing higher expression levels in the heart, although different splice variants need to be considered [202, 203] and γ3 almost exclusively found in fast-twitch type IIb glycolytic skeletal muscle [204, 205]. Most of the knowledge of AMPK regulation is based on γ1 complexes since those are the only ones to date that have been crystallised. However, both naturally occurring as well as genetically created mutations *in vivo* and *in vitro* have helped to gain better understanding of the characteristics of the other isoforms.

Perhaps the most known pathological γ subunit mutation is the γ2 mutation R302Q, which is found to cause Wolff-Parkinson White (WPW) syndrome in humans [206]. Among other mutations in this disease, the R302Q mutant renders AMPK constitutively active leading to the accumulation of large glycogen-containing vacuoles within myocytes and a phenotype resembling that of a glycogen storage disease [207]. Mutation of Arg531 (R531G) in γ2 led to cardiac hypertrophy, contractile abnormalities and highly increased glycogen levels in the heart, while AMPK activity was markedly decreased [208], showing that the influence of AMPK activity on WPW phenotypes is not necessarily of a direct nature. Since all of the reported mutations lie within CBS domains, an impairment of nucleotide responses seems likely though [14]. The role of AMPK γ2 on heart is further supported in a study by Yavari *et al*., where they show that AMPK activation (through generation of a R299Q mutant, equivalent to the R302Q in human numbering) in sinoatrial cells lowers intrinsic heart rate and maintains energy demand in the heart. A genetic loss of γ2, representing the genotypical polar opposite of the R299Q, also reflects phenotypical changes with an increase in heart rate and the inability of adaptation thereof in response to endurance exercise [209]. Interestingly, a mutation in the CBS1 of γ3 which naturally occurs in pigs (R200Q) [181] corresponds to the same CBS domain in γ2. The mutation was later found to exist also in humans as R225W mutation [182]. The pig mutation, once known as rendement napole (RN⁻) mutation was shown to have increased muscle glycogen content which was initially thought to increase meat quality [210]. An equivalent mouse mutant model was generated and showed similar increases in muscle glycogen content as well as increased AMPK γ3 activity concomitant with increased fatty acid oxidation and protection from insulin resistance in skeletal muscle on high fat diet [70], without change in muscle fibre type composition [211]. Transcriptional studies support these observations, with signalling pathways related to glycogen synthesis, glucose uptake and fatty acid oxidation being upregulated in the R225Q mouse model [212].

The same study compared the presumed "opposite" γ3 KO (Prkag3$^{-/-}$) genotype of the activating mutant and confirmed an opposite transcriptomic signature of the γ3 KO model [212].

Equivalent models of CBS-domain mutants were also generated in γ1 with the R70Q mutant *in vitro*, resulting in greatly increased AMPK activity [213] and increased glycogen accumulation in transgenic mice [183]. Other models with mutations in CBS 2 (H151R) generated by crossing of cre-inducible γ1 transgenic H151R with mice expressing cre in myosin light chain in skeletal muscle. This point mutation led to increased muscle, but not cardiac glycogen levels by more than 10-fold, while also improving insulin sensitivity and glucose oxidation [214]. As described above, the more recent, chronically active γ1 D316A transgenic model was found to increase energy expenditure likely through increased WAT thermogenesis [198] while a liver-specific D316A model exhibited protective effects against lipid accumulation through decreased lipogenesis [197].

The findings of activating AMPK and mutations in skeletal muscle complexes warrant further research of AMPK activation pharmacologically with direct activators, making use of advanced knowledge of regulation and novel compounds. Notably, two seminal papers of pan-AMPK activators mirrored beneficial effects on whole-body energy homeostasis largely through effects on skeletal muscle [23, 24]. Although muscle-specific KO models (mDKO) confirmed the requirement of AMPK for those compounds, the role of AMPK γ3 was not evaluated. Previous studies by Barnes *et al.* took advantage of the mentioned γ3 KO model to assess effects of exercise and the AMP-analogue AICAR on muscle glucose uptake *ex vivo* [70]. Importantly, AICAR-induced glucose uptake into EDL was impaired in γ3 KO muscles, while insulin- and contraction mediated glucose uptake remained unchanged. Additionally, glycogen re-synthesis after exercise [70] and basal glycogen levels [184] appeared reduced in γ3$^{-/-}$ EDL muscle. A more recent study found AMPK γ3 to be required for *ex vivo* EDL glucose uptake, AMPK and ACC phosphorylation in response to SPARC (secreted protein acidic and rich in cysteine), a small protein that acts as a myokine in response to exercise [215]. Indeed, a SPARC KO genotype showed reduced abilities of glucose clearance in response to exercise or insulin but could be rescued by supplementation of recombinant SPARC protein. Interestingly, SPARC seems to increase and depends on intracellular Calcium levels for its function, further linking second messengers to AMPK signalling in glucose homeostasis [215].

Despite the availability of new direct AMPK activators as described above, the effect of this new class of activators on AMPK γ3 KO models has not yet been investigated. Non-specific effects of the early activator AICAR have been described in a plethora of literature before, based on the lack of specificity of ZMP/protein interactions [216]. This limits the study of a potential role of AMPK or specific subunit

isoforms and new drugs should help to shed light on AMPK activation and involvement of downstream targets. *In vitro* studies already made use of the ADaM-site binding compound 991 to determine whether the γ subunit isoform plays a role in AMPK activation. AMPK γ2 complexes were found to be activated to a greater extent than their respective γ1 and γ3 counterparts. For β2 complexes, this did not seem to depend on phosphorylation of Ser108, but on the N-terminal region of the γ subunit [107]. This indicates that AMPK complexes may be activated and regulated differently depending on the γ subunit isoform they carry. Further studies of the roles and functions of different AMPK heterotrimers and their downstream effectors are needed to understand the physiological implications of targeted activation of AMPK complexes. Heterotrimer- or isoform-specific activators would greatly improve the possibilities of those studies. Targeting skeletal muscle seems particularly intriguing given its contribution to whole body-glucose metabolism. Within that tissue, the AMPK γ3 isoform stands out due to its unique expression pattern and clearly more understanding of molecular mechanisms underlying muscle glucose metabolism is needed to identify potential γ3-specific targets. The lack of isoform-specific activators and crystal structures of γ3-containing complexes remains a major caveat for that exploration path, but advances in drug development activating β2 complexes [51] or insights from cytokine effects on skeletal muscle glucose uptake may open new doors for research.

2 Aim of the Thesis

AMPK plays a central role in carbohydrate metabolism with glucose uptake being a majorly influenced signalling pathway. It was therefore proposed as drug target for novel and insulin-independent therapies of metabolic disorders and managing glucose homeostasis in the context of type 2 diabetes. Skeletal muscle is of particular interest due to its important role in blood glucose clearance after food intake.

Interestingly, AMPK subunit/isoform expression patterns vary across tissues in most species and a subgroup of AMPK heterotrimers seems to be muscle selective. These complexes share the AMPKγ3 isoform, the regulation and structure of which is not very well understood. Most regulatory and all crystallography studies were performed on γ1 complexes and may therefore not capture unique aspects of other γ isoforms. The development of more potent and specific AMPK activators over time may help to uncover previously missed aspects *in vitro* and *in vivo*.

In this thesis, we aim to investigate the role that the AMPKγ3 subunit and its complexes play on a physiological scale as well as molecular mechanisms that may regulate this isoform on a protein level. For this, we used an AMPKγ3 deficient ($\gamma3^{-/-}$) mouse model to characterise the phenotype by analysing various physiological and metabolic parameters on a whole body-level. We used isolated glycolytic (EDL) and oxidative (SOL) skeletal muscles to perform drug-stimulated *ex vivo* glucose uptake and underlying biochemical analysis of the AMPK signalling pattern. This should give insights into the necessity of AMPKγ3 for glucose uptake into skeletal muscle in response to direct allosteric AMPK activators. Previous studies of such a model only investigated glucose uptake mediated by non-selective AMPK activators such as AICAR (an AMP mimetic), which is known to have profound off-target effects. Further, we studied underlying signalling patterns to identify potential AMPKγ3-specific targets, which would help to better understand the interplay of muscle AMPK and increased glucose uptake.

Additionally, we investigated the role of AMPKγ3 on glucose utilisation by looking into glycogen synthesis and potential targets of AMPK in this pathway.

To have an exhaustive picture of potential physiological roles of AMPKγ3 we also looked into the expression and function in brown adipose tissue (BAT). This could offer another route for therapy of metabolic disorders and help to improve understanding of AMPK regulation of BAT formation and involvement of distinct subpopulations of AMPK which may be targeted pharmacologically.

3 Materials & Methods

Materials

5-aminoimidazole-4-carboxamide riboside (AICAR) was purchased from Apollo Scientific (OR1170T; Bredbury, United Kingdom). 991 (5-[[6-chloro-5-(1-methylindol-5-yl)-1H-benzimidazol-2-yl]oxy]-2-methyl-benzoic acid) (CAS#: 129739-36-2) was synthesised by Spirochem (Basel, Switzerland) as previously described [217]. MK-8722 ((3R,3aR,6R,6aR)-6-((5-([1,1'-Biphenyl]-4-yl)-6-chloro-1H-imidazo[4,5-b]pyridin-2-yl)oxy)hexahydrofuro[3,2-b]furan-3-ol) (CAS: 1394371-71-1) was purchased from Glixx Laboratories Inc (GLXC-11445; Hopkinton, MA, USA) Protein G Sepharose and P81 paper were purchased from GE Healthcare (Chicago, IL, USA). [γ-^{32}P]-ATP was purchased from PerkinElmer (Waltham, MA, USA). The substrate peptide AMARA (AMARAASAAALARRR) was synthesised by GL Biochem (Shanghai, China). All other reagents were from MilliporeSigma (Burlington, MA, USA) if not otherwise stated.

Antibodies

The following antibodies were obtained from Cell Signaling (Danvers, MA, USA): AMPKα1/α2 (#2532), AMPKβ1/β2 (#4150) TBC1D1 (#6929), Akt (#4691), phospho-Akt (Ser473, #4060), GAPDH (#2118), Vinculin (#13901), Hexokinase II (#2867). AMPKα1 (#07-350) and AMPKα2 (#07-363), pospho-TBC1D1 (Ser237, #07-2268) were purchased from MilliporeSigma. UCP1 (#UCP11-A) antibody was purchased from Alpha Diagnostic International (San Antonio, TX, USA) and β-tubulin (#32-2600) from Invitrogen (Waltham, MA, USA). For immunoprecipitation experiments, AMPKα1 and AMPKα2 were used as previously described [218] and AMPKβ1 (#26907-1-AP), AMPKβ2 (#14429-1-AP) as well as UGP2 (10391-1-AP) were used from Proteintech (Manchester, United Kingdom). GLUT4 (ab654) and Total OXPHOS Rodent WB Antibody Cocktail (ab110413) antibodies were purchased from abcam (Cambridge, United Kingdom). AMPKγ3 and AMPKγ1 polyclonal antibodies were generated by YenZym Antibodies (San Francisco, CA, USA) as previously described [73]. Rabbits were immunised with the indicated peptides: a combination of human and mouse AMPKγ3 peptide, human AMPKγ3 [residues S45–S65: *CSSERIRGKRRAKALRWTRQKS], mouse AMPKγ3 [residues S44–S64: *CSSERTCAIRGVKASRWTRQEA]; and AMPKγ1 peptide (residues E7–S26 of mouse AMPKγ1: *CESSPALENEHFQETPESNNS). A terminal cysteine (*C) was added to the peptide sequence to allow peptide conjugation to carrier proteins. The produced antibodies were affinity purified using respective antigen-specific peptide columns by YenZym Antibodies. Horseradish peroxidase (HRP)-

conjugated secondary antibodies were purchased from Jackson ImmunoResearch (West Grove, PA, USA). LiCOR secondary antibodies were purchased from ThermoFisher (#A10038 & #A21109; Carlsbad, CA, USA). Primary (Supplementary Table 1) and secondary antibodies (Supplementary Table 2) are listed in the appendix.

Animal studies

Animal experiments were approved by the internal and local ethics committee and conducted in accordance with the European Convention for the Protection of Vertebrate Animals used for Experimental and Other Scientific Purposes. Protocols used were approved by the Service Vétérinaire Cantonal (Lausanne, Switzerland) under licenses VD3332 and VD3465, in accordance with McMaster Animal Care Committee guidelines (AUP #: 16-12-41, Hamilton, ON) and the Ethics Committees at Nanjing University with involved personnel having personal licences from the regional authority. In compliance with ethical rules and regulatory requirements on use and welfare of laboratory animals, this protocol and all procedures have been reviewed and approved by an ethical committee (Com'Eth, CE17) registered at the French Ministry of Research under the reference 10261.

The generation of AMPKγ3$^{-/-}$ mice was performed by Taconic (Denmark) (Appendix Figure 1A). The animals were kept and maintained according to local regulations and had free access to a standard chow diet or high fat/ high carbohydrate diet (HFHCD) (RD 12492, Research Diet).

Animal phenotyping

Body weight and scoring

Body weight was evaluated once a week on all the mice. Monitoring of hair/coat, eye and nose, breath, activity, posture, and behaviour were recorded on a score sheet following the recommendations of the customer.

qNMR analysis

This procedure is used to give precise analysis of the body composition for fat content, lean tissues and free body fluid. The method uses the Minispec+ analyser (Bruker) by Nuclear Magnetic Resonance (NMR). The test is conducted on conscious fed mice.

TSE cages: energy expenditure, activity, food and water intake

The energy expenditure is evaluated through indirect calorimetry by measuring oxygen consumption with an open flow respirometry system (TSE system, Labmaster, Germany). Very precise CO_2 and O_2 sensors measure the difference in CO_2 and O_2 concentrations in air volumes flowing through control or animal cages. The amount of oxygen consumed over a given period of time can thus be calculated, as far as the air flow through the cage is known. Data from gas exchange are expressed as ml/h/mouse. The system also monitors CO_2 production, thus the respiratory exchange ratio (RER = VCO_2/VO_2; which define fuel preference between glucose vs. lipid metabolism) and finally, heat production (Kcal/h/mouse) can be calculated. An activity and food intake monitoring system is integrated to the set up for the measurement of activity and feeding/drinking behaviour which are involved in the whole energy expenditure.

Following a 3h acclimatisation period, the experiment was performed over 21h, overlapping both with light period of day 1 and day 2 (from 2pm day 1 to 11pm day 2) under a 12h light:12h dark photoperiod (19:00-07:00), at ambient temperature (21°C ± 2).

Oral glucose tolerance test (oGTT)

The glucose tolerance test is used to value the regulation of the glycemia after an induced hyperglycaemia by injection of a standardized glucose bolus (2g/kg). The glucose solution is administered by oral gavage. Blood glucose is measured at different time points over 120 minutes after the injection on a drop of blood collected at the tail using blood glucose monitor and glucose test strips (Roche Diagnostics, Accu-Chek). The test was conducted during the light period, after overnight fasting (16 h).

Blood chemistry

Blood was collected by retro orbital puncture under isoflurane anaesthesia at noon on mice fasted for 4 h. Blood chemistry was performed on an OLYMPUS AU-400 automated laboratory workstation (Beckmann Coulter) with kits and controls supplied by Beckmann Coulter. Free fatty acid was measured on the AU400 using a kit from Wako (Wako Chemical Inc, Richmond, USA). Glycerol was measured using a kit from Randox (Randox Laboratories, UK). Adiponectin levels were measured by ELISA using the Quantikine Adiponectin/Acrp30 immunoassay kit (Ref MRP300 R&D system). Insulin and leptin levels were measured on a BioPlex analyser (BioRad) using the Mouse Metabolic Magnetic bead panel kit (Reference: *MMHMAG-44K* – Milliplex map by Millipore).

Tissue Preparation and Lysis

Tissues were dissected and immediately frozen in liquid nitrogen. Tissues were homogenised in ice-cold lysis buffer (270 mM sucrose, 50 mM Tris·HCl (pH 7.5), 1 mM EDTA, 1 mM EGTA, 1% (w/v) Triton X-100,

20 mM glycerol-2-phosphate, 50 mM NaF, 5 mM $Na_4P_2O_7$, 1 mM DTT, 0.1 mM PMSF, 1 mM benzamidine, 1 µg/ml microcystin-LR, 2 µg/ml leupeptin, and 2 µg/ml pepstatin A) using a tissue lyser (Tissue Lyser II; Qiagen). Lysates were centrifuged at 15,000 rpm for 15 min and the supernatant was snapfrozen in liquid nitrogen for storage.

Quantitative Real Time PCR for Gene Expression

Total RNA was extracted from whole muscles using RNAdvance Tissue Kit (A32645; Beckman Coulter) and quantified by RiboGreen (R11490; Thermo Fisher Scientific). RNA integrity was verified by capillary electrophoresis on a Fragment Analyzer, (DNF-471; Agilent Technologies) and an RNA Quality Number >8 was observed.

To quantify the AMPK subunit isoforms mRNA in mouse muscle, reverse transcription and real time PCR were performed. 500 ng of total muscle RNA was taken as starting material for the reverse transcription using the PrimeScript RT Kit (Takara, #RR037A). RT-qPCR was performed on a LightCycler 480 using the SYBR Green Assay (Roche, #04707516001), with all primers at a final concentration of 0.3 µM per reaction.

All the primers and sequences are listed in the table below. Relative mRNA quantities were calculated for triplicate muscle samples from 4-5 animals and normalised for the three genes *Hprt1* (hypoxanthine ribosyltransferase, HPRT), *GusB* (beta-glucuronidase) and *Pgk1* (Phosphoglycerate Kinase 1). Their stability was validated using GeNorm (M value < 0.6)[219]. Normalised values were calculated by dividing the average expression value by a factor equal to the geometric mean of the normalisation genes [220].

Table 2 Primer sequences used for rt-qPCR of AMPK subunits.

Primer	Forward	Reverse
Prkaa1	5'-AGA GGG CCG CAA TAA AAG AT-3'	5'-CTT TCA AGG CTT CGT CAT CG-3'
Prkaa2	5'-TGA AGC GAG CGA CTA TCA AA-3'	5'-CTT CAC AGC CTC ATC GTC AA-3'
Prkab1	5'-TGC TGC AGG TCA TCT TGA AC-3'	5'-TTG TAC CGG TGT GTT GCA CT-3'
Prkab2	5'-CTT CCT GAG CCC AAT CAT GT-3'	5'-CAG CAG CGT GGT GAC ATA CT-3'
Prkag1	5'-CTC CGC CTT ACC TGT AGT GG-3'	5'-AAG TAG TGG GAC CGA TGC TG-3'
Prkag3	5'-GGA AAC AGC TCC TGT CCT GA-3'	5'-CAT CAA AGC GGG AGT AGA GG-3'
Hprt	5'-CAG TCC CAG CGT CGT GAT TA-3'	5'-TGG CCT CCC ATC TCC TTC AT-3'
GusB	5'-AAC AAC ACA CTG ACC CCT CA-3'	5'-ACC ACA GAT CGA TGC AGT CC-3'
Pgk1	5'-GGG TGG ATG CTC TCA GCA AT-3'	5'-GTT CCT GGT GCC ACA TCT CA-3'

BAT rt-qPCR was performed separately as previously described [80]. Briefly, adipose tissues were lysed in TRIzol reagent (Invitrogen) to remove lipid and the aqueous phase was applied to an RNeasy kit (QIAGEN) column for subsequent purification. Relative gene expression was calculated using the comparative Ct (2-ΔCt) method, where values were normalized to a housekeeping gene (*Ppia*). All Taqman primers were purchased from Invitrogen: *Ppia* (Mm02342430_g1), *Cox2* (Mm03294838_g1), *Cox8b* (Mm00432648_m1), *Cidea* (Mm00432554_m1), *Ucp1* (Mm01244861_m1), *Dio2* (Mm00515664_m1), *Pdk4* (Mm01166879_m1), *Ppargc1a* (Mm01208835_m1), *Pparγ* (Mm00440940_m1), *Prdm16* (Mm00712556_m1).

Quantitative Real Time PCR for Mitochondrial DNA Copy Number measures

Total DNA isolation was performed using the DNAdvance Kit (A48705, Beckmann Coulter). To quantify the amount of mtDNA present per nuclear genome by qPCR, mtDNA (16S) and mtDNA(ND4) primers and probes were used, the sequences of which are shown below. To quantify nuclear DNA, primer and probe sets that detect the PMP22 and Titin genes also shown below were used. The relative mt copy number was determined based on the relative abundance of nuclear and mtDNA, calculated as average of the two targets respectively. The relative mt copy number was determined based on the relative abundance of nuclear and mtDNA, calculated as average of the two targets respectively. The relative abundance is then expressed by ΔCT or CT(nDNA) - CT(mtDNA). Results are displayed as fold change of copy number of mtDNA per nuclear genome compared to the WT muscle.

Table 3 Primer sequences used for mtDNA quantification.

Primer	Forward	Reverse
mtDNA-16S	5'-CGT CTA TGT GGC AAA ATA GTG AGA A-3'	5'-CCA GCT ATC ACC AAG CTC GTT-3'
mtDNA-16S-Probe	5'-(fuorescein)TAG AGG TGA AAA GCC- (MGB-Q500)- 3'	
mtDNA-ND4	5'-CAC ATG GCC TCA CAT CAT CAC-3'	5'-GTG GAT CCG TTC GTA GTT GGA-3'
mtDNA-ND4-Probe	5'-(fuorescein)CCT ATT CTG CCT AGC AAA- (MGB-Q500)- 3'	
PMP22	5'-TTC GTC AGT CCC ACA GTT TTC TC-3'	5'-ACT CGC TAG TCC CAA GGG TCT A-3'
PMP22-Probe	5'-(fuorescein)CGG TCG GAG CAT CAG GAC GAG C- (MGB-Q500)- 3'	
Titin	5'AAA ACG AGC AGT GAC GTG AGC-3'	5'-TTC AGT CAT GCT GCT AGC GC-3'
Titin-Probe	5'-(fuorescein)TGC ACG GAA GCG TCT CGT CTC AGT C- (MGB-Q500)- 3'	

Immunoprecipitation and AMPK Activity Assay

200 µg of muscle lysate or 1,000 µg of BAT lysate were incubated on a rotating platform at 4°C overnight with a mix of 5 µL protein G-sepharose and the indicated antibodies. The beads were pelleted at 500 g for 1 min and initially washed twice with 0.5 mL lysis buffer containing 150 mM NaCl and 1 mM DTT and subsequently washed twice with the same amount of buffer A [50 mM HEPES (pH 7.4), 150 mM NaCL, 1 mM EGTA and 1 mM DTT]. The AMPK complexes were either eluted with Laemmli buffer for immunoblot analysis or taken directly for AMPK activity measurement. The AMPK activity assay was performed by incubating the beads for 30 min at 30°C on a heated shaker (Thermomixer R, Eppendorf) in buffer A with additional 10 mM Mg2+ and 100 µM ATP in presence of 200 µM AMARA peptide (AMARAASAAALARRR) and 1 µCi of [γ-32P] ATP. Reactions were stopped by spotting the reaction mix onto P81 filter paper and washing in 75 mM phosphoric acid. The P81 papers were dried after three washes and the 32P incorporation into the substrate peptide measured by Cherenkov counting (5 min) using a scintillation counter (Tri-Carb 2810TR, PerkinElmer).

Western Blotting

Protein concentrations were determined by Bradford assay (23200, ThermoFisher) before denaturation in Laemmli buffer at 95°C for 5 min. 20 µg of protein was separated by SDS-PAGE on 4-12% gradient gels (NW04127, ThermoFisher) and transferred onto nitrocellulose membranes (#926-31090, LiCOR). Membranes were blocked for 1 h at ambient temperature in LiCOR blocking buffer (#927-60001, LiCOR). Membranes were subsequently incubated in TBST containing 5% (w/v) BSA and the primary antibody overnight at 4 °C. After rigorous washing, the membranes were incubated for 1h in either HRP-conjugated or LiCOR secondary antibodies diluted 1:10,000. Signal imaging was performed either using enhanced chemiluminescence (ECL) reagent (GE Healthcare) or a LiCOR Odyssey CLx imaging system. Densitometry for ECL blots was performed using Image J Software (NIH).

Capillary Western Blot Analysis

Due to sample limitation, incubated mouse muscles were blotted using an automated capillary Western Blot system (Sally Sue) from ProteinSimple (San Jose, CA, USA) (http://www.proteinsimple.com/sally_sue.html). Experiments were performed according to the manufacturer's protocol using the indicated standard reagents for the Sally Sue system (SM-S001, ProteinSimple). Briefly, all samples were first diluted to 2 mg/mL in lysis buffer and then further diluted

to 0.5 mg/mL in 0.1% SDS. Following the manufacturer's instructions for sample preparation, this resulted in an assay protein concentration of 0.4 mg/mL.

Ex vivo Glucose Uptake

Animals were sacrificed by cervical dislocation, and extensor digitorum longus (EDL) or soleus (SOL) muscles were rapidly dissected and mounted on an incubation apparatus. The respective muscles were incubated as previously described [98] in the presence of the indicated drug or vehicle for 60 min or their contraction evoked via electrical stimulation for 15 min. 2-Deoxy-[^{3}H] glucose uptake was measured during the last 10 min of the incubation or contraction period of each experiment, as described previously [98].

Ex Vivo Glycogen Synthesis

Ex vivo glycogen synthesis was measured as previously described [221]. Briefly, EDL muscles were harvested and incubated in KRB buffer containing 5.5 mM *D*-glucose and 0.5 µCi/ml of [^{14}C]-glucose for 40 min at 37°C in the presence or absence of the indicated AMPK activator. Snap-frozen muscles were were digested in 30% KOH at 95°C for 20 min. Glycogen solution (50 µl of a 5% glycogen solution) was added to each sample, and 100% ethanol was added to a final concentration of 70%, and then glycogen was allowed to precipitated at −20°C overnight and centrifuged to pellet glycogen. The glycogen pellets were washed four times with 66% ethanol and dissolved in 50 µl of deionized water. Samples were spotted on filter paper (Whatman 3MM) and washed three times with 66% ethanol. The dried papers were subjected to scintillation counting to determine [^{14}C]-glycogen.

AICAR and MK-8722 Tolerance Test

AICAR tolerance was performed as previously described by Goodyear *et al.* [222]. In brief, water or AICAR was injected intraperitoneally at a dose of 250 mg/kg body weight and blood from the tail was used to measure blood glucose levels before (t=0) and after injection of AICAR using a Contour XT glucometer (Bayer, Leverkusen) and single use glucose sensors (Ascensia, Basel). MK-8722 tolerance was tested by oral administration of either vehicle (0.25% (w/v) methylcellulose, 5% (v/v) Polysorbate 80, and 0.02% (w/v) sodium lauryl sulfate in deionised water) or 10 mg/kg body weight MK-8722. Blood glucose measurement was measured as described for AICAR above.

Citrate Synthase Activity Assay

Citrate synthase activity was measured in EDL, SOL and gastrocnemius (GAS) muscle lysates. After lysis, protein concentration was determined by Bradford assay and samples equally diluted to 2 mg/mL. 10 µg of protein was assayed in duplicates using a citrate synthase assay kit (CS0720, MilliporeSigma) using the manufacturer's protocol and recombinant citrate synthase as positive control. Briefly, the formation of 2-nitro-5-thiobenzoic acid was measured at a wavelength of 412 nm over time using a spectrophotometer (Spectramax, Molecular Devices). The baseline absorbance of the reaction mix was measured and the reaction initiated by the addition of oxaloacetic acid. The change of absorbance was recorded every 10 seconds for 1.5 minutes.

Infrared Thermography

UCP1-mediated thermogenesis was assessed in 14-week-old male WT and Prkag3 KO mice as previously described [223]. Briefly, mice were anaesthetised with an intraperitoneal injection of 0.5 mg/g bw Avertin (2,2,2-Tribromoethanol dissolved in 2-methyl-2-butanol; Sigma Aldrich) then, 2 minutes later, injected with either saline or the highly selective β3-adrenergic receptor agonist CL 316,243 (Tocris, Bristol, United Kingdom). Mice were subsequently placed dorsal side up onto an enclosed stationary treadmill to measure oxygen consumption (VO_2) with a Comprehensive Laboratory Animal Monitoring System (CLAM) (Columbus Instruments, OH, USA) and 18 minutes after the second injection a static dorsal thermal image was taken with an infrared camera (FLiR Systems, Wilsonville, OR, USA). Serum samples were collected via tail-nick just after the infrared image was taken and non-esterified free fatty acid (NEFA) concentration was determined using manufacturer´s instructions with a two-step kit (NEFA-HR 2, WAKO).

Metabolic Monitoring

Metabolic monitoring was performed as previously described [72] in a Comprehensive Laboratory Animal Monitoring System (CLAMS). For the chronic 5 day CL 316,243 (5D CL) challenge, mice were injected intraperitoneally with saline or CL 316,243 (First 4 days 0.5 mg/kg and last day 1.0 mg/kg) at 0930 hrs and measurements for VO_2 were calculated 6 hours post-injection. Mice were sacrificed 24 hours after the last injection.

Tissue Histology

Tissues were fixed in 10% formalin for 24-48 hours at 4 °C and processed for paraffin embedding and hematoxylin and eosin (H&E) staining by the core histology laboratory at the McMaster Immunology Research Centre (Hamilton, Canada).

Immunohistochemistry

For immunostaining against MYH4, MYH2, MYH7 and Laminin, adult legs without fixation and without skin were embedded with Tissue-TEK OCT (Sakura Finetek, Netherlands) and directly frozen in cold isopentane pre-cooled in liquid nitrogen. Muscles were conserved at -80 °C and cut with a cryostat (Leica 3050s) with a thickness of 10 µm. Cryostat sections were washed 3 times 5 minutes with PBS and then incubated with blocking solution (PBS and 10% goat serum) for 30 minutes at room temperature. Sections were incubated overnight with primary antibody diluted in PBS + 10% goat serum solution at 4 °C and washed repeatedly as described above. The sections were incubated with secondary antibody, diluted in PBS + 10% goat serum solution for 1 hour at room temperature. Sections were further washed and mounted with Mowiol solution and a glass coverslip. Images were collected with a microscope (Olympus BX63F) and a camera (Hamamatsu ORCA-Flash 4.0). Images were analysed with ImageJ (NIH). The antibodies used are listed in Supplementary Table 1 and Supplementary Table 2. Fibre boundaries were defined by the laminin signal and myosin type I, type IIA and type IIB heavy chains were quantified. Remaining unlabelled fibres were included for total fibre number and individual proportions of type I, type IIA and type IIB of that total number calculated.

Statistical Analysis

Data is displayed as means ± SEM and statistical analysis was performed using GraphPad Prism software. Differences between only two groups were analysed using an unpaired two-tailed Student's t-test and otherwise by one-way ANOVA with Bonferroni post hoc test for multiple comparisons. Repeated measures two-way ANOVA was used to analyse infrared thermography, VO_2 data from the 5D CL challenge and *in vivo* blood glucose measurements. Statistical significance was accepted at $P< 0.05$.

4 Results I

Role of AMPKγ3 in Skeletal Muscle

4.1 Role of AMPKγ3 on General Metabolic Parameters

In order to assess physiological roles of AMPKγ3, we generated a constitutive whole-body γ3 knock-out (KO) mouse model (in labels referred to as γ3$^{-/-}$) in collaboration with Taconic Bioscience (Cologne, Germany). The targeting strategy is shown in (Appendix Figure 1A). Briefly, exons 5-10 of the *Prkag3* gene encoding AMPKγ3 were flanked by loxP sites, resulting in a constitutive knock-out by deletion of CBS2 and parts of CBS1 and CBS3. This results in joined exons 1-4 and exons 11-13 (premature stop codon in exon 12). In addition, the resulting transcript may be a target for non-sense mediated RNA decay and thereby may not be expressed at significant level. In support of this, we were unable to detect faster migrating polypeptides using an antibody raised against residues 44–64 within exon 1-3 of the mouse γ3 (Appendix Figure 1C). AMPKγ3$^{-/-}$ mice were born at expected Mendelian frequency (Appendix Figure 1B) and showed similar body weight/growth (data not shown). Food intake, spontaneous physical activity, as well as oxygen consumption (Appendix Figure 1D-F) and respiratory exchange ratio (Figure 8C) are similar between wild-type (WT) and γ3$^{-/-}$ mice.

Metabolic phenotyping of the mice was performed at Phnomin (Illkirch, France) according to a design study plan laid out in Figure 7. Ten WT and γ3$^{-/-}$ mice were delivered at seven weeks of age and housed at the facility from that moment onwards. Body weight was constantly recorded and did not reveal any differences on either chow or high fat diet (HFD) (Figure 8A) over the duration of the study.
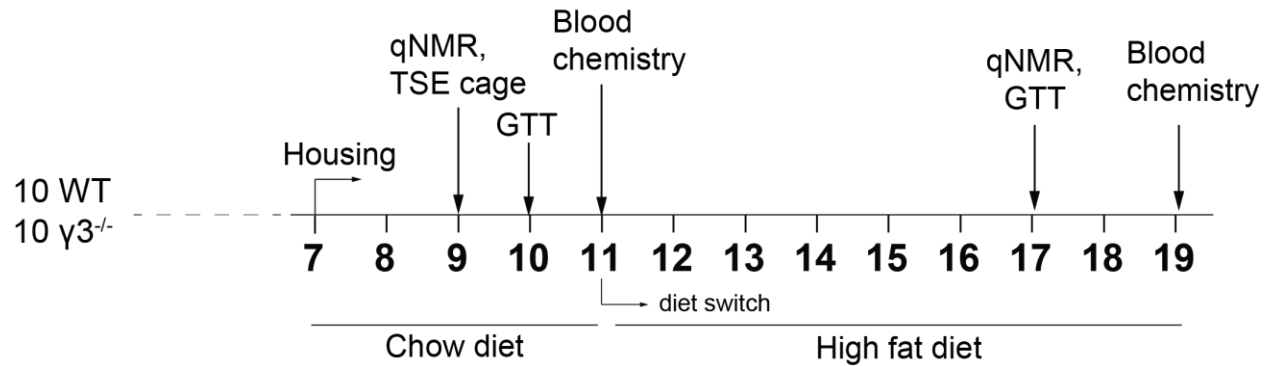
Figure 7 Study design plan for mouse metabolic phenotyping at Phenomin (Illkirch, France).
10 WT and 10 Prkag3^{-/-} (γ3^{-/-}) were delivered at the facility at an age of 7 weeks, where they were housed and fed chow diet for 4 weeks. In week 11, a diet switch occurred from chow to high fat diet. Experiments and measurements were conducted following the indicated scheme.

The body composition of the animals was monitored by quantitative nuclear magnetic resonance (qNMR) twice, representing a chow measurement and a HFD equivalent. As the switch to HFD in week 7 led to an increase in body weight (Figure 8A), this was primarily due to an increased fat mass in both genotypes (Figure 8B) indicating similar metabolic responses to the diet switch. This is also supported by measured blood plasma levels of insulin and leptin (Figure 8D, E), which both increase to similar degrees in WT and γ3^{-/-} mice when fed with HFD. Glucose tolerance is similar between genotypes on chow diet or HFD (Figure 8F) despite increased blood sugar levels on HFD feeding, further supporting the findings above and indicating a developing insulin resistance/overt diabetes (Figure 8D, F) due to the HFD. Collectively, the metabolic phenotyping of the γ3^{-/-} mice does not suggest an altered glucose homeostasis in the KO model.
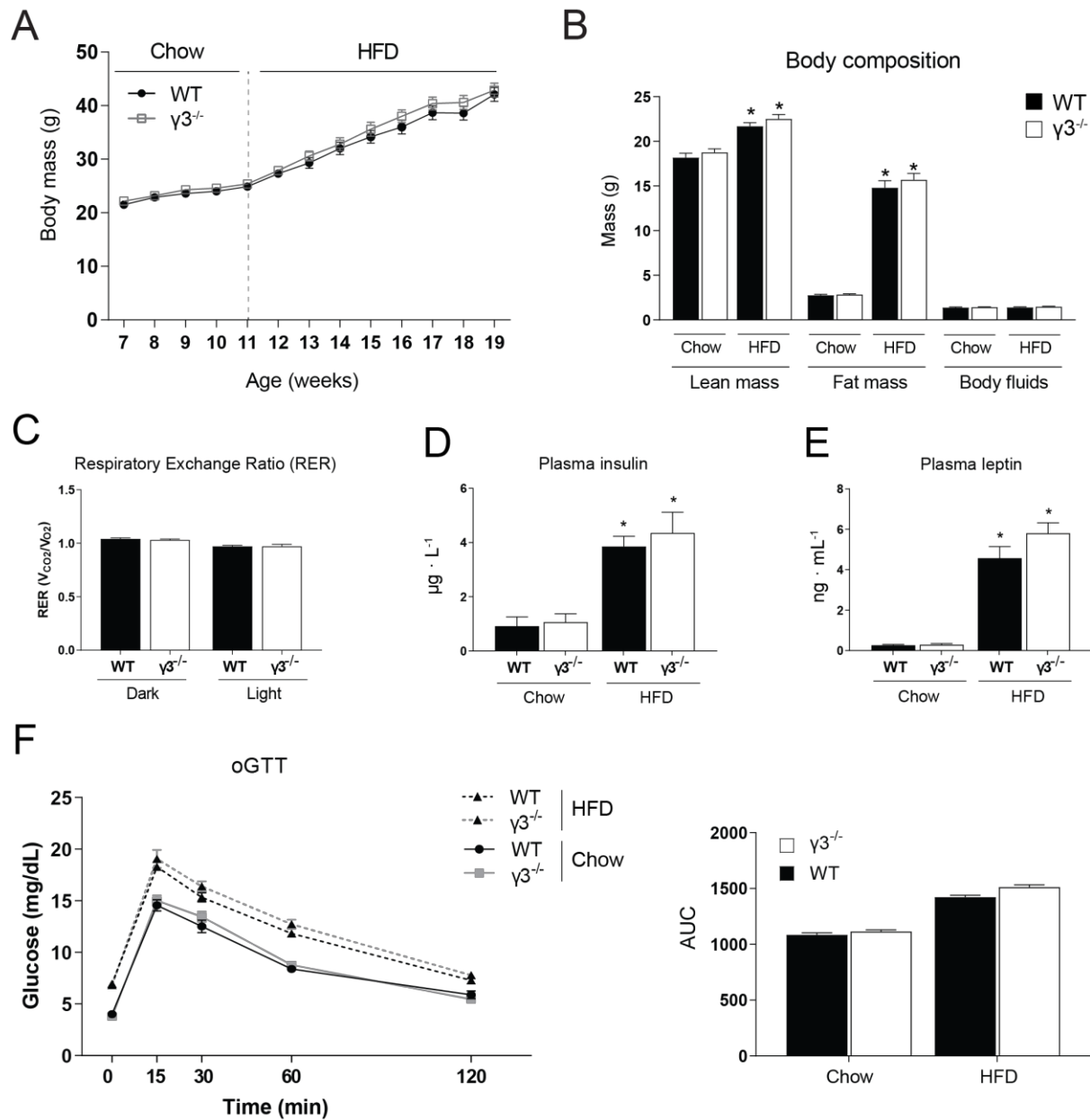
Figure 8 AMPKγ3^{-/-} mice do not show changes in glucose homeostasis under chow or in adaptation to high fat diet (HFD).

A) Body weight over time of WT and γ3^{-/-} mice. Mice were fed chow diet until week 11 before switching to HFD. Resutls are shown as means ± SEM for n=10 animals per genotype and analysed by two-way ANOVA, using Bonferroni correction. **B)** Body composition measured by qNMR and broken down into lean mass, fat mass and body fluids of WT and γ3^{-/-} mice fed with chow diet and high fat diet (HFD). Data are shown as mean ± SEM of n=10 mice per genotype and analysed by two-way ANOVA, using Bonferroni correction. *$P<0.05$ was accepted as significant and indicates an effect of chow versus HFD. **C-E)** Respiratory exchange ratio (RER) **(C)**, plasma insulin **(D)** and plasma leptin **(E)** levels of WT and γ3^{-/-} mice measured in week 11 (chow diet) and week 19 (HFD) respectively. Data is shown as mean ± SEM of n=10 mice per genotype and two-way ANOVA, using Bonferroni correction. *$P<0.05$ was accepted as significant and indicates an effect of chow versus high fat diet. **F)** Oral glucose tolernace test (oGTT) of WT and γ3^{-/-} mice performed in week 10 (chow diet) and week 17 (HFD) respectively. Blood glucose levels were measured over 120 min after an oral glucose bolus. The data are plotted over time as mean ± SEM. n=10 animals per genotype were used and data analysed by two-way ANOVA with Turkey's Honest Significant Difference correction.

4.2 Role of AMPKγ3 on AMPK Subunit/Isoform Expression and AMPK Complex Formation

After verification of our AMPKγ3 antibody in gastrocnemius (GAS) (Appendix Figure 1C) as also done previously [73], we wanted to assess the expression of γ3 in skeletal muscle. Previous reports suggest AMPKγ3 expression are detected primarily in glycolytic/fast-twitch muscles like extensor digitorum longus (EDL) and GAS [70] predominantly as α2β2γ3-complex [224] and to a small degree in the more oxidative/slow-twitch soleus (SOL) [225]. Indeed, we observed expression and activity of γ3 complexes to be the highest in GAS and EDL and rather low in SOL (Figure *9*A, C). Expression of γ3 in SOL lysate proved to be below the detection limit by direct immunoblotting (IB) (Appendix Figure 2A), but could be seen after immunoprecipitation (IP) followed by immunoblotting (Figure *9*A and Appendix Figure 2B) or AMPK activity assay (Figure *9*C). Liver lysates and immunoprecipitated samples showed a non-specific band in the γ3 blot (Figure *9*A), which could be confirmed by equal detection of the band in immunoglobulin G (IgG) IP samples (Figure *9*B). AMPK activity assays showed only negligible background activity of γ3-associated activity in liver and heart samples (Figure *9*C). To investigate if a genetic deletion of γ3 affects AMPK activities of α1- or α2-containing complexes, we used GAS lysates to immunoprecipitate those complexes with isoform-specific antibodies and subsequently performed *in vitro* AMPK activity assays. We could observe that AMPKα1-associated activity was unchanged (Figure *9*D), whereas AMPKα2-activty was decreased by approximately 50% (Figure *9*E).
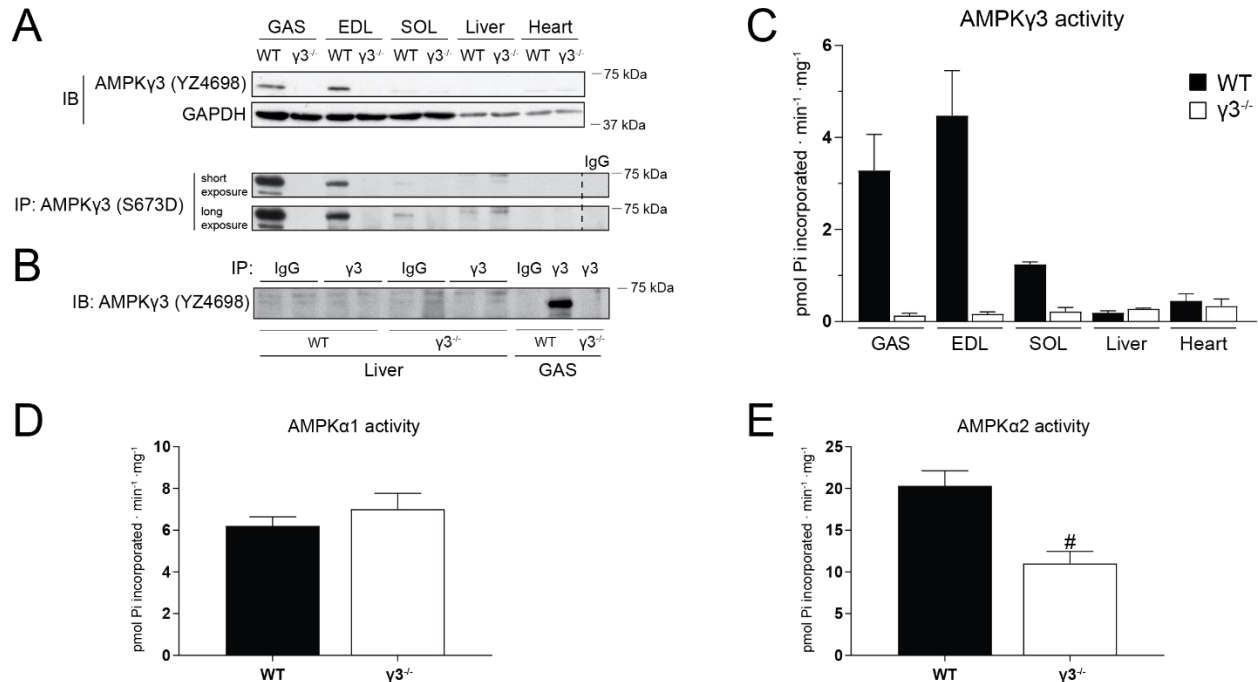
Figure 9 AMPKγ3 is expressed primarily in glycolytic muscles and its genetic deletion causes reduced activity of AMPKα2 in GAS.
A) Immunoblot (IB) analysis of γ3 expression in a panel of mouse tissues using 20 µg of protein extract of wild-type (WT) and AMPKγ3 knock-out (γ3⁻/⁻) tissues. 200 µg of tissue extract was used for immunoprecipitation (IP) and subsequent IB of AMPK γ3. **B)** 200 µg of liver and GAS extract were used for IP with either AMPKγ3-specific antibody or species-matched IgG and immunoblotted with the AMPKγ3 antibody. **C-E)** *In vitro* AMPK activity assays (in duplicate) were performed on 200 µg of immunoprecipitated extract of the indicated tissue using AMPKγ3-specific antibody (C) or 100 µg of GAS extract (D + E) using either AMPKα1-(D) or AMPKα2-(E) specific antibodies as described in MATERIALS and METHODS. Values are plotted as means ± SEM and represent n=3 samples per tissue and genotype (C) or n=9-10 samples per genotype(D-E). Statistically significant results were determined by an unpaired Student's t-test and are shown as #P<0.05. GAS; gastrocnemius, EDL; extensor digitorum longus, SOL; soleus, IgG; immunoglobulin G.

Given the preferential assembly of γ3 complexes with α2 and β2 isoforms and the apparent decrease in α2 activity, we thought that the complex formation may be hindered or destabilised due to the lack of γ3 and therefore cause a change in expression in the α2 and β2 subunit isoforms. We therefore performed a quantitative IB analysis of AMPK subunit isoforms of both glycolytic/fast-twitch (EDL, GAS) and oxidative/slow-twitch (SOL) muscle types in WT and γ3⁻/⁻ animals (Figure 10). For this analysis, we used a capillary immunoblotting system (Sally Sue, Protein Simple), which enables improved reproducibility and quantitative analysis of immunoblots (described in MATERIALS and METHODS). We performed extensive antibody validation previously [73] and here in form of signal linearity and working antibody concentration on the Sally Sue system of all used antibodies (Appendix Figure 3). Quantification of the immunoblots revealed that expression of α2 (and total AMPKα as a result thereof) and β2 subunit isoforms was reduced by approximately 20-30% in EDL as well as GAS (Figure 10A, B), but not in SOL (Figure 10C). To determine if this effect is also seen at the transcript level, we performed qPCR analyses (Appendix Figure 5). We did not detect any difference in mRNA expression levels of *Prkaa2*, *Prkab2* (encoding AMPKα2 and AMPKβ2

respectively) or any other AMPK subunit isoform in either GAS (Appendix Figure 5A) or SOL (Appendix Figure 5B) between WT and γ3$^{-/-}$ animals, while confirming no *Prkag3* (AMPKγ3) mRNA was detected. To examine whether loss of one γ3 allele would cause similar effects, we applied similar measurements to EDL muscles from heterozygous (HET) mice (Figure 11). As expected, AMPKγ3 expression was decreased by about half which confirmed the genotype of the animals. However, AMPKα2 and AMPKβ2 were not significantly reduced in the HET muscles.

Collectively, this shows that total, but not partial genetic loss of AMPKγ3 causes a reduction of protein expression of AMPKα2 and AMPKβ2 in glycolytic muscles. Loss of γ3 does not impact mRNA expression or AMPK subunit expression in oxidative muscles.
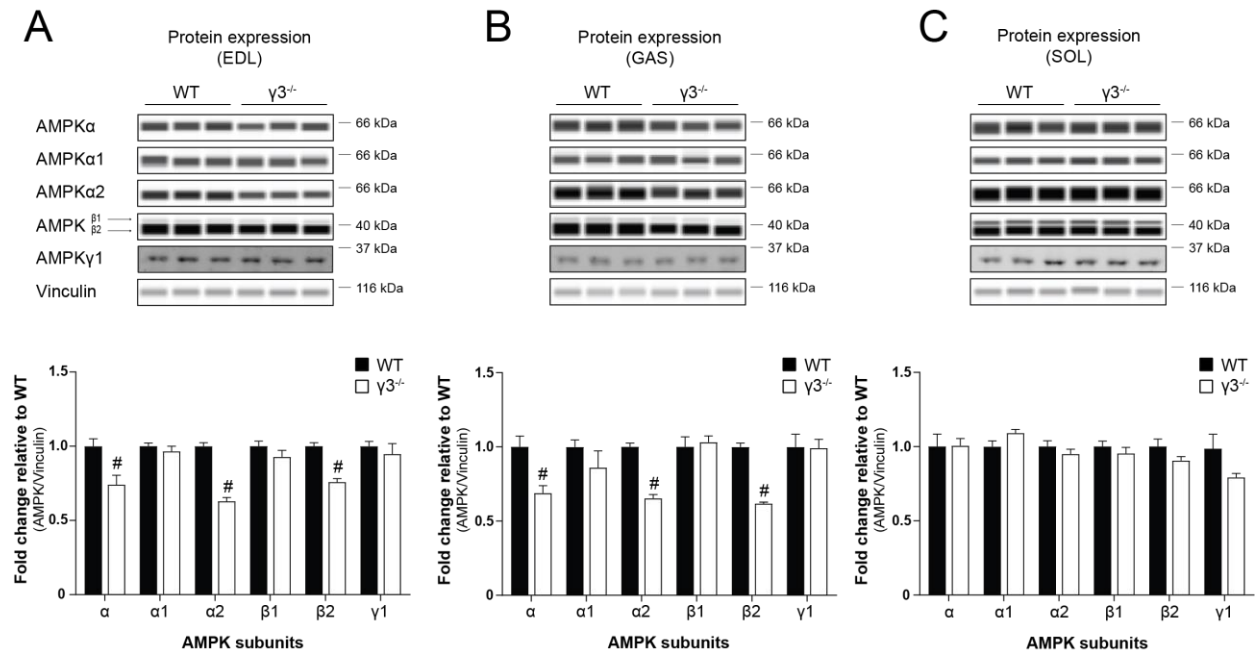
Figure 10 Genetic deletion of the AMPKγ3 isoform causes reduced expression of AMPK α2 and AMPK β2 isoforms in glycolytic muscles.
A-C) Representative immunoblots and quantification of AMPK subunit expression in EDL (A), GAS (B) and SOL (C) muscles using an automated capillary Western Blot system (Sally Sue, Protein Simple). Immunoblots were performed using 16 ng of muscle extract and the indicated AMPK isoform-specific and or pan-AMPKβ1/2 antibody. AMPKγ1 expression was quantified using 20 µg of muscle extract and quantification on a fluorescence-based Western Blot system (LiCOR) due to antibody compatibility. AMPK subunit isoform expressions were normalised by their respective Vinculin expression and are shown as fold change relative to WT muscle. Values are plotted as means ± SEM and represent n=5-11 samples per muscle/genotype. Statistically significant changes in expression were determined by an unpaired Student's t-test and are shown as #*P*<0.05. GAS; gastrocnemius, EDL; extensor digitorum longus, SOL; soleus.

Figure 11 Loss of one allele of AMPKγ3 is not sufficient to cause a change in AMPK subunit expression.
Representative immunoblot (A) and quantification (B) of AMPK subunit isoforms in WT and heterozygous (HET) EDL muscles. Immunoblots were performed using 16 ng of muscle extract and the indicated AMPK isoform-specific and or pan-AMPKβ1/2 antibody. AMPKγ3 expression was compared using 20 μg of muscle extract and detection using horseradish peroxidase (HRP)-conjugated secondary antibodies and enhanced chemiluminescence (ECL) reagent due to antib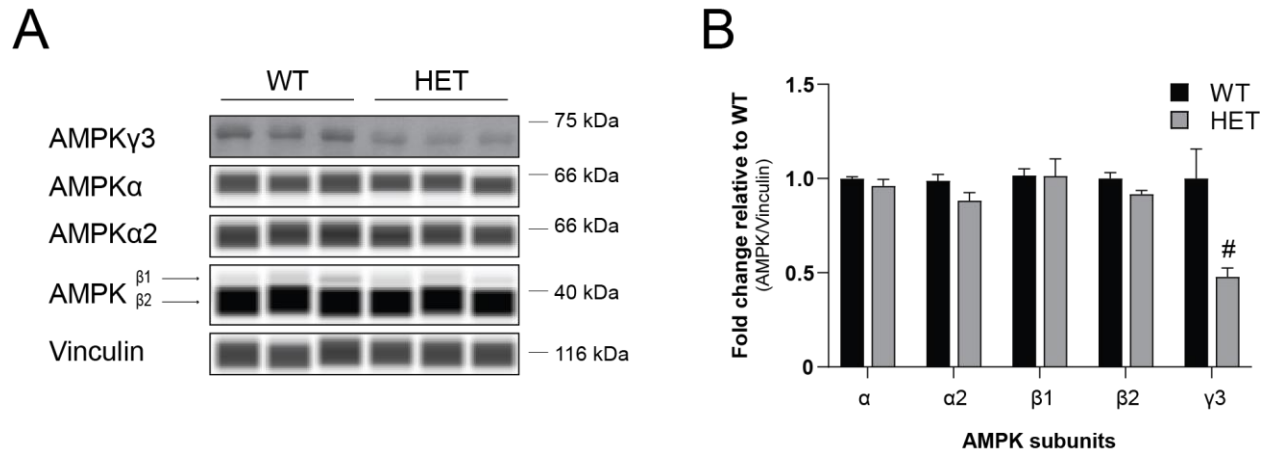ody compatibility. Bands were quantified using densitometry analysis of the ImageJ software (Java-based image-processing and analysis software). AMPK subunit isoform expressions were normalised by their respective Vinculin expression and are shown as fold change relative to WT muscle. Data is shown as means ± SEM and represent n=5-6 samples per genotype. Statistically significant changes in expression were determined by an unpaired Student's t-test and are shown as #$P<0.05$.

The reduced expression of α2 and β2 in glycolytic γ3$^{-/-}$ muscles pointed towards a role of γ3 in formation or stability of AMPK complexes containing those three subunit isoforms. To further investigate this, we aimed to identify the identity of those complexes by immunoprecipitation. We therefore used α- and β-isoform-specific antibodies to immobilise complexes containing these subunits and detect if γ3 is part of the heterotrimer.

Figure 12 AMPK γ3 primarily forms complexes with α2, but not with α1.
A-B) Immunoprecipitation (IP) of 200 μg of GAS lysate with either α1-(A) or α2-specific antibodies. Immunoprecipitates were used for subsequent immunoblot (IB) analysis with the indicated AMPK isoform-specific and or pan-AMPKβ1/2 antibody. Horseradish peroxidase (HRP)-conjugated secondary antibodies and enhanced chemiluminescence (ECL) reagent were used for signal detection. GAS; gastrocnemius.
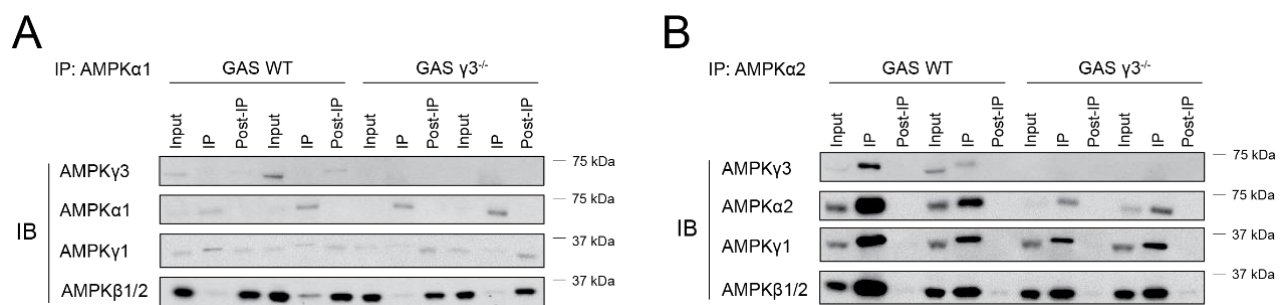
Figure 13 AMPK γ3 primarily forms complexes with β2, but not with β1.
A-B) Immunoprecipitation (IP) of 200 µg of GAS lysate with either α1-(A) or α2-specific antibodies. Immunoprecipitates were used for subsequent immunoblot (IB) analysis with the indicated AMPK isoform-specific and or pan-AMPKβ1/2 antibody. Horseradish peroxidase (HRP)-conjugated secondary antibodies and enhanced chemiluminescence (ECL) reagent were used for signal detection. GAS; gastrocnemius.
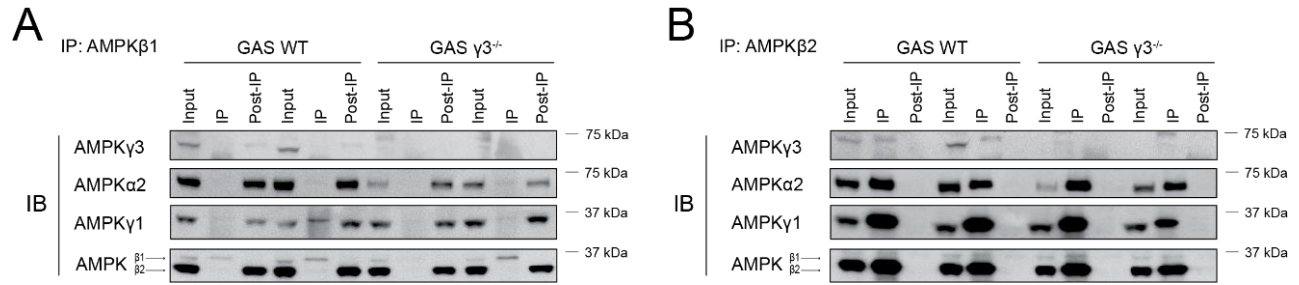
Immunoprecipitation experiments revealed that γ3 can readily be detected in α2-IP (Figure 12A), but not in α1-IP (Figure 12B) samples. A similar selectivity can be seen when comparing β1-IP (Figure 13A) with β2-IP (Figure 13B), suggesting that γ3 forms complexes with both α2 and β2 subunit isoforms in GAS, thus confirming previous observations [224] and supporting our hypothesis above.

4.3 Role of AMPKγ3 on Mitochondrial Content and Function

As previous muscle-specific AMPK KO models of either α [137] or β subunits [72] suggested reduced mitochondrial content and function, we aimed to investigate whether genetic loss of AMPKγ3 will cause similar effects. On the opposite spectrum of mitochondrial content, the gain-of-function γ3 R225Q mutant was reported to have increased mitochondrial content, while γ3$^{-/-}$ mice did not show any alterations in GAS [211]. Importantly, this γ3$^{-/-}$ model did not show alterations in α2 or β2 expression [70], leaving an open question whether a reduction of expression of α2 and β2 as well as α2 activity without complete loss thereof is enough to cause negative effects on mitochondrial content or function.

To assess this, we compared parameters of mitochondrial content and function (Figure 14C, D) in both glycolytic EDL and oxidative SOL muscles. We did not detect any difference in mitochondrial DNA (mtDNA) copy numbers (Figure 14A, B) or expression of mitochondrial respiratory chain complexes (Figure 14 E, F) in either muscle type, suggesting no impact of γ3 on mitochondrial content and integrity. Equally, mitochondrial function as represented by citrate synthase (CS) activity is not affected by loss of γ3 (Figure 14C, D).
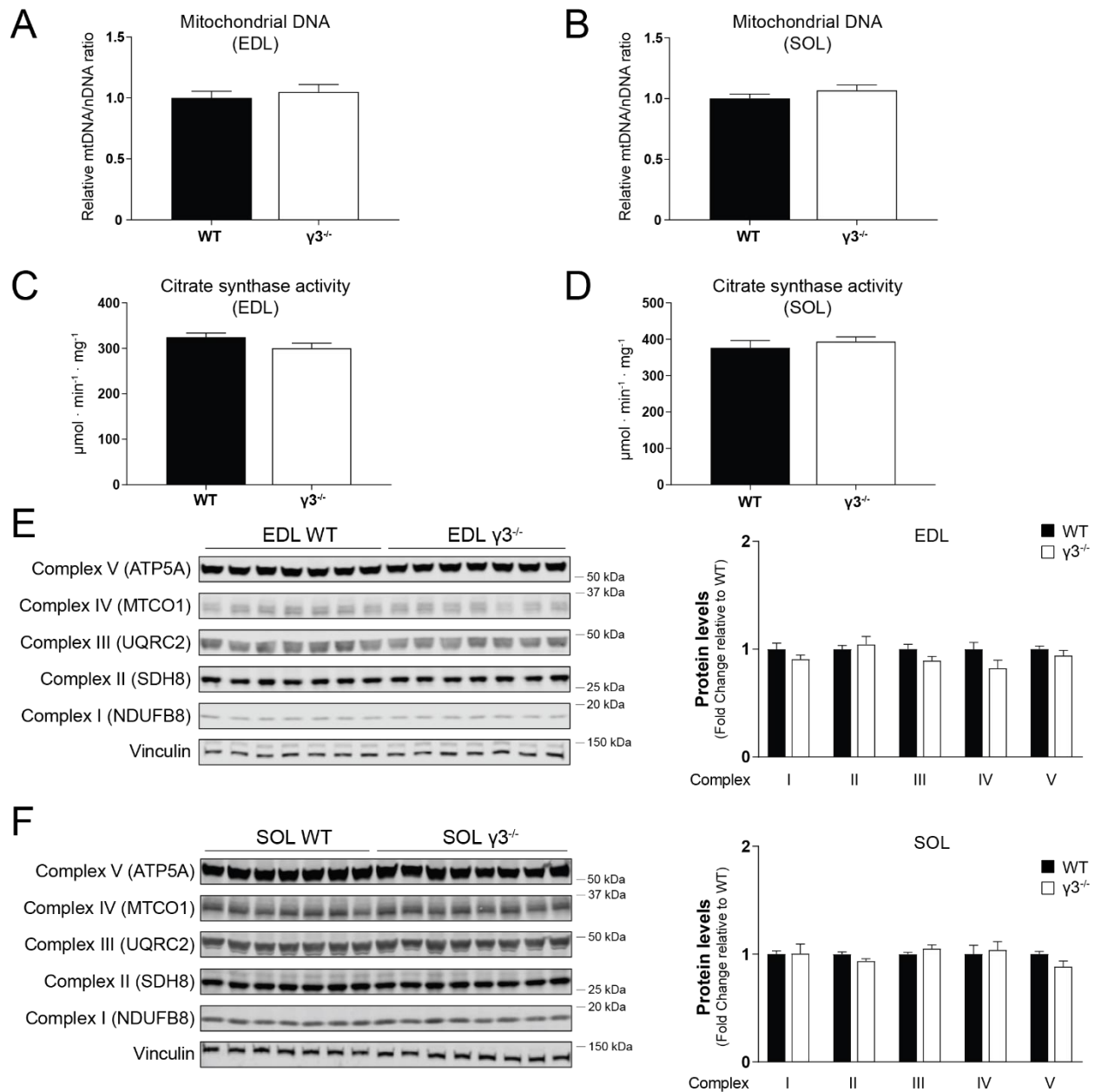
Figure 14 AMPK γ3$^{-/-}$ mice do not show impairments in mitochondrial integrity or complex expression. (mtDNA measurement performed by Jens Stolte)

A+B) Relative quantification of mitochondrial DNA (mtDNA) was performed using qPCR by quantification and normalisation of stable mitochondrial genes for EDL (A) and SOL (B) muscles as described in MATERIALS and METHODS. Results are shown as means ± SEM and represent n=5 samples per genotype. **C+D)** Citrate synthase activity was measured in GAS (C) and SOL (D) lysates using 10 μg of muscle lysate. Results are shown as means ± SEM and represent n=8 samples per genotype. **E+F)** Immunoblot (IB) analysis and quantification of mitochondrial complexes in EDL (E) and SOL (F) using 20 μg of muscle extract and an antibody mix detecting the indicated mitochondrial complexes. Quantification was performed on a fluorescence-based Western Blot system (LiCOR), normalised with Vinculin and shown as fold change relative to wild-type (WT) muscle. All the data was analysed by unpaired two-tailed Student's t-test. EDL; extensor digitorum longus, SOL; soleus.

4.4 Role of AMPKγ3 on Muscle Fibre Type

Fibre-type shifts in GAS were among previous reports of gain-of-function γ3 mutants [211], but did not occur in muscles lacking AMPKβ1/2 [72]. To assess the fibre types of WT and γ3$^{-/-}$ mice we examined whole-leg cross-sections by immunofluorescence staining using myosin heavy chain specific antibodies. We did not observe any difference in fibre-type composition when comparing γ3$^{-/-}$ EDL or SOL with their WT littermates. Together with the data on mitochondria, γ3 seems to be dispensable for regulating mitochondrial content and function as well as fibre-type composition in either glycolytic or oxidative muscle.
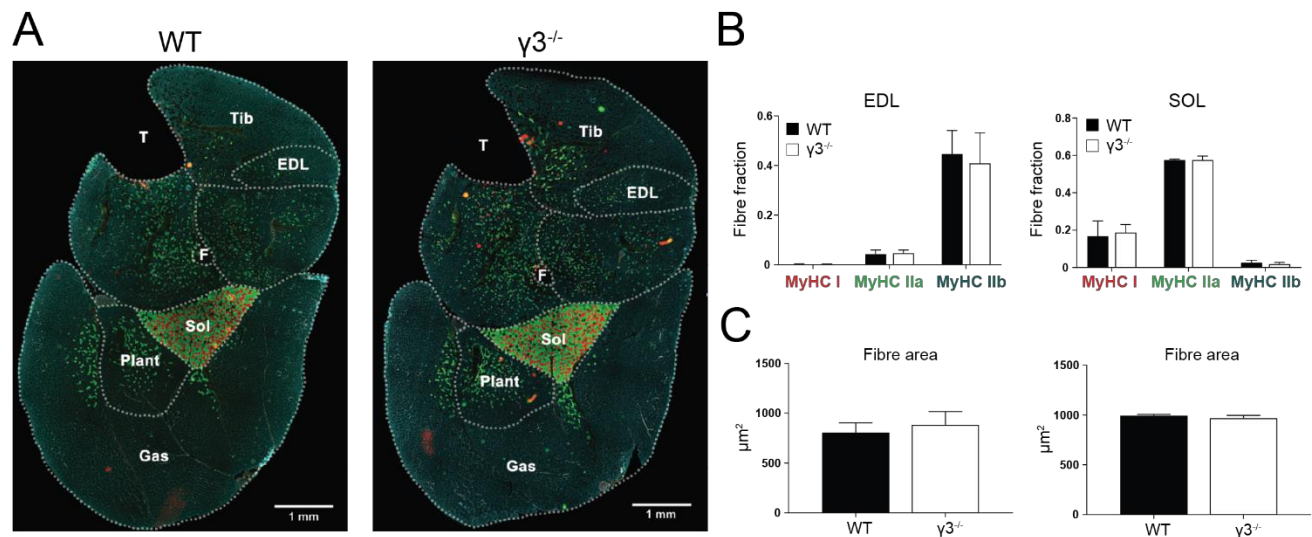
Figure 15 AMPK γ3$^{-/-}$ mice do not show changes in fibre-type composition or fibre area. (Staining work performed by Dr Matthieu Ferreira Dos Santos, Institut Cochin, Paris, France)
A) Representative images of whole-leg fibre-typing analysis of WT and γ3$^{-/-}$ mice using myosin heavy chain (MyHC) and laminin specific antibodies for section staining. (Scale bar, 1 mm) **B+C)** Quantification of relative MyHC content (B) and fibre area (C) in EDL and SOL muscles. Results are shown as means ± SEM and represent n=4 samples per genotype. Fibre boundaries were defined by the laminin signal and myosin type I, type IIA and type IIB heavy chains were quantified. Remaining unlabelled fibers were included for total fibre number and individual proportions of type I (**red**), type IIA (**green**) and type IIB (**blue**) of that total number calculated. All the data was analysed by unpaired two-tailed Student's t-test. GAS; gastrocnemius, EDL; extensor digitorum longus, SOL; soleus, Tib; tibialis anterior, Plant; plantaris, F; fibula, T; tibia.

4.5 Role of AMPKγ3 in Glucose Uptake into Skeletal Muscle

4.5.1 Role of AMPKγ3 in Insulin-mediated Glucose Uptake

Following our initial metabolic phenotyping *in vivo* (Figure 8) and as a verification for our *ex vivo* muscle incubation set-up for glucose uptake measurements, we investigated the effect of insulin on glucose uptake and the underlying signalling in incubated EDL. In line with the finding on basal glucose homeostasis (Figure 8D, F), basal glucose uptake was unchanged and insulin increased glucose uptake in both genotypes (Figure 16A) to the same extent. We performed immunoblot analysis of the incubated EDL lysates after glucose uptake (Figure 16B) and saw increased levels of Akt phosphorylation without difference between WT and γ3$^{-/-}$ samples (Figure 16C). We also confirmed that expression of glucose transporter 4 (GLUT4) (Figure 16D) and hexokinase II (HXKII) (Figure 16E) was unchanged in γ3$^{-/-}$ EDL, thus confirming and augmenting the finding of unchanged glucose homeostasis in the KO model.
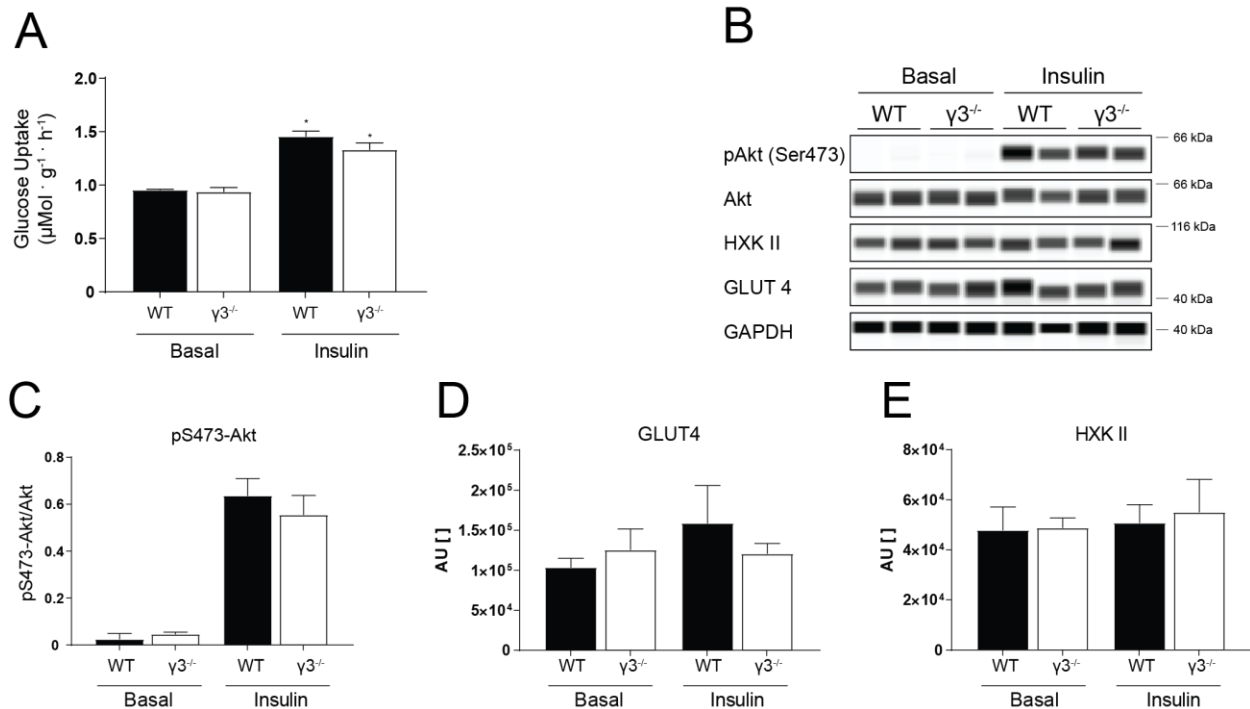
Figure 16 Deficiency of AMPKγ3 does not impact insulin-mediated glucose uptake *ex vivo*.
A+B) Glucosue uptake (A) and immunoblot (IB) of *ex vivo* incubated EDL muscles (B) incubated with either water (Vehicle) or 100 nM Insulin. *Ex vivo* muscle incbation is described in detail in MATERIALS & METHODS. **C-E)** IB analysis of lysate prepared from the incubated muscles with the indicated antibodies using an automated capillary Western Blot system (Sally Sue, Protein Simple). Immunoblots were performed using 16 ng of muscle extract and the indicated phospho-specific and total protein antibodies with representative blots shown. Results are shown as means ± SEM and represent n=2-5 samples per genotype/treatment and were analysed by one-way ANOVA, using Bonferroni correction. *$P<0.05$ was accepted as significant and indicates an effect of Insulin vs Basal.

4.5.2 Role of AMPKγ3 in Insulin-independent Glucose Uptake

It has been shown that stimulation of glucose uptake *ex vivo* in skeletal muscle through AICAR requires functional AMPK in both SOL and EDL [68, 164]. In line with those findings, we found AICAR to increase *ex vivo* glucose uptake into WT muscles by about 2.5-fold for EDL (Figure 17A) and 1.6-fold in SOL (Figure 17B). Remarkably, we found AICAR-stimulated glucose uptake to be markedly reduced in γ3$^{-/-}$ EDL muscles, but not in their SOL counterparts (Figure 17A, B). We further investigated the underlying signalling by immunoblots of the incubated muscle lysates and measured phosphorylation levels of known AMPK targets such as ACC and TBC1D1 (Figure 17C, D). We show that ACC phosphorylation of Ser212 (Figure 17E, F) and TBC1D1 phosphorylation of Ser231 (Figure 17G, H) is increased in AICAR treated EDL and SOL muscles in WT mice, but significantly reduced in only γ3$^{-/-}$ EDL samples (Figure 17E, G), linking γ3 expression to phosphorylation status of AMPK targets in response to AICAR stimulation.

We next wanted to examine whether partial loss of γ3 in HET mice would show similar effects in glucose uptake and AMPK signalling. We examined glucose uptake (Figure 18A) and the underlying phosphorylation patterns of ACC and TBC1D1 (Figure 18AC, D) and observed an increase in both pS212-ACC and pS231-TBC1D1 to similar levels in both genotypes. AMPKγ3 activity was decreased by approximately 50% in HET samples, but AICAR activation was not affected as both genotypes increase by about 3-fold (Figure 18B).

A. *Ex vivo* EDL — Glucose uptake (μMol $\cdot$ g^{-1} $\cdot$ h^{-1}) for WT and γ3$^{-/-}$ under Vehicle and AICAR conditions.

B. *Ex vivo* SOL — Glucose uptake (μMol $\cdot$ g^{-1} $\cdot$ h^{-1}) for WT and γ3$^{-/-}$ under Vehicle and AICAR conditions.

C. Western blots (EDL): pACC (S212), ACC, pTBC1D1 (S231), TBC1D1, pAMPK (T172), AMPKα, Vinculin.

D. Western blots (SOL): pACC (S212), ACC, pTBC1D1 (S231), TBC1D1, pAMPK (T172), AMPKα, Vinculin.

E. pS212-ACC — pS212-ACC/ACC (EDL).

F. pS212-ACC — pS212-ACC/ACC (SOL).

G. pS231-TBC1D1 — pS231-TBC1D1/TBC1D1 (EDL).

H. pS231-TBC1D1 — pS231-TBC1D1/TBC1D1 (SOL).

Figure 17 AICAR-stimulated glucose uptake and phosphorylation of ACC and TBC1D1 is blunted in AMPKγ3^{-/-} EDL but not SOL.

EDL and SOL muscles from wild-type (WT) and AMPKγ3^{-/-} mice were isolated and incubated with 0.1% DMSO (Vehicle) or 2 mM AICAR for 50 min in Krebs-Ringer buffer (KRB) containing 2 mmol/L pyruvate. Muscles were transferred to vials containing 2-deoxy-[^{3}H] glucose (2-DG) with or without 2mM AICAR for 10 min. At the end of the incubation, muscles were immediately snap frozen in liquid nitrogen for further analysis. Lysates were split for glucose uptake analysis and immunoblots. **A-B)** Glucose transport in EDL (A) and SOL (B) was assayed from muscle lysates as described above. **C-H)** Immunoblot (IB) analysis and quantification of lysates prepared from the incubated muscles. Blots and quantification were performed using an automated capillary Western Blot system (Sally Sue, Protein Simple). IBs were performed using 16 ng of muscle extract and the indicated phospho-specific and total protein antibodies. Phosphorylation of ACC and TBC1D1 was quantified as ratio of the phosphorylated protein and the respective total protein. Results are expressed as means ± SEM with n=4-6 animals per treatment/genotype. Statistical analysis was performed by one-way ANOVA with Bonferroni correction and statistical significance shown as *$P< 0.05$ (Vehicle vs AICAR) and #$P<0.05$ (WT vs γ3^{-/-}). EDL; extensor digitorum longus, SOL; soleus, AICAR; 5-aminoimidazole-4-carboxamide ribonucleoside.
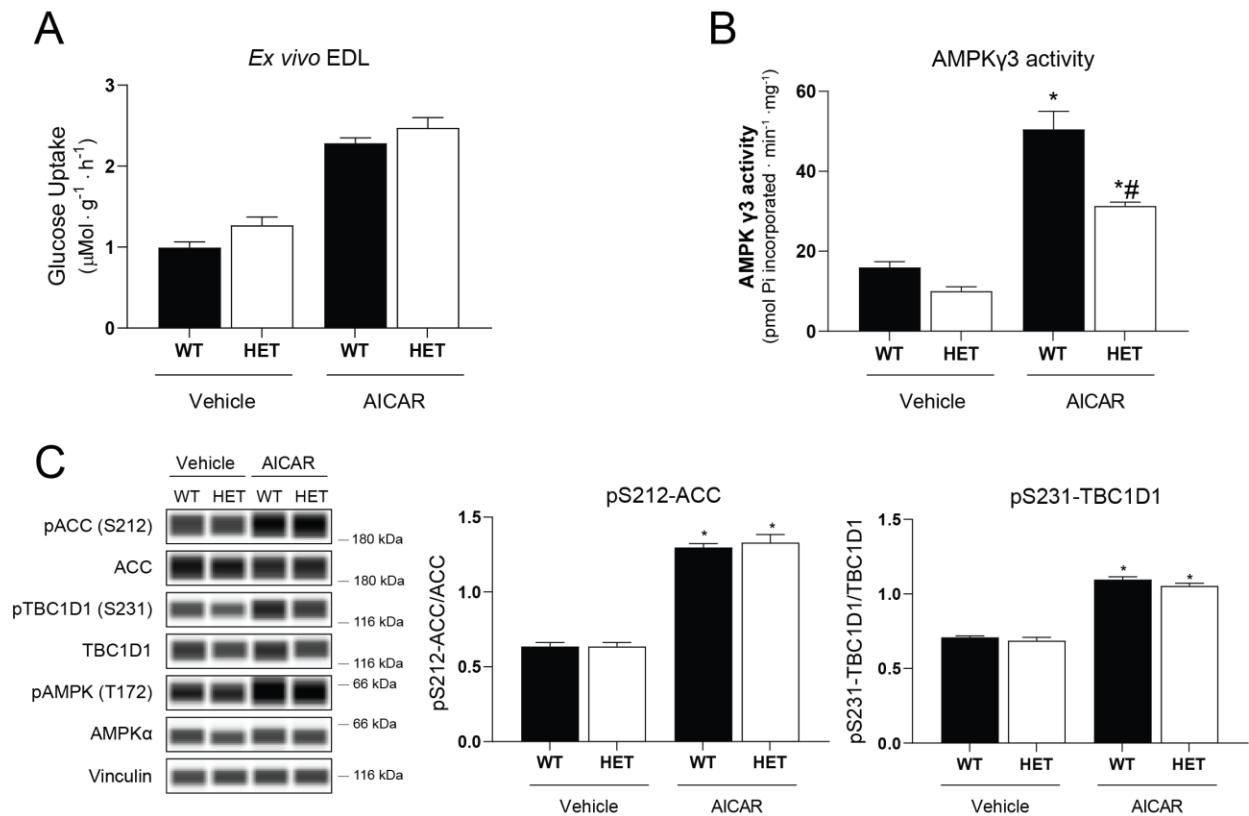
Figure 18 Partial ablation of AMPKγ3 is not sufficient to reduce AICAR-stimulated glucose uptake or phosphorylation of ACC and TBC1D1 in EDL.

EDL muscles from wild-type (WT) and heterozygous AMPKγ3$^{+/-}$ (HET) mice were isolated and incubated with 0.1% DMSO (Vehicle) or 2 mM AICAR for 50 min in Krebs-Ringer buffer (KRB) containing 2 mmol/L pyruvate. Muscles were transferred to vials containing 2-deoxy-[^{3}H] glucose (2-DG) with or without 2mM AICAR for 10 min. At the end of the incubation, muscles were immediately snap frozen in liquid nitrogen for further analysis. Lysates were split for glucose uptake analysis and immunoblots. A) Glucose transport in EDL was assayed from muscle lysates as described above. **B)** *In vitro* AMPK activity assays (in duplicate) were performed on 100 μg of immunoprecipitated EDL extracts using AMPKγ3-specific antibody as described in MATERIALS and METHODS. **C)** Immunoblot (IB) analysis and quantification of lysates prepared from the incubated muscles. Blots and quantification were performed using an automated capillary Western Blot system (Sally Sue, Protein Simple). IBs were performed using 16 ng of muscle extract and the indicated phospho-specific and total protein antibodies. Phosphorylation of ACC and TBC1D1 was quantified as ratio of the phosphorylated protein and the respective total protein. Results are expressed as means ± SEM with n=5-6 animals per treatment/genotype. Statistical analysis was performed by one-way ANOVA with Bonferroni correction and statistical significance shown as *$P < 0.05$ (Vehicle vs AICAR) and #$P < 0.05$ (WT vs HET). EDL; extensor digitorum longus, AICAR; 5-aminoimidazole-4-carboxamide ribonucleoside.

With the availability of potent ADaM-site-binding AMPK activators that were shown to increase glucose uptake into skeletal muscle in an AMPK-dependent manner [23, 24], we wanted to investigate further whether the lack of γ3 causes similar impairments in allosteric activator-stimulated glucose uptake. We took compound 991, which was previously shown to stimulate glucose uptake in skeletal muscle *ex vivo* [73, 76] and in an AMPK-dependent fashion in myotubes [76]. We confirmed its action through AMPK in muscle by using a previously described muscle-specific AMPKα1/α2 double knock-out (m-α1/α2 DKO) mouse model [164]. This work was conducted at the University of Nanjing by the group of Prof Shuai Chen

and shows that 991-induced glucose uptake is fully depended on the presence of skeletal muscle AMPK in both EDL and SOL (Appendix Figure 7A, B). This is complemented by immunoblots and the virtual absence of total AMPK protein and phosphorylation of ACC and TBC1D1 respectively (Appendix Figure 7C, D).

We then assessed the effect of two ADaM-site binding drugs, namely 991 and the structurally related MK-8722 [24] on *ex vivo* glucose uptake. Both 991 and MK-8722 increase glucose uptake in EDL muscles *ex vivo* by about 2-fold and 1.7-fold, respectively (Figure 19A). Contrary to AICAR-stimulated glucose uptake, there was no reduction of glucose uptake in $\gamma 3^{-/-}$ EDL with either compound. AMPKγ3-associated activity was increased modestly with both 991 and MK-8722 in WT muscles, while AICAR shows a much greater increase of γ3-activity. Confirming expectations, $\gamma 3^{-/-}$ samples did not show any γ3-activity beyond background (Figure 19B). We again looked at underlying signalling and AMPK target phosphorylation by immunoblot (Figure 19C, D). We found that both 991 and MK-8722 increased phosphorylation levels of ACC and TBC1D1 in WT EDL to a similar degree. However, in contrast to the AICAR experiment, but in line with the unchanged glucose uptake, we did not detect any difference in either pS212-ACC (Figure 19E) or pS231-TBC1D1 (Figure 19F) when comparing WT and $\gamma 3^{-/-}$ EDL. Collectively, this suggests that AMPKγ3 is not required for ADaM-site binding allosteric activators to increase *ex vivo* glucose uptake or phosphorylate the AMPK targets ACC and TBC1D1.

To verify that this effect is not restricted to glycolytic muscles, we performed similar experiments using SOL muscles as representative for an oxidative muscle phenotype. We subjected *ex vivo* incubated SOL muscles to the same dose of 991 and measured glucose uptake, γ3-associated AMPK activity as well as phosphorylation of ACC and TBC1D1. Likewise, 991 treatment increased glucose uptake by about 2-fold but without any difference between WT and $\gamma 3^{-/-}$ muscles (Figure 20A). Even though basal γ3-acitivity in SOL is rather low, 991 treatment increased the latter also by 2-fold in WT, with no detectable activity in the KO counterpart (Figure 20B).

Figure 19 AMPKγ3 is not required for either 991- or MK-8722-mediated glucose uptake in EDL *ex vivo*.
EDL muscles from wild-type (WT) and AMPKγ3⁻/⁻ mice were isolated and incubated with 0.1% DMSO (Vehicle), or 10 µM of either 991 or MK-8722 for 50 min in Krebs-Ringer buffer (KRB) containing 2 mmol/L pyruvate. Muscles were transferred to vials containing 2-deoxy-[³H] glucose (2-DG) with or without AMPK activator for 10 min. At the end of the incubation, muscles were immediately snap frozen in liquid nitrogen for further analysis. Lysates were split for glucose uptake analysis and immunoblots. **A)** Glucose transport in EDL was assayed from muscle lysates as described above. **B)** *In vitro* AMPK activity assays (in duplicate) were performed on 100 µg of immunoprecipitated EDL extracts using AMPKγ3-specific antibody as described in MATERIALS and METHODS. (n=4-14 per treatment/genotype) **C-F)** Immunoblot (IB) analysis and quantification of lysates prepared from the incubated muscles. Blots and quantification were performed using an automated capillary Western Blot system (Sally Sue, Protein Simple). IBs were performed using 16 ng of muscle extract and the indicated phospho-specific and total protein antibodies.

Phosphorylation of ACC and TBC1D1 was quantified as ratio of the phosphorylated protein and the respective total protein. Results are expressed as means ± SEM with n=4-9 animals per treatment/genotype. Statistical analysis was performed by one-way ANOVA with Bonferroni correction and statistical significance shown as *$P < 0.05$ (Vehicle vs Activator). EDL; extensor digitorum longus, AICAR; 5-aminoimidazole-4-carboxamide ribonucleoside.

Immunoblot analysis of phosphorylation of ACC and TBC1D1 show modest increases, but also here we did not observe any difference between genotypes (Figure 20C). Taken together, both EDL and SOL experiments show that γ3 is not required to mediate glucose uptake or AMPK signalling of direct allosteric activators in skeletal muscle.
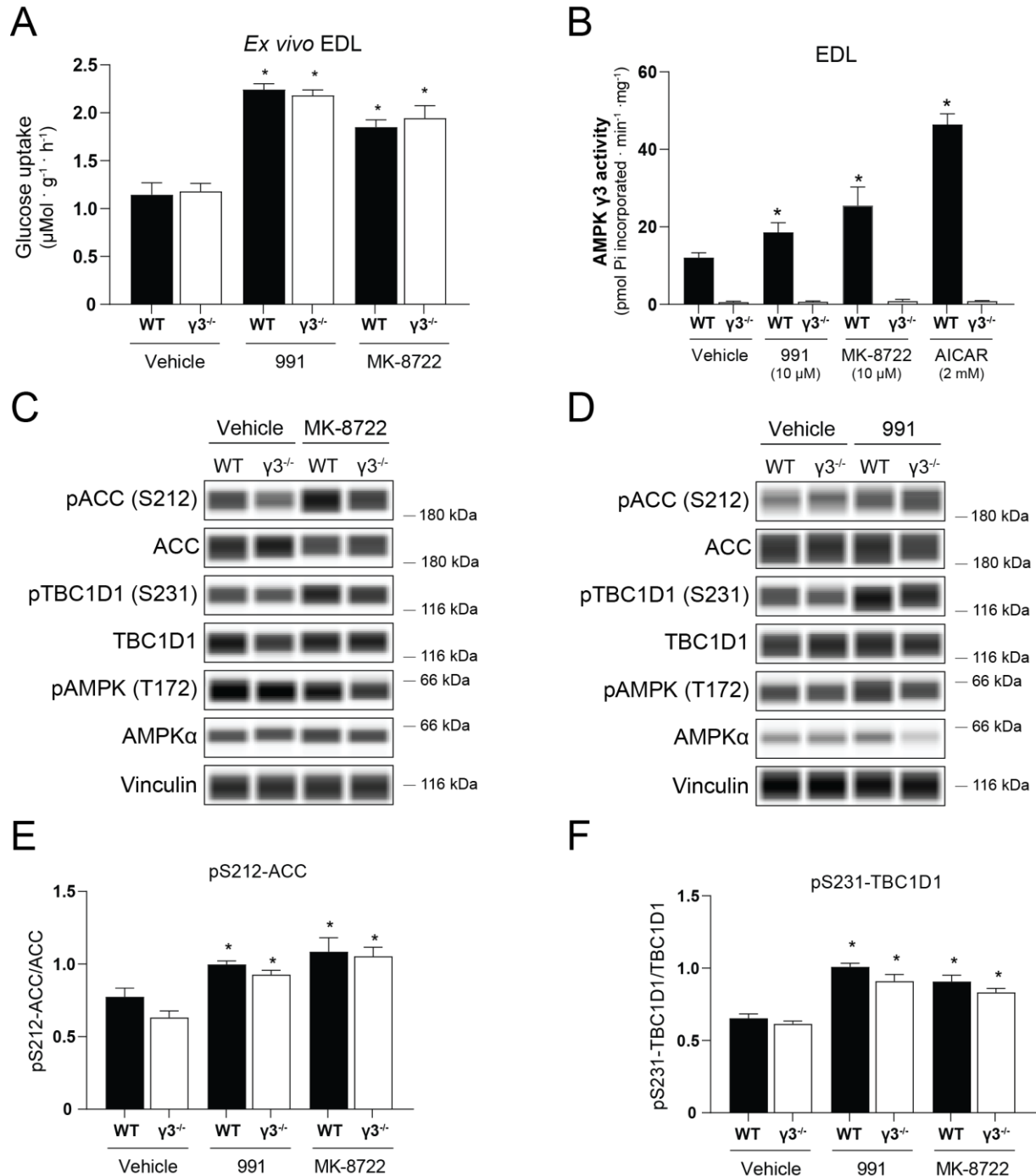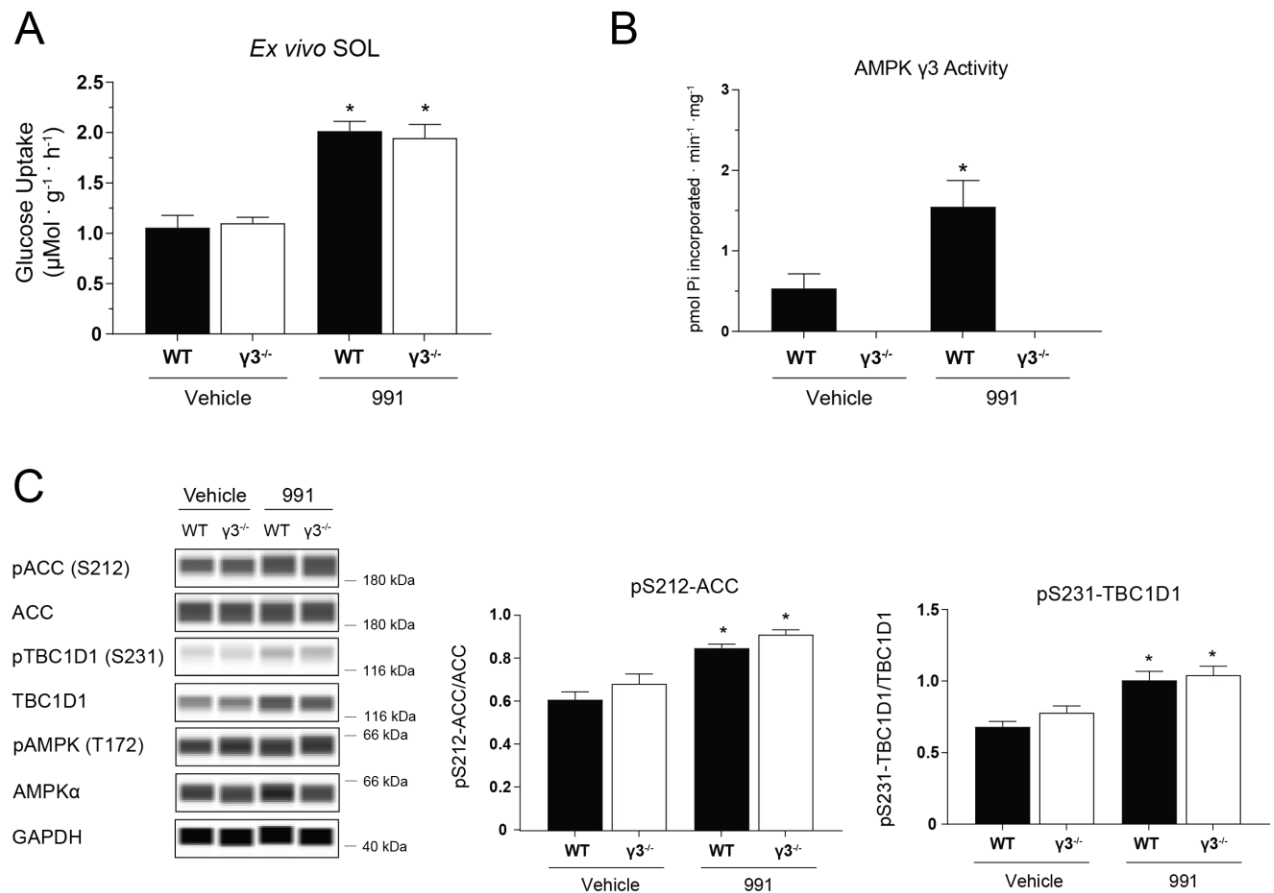

Figure 20 AMPKγ3 is not required for either 991-mediated glucose uptake in SOL *ex vivo*.
SOL muscles from wild-type (WT) and AMPKγ3^{-/-} mice were isolated and incubated with 0.1% DMSO (Vehicle) or 10 µM 991 for 50 min in Krebs-Ringer buffer (KRB) containing 2 mmol/L pyruvate. Muscles were transferred to vials containing 2-deoxy-[³H] glucose (2-DG) with or without 991 for 10 min. At the end of the incubation, muscles were immediately snap frozen in liquid nitrogen for further analysis. Lysates were split for glucose uptake analysis and immunoblots. **A)** Glucose transport in SOL was assayed from muscle lysates as described above. **B)** *In vitro* AMPK activity assays (in duplicate) were performed on 100 µg of immunoprecipitated SOL extracts using AMPKγ3-specific antibody as described in MATERIALS and METHODS. (n=4-7 per treatment/genotype) **C-F)** Immunoblot (IB) analysis and quantification of lysates prepared from the incubated muscles. Blots and quantification were performed using an automated capillary Western Blot system (Sally Sue, Protein Simple). IBs were performed using 16 ng of muscle extract and the indicated phospho-specific and total protein antibodies. Phosphorylation of ACC and TBC1D1 was quantified as ratio of the phosphorylated protein and the respective total protein. Results are expressed as means ± SEM with n=4 animals per treatment/genotype. Statistical analysis was performed by one-way ANOVA with Bonferroni correction and statistical significance shown as *$P < 0.05$ (Vehicle vs 991). SOL; soleus.

4.5.3 Role of AMPKγ3 in Whole-body Glucose Metabolism

After having observed results on *ex vivo* glucose uptake in different muscle types, we aimed to investigate whether this translates into *in vivo* hypoglycaemic impairments as seen in muscle-specific AMPKα double KO [164] or α2 KO mice when challenged with AICAR [68].
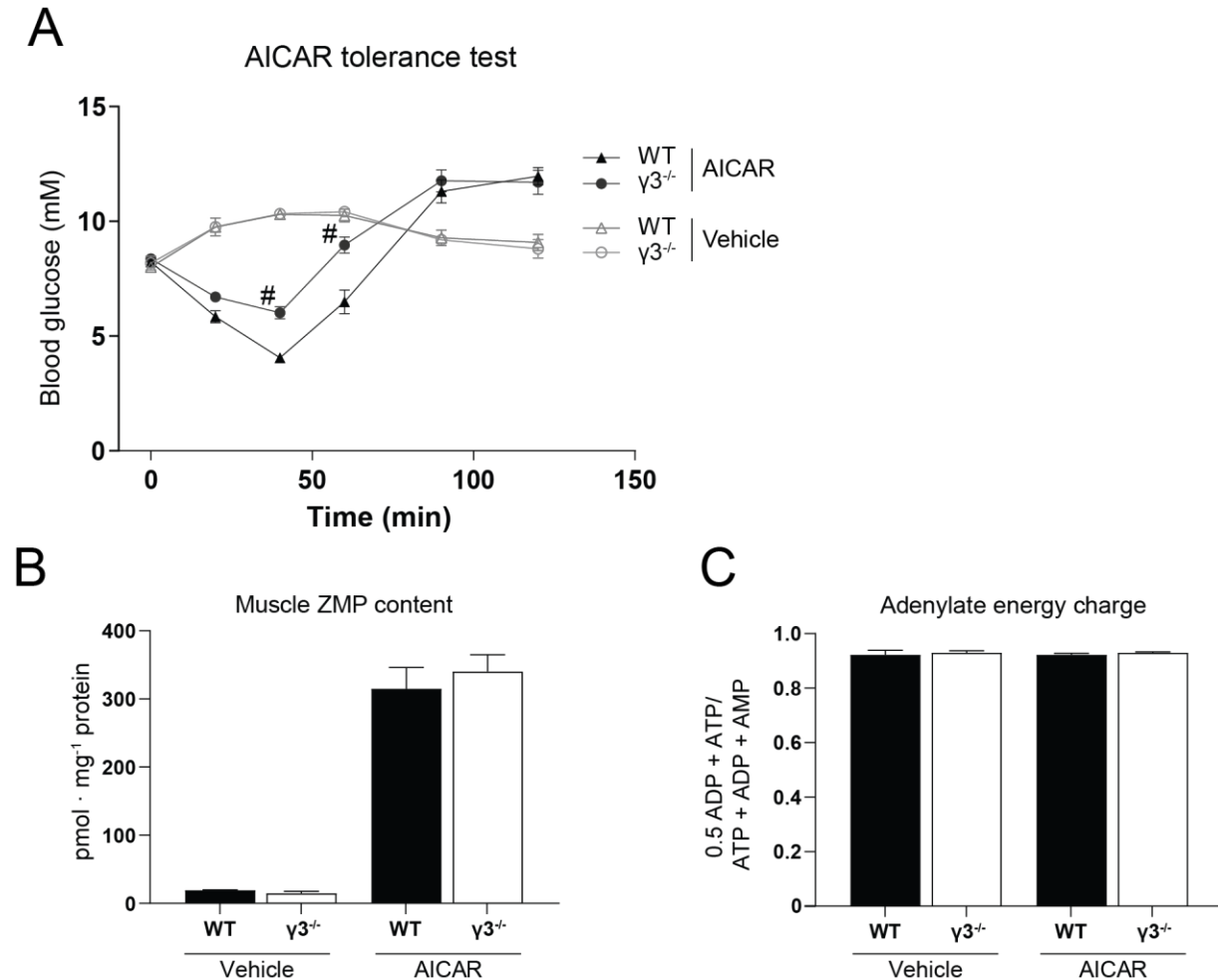
Figure 21 AMPKγ3 is required for AICAR-induced whole-body glucose clearance.
A) AICAR tolerance test (ATT) of male WT and γ3⁻/⁻ mice (10-12 weeks old). Mice were fasted for 3h in the morning and then injected intraperitoneally with either water (vehicle) or AICAR (250 mg/kg body weight) and blood glucose levels were monitored for 2h. GAS muscles were harvested and snap-frozen immediately after competition of the ATT at t=120 min. n =5-12 per genotype/treatment. Data is shown as means ±SEM. Statistical significance of blood glucose levels at the indicated timepoints was determined by two-way ANOVA with Bonferroni correction with #$P<0.05$ (WT versus γ3⁻/⁻) representing significance. **B+C)** HPLC analysis of ZMP content (B) and adenylate energy charge (C) of GAS muscles harvested after competition of the ATT. Results are expressed as means ± SEM with n=5-12 animals per treatment/genotype. Statistical analysis was performed by one-way ANOVA with Bonferroni correction. AICAR; 5-aminoimidazole-4-carboxamide ribonucleoside; ZMP; AICAR monophosphate.

We injected either water (vehicle) or a dose of AICAR (250 m/kg body weight) intraperitoneally into 3h-fasted mice and monitored blood glucose levels for 120 min. Injection of AICAR robustly reduced blood glucose levels of both WT and γ3⁻/⁻ animals. Interestingly the hypoglycaemic effect of AICAR was blunted

in γ3$^{-/-}$ mice at two time-points (t= 40 min and t=60min) within an hour of injection (Figure 21A). We confirmed similar ZMP content (Figure 21B) and adenylate energy charge (Figure 21C) in WT and γ3$^{-/-}$ GAS muscles harvested after completion of the tolerance test, indicating unchagend drug delivery and adenosine nucleotide balance. Together with the *ex vivo* results, this suggests that AMPKγ3 plays an important role AICAR-mediated glucose uptake in glycolytic muscle which contributes to whole-body glucose homeostasis in response to AICAR/ZMP.

In a similar approach to the *ex vivo* experiments, we also wanted to inestigate the effect of allosteric activators binding to the ADaM site on whole-body glucose disposal. We chose MK-8722 due to its oral efficacy shown in previous models [24]. We challenged 3h-fasted mice with an oral dose of 10 mg/kg or 30 mg/kg MK-8722 (or vehile). Corresponding to our observations *ex vivo*, MK-8722 lowered blood glucose levels to a similar extent in both genotypes, indicating that γ3 is dispensible for ADaM site activator-mediated glucose homeostasis *in vivo* (Figure 22). Consistent with this result, a higher dose of 30 mg/kg also showed similar glucose clearance effects in WT and γ3$^{-/-}$ mice (Appendix Figure 8A), while our collaborators from the University of Nanjing could confirm the dependence of glucosue clearance on skeletal msucle AMPK (Appendix Figure 8B).
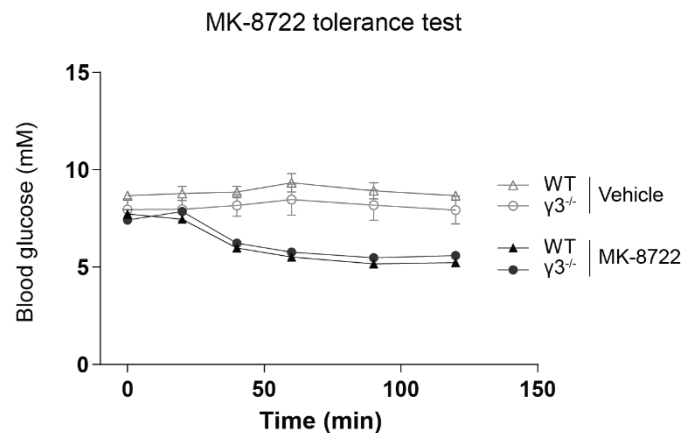
Figure 22 AMPKγ3 is dispensable for MK-8722-induced whole-body glucose clearance.
MK-8722 tolerance test of male WT and γ3$^{-/-}$ mice (10-12 weeks old). Mice were fasted for 3h in the morning and then orally administered with either vehicle (0.25% (w/v) methylcellulose, 5% (v/v) Polysorbate 80, and 0.02% (w/v) sodium lauryl sulfate in deionized water) or MK-8722 (10 mg/kg body weight) and blood glucose levels were monitored for 2h. GAS muscles were harvested and snap-frozen immediately after competition of the experiment. n=3-14 per genotype/treatment. Data are shown as means ±SEM. Statistical significance of blood glucose levels at the indicated timepoints was determined by two-way ANOVA with Bonferroni correction.

4.5.4   Role of AMPKγ3 in Glycogen Metabolism

While glucose uptake is broadly described as the process of glucose entering the cell through glucose transporters (e.g. GLUT1/GLUT4 in the case of skeletal muscle), this glucose transport is part of a three-step process also referred to as "glucose flux" [226]. Prior to glucose transport, glucose supply or delivery plays an important role and after the glucose transport, glucose metabolism determines the molecular fate of glucose inside the cell [60, 226]. Exercise studies in humans show a suppression of glucose oxidation to promote re-synthesis of glycogen, thus shifting the utilisation of glucose in favour of recovery [227]. Lack of AMPKγ3 [184] and α2 [228] was shown to increase glucose oxidation after exercise, suggesting a role of AMPK in this shift/suppression of glucose oxidation. This line of thought is supported by previous studies of a gain-of-function γ3 mutant which showed increased glycogen storage in mice [70] and humans [182], while a genetic loss thereof showed reduced glycogen levels in EDL [184].

To investigate the role of γ3 in glucose utilisation, we focused primarily on glycogen synthesis, although there are other pathways as shown in Figure 25. We initially measured *de novo* glycogen synthesis in *ex vivo* EDL in response to AICAR and MK-8722 Both activators increased glycogen synthesis by about 3-fold in WT muscles. Similar to results in glucose uptake (Figure 17A, Figure 19A), deletion of γ3 lead to blunted glycogen synthesis in response to AICAR, while MK-8722 stimulation was unaffected and showed a similar in glycogen synthesis in WT and γ3$^{-/-}$ muscles (Figure 23A).
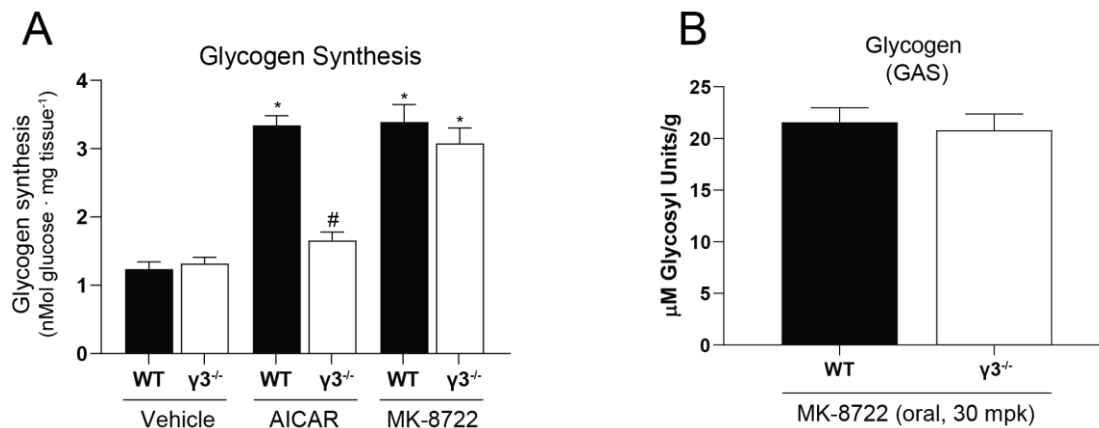
Figure 23 AMPKγ3 is required for AICAR-stimulated glycogen synthesis, but not for MK-8722.
A) EDL muscles were incubated in 2 ml of KRB buffer containing 5.5 mM d-glucose and 0.5 µCi/ml of [^{14}C]glucose for 80 min at 37°C in the presence or absence of either 2mM AICAR or 10 µM MK-8722. At the end of the incubation, muscles were rinsed with ice-cold KRB buffer, blotted on the paper, and quickly snap-frozen and glycogen levels measured as describd in MATERIALS and METHODS. Results are shown as means ± SEM and represent n=5-12 samples per genotype/treatment. Statistical significance was analysed by one-way ANOVA, using Bonferroni correction. *$P<0.05$ was accepted as significant and indicates an effect of activator (AICAR or MK-8722) vs Vehicle and #$P<0.05$ for an effect of WT vs γ3$^{-/-}$. **B)** Glycogen content of GAS muscles after oral MK-8722 tolerance test (30 mg/kg body weight). Results are shown as means ± SEM and represent n= 8-10 samples per genotype/treatment. Statistical analysis was performed by two-sided unpaired Student's t-test. GAS; gastrocnemius.

We wanted to take this observation one step further and measured glycogen levels in GAS muscles harvested after oral administration of MK-8722, resulting in lowered blood glucose levels without any difference in WT and γ3$^{-/-}$ mice (Figure 22). In line with this, glycogen levels in GAS after an oral dose of MK-8722 are unchanged in both genotypes (Figure 23A).
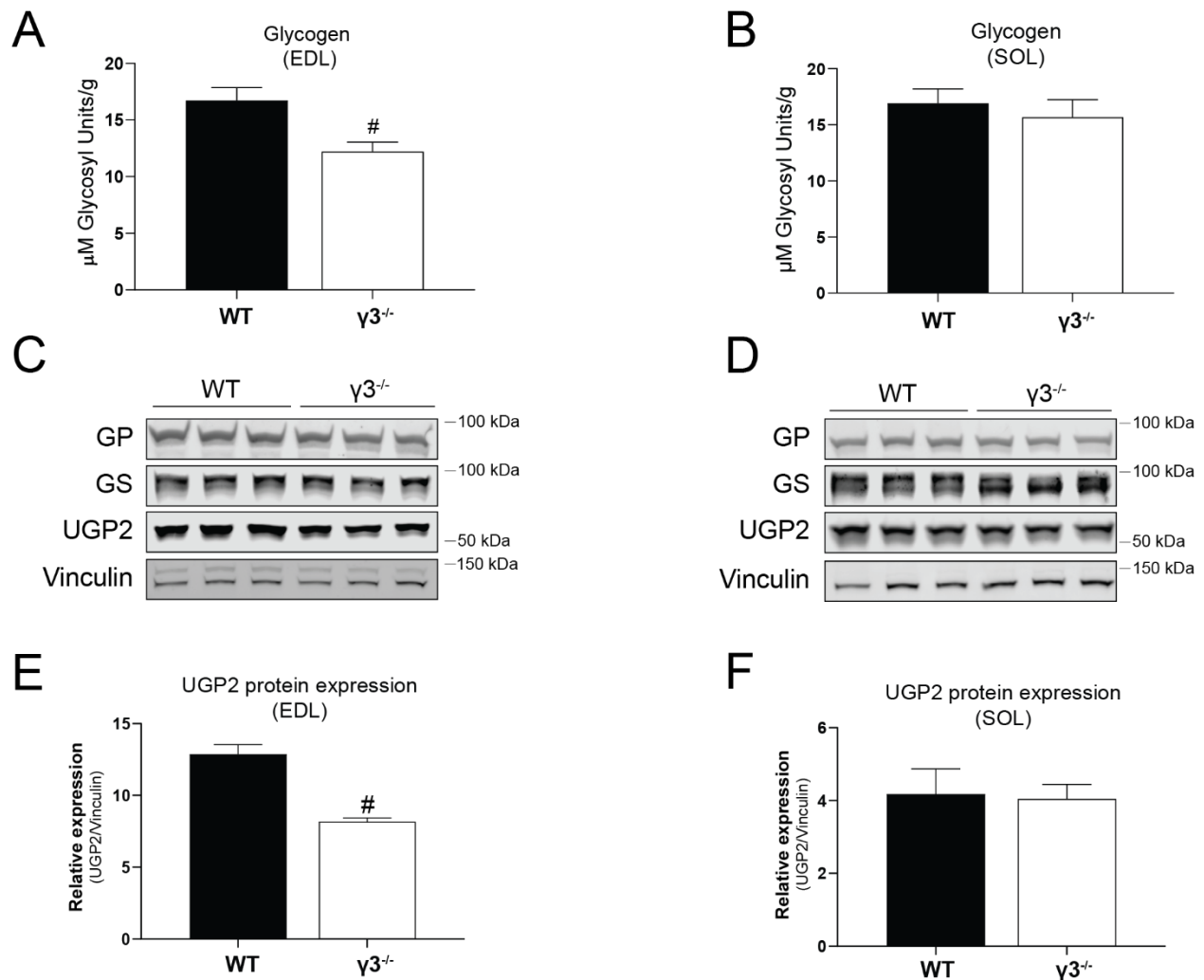
Figure 24 AMPKγ3 deficiency causes reduced glycogen and UGP2 expression in glycolytic muscles.
A-B) Glycogen content of basal EDL (A) and SOL (B) muscles.Results are shown as means ± SEM and represent n= 8-10 samples per genotype/treatment. Statistical analysis was performed by two-sided unpaired Student's t-test. **C-F)** Immunoblot (IB) analysis of key enzymes in glycogen synthesis and quantifications of UGP2 expression in EDL (C, E) and SOL (D, F). Blots and quantification were performed using a LiCOR system. IBs were performed using 20 µg of muscle extract and the indicated antibodies. Results are expressed as means ± SEM with n=7-8 animals per genotype. Statistical analysis was performed by two-sided unpaired Student's t-test and statistical significance shown as #P< 0.05 (WT vs γ3$^{-/-}$). EDL; extensor digitorum longus, SOL; soleus, UGP2; UDP-glucose pyrophosphorylase 2, GP; glycogen phosphorylase, GS; glycogen synthase [*Gys*1].

To validate also basal steady-state glycogen status, we measured glycogen levels in both EDL and SOL and analysed expression levels of key players in glycogen metabolism displayed in Figure 25. Previously, γ3$^{-/-}$

EDL was shown to have lower glycogen levels in fed and fasted state, while the gain-of-function γ3 R225Q mutant showed increased glycogen levels [184]. Confirming this finding, we observed 20-30% decreased glycogen levels in γ3$^{-/-}$ EDL but not SOL muscles (Figure 24A, B). By immunoblot analysis we could see similar levels of expression of glycogen phosphorylase (GP) and muscle glycogen synthase (encoded by GYS1) (GS) in both WT and γ3$^{-/-}$ muscles (Figure 24A, B). Intriguingly, we could detect a decreased expression in an ezyme catalysing the reaction from glucose-1-phosphate to the glycogen precursor UDP-glucose, namely UDP-glucose pyrophosphorylase 2 (UGP2). We found this decrease to be distinct in the glycolytic EDL (Figure 24C, E) and GAS (Appendix Figure 10C, E) muscles with 30-40% and 20-30% respectively as opposed to the oxidative SOL (Figure 24D, F). Further, we measured mRNA levels of *Ugp2* and saw a similar 20-30% decrease on the transcript level in GAS (Appendix Figure 10 E), but not SOL (Appendix Figure 10F). To test whether a reduction of UGP2 expression translates into reduced UDP-glucose and therefore reduced substrate availability for GS, we measured the content of UDP-linked hexose sugars, but did not see a difference in WT and γ3$^{-/-}$ mice (Appendix Figure 11). We verfied the specificity of the UGP2 antibody (#10391-1-AP, Proteintech) extensively in differentiating C2C12 myoblasts (Appendix Figure 12A), where UGP2 expression increases with in parallel with AMPKβ2 which was used as differentiation/myogenesis marker (Appendix Figure 12A, B). We also performed a siRNA knock down of UGP2 on day 4 during differentiation of myoblasts, which yielded in a 50% reduction of UGP2 expression (Appendix Figure 12C, D). Taken together, this indicates a role for γ3 in basal glycogen metabolism, possibly due to reduction in UGP2 expression, while expression of other key enzymes remains unchanged.
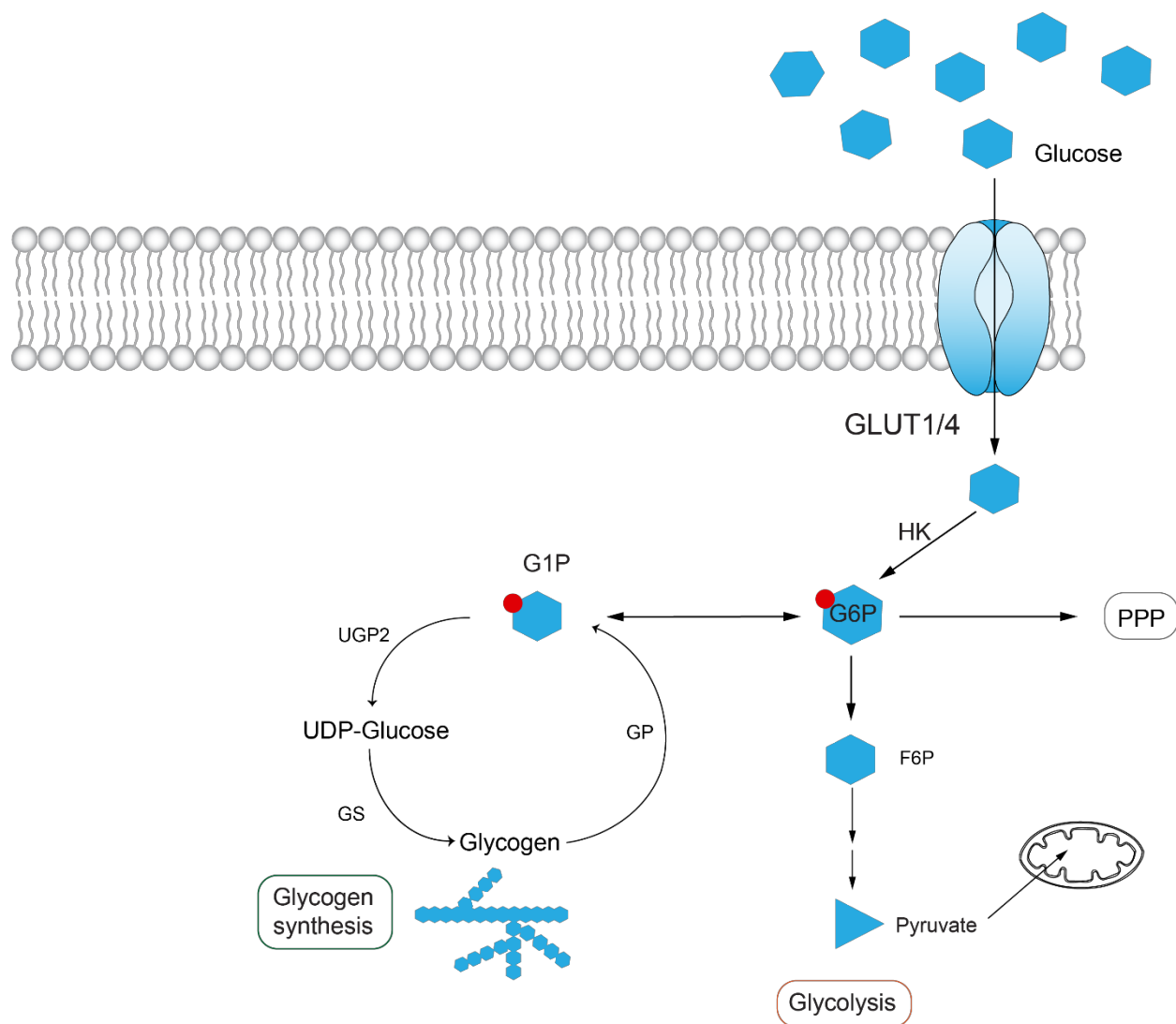
Figure 25 Simplified schematic representation of "glucose flux" in muscle cells.
Circulating glucose is transferred into the cell and phosphorylated by Hexokinase (HK) to form glucose-6-phosphate (G6P). G6P can be metabolised broadly in three different pathways, determining the cellular fate of glucose in the cell. The glycogen synthesis pathway comprises the formation of glucose-1-phosphate (G1P) which is the substrate for UDP-glucose pyrophosphorylase 2 (UGP2) to for UDP-Glucose. Glycogen synthase (GS) (GYS2 in muscle) uses the latter as substrate to form glycogen, which is readily broken down by glycogen phosphorylase (GP). PPP; pentose phosphate pathway, F6P; fructose-1,6-bisphosphate.

Given that genetic ablation of γ3 reduced UGP2 expression, we wanted to see if treatment with AMPK activators would in turn increase UGP2 expression and potentially play a role in accelerating the rate of glycogen synthesis as seen in (Figure 23A). We therefore analysed expression of the latter in AMPK activator (991) incubated EDL muscle.
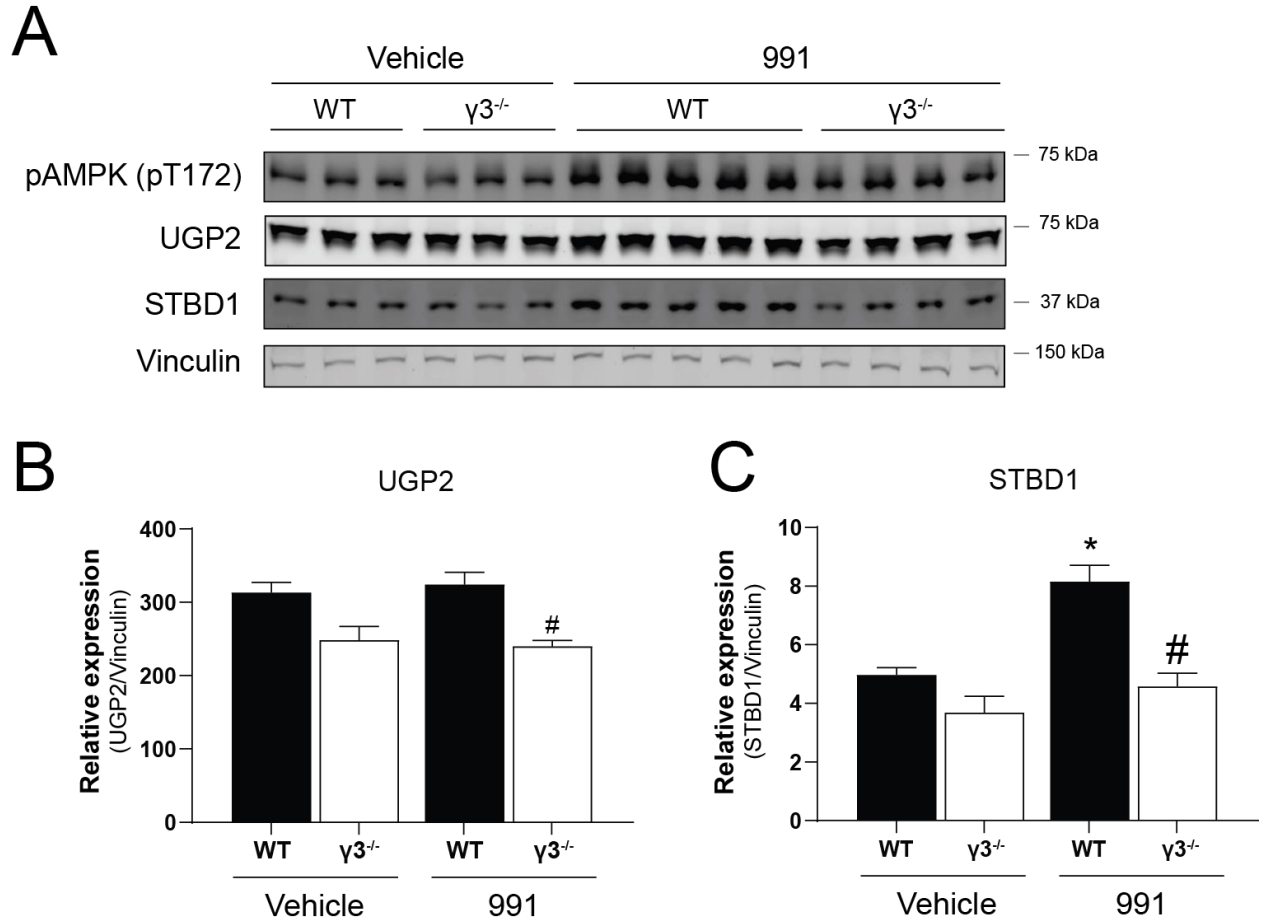
Figure 26 991 treatment increases STBD1 expression in WT EDL, but not in γ3^{-/-}.
A-C) Immunoblot (IB) analysis and quantification of lysates prepared from the *ex vivo* incubated EDL muscles. Blots and quantification were performed using a LiCOR system. IBs were performed using 20 µg of muscle extract and the indicated antibodies. UGP2 (B) and STBD1 (C) expressions were quantified by normalising to Vinculin. Phosphorylation of STBD1 was quantified as ratio of the phosphorylated protein and total protein (C). Results are expressed as means ± SEM with n=4-9 animals per treatment/genotype. Statistical analysis was performed by one-way ANOVA with Bonferroni correction and statistical significance shown as *$P< 0.05$ (Vehicle vs 991) and #$P<0.05$ (WT vs γ3^{-/-}). UGP2; UDP-glucose pyrophosphorylase 2, STBD1; starch binding domain-containing protein 1.

Despite a robust increase in AMPK phosphorylation (pT172), UGP2 expression did not change in WT EDL with 991 treatment. Lack of γ3 caused decreased UGP2 expression in 991-treated EDL muscles, while non-treated muscles showed a similar trend without reaching significance (Figure 26A, B). Initial experiments with MK-8722 incubated EDL muscles support the findings of unchanged UGP2 expression, while STBD1 expression increases with AMPK activation (Appendix Figure 13). Further, we performed qPCR on 991 and MK-8722 treated C2C12 cells, but equally could not detect any change in *Ugp2* transcript (Appendix Figure 14). Interestingly, another previously described AMPK target, starch binding domain-containing protein 1 (STBD1) [229] showed an increase of expression of about 50% in WT, but not in γ3^{-/-} EDL (Figure 26C). STBD1 was recently shown to promote clustering of glycogen in response to ER stress in C2C12 cells [230]

and to be involved in intracellular trafficking of glycogen to lysosomes [231]. Both studies also showed co-localisation of the protein to glycogen, thus indicating a spatial linking to a known AMPK target.
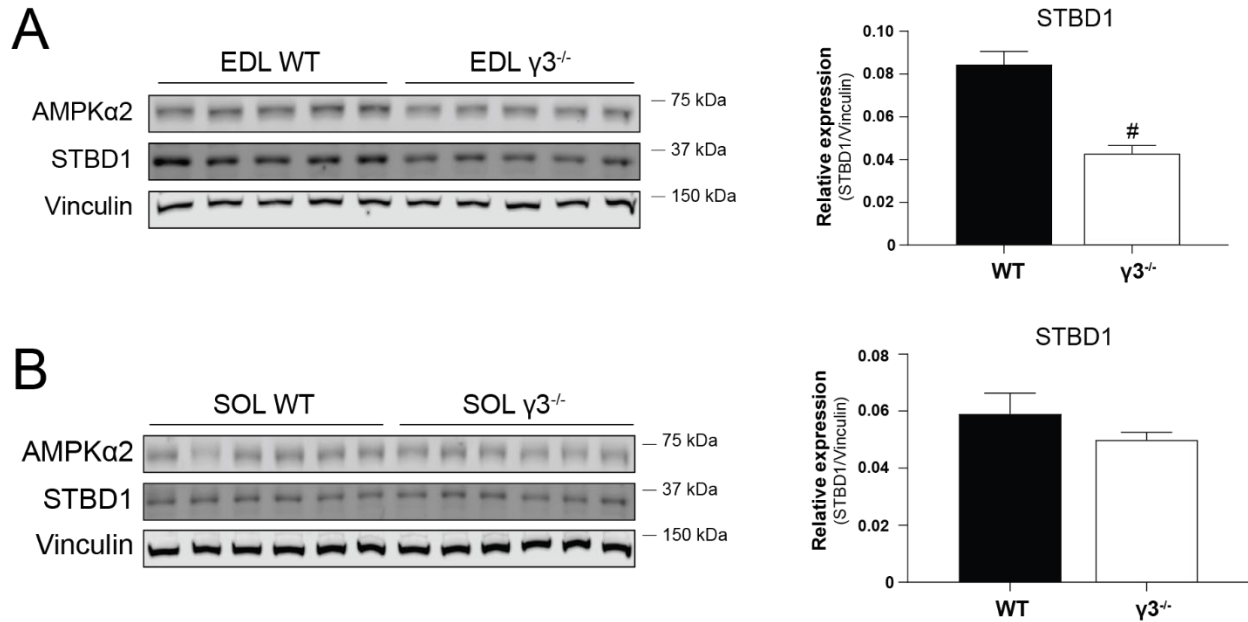
Figure 27 STBD1 expression is decreased in glycolytic γ3$^{-/-}$ muscles.
A-B) Immunoblot (IB) analysis and quantification of lysates prepared from either basal EDL (A) or SOL (B) muscles. Blots and quantification were performed using a LiCOR system. IBs were performed using 20 µg of muscle extract and the indicated antibodies. STBD1 expressions were quantified by normalising to Vinculin. Results are expressed as means ± SEM with n=5-6 animals per genotype. Statistical analysis was performed by unpaired two-sided Student's t-test and significance is shown as #P<0.05 (WT vs γ3$^{-/-}$). STBD1; starch binding domain-containing protein 1, EDL; extensor digitorum longus, SOL; soleus.

This led us to examine whether we see a link between decreased glycogen levels in basal glycolytic muscles (as shown in Figure 24A) and STBD1 expression. We compared STBD1 expression in EDL and SOL muscles and observed a decrease of STBD1 expression by about 50% in γ3$^{-/-}$ EDL, but not in SOL (Figure 27A, B). This correlates roughly with the previously seen 40-50% decrease in AMPKα2 expression (Figure 10A) in γ3 deficient EDL. Additionally, STBD1 expression was also reduced to a similar extent in GAS (Appendix Figure 15), indicating an effect in glycolytic muscles overall.

Given the previous reports on increased STBD1 expression in response to ER stress in myoblasts [230], we wanted to study the effects of AMPK activation (which physiologically happens by cellular energy stress) in the same system. We therefore treated C2C12 cells with direct AMPK activators with the aim to quantify STBD1 expression in response. In line with the *ex vivo* EDL results, 991 also increased STBD1 expression by about 50% in a time-dependent manner (Figure 28A, C). As a control, phosphorylation of ACC was also seen to increase by the same extent (Figure 28B).
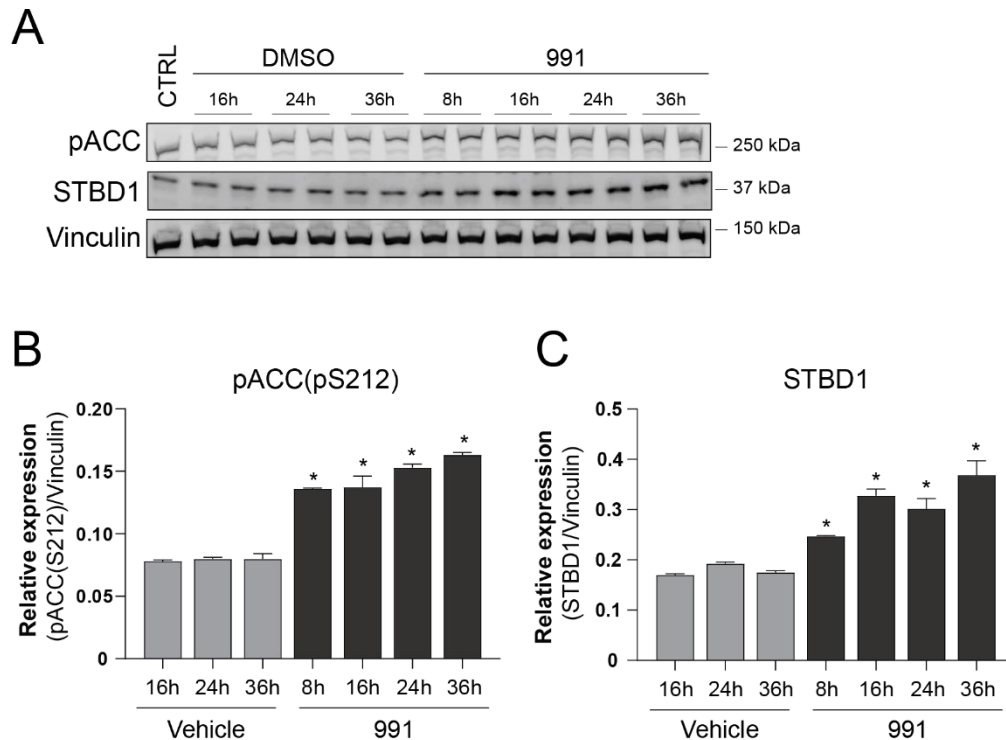
Figure 28 STBD1 expression increases in response to 991 treatment in C2C12 cells.
C2C12 myoblasts we treted with 10 μM 991 or 0.1% DMSO (Vehicle) (in duplicate) at day 7 of differentiation. **A-C)** Immunoblot (IB) analysis and quantification of cell lysates lysed after the indicated time of treatment.Blots and quantification were performed using a LiCOR system. IBs were performed using 20 μg of cell extract and the indicated antibodies. STBD1 expressions and ACC phosphorylation (pACC (pS212)) were quantified by normalising to Vinculin. Results are expressed as means ± SEM. Statistical analysis was performed by one-way ANOVA with Bonferroni correction (8h treatment was compared to 16h Vehicle treatment) and statistical significance shown as *$P < 0.05$ (Vehicle vs 991). STBD1; starch binding domain-containing protein 1.

Conform with expectations, treatment with the structural analogue compound MK-8722 showed very similar results of increasing STBD1 expression and ACC phosphorylation (Appendix Figure 16). Collectively, those results suggest that ablation of γ3 leads to lower levels of STBD1 expression in basal muscles and that expression of the latter increases in response to direct AMPK activators in skeletal muscle tisssues and cells.

5 Discussion I

The growing prevalence of type 2 diabetes and obesity-related metabolic diseases has long fuelled research into drug-targets to combat those adverse outcomes. AMPK emerged as an insulin-independent target that may overcome increasing problems of insulin resistance. The development of increasingly potent and direct (ADaM-site binding) AMPK activators with improved bioavailability measures sparked new interest in therapeutic applications thereof [99]. Early developments of allosteric, ADaM-site binding drugs highlighted the importance of targeting specific isoforms since early types of this drug class failed to robustly activate β2 complexes. Until this day, all drugs in this class show a preference to activate β1-containing complexes over their β2 equivalents. This is particularly important when targeting skeletal muscle since β2 is the predominant subunit isoform in skeletal muscle. Thanks to increased potency and binding affinities to β2 subunits of compounds like 991 [41], newly developed allosteric activators can be classed as pan-AMPK activators able to activate both β subunit isoforms. In the view of isoform-selective activation targeting of γ3 seems particularly intriguing as an entry point since its expression is largely restricted to skeletal muscle [67]. Thus, understanding of the physiological role of γ3 in regulation of glucose metabolism/homeostasis at both peripheral and whole-body levels are important for development of skeletal muscle-selective AMPK activators.

Two seminal recent papers particularly highlight the importance of skeletal muscle AMPK in mediation of anti-diabetic effects of allosteric AMPK activators. Both compounds PF-739 and MK-8722 (structurally related to 991) show improved glucose uptake *ex vivo* and glucose lowering effects *in vivo* through skeletal muscle AMPK in rodents and non-human primates [23, 24]. Despite the efforts in development of potent small-molecule allosteric activators, the requirement of γ3 for this activator class has not been explored but would provide important guidance for the evolution of next-generation activators. In this study, we used a whole-body γ3-deficient mouse model to show a selective loss of AICAR-, but not ADaM-site activator-induced glucose uptake both in glycolytic muscles *ex vivo* and on a whole-body level. We found a similar drug-dependent effect in the rate of glycogen synthesis, where AICAR-stimulated glycogen synthesis is blunted in γ3$^{-/-}$ EDL muscles *ex vivo*, but MK-8722 response being unaffected.

We show that γ3 ablation leads to reduction of α2 and β2 subunits of approximately 20-30% specifically in glycolytic EDL and GAS muscles, without translating to oxidative muscles like SOL. Based on previous findings of relatively low expression of γ3 in SOL (about 2% of present AMPK complexes) compared to β2

complexes forming around 80% of all AMPK complexes in the same muscle [224], it seems reasonable to assume that absence of a minor contributor to the whole AMPK pool does not significantly impact overall AMPK protein expression. On the other hand, EDL muscles were reported to express around 20% of γ3-containing complexes and 90-95% α2 and β2-contianing complexes with α2β2γ1 and α2β2γ3 being the predominantly expressed complexes [224]. Thus, lack of γ3 may well cause an excess of monomeric α2 and β2 isoforms which normally form complexes with the former. Excess subunits may then in turn be degraded and result in partial loss and reduced protein levels thereof. A similar effect was observed in γ1-deficient mice where expression of all subunit isoforms relevant for complex formation (α1, α2, β1 and β2) were greatly decreased in SOL [232]. In this regard, the effect size of a 20-30% loss of α2 and β2 in EDL and GAS seems smaller than in the γ1 KO, but appropriate to its overall contribution of AMPK complexes in those muscles. Notably, a previous γ3$^{-/-}$ model did not report a statistically significant reduction of either subunit isoform in GAS muscles. Nonetheless, a decrease of roughly 25% in α2 expression can be seen in γ3$^{-/-}$ GAS [70]. Statistical significance may not have been achieved due to insufficient power of the experiment. Further, the semi-quantitative nature of EDL detection may add to statistical variation and be less accurate than more advanced quantification methods [233]. We used extensive method validation with regard to signal quantification and two independent advanced technologies to confirm our results.

Since first reports of AICAR-mediated glucose uptake in skeletal muscle *ex vivo* [135], several efforts were made to decipher AMPK requirements for this effect. Models including a kinase-dead α2 mutant as well as α2 KO [68, 71] were followed by a β2 KO [69] and a γ3 KO model [70] to point out a dependence on those subunit isoforms, suggesting the AICAR effect to be dependent on a functional α2β2γ3 complex. We show that partial loss of γ3 in heterozygous (γ3$^{+/-}$, HET) EDL is neither sufficient to change protein expression of α2 or β2, nor to impair AICAR-induced glucose uptake *ex vivo*. Other models of partial genetic loss of specific subunit isoforms (e.g. α2$^{+/-}$ or β2$^{+/-}$) and their response to AICAR have not been reported. A model of LKB1 hypomorphic, in which AICAR-stimulated α2 activity is reduced by about 60% may serve as a suitable comparison and shows the intact ability increasing glucose uptake in response to AICAR [136]. Further, we show that the ability of ADaM-site binding AMPK activators 991 and MK-8722 to stimulate glucose is not impaired in γ3$^{-/-}$ EDL, despite depending on total skeletal muscle AMPK (Appendix Figure 7A and [24]). It therefore seems unlikely that a partial reduction of α2 (and as a result total α) and β2 alone causes the impairment of AICAR to increase glucose uptake in γ3 deficient glycolytic muscles.

Following our findings *ex vivo*, we also show that the AICAR-, but not MK-8722-mediated glucose clearance is impaired on a whole-body level in γ3$^{-/-}$ mice. As we see similar potencies of MK-8722 and 991

in *ex vivo* glucose uptake, as well as γ3 activation and AMPK downstream target phosphorylation (Figure 19), we assume that 991 would exhibit similar effects *in vivo* if its bioavailability issues could be overcome. This distinctly different response of AICAR and ADaM-site drugs is particularly intriguing since both activator types require functional AMPK to elicit their effects [23, 24, 71, 72, 76]. Both inactivated α2 and absence of α2 were shown to result in AICAR intolerance [68, 222, 234], supporting the thought of an effect of the predominant skeletal muscle α2 subunit isoform. We augment this line of thought by showing similar effects in γ3-deficient mice. On the contrary, γ3 is not required to produce a glucose-lowering effect with MK-8722 which we demonstrated in with a submaximal and maximal previously reported dose (Figure 22 and Appendix Figure 8A), falling in line with our previous *ex vivo* results.

In our study, we show that γ3-activation by AICAR appears stronger than by 991/MK-8722 (Figure 19B), but it needs to be noted that the applied AMPK activity assay reflects only phosphorylation levels of AMPK-pT172 and not allosteric activation by e.g. ADaM-site binding drugs. This results in a potential under-representation of AMPK activity in this assay and indicates additional comparison of AMPK target phosphorylation. As judged by phosphorylation of known AMPK targets such as ACC and TBC1D1, both AICAR and 991/MK-8722 appear to activate WT muscles to a similar extent. Interestingly though, phosphorylation of ACC and TBC1D1 was reduced in AICAR-, but not MK-8722 treated γ3^{-/-} EDL muscles thus mirroring glucose uptake results. This poses the question whether activation by AICAR or its metabolite product ZMP shows a γ3 subunit isoform-preference (e.g. γ3 over γ1). Despite binding to the same sites as AMP [235], ZMP binding affinity to purified AMPK is much lower than that of AMP [236]. Nonetheless, due to slow metabolisation of ZMP in the cell, AICAR still achieves robust activation of AMPK in most cell types and tissues [237]. So far, our understanding of the nucleotide regulation of AMPK is mostly based on γ1 complexes as no crystal structure of other γ isoform-containing complexes has not been published (or deposited to the database). Some studies examined the nucleotide regulation of multiple AMPK isoforms and have suggested that the isoform composition of the AMPK heterotrimer can influence nucleotide regulation [29, 41]. This offers the intriguing possibility that the various AMPK isoform complexes may play different roles in tissues in response to changes in the AMP/ADP to ATP ratio [21]. A comparison between the individual AMP binding sites revealed that AMP binding affinity to site 3 ("weak site", refer to Figure 1) of α2β2γ3 complexes is by an order of magnitude higher than that of the α2β2γ1 counterpart (K_d= 42±4 μM and 560±90 μM, respectively) [54]. Allosteric activation of AMP in γ3-containing complexes is somewhat disputed though, with only marginal activation reported in one study [29] and 1.5-fold comparison in another [54]. However, protein purity may be a cause for this disparity and translatability of those findings from recombinant proteins is not clear. Despite having highly

conserved CBS domains, the γ subunits show major differences when it comes to their N-termini. While γ3 and γ2 isoforms show large unrelated N-terminal extensions, γ1 does not. Both the structure and function of those extensions remains elusive to date.

A recent study aimed to shed light at this by comparing 991 activation of AMPK complexes harbouring different γ-N-termini. Interestingly, α2β2γ3 and α2β2γ1 were activated to a similar degree, while α2β2γ2 activation was roughly 50% higher. This effect was maintained in a γ1 chimeric construct containing the γ2 N-terminus and suggested to be due to enhanced protection from dephosphorylation, highlighting the N-terminal effect on AMPK activation [107]. This raises the question of how the γ subunit interacts with the ADaM-site located at the interface of α- and β-subunits and remains to be elucidated for both γ2 and γ3 isoforms. Other drug binding sites on the γ subunit were recently identified and shown to achieve γ1 and γ2 activation without affecting γ3 [238], suggesting the possibility of structural differences that could be exploited for γ isoform selectivity in the future.

After glucose is taken up by the cells, phosphorylation by hexokinase fixates it in the cytosol, which builds the basis for further utilisation in several metabolic pathways including glycolysis and glycogen synthesis. Although AMPK itself inhibits GS through phosphorylation in an α2-dependet fashion [239], this effect is overruled by allosteric activation of G6P [175]. Previous studies show increased levels of glycogen after exercise in gain-of-function γ3 mutants, while lack of γ3 resulted in lower glycogen levels [70]. In line with this, basal and *ex vivo* contracted γ3$^{-/-}$ EDL muscles showed lower glycogen levels than WT EDL, while γ3 R225Q mutants showed higher levels when compared to WT. Concomitantly, the authors found increased glucose oxidation in γ3$^{-/-}$ mice, indicating that the γ3 subunit regulates the molecular fate of glucose in skeletal muscle [184]. Suppression of glucose oxidation to favour glycogen re-synthesis was found to be increased in the post-exercise recovery period in humans [227], potentially providing a link to increased α2β2γ3-activity after exercise [65]. Utilising our γ3$^{-/-}$ model, we show that *de novo* glycogen synthesis is impaired in AICAR- but not MK-8722-stimulated EDL muscles, similar to our results of decreased glucose uptake in AICAR-treated γ3$^{-/-}$ EDL. Given the unchanged basal *de novo* glycogen synthesis rate, lower substrate availability through limited glucose uptake is most likely the reason for the decreased rate in glycogen storage. MK-8722 on the other hand increases glycogen synthesis in both WT and γ3$^{-/-}$ EDL and glycogen levels in GAS are unchanged after oral MK-8722 administration. A measurement of muscle glycogen after AICAR injection would add an additional layer of understanding of how the *de novo* glycogen synthesis translates into an *in vivo* system.

Despite unchanged rates of *de novo* glycogen synthesis we observed lower steady state levels of glycogen in both γ3$^{-/-}$ EDL and GAS muscles. Other reports of muscle-specific α1/α2 double KO (m-α1α2$^{-/-}$) also show lower glycogen levels in quadriceps [138]. However, differences in reports of γ3$^{-/-}$ of unchanged levels in γ3$^{-/-}$ GAS [70] while decreased in γ3$^{-/-}$ EDL [184] highlight the importance of consistent measures and comparisons of muscle types. Here, we compare both EDL and GAS as representatives of glycolytic muscles and use SOL as oxidative muscle with very limited expression of γ3. We see decreased steady state basal glycogen levels in both EDL and GAS, but not in SOL. This was accompanied by a reduction of UGP2 protein (and mRNA in GAS), which is essential in catalysing the formation of the glycogen precursor UDP-glucose. A similar decrease in UGP2 expression was reported in m-α1α2$^{-/-}$ quadriceps [138]. Earlier studies suggested a decrease in *Ugp2* mRNA in γ3$^{-/-}$ GAS while and increase was found in the γ3 R225Q mutant [212, 240]. This is consistent with increased protein levels in the equivalent pig γ3R200Q mutant [241, 242] and the γ2N488I heart mutant [243]. Although UGP2 is considered of minor importance for glycogen synthesis, our findings may suggest a partial role for UGP2 in steering glucose flux to glycogen synthesis. As a result, decreased UGP2 in γ3$^{-/-}$ EDL may in turn lead to lower glycogen levels. However, we did not find direct evidence of decreased UDP-hexose metabolite levels in γ3-deficient GAS or increased UGP2 expression with 991/MK-8722 treatment in at least WT EDL (Figure 26 and Appendix Figure 13). This may be due to chronic effects of AMPK activation that are reported in the γ2 mutant [243] and reflect the constitutively active γ3 mutants, but are not captured in our acute activation experiments.

While we could not detect an effect of acute AMPK activation on UGP2 expression, we could see a γ3-dependent increase of STBD1, which has previously been reported to be an AMPK substrate [229] and to be associated with glycogen spatially and metabolically [231]. Interestingly, a genetic loss of muscle GS and thus virtual absence of muscle glycogen correlated with a complete loss of STBD1 expression [231]. Similar to AMPK, STBD1 contains a CBM domain, the mutation of which causes reduced interaction with glycogen-associated proteins [244]. While STBD1 is involved in glycogen trafficking towards lysosomes in a process termed "glycophagy" [245], much of its physiological role remains to be studied. It may serve as a quality-control for newly produced glycogen [170] and thereby increase in expression in response to 991/MK-8722 as seen in EDL and C2C12 cells. If glycogen binding increases stability of STBD1, decreased glycogen levels as seen in γ3$^{-/-}$ EDL may destabilise it and increase its degradation as previously seen in a G6P-insensitive R582A KI model of liver glycogen synthase [246]. Whether the change in expression is merely a product of glycogen levels or specific to AMPK γ3 remains to be elucidated.

6 Results II

Role of AMPKγ3 in Brown Adipose Tissue (BAT)

6.1 Expression of AMPK Subunits and Complexes

Recently, it was suggested that *Prkag3* mRNA (encoding for AMPKγ3) is expressed in mouse brown adipose tissue precursors [77], which led us to investigate whether the same is true in BAT tissue on a protein level and whether γ3 is present as active AMPK heterotrimer. At first, we compared AMPK subunit isoform expression between skeletal muscle (EDL) and BAT from WT mice, which showed distinct differences between both tissues (Figure 29A). Both α and β subunit isoforms showed almost an inverted pattern, where skeletal muscle expression of α2 is far greater than that of BAT and α1 in expression is far greater in the latter compared to the former. Total AMPKα (as assessed by a pan AMPKα1/α2 antibody) expression seemed similar between both tissues, but efficacy of isoform-specific detection of this antibody is undocumented. Similarly, β subunit isoform expression covers polar opposites when comparing EDL and BAT. EDL expresses primarily the β2 isoform with barely any β1 detectable, while BAT shows far greater β1 expression and only small amounts of β2. AMPKγ1 expression is comparable in both tissues. As we could not detect γ3 from BAT lysates, we aimed to detect γ3-associated AMPK activity after immunoprecipitation with a γ3-specific antibody using GAS muscle as control. We could indeed detect γ3-activity in WT BAT, thus confirming the presence of γ3 in BAT and the presence of active/functioning AMPK complexes containing the latter (Figure 29B). To complement this finding, we wanted to investigate the identity of the AMPK complex containing γ3 in BAT. Similar to the previous activity assay, we immunoprecipitated BAT and GAS extracts to enrich either γ3-containing AMPK complexes and immunoblotted the precipitates with isoform-specific antibodies. The supernatants of this IP were taken for a further γ1-IP to compare subunit identities of γ1- and γ3-complexes (Figure 29B, C). We observed that γ3 forms complexes with α2 an β2 subunits, while only marginally interacting with their α1 and β1 counterparts (Figure 29B). This mirrors our finding in skeletal muscle, where γ3 also interacts primarily with α2 and β2. On the other hand, γ1-IP of BAT shows no preference for α subunit isoforms since both α1 and α2 are readily detected in BAT γ1 complexes. When comparing β subunits however, β1 is the preferred interaction partner for γ1 while almost barely any β2 is detected in the IP.

Further, we compared AMPK subunit expression in γ3-deficient BAT, but could not detect any significant change related to the genotype in either subunit isoform expression (Figure 29E, F) or AMPKγ1-activity (Appendix Figure 9).
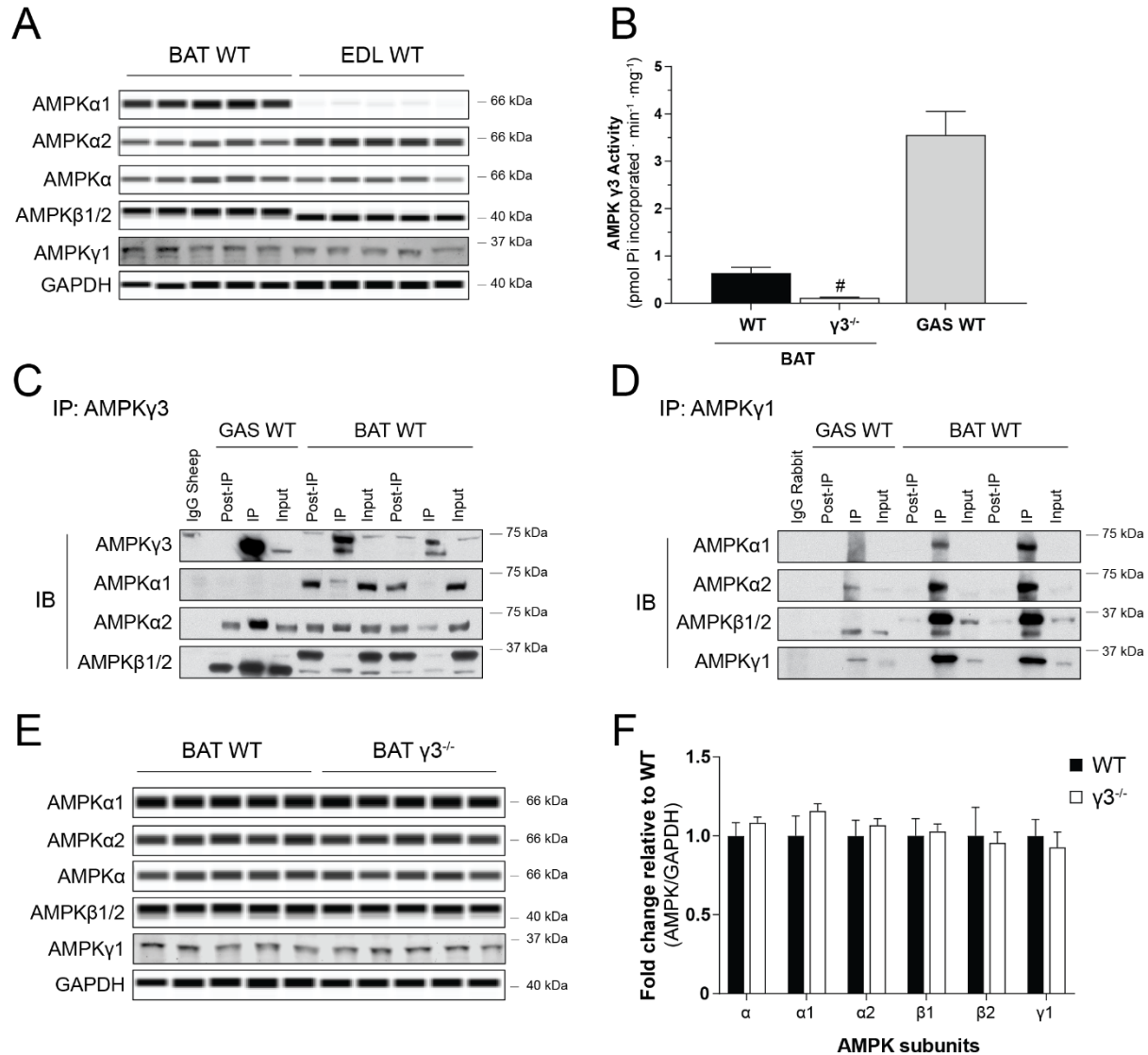
Figure 29 AMPKγ3 is expressed in mouse brown adipose tissue (BAT) and forms heterotrimeric complexes with α2 and β2 subunit isoforms.
A) Immunoblot (IB) analysis of AMPK subunit expression of BAT and EDL lysates from WT mice. Immunoblots were performed using 16 ng of muscle extract and the indicated AMPK isoform-specific and or pan-AMPKβ1/2 antibody using an automated capillary Western Blot system (Sally Sue, Protein Simple). AMPKγ1 was immunoblotted using 20 μg of tissue extract on a LiCOR-system due to antibody compatibility. **B)** *In vitro* AMPK activity assays (in duplicate) were performed on either 100 μg of immunoprecipitated GAS (n=3) or 1,000 μg of BAT extract (n=7) using AMPKγ3-specific antibody as described in MATERIALS and METHODS. **C-D)** Immunoprecipitation (IP) of 150 μg of GAS and 1,000 μg BAT lysate with an AMPKγ3-specific antibody (C). Immunoprecipitates were used for subsequent immunoblot (IB) analysis with the indicated AMPK isoform-specific and or pan-AMPKβ1/2 antibody and supernatants were subjected to another IP with with an AMPKγ1-specific antibody followed by IB as indicated (D). Horseradish peroxidase (HRP)-conjugated secondary antibodies and enhanced chemiluminescence (ECL) reagent were used for signal detection. GAS; gastrocnemius, BAT; brown adipose tissue.

6.2 Functional Role of AMPKγ3 in BAT

After confirming the expression and complex identity of γ3 containing AMPK complexes, we wanted to study potential physiological effects γ3 may have in BAT. Since it was shown that lack of AMPK impairs BAT-mediated thermogenesis [80], we wanted to test the hypothesis that γ3 would play a role in this effect. We therefore subjected mice to a 6h cold challenge and measured body temperature over time (Figure 30A). However, we could not see any difference in body temperature of the animals, pointing towards only a minor, if any role of γ3 in cold tolerance. We looked at AMPK activity to see if any change occurred between the genotypes during the cold challenge (Figure 30B, C). Confirming our previous finding, we could detect γ3-associated activity in BAT WT, yet seemed unchanged to basal conditions and still far below γ3-activity in GAS muscle (Figure 30B). AMPKγ1-activity should reflect all the non-γ3 activity in BAT and therefore act as somewhat of a proxy for overall AMPK activity in the tissue. When looking at γ1-assocaited activity though, no change between WT and γ3$^{-/-}$ mice could be detected (Figure 30C), suggesting that lack of γ3 does not impact BAT thermogenic function.
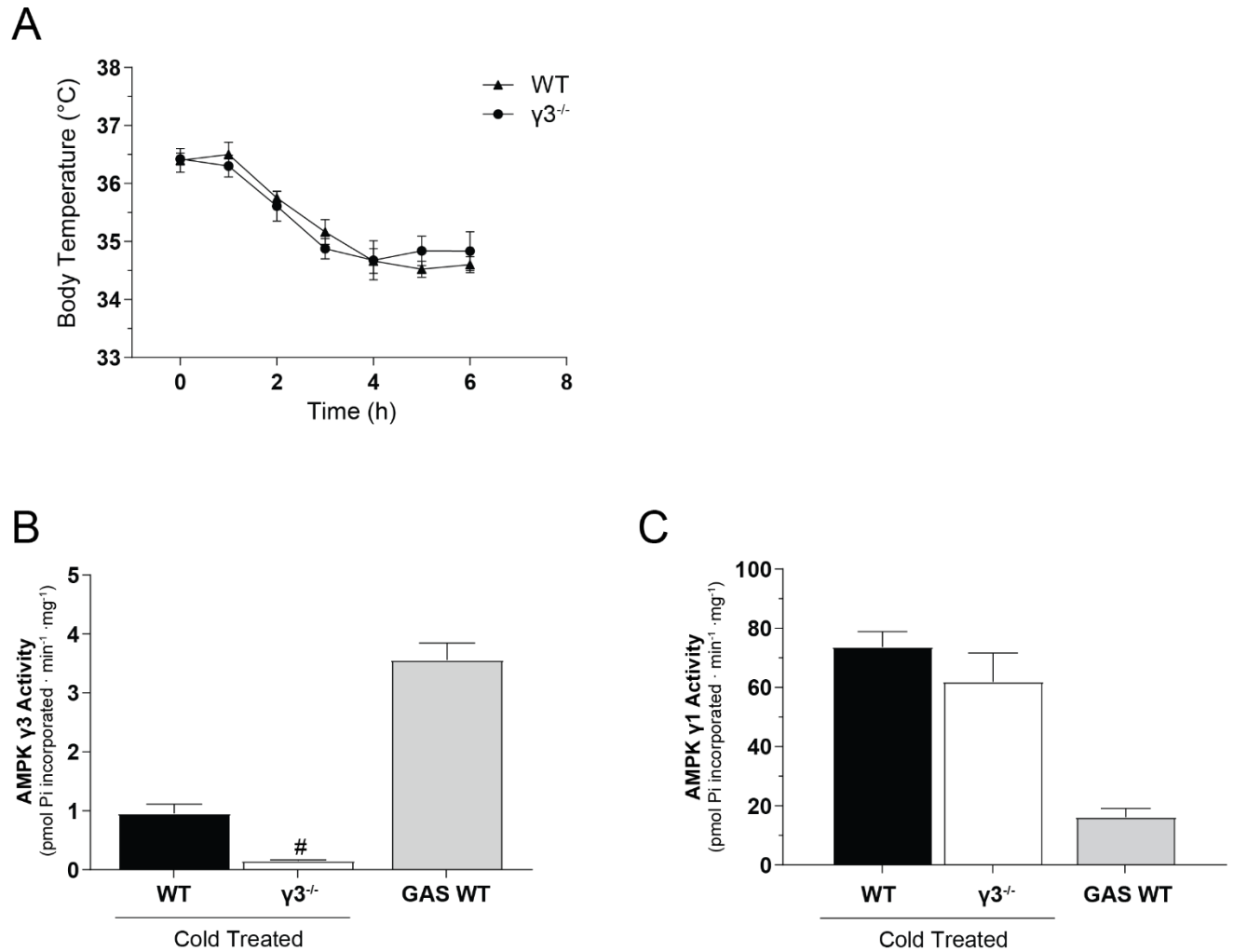
Figure 30 AMPKγ3 is dispensable for acute cold tolerance *in vivo*.
A) WT and AMPKγ3⁻/⁻ mice were subjected to a cold test of 4°C ambient temperature and body temperature was measured once per hour. Results are shown as means ± SEM for n=8 animals per genotype and analysed by two-way ANOVA, using Bonferroni correction. **B-C)** *In vitro* AMPK activity assays (in duplicate) were performed on either 100 µg of GAS (n=3) or 1,000 µg of BAT extract (n=8) using AMPKγ3-specific antibody (B). Supernatants were subjected to IP using AMPKγ1-specific antibody (C) and kinase assays were performed as described in MATERIALS and METHODS. GAS; gastrocnemius, BAT; brown adipose tissue.

To further validate our hypothesis of γ3 being dispensable for BAT thermogenic function, we collaborated with Prof Gregory Steinberg (McMaster University, Hamilton, ON, Canada) who performed experiments using β3-adrenoreceptor (β3-AR) agonists and sophisticated thermographic imaging to measure acute induction of UCP1-mediated thermogenesis and browning of inguinal white adipose tissue (iWAT). These experiments (Figure 31) were performed by Eric Desjardins (MSc).

In line with our findings, a single injection of β3-AR agonist CL-316,243 (CL) significantly increased oxygen consumption (Figure 31A), interscapular (IS) BAT surface area temperature (Figure 31B, C) and serum non-esterified free fatty acid (NEFA) concentration (Figure 31D) all to similar extent in WT and γ3⁻/⁻ mice.
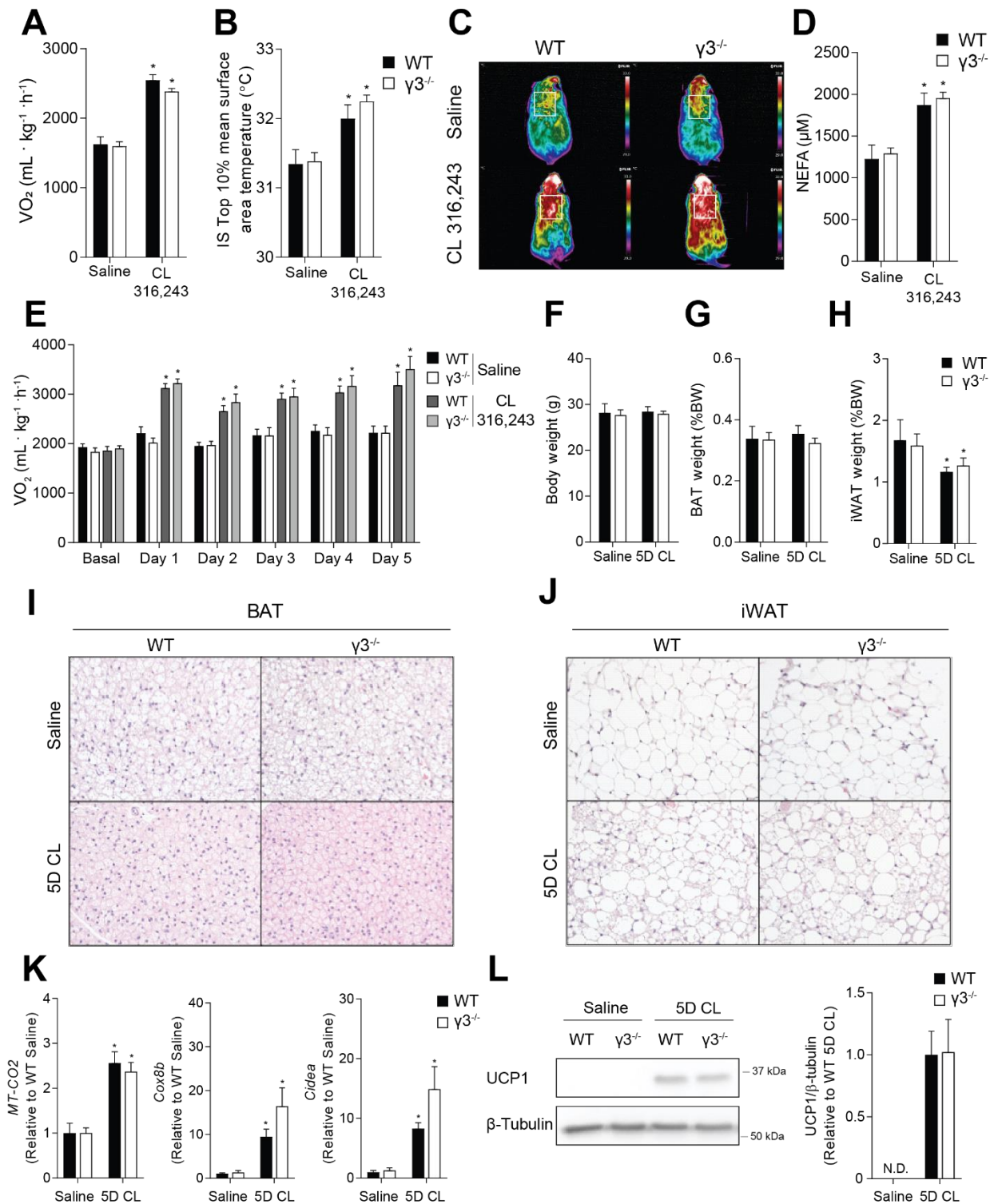
Figure 31 AMPKγ3 is not required for the acute induction of UCP1-mediated non-shivering thermogenesis in brown adipose tissue (BAT) or the adaptive response to non-shivering thermogenesis or the browning of inguinal WAT in mice. (Work performed by Eric Desjardins and Julian Yabut, McMaster University, Hamilton, ON, Canada)
A-D) Oxygen consumption (VO₂), (B) interscapular (IS) BAT surface area temperature with representative thermal images (C) and serum non-esterified free fatty acid (NEFA) concentration (D) in response to a single injection of saline or CL 316,243 (CL) in male

WT or γ3$^{-/-}$ mice (0.033 nmol/g, 20 min time-point), n=9-13 per group. Data are means ± SEM with a CL 316,243 effect shown as *P < 0.05, as determined via repeated measures two-way ANOVA. **E)** Oxygen consumption (VO$_2$) basally and 6h post-injection of saline or CL in male WT or γ3$^{-/-}$ mice on indicated days, n=5-8 per group. **F-J)** Final body weight (F), BAT weight (G), and inguinal WAT (iWAT) depot weight (H) after 5 consecutive days of saline or CL 316,243 (5D CL) injections in male WT or γ3$^{-/-}$ mice, n=5-8 per group. Representative histological images of H&E-stained (I) BAT and (J) iWAT (10X magnification) from male WT or γ3$^{-/-}$ mice treated with saline or 5D CL. **K)** mRNA expression of genes indicative of iWAT browning in male WT or γ3$^{-/-}$ mice treated with saline or CL for 5 days. (n=4-7 per group). **L-M)** Immunoblot (IB) analysis (L) and densitometry quantification (M) of UCP1 in male WT and γ3$^{-/-}$ mice treated with saline or CL for 5 days (n=6-8 per group). Data are means ± SEM with *P < 0.05 denoting a 5D CL effect, as determined via repeated measures two-way ANOVA (A) and regular two-way ANOVA. BAT; brown adipose tissue, iWAT; inguinal white adipose tissue.

We also studied a potential chronic and adaptation effect of β-adrenergic stimulation by administering CL for 5 days (5D CL) and analysing effects on BAT and browning of iWAT (Figure 31E-M). Daily injection of CL showed a significantly increased oxygen consumption (Figure 31E) as seen after a single injection. However, overall body weight and BAT weight were unaffected (Figure 31F, G). The total iWAT weight decreased after 5 days of treatment (Figure 31H) and the tissue appeared more multilocular, indicative of browning (Figure 31J). Both effects were similar between genotypes though and BAT morphology (Figure 31I) also seemed unaffected by lack of γ3. Chronic CL treatment significantly increased UCP1 protein expression as well as levels of other thermogenic and mitochondrial genes such as *Cox8b*, *Cidea* and *Cox2* (Figure 31K, L). These results demonstrate that γ3 is not required for β3-AR agonist-induced remodelling of BAT and iWAT in mice.

7 Discussion II

Recent research increasingly augments the traditional understanding of BAT beyond UCP1-mediated non-shivering thermogenesis [185, 186]. Despite BAT showing some of the highest AMPK activity of any tissues assessed [81], studies exploring a physiological role of AMPK in BAT only emerged rather recently. In a recent study, genetic models of an inducible adipocyte-specific AMPKβ1/β2 KO showed that AMPK plays a crucial role for mitochondrial integrity/function in BAT as well as being required for cold tolerance and β-adrenergic activation of brown and beige adipose tissues [80]. This provided a important insight into AMPK regulation of BAT and WAT metabolism but left open questions regarding the individual subunits and isoforms involved in this regulation. Previous studies showed α1 being highly expressed and active in BAT, yet fall short of information on the involved AMPK heterotrimer. Here, we show that γ3 is dispensable for acute β-adrenergic induction of UCP1-mediated non-shivering thermogenesis in BAT and chronic adaptive response to non-shivering thermogenesis and WAT browning.

Detailed studies of AMPK complex identity have not been performed, and to our knowledge presence of γ3 protein in BAT has not been demonstrated. Transcriptome profiling by RNA sequencing results from Perdikari *et al*. identified AMPKγ3 in mouse brown preadipocytes, but did not report protein expression [77]. Strikingly, they showed that RNAi-mediated knockdown of either γ1 or γ3 (but not γ2) in brown adipocyte precursors was enough to profoundly reduce UCP1 protein expression by approximately 80%. We used previously and extensively validated γ3-specific antibodies [73] (and Appendix Figure 1C) to show AMPKγ3 protein expression and γ3-associated AMPK activity in BAT. Moreover, we could confirm preferential expression of α1 and β1 subunits in BAT as compared to their α2 and β2 counterparts in skeletal muscle. Despite this shift in subunit isoform expression, γ3 still occurs in complexes comprised of α2 and β2, similar to what we observed in skeletal muscle.

Even though we showed that γ3 is dispensable for β-adrenergic agonist-induced thermogenesis and remodelling of BAT and iWAT, future studies are of potentially γ3 specific activation or γ3-transgenic models are warranted to investigate roles in adipose browning and subsequent amelioration of insulin resistance and fatty liver. Limitations of this approach may be posed by the overall relatively low activity of γ3 compared to other AMPK subunit isoforms. Likely, only a robust isoform-specific activation may be enough to cause γ3-mediated effects on overall BAT metabolism. Recent studies of a constitutively active gain-of-function AMPKγ1 (D316A) mutant highlight potential benefits in high fat diet-induced weight gain

and energy expenditure possibly independently of BAT or UCP1 through other adipocyte subpopulations [191, 198]. This shows the heterogeneity of adipocytes and the need for a more differentiated approach of targeting. Expression and potential roles of AMPKγ3 in those subpopulations as well as potential therapeutic benefits remain to be explored.

8 Conclusion and Outlook

In this study we investigated the role of AMPK from a focus of skeletal muscle as a key tissue of glucose homeostasis in physiological responses like exercise- or insulin-stimulated glucose uptake. An increasing amount of interest is building up to understand the metabolic regulation of this tissue as a therapeutic target for type 2 diabetes since it may open the door to avoid critical side effects which limit pharmacological potential. AMPK-mediated glucose uptake as such acts independently form insulin signalling and may therefore be of great benefit in settings of increasing insulin resistance and the recognition of severity [247].

We used a constitutive knock-out of the muscle-selective AMPKγ3 isoform to compare effects of the AMP-mimetic AICAR and a novel class of direct allosteric activators represented by compounds 991 and MK-8722. We show that a lack of γ3 in glycolytic muscles blunts *ex vivo* glucose transport in response to AICAR, but not to direct AMPK activators (991 and MK-8722). We could see this effect translating into a whole-body glucose clearance phenotype, which raises the intriguing question of differential activation of γ subunit isoforms by different activators. A difference in AICAR response is particularly interesting since the acting AMP analogue ZMP may indicate differences in AMP response in natural physiological settings. Although chronic AICAR-exposure improves diabetic and insulin resistance phenotypes in rodents [248-250], results in humans are far more ambiguous (or marginal) [251-253] and given its lack of oral availability and known side-effects [254, 255] it is unlikely to be suitable for therapies and even as AMPK-targeted drug. Compounds like R419 were shown to activate AMPK by inhibition of mitochondrial complex I, in effect raising AMP levels [97, 100].Future developments of skeletal muscle targeted or tissue-specific drugs raising AMP-levels, could take advantage of activation of γ3 complexes and elicit beneficial effects with the potential of lower side-effects.

Based on available reports using pre-clinical models (up to non-human primates) *in vivo* ADaM site binding drugs appear AMPK-selective, but may not necessarily be the ideal way of achieving a γ3 and thus potentially skeletal muscle-specific AMPK activation either since the link of that binding site to the identity of the γ3 subunit isoform is unclear. Nonetheless, recent cellular studies indicate a difference in response to 991 may depend on the γ subunit isoform, with γ2 being more potent than its γ1 and γ3 counterparts [107]. However, the translation of this effect into *in vivo* settings remains to be proven. Additionally, β2-selective ADaM site binding drugs and crystal structures of β2-contianing complexes were recently

reported [51], possibly achieving somewhat of a similar feat of selective activation of skeletal muscle AMPK. Clearly, crystal structures of γ3-complexes would aid to select the best strategy to achieve γ3-selectivity and clarify if that can be achieved by the ADaM site. We and others before [54, 256] managed to express bacterial α2β2γ3 complexes of high purity, but this has yet to translate into structural information.

Another strategy may be to exploit binding sites in the γ subunit other than that of AMP as shown with the prodrug compound 13 and the acting compound C2 [257] and its selectivity of γ1 and γ2 complexes over their γ3 equivalents [238]. It should be noted that competition with AMP [257] poses a risk of adverse effects in physiological environments. However, the differences in responses to γ subunit isoforms of multiple compounds highlight the possibility of potential structural differences between the three isoforms and future discoveries of more detailed structural elements should be able to advance knowledge on specific activation thereof. Interestingly, a recent study investigated the possibility of exercise-responsive myokines to increase glucose uptake and found that this may be mediated by γ3 [215], suggesting that a field of endogenous AMPK ligands may be underexplored and offer an alternative approach in the search of isoform-specific ligand binding.

Glycogen metabolism is known to be affected by either loss- or gain-of-function γ3 mutations [70, 184, 211, 258]. We show that acute glycogen synthesis in response to increased glucose uptake is unchanged following treatment with direct AMPK activators. Reduced AICAR-stimulated glucose uptake is likely to reduce glycogen synthesis in turn, suggesting that the ability of *de novo* glycogen synthesis is not changed in γ3$^{-/-}$ muscles. However, reduced steady-state glycogen levels in basal glycolytic γ3$^{-/-}$ muscles suggest an effect of γ3 on the molecular fate of glucose in the cell. This may partly be mediated by reduced expression of UGP2, which may act as a minor fine-tune mechanism to direct glucose flux towards glycogen synthesis. We also saw increased expression of STBD1 but were unable to propose a comprehensive mechanism for this. It is important to consider that steady-state measurement of metabolites such as glycogen do not provide any information on metabolic mechanisms *per se* but provide a single timepoint assessment. Analysis of the glycolytic flux would provide an additional layer of information and the existence of modern techniques (e.g. metabolomics coupled with isotope labelled precursors) are already established and positioned for this type of analysis [259, 260].

9 Appendix

Supplementary Table 1 List of the primary antibodies.
IB; immunoblot, IP; immunoprecipitation, IF; immunofluorescence.

Primary antibody	Application (IP/IB/IF)	Supplier	Reference
AMPKα1	IP	Custom-made (MRC PPU Reagents & Services, University of Dundee)	[73]
AMPKα2	IP		[73]
AMPKγ3	IP		S673D, [73]
AMPKα1/α2	IB	Cell Signaling	2532
AMPKβ1/β2	IB	Cell Signaling	4150
TBC1D1	IB	Cell Signaling	6929
Akt	IB	Cell Signaling	4691
phospho-Akt (Ser473)	IB	Cell Signaling	4060
GAPDH	IB	Cell Signaling	2118
Vinculin	IB	Cell Signaling	13901
Hexokinase II	IB	Cell Signaling	2867
GLUT4	IB	Abcam	ab654
AMPKα1	IB	MilliporeSigma	07-350
AMPKα2	IB	MilliporeSigma	07-363
pospho-TBC1D1 (Ser231)	IB	MilliporeSigma	07-2268
UCP1	IB	Alpha Diagnostic International	UCP11-A
β-tubulin	IB	Invitrogen	32-2600
AMPKβ1	IB	Proteintech	26907-1-AP
AMPKβ2	IB	Proteintech	14429-1-AP
UGP2	IB	Proteintech	10391-1-AP
Total OXPHOS Cocktail	IB	Abcam	ab110413
AMPKγ3	IP/IB	Custom-made (YenZym)	YZ4698, [73]
AMPKγ1	IP/IB	Custom-made (YenZym)	YZ5115, [73]
Myh7 (MyHCI)	IF	DHSB	BA-F8
Myh2 (MyHCIIa)	IF	DHSB	SC-71
Myh4 (MyHCIIb)	IF	DHSB	BF-F3
Laminin	IF	Sigma	L9393

Supplementary Table 2 List of the secondary antibodies.

Secondary antibodies	Supplier	Reference
Peroxidase AffiniPure Goat Anti-Rabbit IgG	Jackson ImmunoResearch	111-035-144
Donkey anti-Mouse IgG Alexa Fluor 680	ThermoFischer	A10038
Goat anti-Rabbit IgG Alexa Fluor 680	ThermoFischer	A21109
Goat anti-Mouse IgG2b Alexa Fluor 350	ThermoFischer	A-21140
Goat anti-Mouse IgG1 Alexa Fluor 594	ThermoFischer	A-21125
Goat anti-Mouse IgM Alexa Fluor 647	ThermoFischer	A-21238
Goat anti-Rabbit IgG Alexa Fluor 488	ThermoFischer	A-11008

A

Mouse genomic locus

5` UTR  1  2  3  4  5  6  7  8  9  10  11  12  13  3` UTR

Targeting locus

Targeting allele

1 2 3 4 5 6 7 8 9 10 Puro 11 12

LHA: 5.9 kb   FR: 2.3 kb   SHA: 3.2 kb

1 2 3 4 5 6 7 8 9 10 Puro 11 12 13

Conditional KO

1 2 3 4 5 6 7 8 9 10 11 12 13

Constitutive KO

1 2 3 4 11 12 13

loxP site

FRT site

B

	WT	HET	γ3⁻/⁻
n	50	98	52

C

GAS

WT   γ3⁻/⁻

AMPK γ3 →

— 75 kDa
— 50 kDa
— 37 kDa
— 25 kDa
— 20 kDa
— 15 kDa
— 10 kDa

D

Total activity (motion)

Activity counts/h

20,000
15,000
10,000
5,000
0

WT   γ3⁻/⁻   WT   γ3⁻/⁻
Dark   Light

E

VO$_2$ mean

mL · h^{-1} · g^{-1} (bw)

5,000
4,000
3,000
2,000
1,000
0

WT   γ3⁻/⁻   WT   γ3⁻/⁻
Dark   Light

F

Cumulative food intake

Food intake (g)

5
4
3
2
1
0

WT   γ3⁻/⁻   WT   γ3⁻/⁻
Dark   Light

Appendix Figure 1 Strategy of generating AMPKγ3-deficient mice and antibody verfication.

A) Genomic targeting strategy for creating AMPKγ3$^{-/-}$mice. **B)** Genotype frequency during breeding of AMPKγ3$^{-/-}$ mice. **C)** Verification of γ3-specific antibody (YZ4698) raised against a combination of human and mouse AMPKγ3 peptide, human AMPKγ3 [residues S45–S65: *CSSERIRGKRRAKALRWTRQKS], mouse AMPKγ3 [residues S44–S64: *CSSERTCAIRGVKASRWTRQEA] by YenZyme (San Francisco, CA, USA). 20 μg of WT and γ3$^{-/-}$ GAS lysate was immunoblotted as a whole membrane with 1 μg/mL antibody in 5% BSA. Horseradish peroxidase (HRP)-conjugated secondary antibodies and enhanced chemiluminescence (ECL) reagent were used for signal detection. D-F) Total activity (D), oxygen consumption (E) and food intake (F) of WT and γ3$^{-/-}$ mice was measured in week 9 with 12h light/dark cycles. Data is shown as mean ± SEM of n=10 mice per genotype and two-way ANOVA, using Bonferroni correction. GAS; gastrocnemius.

Appendix Figure 2 Verification of AMPKγ3 expression in soleus muscle.

A) Immunoblot (IB) analysis of soleus (SOL) muscles with the indicated AMPK isoform-specific antibodies. Horseradish peroxidase (HRP)-conjugated secondary antibodies and enhanced chemiluminescence (ECL) reagent were used for signal detection. **B)** Immunoprecipitation (IP) of 200 μg of S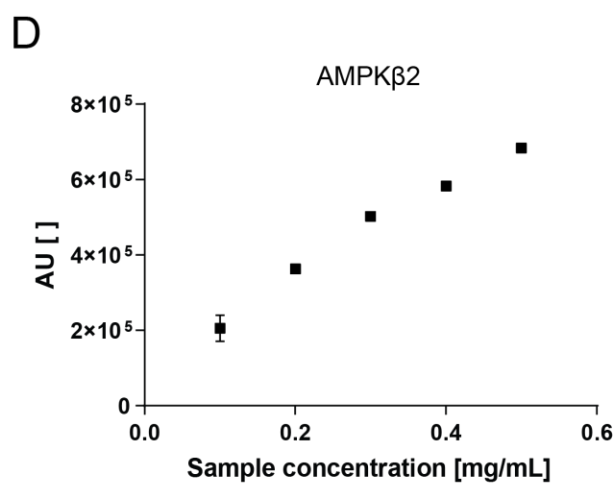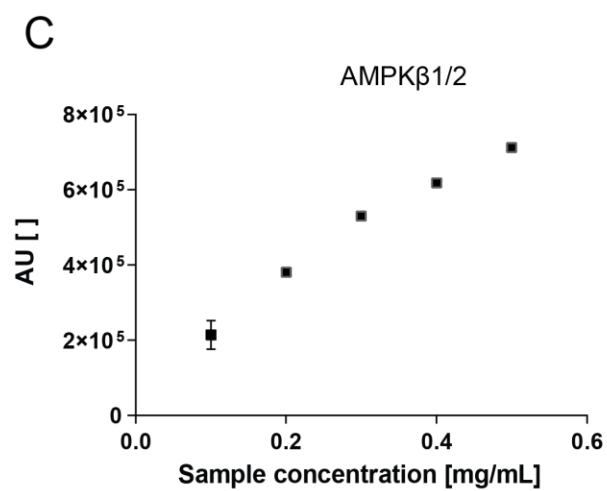OL lysate with either γ3-specific antibody (S673D) or species-matched immunoglobulin G (IgG) and subsequent IB with another γ3-specific antibody (YZ4698). Horseradish peroxidase (HRP)-conjugated secondary antibodies and ECL reagent were used for signal detection and two exposure times are shown. SOL; soleus.
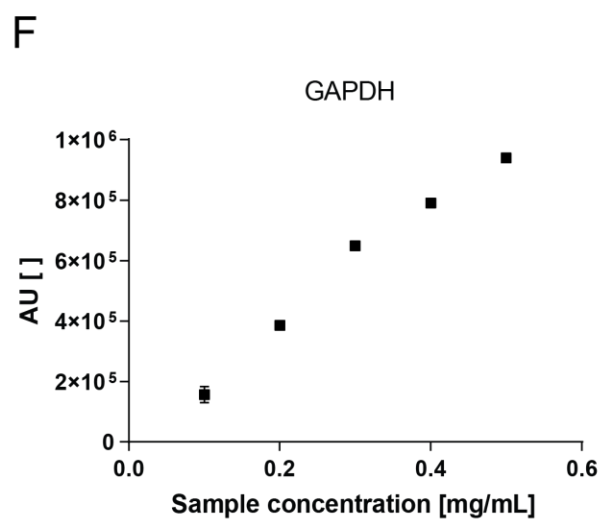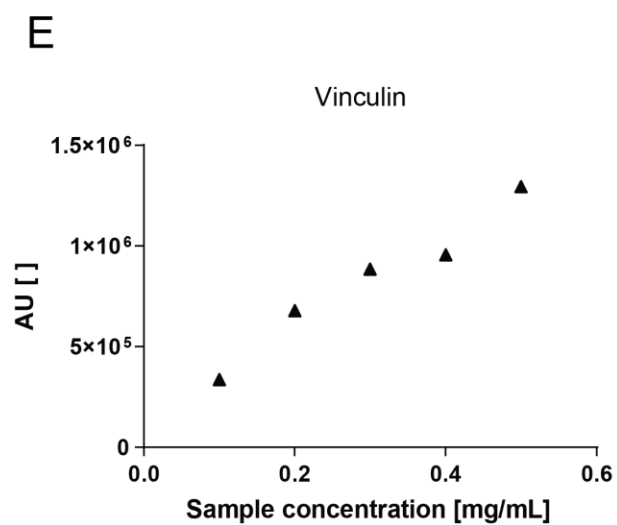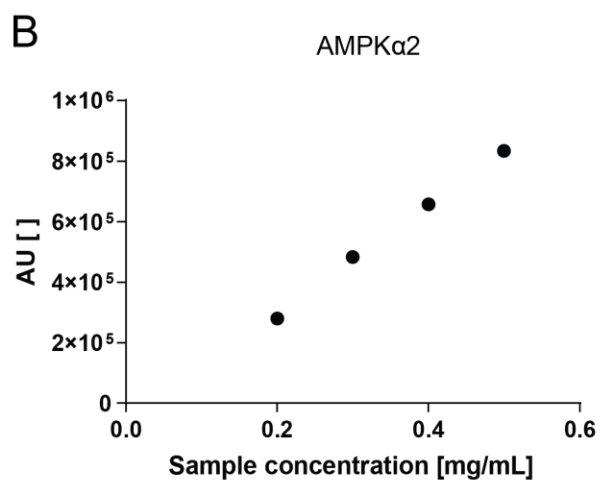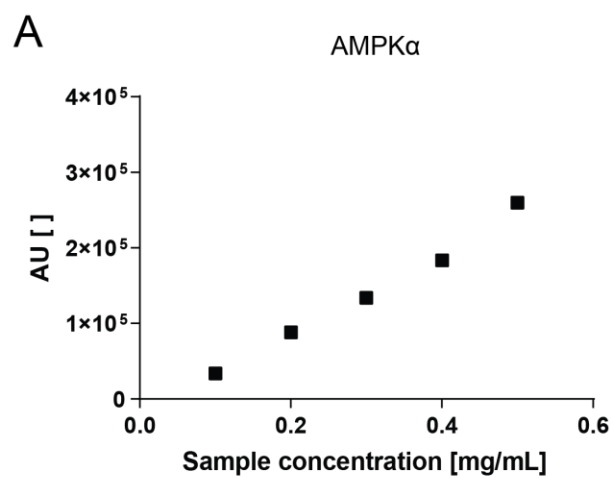
Appendix Figure 3 Verification of signal linearity of either AMPK subunit-specific antibodies (A-D) or loading controls (E, F) using an automated capillary Western Blot system (Sally Sue, Protein Simple).
Immunoblots were performed using varying sample concentrations of EDL extract and the indicated AMPK isoform-specific and or pan-AMPKβ1/2 antibody. The system uses 40 nanolitres (nL) of sample for an individual capillary, yielding in 4-24 ng of total protein used for the blots.
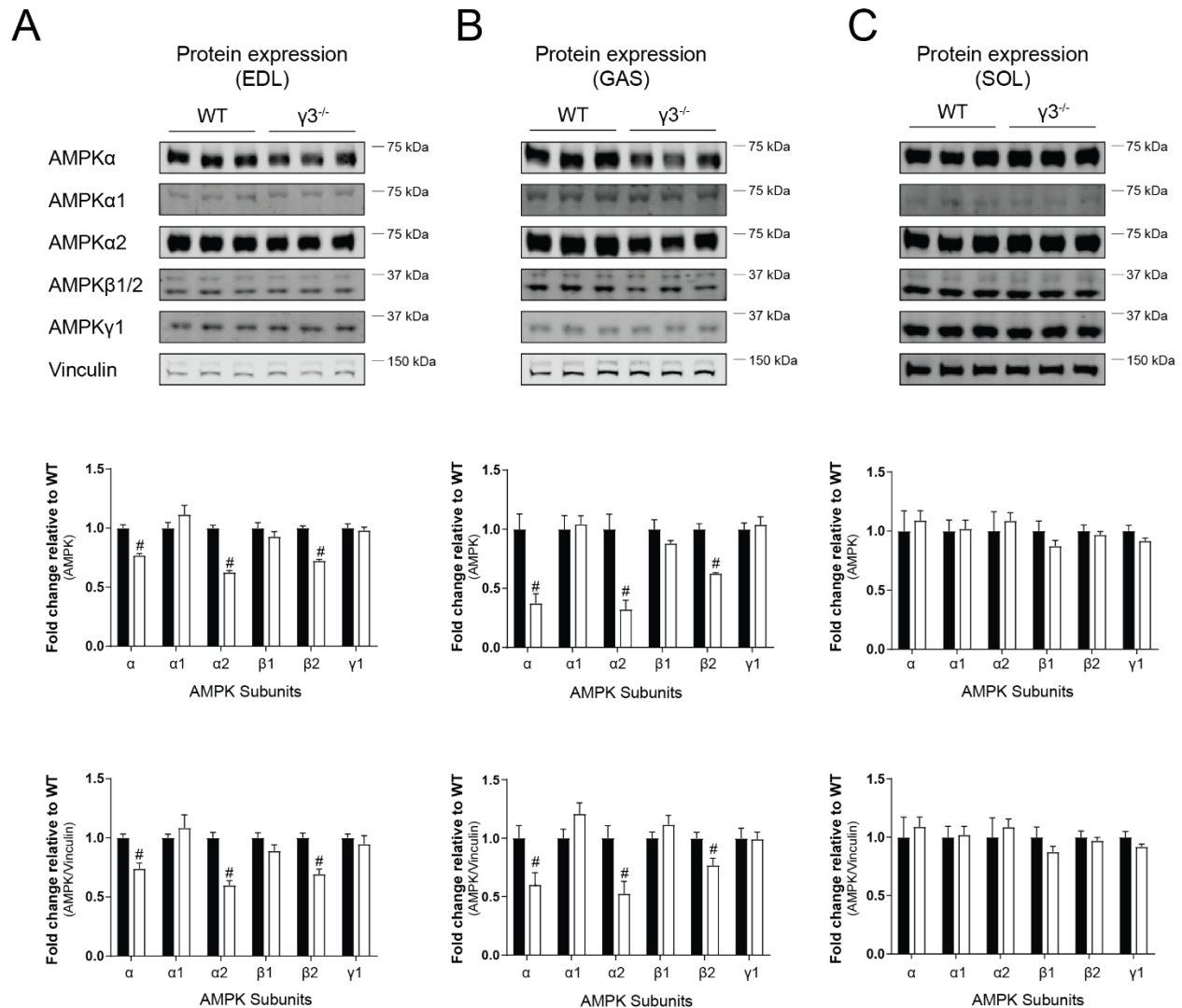
Appendix Figure 4 Genetic deletion of the AMPKγ3 isoform causes reduced expression of AMPK α2 and AMPK β2 isoforms in glycolytic muscles.
A-C) Representative immunoblots and quantification of AMPK subunit expression in EDL (A), GAS (B) and SOL (C) muscles using a fluorescence-based Western Blot system (LiCOR). Immunoblots were performed using 20 μg of muscle extract and the indicated AMPK isoform-specific and or pan-AMPKβ1/2 antibody. AMPK subunit isoform expressions were normalised by their respective Vinculin expression and are shown as fold change relative to WT muscle. Values are plotted as means ± SEM and represent n=5-8 samples per muscle/genotype. Statistically significant changes in expression were determined by an unpaired Student's t-test and are shown as #$P<0.05$. GAS; gastrocnemius, EDL; extensor digitorum longus, SOL; soleus.

Appendix Figure 5 Genetic deletion of the AMPKγ3 isoform does not change mRNA levels of AMPK subunit transcripts.

Relative levels of mRNA of the indicated genes (encoding AMPK subunit isoforms) in GAS (A) and SOL (B) were assessed by qPCR (n=5 muscle/genotype). Results are shown as means ± SEM. Statistically significant changes in expression were determined by an unpaired Student's t-test. GAS; gastrocnemius, SOL; soleus.
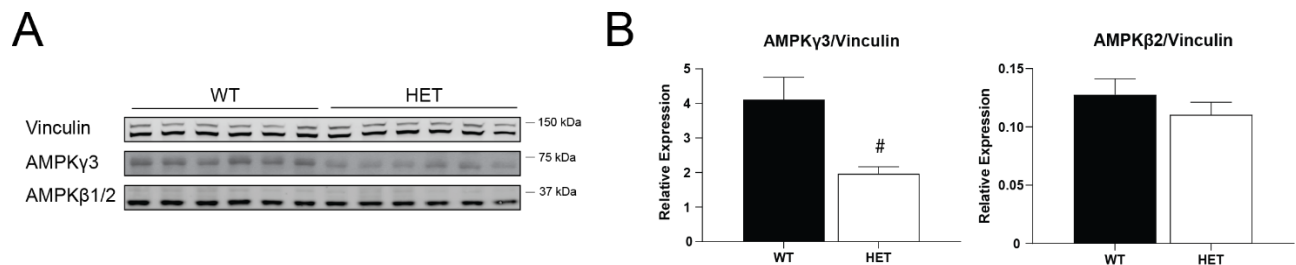
Appendix Figure 6 Partial loss of AMPKγ3 is not sufficient to cause a change in AMPKβ2 subunit expression. **A-B)** Representative immunoblot (A) and quantification (B) of AMPK subunit isoforms in WT and heterozygous (γ3$^{+/-}$, HET) EDL muscles. Immunoblots were performed using 20 μg of muscle extract and the indicated AMPK isoform-specific and or pan-AMPKβ1/2 antibody using the LiCOR system. AMPKγ3 expression was compared using 20 μg of muscle extract and detection using horseradish peroxidase (HRP)-conjugated secondary antibodies and enhanced chemiluminescence (ECL) reagent due to antibody compatibility. Bands were quantified using densitometry analysis of the ImageJ software (Java-based image-processing and analysis software). AMPK subunit isoform expressions were normalised by their respective Vinculin expression. Data are shown as means ± SEM and represent n=6 samples per genotype. Statistically significant changes in expression were determined by an unpaired Student's t-test and are shown as #P<0.05.
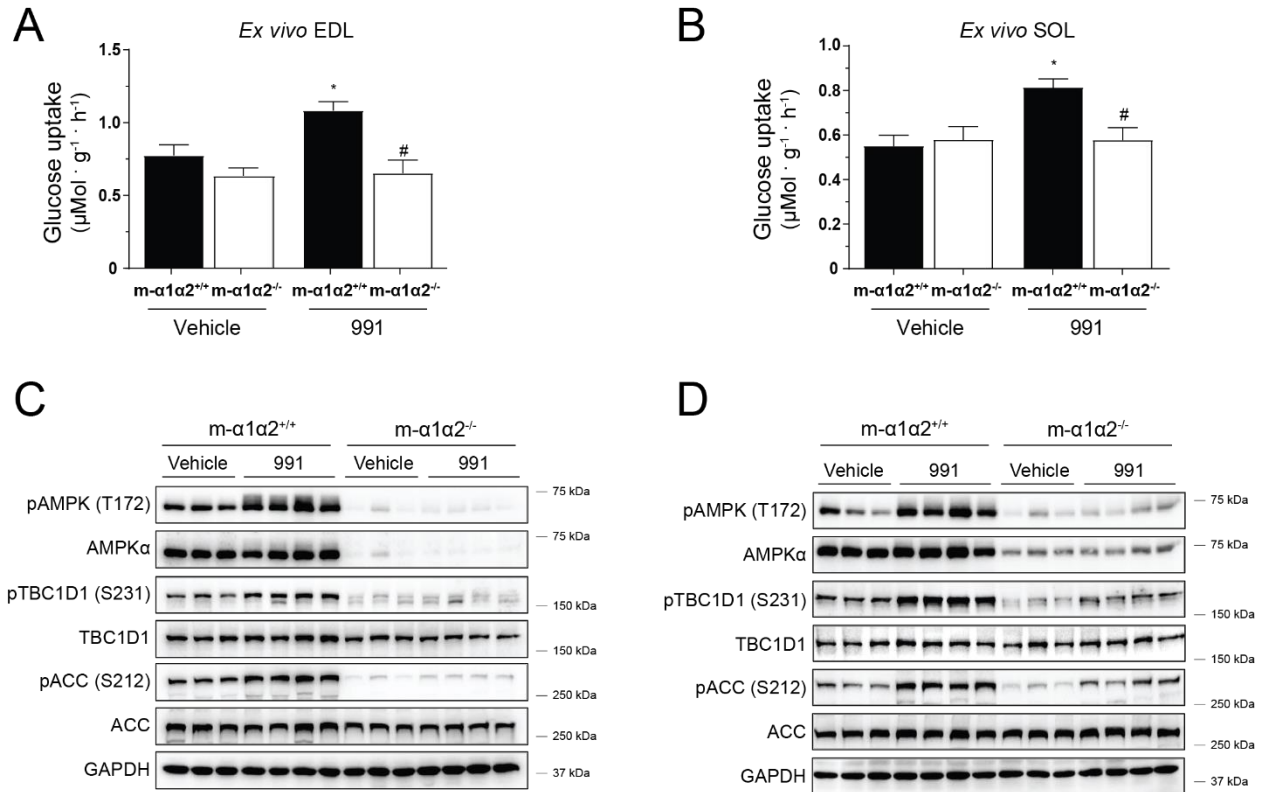
Appendix Figure 7 AMPK α1/α2 is required for 991-mediated glucose uptake in skeletal muscle. (Work performed in group of Prof Shuai Chen, University of Nanjing, China)

EDL and SOL muscles from wild-type (WT) and muscle-specific AMPKα1/α2$^{-/-}$(m-α1α2$^{-/-}$) mice were isolated and incubated with 0.1% DMSO (Vehicle) or 10 μM 991 for 50 min in Krebs-Ringer buffer (KRB) containing 2 mmol/L pyruvate. Muscles were transferred to vials containing 2-deoxy-[^{3}H] glucose (2-DG) with or without 10 μM 991 for 10 min. At the end of the incubation, muscles were immediately snap frozen in liquid nitrogen for further analysis. Lysates were split for glucose uptake analysis (A, B) and immunoblots using a LiCOR detection system (C, D). **A-B)** Glucose transport in EDL (A) and SOL (B) was assayed from muscle lysates as described above. C-D) Immunoblot (IB) analysis of lysates prepared from the incubated muscles. IBs were performed using 20 μg of muscle extract and the indicated phospho-specific and total protein antibodies. Results are expressed as means ± SEM with n=3-4 animals per treatment/genotype. Statistical analysis was performed by one-way ANOVA with Bonferroni correction and statistical significance shown as *$P< 0.05$ (Vehicle vs 991) and #$P<0.05$ (WT vs m-α1α2$^{-/-}$). EDL; extensor digitorum longus, SOL; soleus.
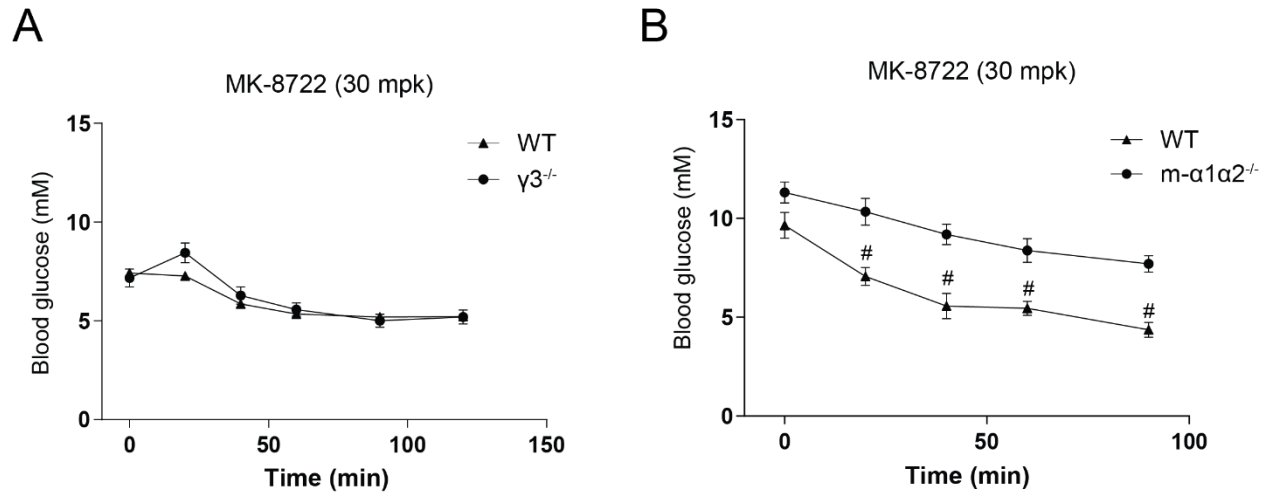
Appendix Figure 8 AMPK α1/α2 but not AMPKγ3 is required for MK-8722-induced whole-body glucose clearance. MK-8722 tolerance test of male WT and either γ3$^{-/-}$ mice (A) or muscle-specific AMPKα1/α2$^{-/-}$(m-α1α2$^{-/-}$) mice (B) (10-16 weeks old). Mice were fasted for 3-4h in the morning and then orally administered with either vehicle (0.25% (w/v) methylcellulose, 5% (v/v) Polysorbate 80, and 0.02% (w/v) sodium lauryl sulfate in deionized water) or MK-8722 (30 mg/kg body weight) and blood glucose levels were monitored for either 2h or 90min. GAS muscles were harvested and snap-frozen immediately after completion of the experiment. n=3-14 per genotype/treatment. Data are shown as means ±SEM. Statistical significance of blood glucose levels at the indicated timepoints was determined by two-way ANOVA with Bonferroni correction. and statistical significance shown as #P< 0.05 (WT vs KO).
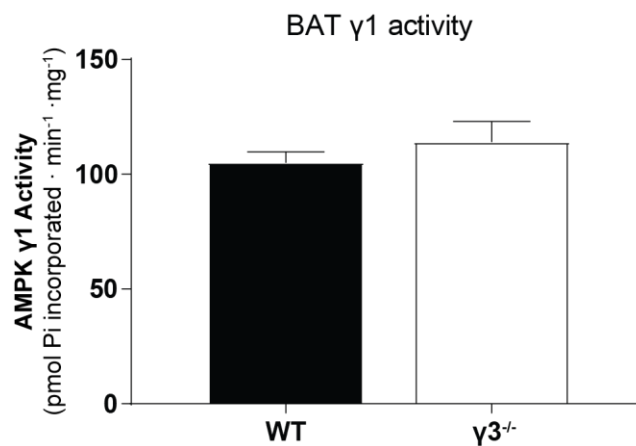
Appendix Figure 9 Genetic deletion of AMPKγ3 does not alter γ1-associated AMPK activity in mouse brown adipose tissue (BAT).
In vitro AMPK activity assays (in duplicate) were performed on 100 μg of immunoprecipitated BAT extract using AMPKγ3-specific antibody or species-matched immunoglobulin G (IgG) as described in MATERIALS and METHODS. Values are plotted as means ± SEM and represent n=9 samples per tissue and genotype. Statistically significant results were determined by a two-tailed unpaired Student's t-test.
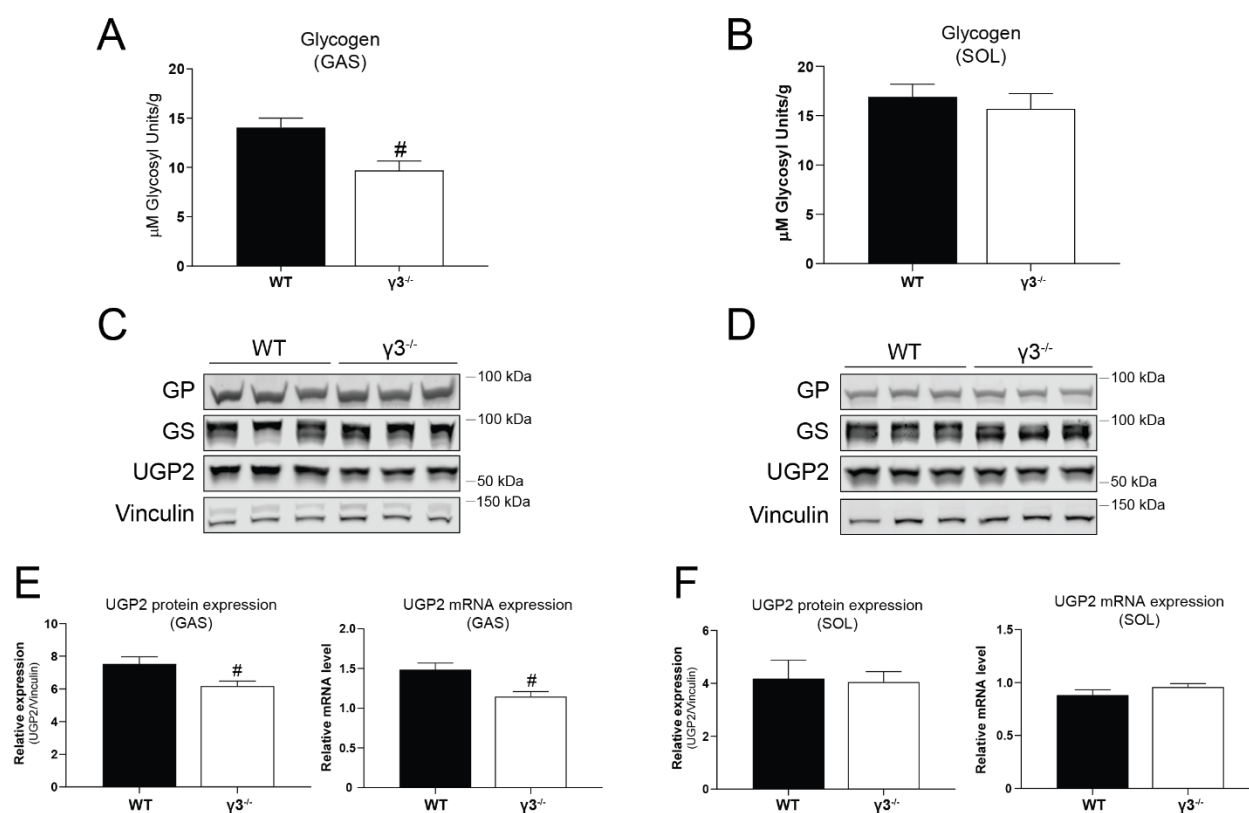
Appendix Figure 10 Glycogen content and expression of UDP-Glucose Pyrophosphorylase 2 (UGP2) is decreased in γ3$^{-/-}$ GAS muscle.

A-B) Glycogen content measurement in GAS (A) and SOL (B) muscles as described in MATERIALS & METHODS. **C-D)** Representative Immunoblot (IB) analysis of basal GAS (C) and SOL (D) muscles with the indicated antibodies. IBs were performed using 20 µg of muscle extract and detection on a LiCOR system.

E-F) Quantification of UGP2 expression (mRNA and protein) of GAS (E) and SOL (F) muscles. Results are expressed as means ± SEM with n=7-8 animals per treatment/genotype. Statistical analysis was performed by a two-tailed unpaired Student's t-test with significance shown as #P<0.05 (WT vs γ3$^{-/-}$). GAS; gastrocnemius, SOL; soleus, GP; glycogen phosphorylase, GS; glycogen synthase [*Gys2*], UGP2; UDP-glucose pyrophosphorylase 2.

UDP-Hexose

Lactate

Pyruvate
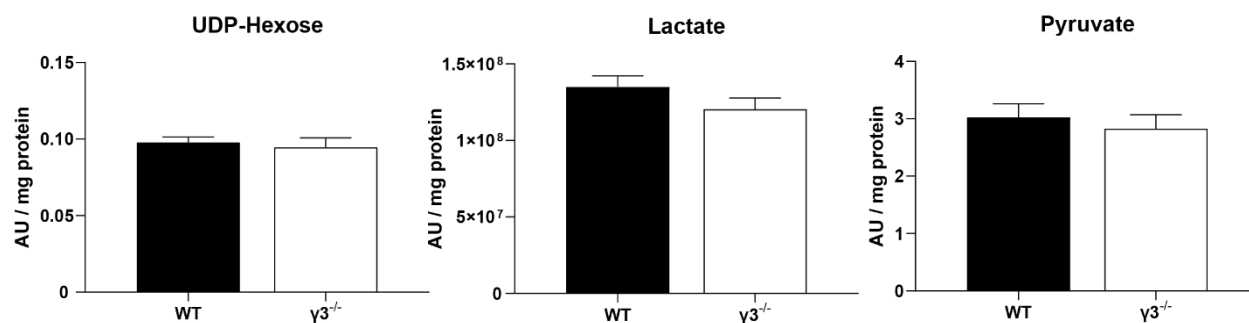
Appendix Figure 11 Metabolite contents in GAS muscle measured by LC-MS.
Frozen GAS muscles were used for liquid-liquid extraction with chloroform, methanol and water and metabolites measured by LC-MS. All metabolite data was normalised to internal standards and to protein amount. Results are expressed as means ± SEM with n=10 animals per genotype. Statistical analysis was performed by a two-tailed unpaired Student's t-test.

A

B

C

D
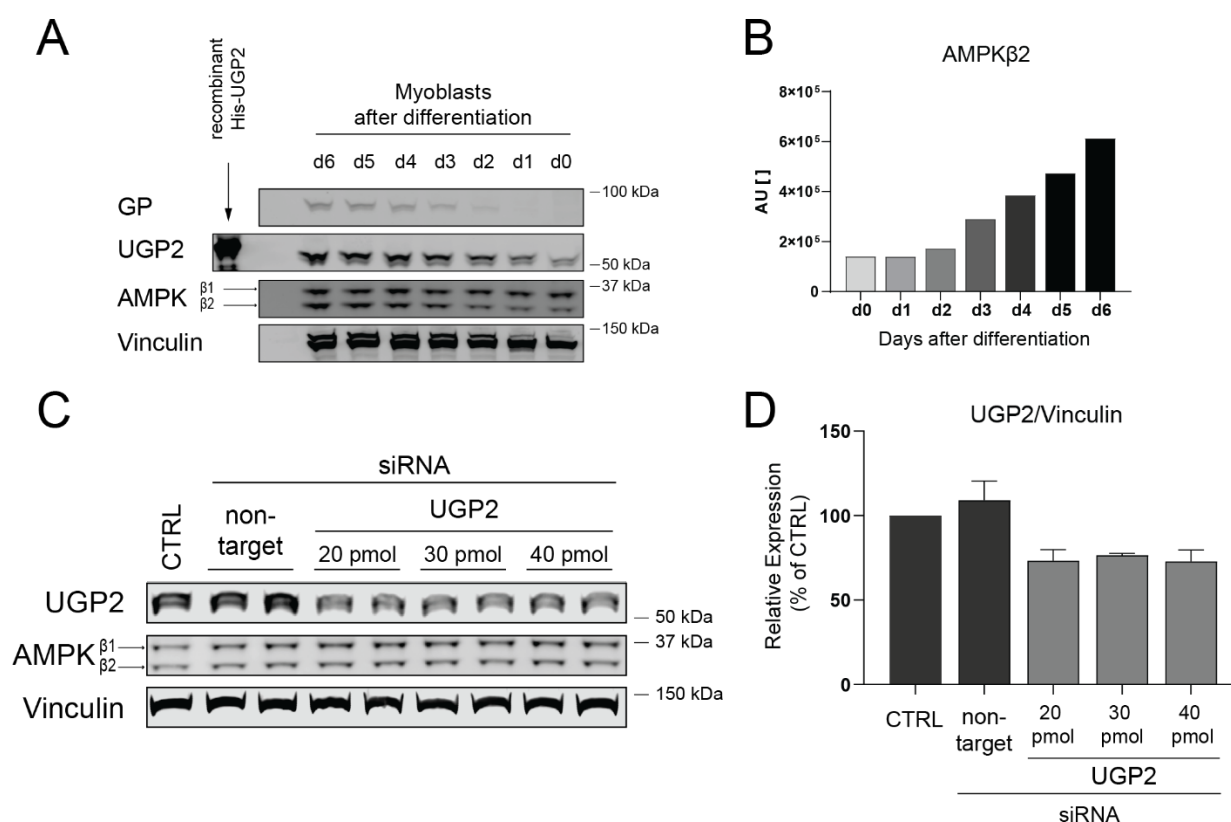
Appendix Figure 12 UGP2 expression increases in with progressing myogenesis in C2C12 cells.
A-B) Immunoblot (IB) analysis of myoblasts at different stages of differentiation with the indicated antibodies. IBs were performed using 20 µg of cell lysate and AMPKβ2 quantified (B) using a LiCOR system. **C-D)** IB analysis for validation of UGP2 antibody (Proteintech #10391-1-AP) by siRNA knock down of the target. IBs were performed using 20 µg of cell lysate either not transfected with siRNA (CTRL), transfected with 40 pmol of scramble siRNA (non-target) or varying amounts UGP2-targeting siRNA (A) for 24h on day 4 of differentiation before changing medium and harvesting after 48h. UGP2 was normalised by Vinculin and quantified relatively to the non-transfected control. UGP2; UDP-glucose pyrophosphorylase 2.
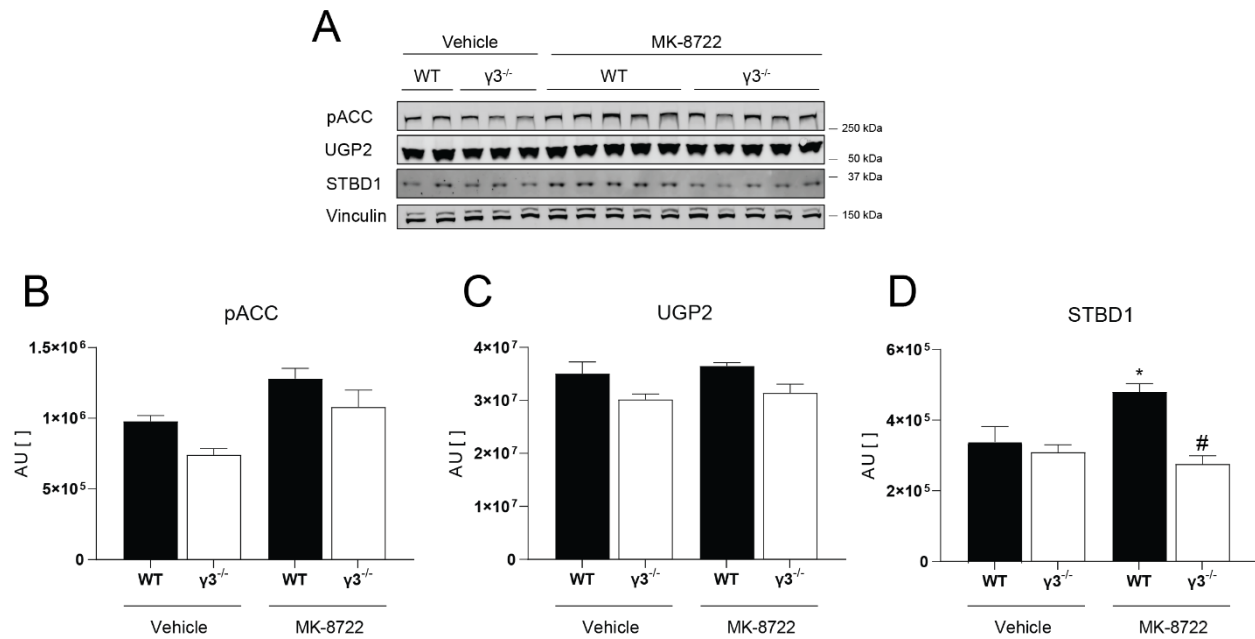
Appendix Figure 13 MK-8722 treatment increases STBD1 expression in WT EDL, but not in γ3$^{-/-}$.

A-D) Immunoblot (IB) analysis and quantification of lysates prepared from the ex vivo incubated EDL muscles. Blots and quantification were performed using a LiCOR system. IBs were performed using 20 µg of muscle extract and the indicated phospho-specific and total protein antibodies. Expressions were quantified as direct signals due to low power for Vehicle treatments. Results are expressed as means ± SEM with n=2-5 animals per treatment/genotype. Statistical analysis was performed by one-way ANOVA with Bonferroni correction and statistical significance shown as *$P<$ 0.05 (Vehicle vs 991) and #$P<$0.05 (WT vs γ3$^{-/-}$). UGP2; UDP-glucose pyrophosphorylase 2, STBD1; starch binding domain-containing protein 1.
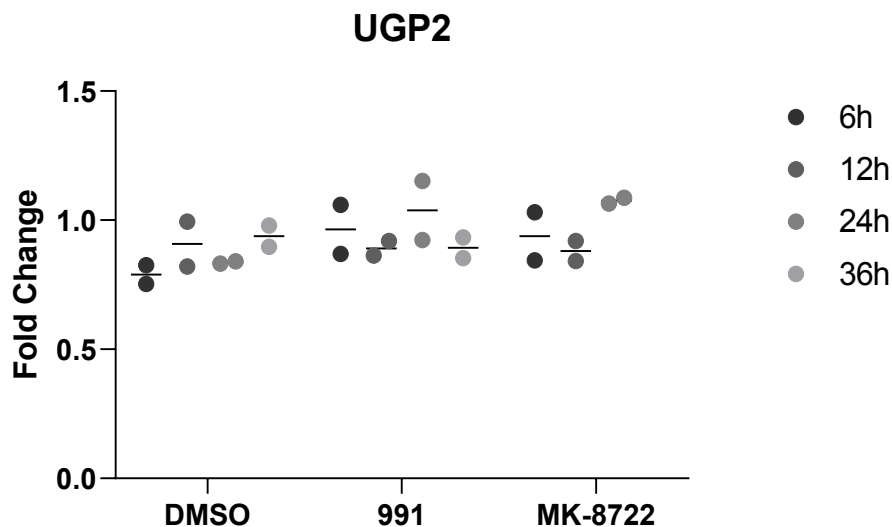
Appendix Figure 14 Treatment with direct AMPK activators does not change *Ugp2* mRNA levels in C2C12.

Relative levels of mRNA of Ugp2 (encoding UDP-glucose pyrophosphorylase 2) in C2C12 were assessed by qPCR (n=2 timepoint/treatment) and normalised against untreated control cells. Results are shown as means ± SEM. Statistical analysis was performed by one-way ANOVA with Bonferroni correction. UGP2, UDP-glucose pyrophosphorylase 2.
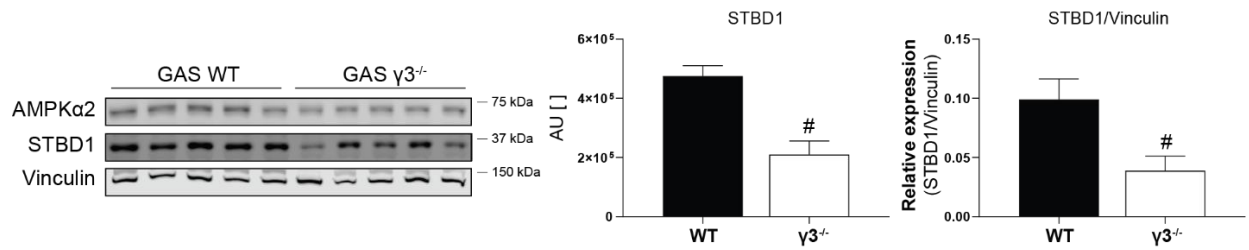
Appendix Figure 15 STBD1 expression is decreased in γ3$^{-/-}$ GAS muscles.
Immunoblot (IB) analysis and quantification of lysates prepared from basal GAS muscles. Blots and quantification were performed using a LiCOR system. IBs were performed using 20 µg of muscle extract and the indicated antibodies. STBD1 expressions were quantified by direct signal and normalisation to Vinculin. Results are expressed as means ± SEM with n=5 animals per genotype. Statistical analysis was performed by unpaired two-sided Student's t-test and significance is shown as #P<0.05 (WT vs γ3$^{-/-}$). STBD1; starch binding domain-containing protein 1.
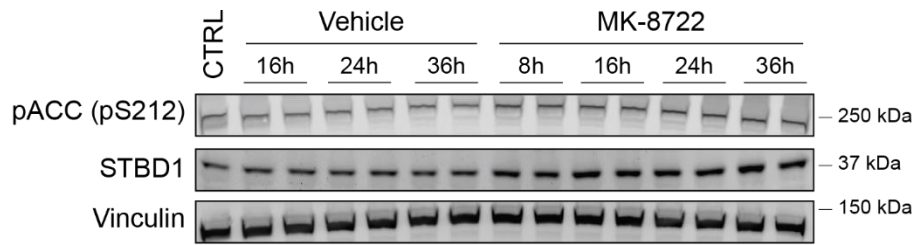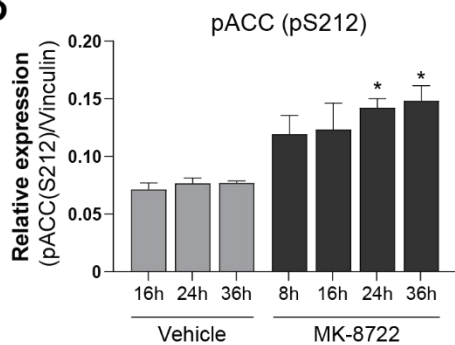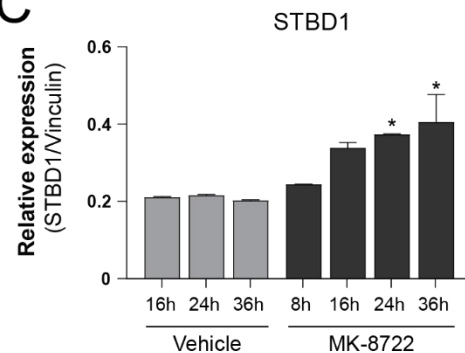
Appendix Figure 16 STBD1 expression increases in response to 991 treatment in C2C12 cells.
C2C12 myoblasts we treated with 10 µM MK-8722 (in duplicate) or 0.1% DMSO (Vehicle) at day 7 of differentiation. **A-C)** Immunoblot (IB) analysis and quantification of cell lysates lysed after the indicated time of treatment.Blots and quantification were performed using a LiCOR system. IBs were performed using 20 µg of cell extract and the indicated antibodies. STBD1 expressions and ACC phosphorylation (pACC (pS212)) were quantified by normalising to Vinculin. Results are expressed as means ± SEM. Statistical analysis was performed by one-way ANOVA with Bonferroni correction (8h treatment was compared to 16h Vehicle treatment) and statistical significance shown as *P< 0.05 (Vehicle vs 991). STBD1; starch binding domain-containing protein 1.
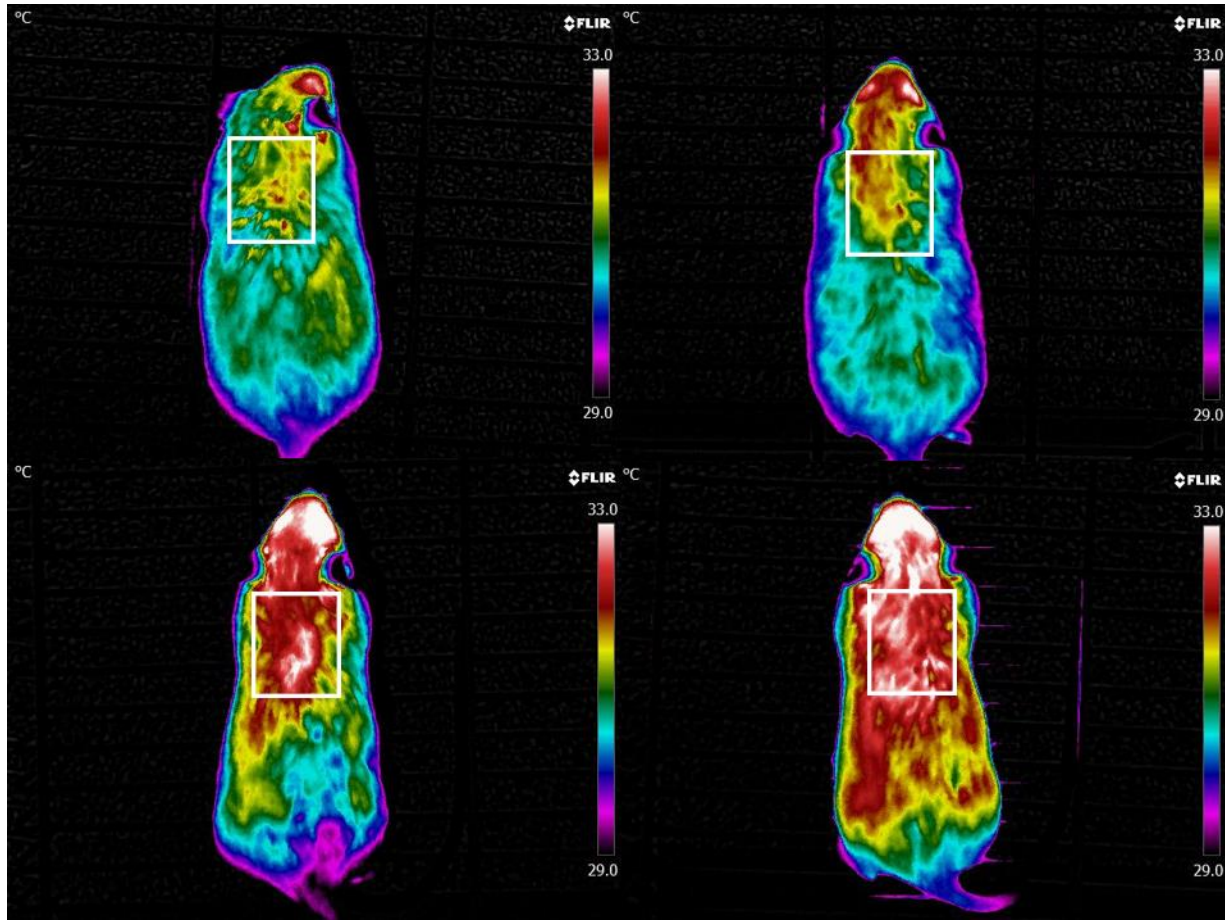
Appendix Figure 17 Large-scale, high-resultion image of thermography and BAT surface temparature measurement depicted and described in Figure 31C. (Imaging performed by Eric Desjardins, McMaster University, Hamilton, ON, Canada)

9.1 Manuscript prepared for preprint and publication

Following a copy of the work accepted in Molecular Metabolism on 26th March 2021

Compound- and fiber type-selective requirement of AMPKγ3 for insulin-independent glucose uptake in skeletal muscle

Philipp Rhein, Eric M. Desjardins, Ping Rong, Danial Ahwazi, Nicolas Bonhoure, Jens Stolte, Matthieu D. Santos, Ashley J. Ovens, Amy M. Ehrlich, José L. Sanchez Garcia, Qian Ouyang, Mads F. Kjolby, Mathieu Membrez, Niels Jessen, Jonathan S. Oakhill, Jonas J. Treebak, Pascal Maire, John W. Scott, Matthew Sanders, Patrick Descombes, Shuai Chen, Gregory R. Steinberg, Kei Sakamoto.

MOLECULAR METABOLISM

Original Article

Compound- and fiber type-selective requirement of AMPKγ3 for insulin-independent glucose uptake in skeletal muscle

Philipp Rhein [1,2], Eric M. Desjardins [3,4,14], Ping Rong [5,14], Danial Ahwazi [6], Nicolas Bonhoure [1], Jens Stolte [1], Matthieu D. Santos [7], Ashley J. Ovens [8,9], Amy M. Ehrlich [6], José L. Sanchez Garcia [1], Qian Ouyang [5], Mads F. Kjolby [10,11], Mathieu Membrez [1], Niels Jessen [10,11], Jonathan S. Oakhill [8,9], Jonas T. Treebak [6], Pascal Maire [7], John W. Scott [9,12,13], Matthew J. Sanders [1], Patrick Descombes [1], Shuai Chen [5], Gregory R. Steinberg [3,4], Kei Sakamoto [1,6,*]

ABSTRACT

Objective: The metabolic master-switch AMP-activated protein kinase (AMPK) mediates insulin-independent glucose uptake in muscle and regulates the metabolic activity of brown and beige adipose tissue (BAT). The regulatory AMPKγ3 isoform is uniquely expressed in skeletal muscle and potentially in BAT. Herein, we investigated the role that AMPKγ3 plays in mediating skeletal muscle glucose uptake and whole-body glucose clearance in response to small-molecule activators that act on AMPK via distinct mechanisms. We also assessed whether γ3 plays a role in adipose thermogenesis and browning.

Methods: Global AMPKγ3 knockout (KO) mice were generated. A systematic whole-body, tissue, and molecular phenotyping linked to glucose homeostasis was performed in γ3 KO and wild-type (WT) mice. Glucose uptake in glycolytic and oxidative skeletal muscle *ex vivo* as well as blood glucose clearance in response to small molecule AMPK activators that target nucleotide-binding domain of γ subunit (AICAR) and allosteric drug and metabolite (ADaM) site located at the interface of the α and β subunit (991, MK-8722) were assessed. Oxygen consumption, thermography, and molecular phenotyping with a β3-adrenergic receptor agonist (CL-316,243) treatment were performed to assess BAT thermogenesis, characteristics, and function.

Results: Genetic ablation of γ3 did not affect body weight, body composition, physical activity, and parameters associated with glucose homeostasis under chow or high-fat diet. γ3 deficiency had no effect on fiber-type composition, mitochondrial content and components, or insulin-stimulated glucose uptake in skeletal muscle. Glycolytic muscles in γ3 KO mice showed a partial loss of AMPKα2 activity, which was associated with reduced levels of AMPKα2 and β2 subunit isoforms. Notably, γ3 deficiency resulted in a selective loss of AICAR-, but not MK-8722-induced blood glucose-lowering *in vivo* and glucose uptake specifically in glycolytic muscle *ex vivo*. We detected γ3 in BAT and found that it preferentially interacts with α2 and β2. We observed no differences in oxygen consumption, thermogenesis, morphology of BAT and inguinal white adipose tissue (iWAT), or markers of BAT activity between WT and γ3 KO mice.

Conclusions: These results demonstrate that γ3 plays a key role in mediating AICAR- but not ADaM site binding drug-stimulated blood glucose clearance and glucose uptake specifically in glycolytic skeletal muscle. We also showed that γ3 is dispensable for β3-adrenergic receptor agonist-induced thermogenesis and browning of iWAT.

© 2021 The Authors. Published by Elsevier GmbH. This is an open access article under the CC BY-NC-ND license (http://creativecommons.org/licenses/by-nc-nd/4.0/).

Keywords AMP-activated protein kinase; 5-Aminoimidazole-4-carboxamide riboside; MK-8722; Glucose uptake; TBC1D1; Brown adipose tissue

[1]Nestlé Research, Société des Produits Nestlé S.A., EPFL Innovation Park, Lausanne, 1015, Switzerland [2]School of Life Sciences, EPFL Innovation Park, Lausanne, 1015, Switzerland [3]Centre for Metabolism, Obesity, and Diabetes Research, McMaster University, Hamilton, ON, L8N3Z5, Canada [4]Department of Medicine and Department of Biochemistry and Biomedical Sciences, McMaster University, Hamilton, ON, L8N3Z5, Canada [5]MOE Key Laboratory of Model Animal for Disease Study, Model Animal Research Center, School of Medicine, Nanjing University, Nanjing, 210061, China [6]Novo Nordisk Foundation Center for Basic Metabolic Research, University of Copenhagen, Copenhagen, 2200, Denmark [7]Université de Paris, Institut Cochin, INSERM, CNRS, 75014, Paris, France [8]Metabolic Signalling Laboratory, St Vincent's Institute of Medical Research, School of Medicine, University of Melbourne, Fitzroy, VIC, 3065, Australia [9]Mary MacKillop Institute for Health Research, Australian Catholic University, Fitzroy, VIC, 3000, Australia [10]Department of Biomedicine, Aarhus University, Aarhus, Denmark [11]Department of Clinical Pharmacology and Steno Diabetes Center Aarhus, Aarhus University Hospital, Aarhus, Denmark [12]Protein Chemistry and Metabolism Unit, St Vincent's Institute of Medical Research, Fitzroy, VIC, 3065, Australia [13]The Florey Institute of Neuroscience and Mental Health, Parkville, VIC, 3052, Australia

[14] These authors contributed equally.

*Corresponding author. Novo Nordisk Foundation Center for Basic Metabolic Research, University of Copenhagen, Blegdamsvej 3B, Copenhagen, DK-2200, Denmark. E-mail: kei.sakamoto@sund.ku.dk (K. Sakamoto).

Original Article

1. INTRODUCTION

AMP-activated protein kinase (AMPK) is an evolutionary conserved energy sensor that functions to maintain energy homeostasis through coordinating metabolic pathways [1,2]. AMPK exists as complexes of three subunits: a catalytic α and two regulatory β and γ subunits. Each exists as multiple isoforms (α1/α2, β1/β2, and γ1/γ2/γ3), generating up to 12 possible combinations [1]. AMPK heterotrimers are active when a conserved threonine (Thr172) residue within the activation loop of the α subunit kinase domain is phosphorylated [3]. The major upstream kinase phosphorylating Thr172 in metabolic tissues (e.g., muscle, liver) is a complex containing LKB1 [4,5]. The γ-subunits contain four tandem cystathionine β-synthase (CBS) motifs that bind adenine nucleotides. Binding of ADP and/or AMP to CBS motifs causes conformational changes that promote net Thr172 phosphorylation [6–8]. Moreover, the binding of AMP, but not ADP, further increases AMPK activity by direct allosteric stimulation [6]. Prodrugs of AMP-mimetics such as 5-aminoimidazole-4-carboxamide riboside (AICAR) have been widely used as pharmacological AMPK activators that target the CBS motifs [9]. Proof-of-concept preclinical studies demonstrated that AICAR treatment improved insulin sensitivity in animal models of insulin resistance [10]. However, AICAR produces numerous AMPK-independent metabolic actions [11]. For example, we have recently demonstrated that AICAR suppresses hepatic glucose production independently of AMPK [12] through inhibition of fructose-1,6-bisphosphatase-1, an AMP-sensitive enzyme involved in gluconeogenesis, in vivo [13]. We also showed that AICAR regulated >750 genes in AMPK-null mouse primary hepatocytes [14].

A nucleotide-independent regulation of AMPK was discovered when a novel small-molecule activator, A-769662, was identified [15] and its mechanism of action was explored [16–18]. The crystallographic structures of AMPK trimeric complexes revealed that A-769662 and 991 (another activator, also known as ex229) bind in a pocket termed allosteric drug and metabolite (ADaM) site located at the interface of the α subunit (kinase domain N-lobe) and β subunit (carbohydrate binding module) [9,19,20]. A-769662 was subsequently found to be selective for the AMPKβ1-containing complexes [17] and failed to stimulate AMPK-dependent glucose uptake due to lack of potency against β2-containing complexes that are prevalent in skeletal muscle [21]. We and others have shown that 991, and its two related benzimidazole derivatives with improved bioavailability (MK-8722, PF-739), are potent and highly specific AMPK activators [14,22,23]. They activate both β1- and β2-containing complexes (thereby activating all 12 possible human AMPK complexes) and have been shown to stimulate glucose uptake in skeletal muscle and lower blood glucose levels in vivo [22,24]. Notably, the administration of PF-739 resulted in attenuated blood glucose reduction in skeletal muscle-specific but not in liver-specific double knockout (KO) of AMPKα1/α2 [23].

AMPK isoform expression varies among different cell and tissue types, with α1, β1, and γ1 appearing the most ubiquitously expressed. Conversely, γ3 is selectively expressed in skeletal muscles containing a high proportion of glycolytic/fast-twitch fibers such as extensor digitorum longus (EDL) muscle [22,25–27]. Interestingly, even though skeletal muscle expresses multiple isoforms, assays of immunoprecipitated isoforms reveal that the α2β2γ1 and α2β2γ3 complexes account for 90% (of which α2β2γ3 accounts for 20%) of the total AMPK trimers in mouse EDL skeletal muscle [21]. Loss of expression/function of α2, β2 or γ3 is sufficient to ablate AICAR-induced glucose uptake in isolated skeletal muscle ex vivo [25,28–32].

In addition to its established metabolic roles in skeletal muscle [33,34], AMPK also plays a vital role in regulating the development of brown adipose tissue (BAT), maintenance of BAT mitochondrial function, and browning of white adipose tissue (WAT) [35]. Adipose-specific AMPKβ1/β2-KO (ad-AMPK KO) mice had a profound defect in thermogenesis [36], and both cold exposure and acute treatment with the β3-adrenergic receptor agonist (CL-316,243) in the ad-AMPK KO mice yielded subnormal increments in oxygen consumption and BAT temperature responses (likely related to impairments in BAT mitochondrial function). A high-throughput screen of protein kinases using a combination of RNAi-mediated knockdown and pharmacological inhibitors identified AMPK as a prominent kinase that promoted the formation of UCP1-abundant brown adipocytes in vitro [37]. Proof of concept experiments in vivo showed that daily treatment of diabetic ZDF rats with an AMPK activator (C163, for six weeks) increased the formation of brown adipocytes [37]. Intriguingly, transcripts of the *Prkag3* (AMPKγ3 gene) were identified in brown adipocyte precursors at intermediate levels, and RNAi-mediated knockdown of *Prkag3* was sufficient to profoundly block the brown adipocyte formation without affecting general adipose differentiation [37]. These results prompted us to assess whether γ3 plays a role in adipose thermogenesis and browning in vivo.

We hypothesized that γ3-containing complexes play an important role for insulin-independent and AMPK activator-mediated glucose uptake in skeletal muscle and for regulating BAT thermogenesis. To test this hypothesis, we generated γ3 KO mice and determined the effect of AICAR and the ADaM site binding drugs (991, MK-8722) on glucose uptake in glycolytic and oxidative skeletal muscles ex vivo and blood glucose kinetics in vivo. In addition, we probed BAT function using the β3-adrenergic receptor agonist CL-316,243. Strikingly, we found that γ3 deficiency resulted in a selective loss of AICAR-, but not 991/MK-8722-induced blood glucose clearance in vivo and glucose uptake specifically in glycolytic muscle ex vivo. We also found that γ3 is not required for the acute β3-adrenergic receptor-induction of UCP1-mediated non-shivering thermogenesis in the BAT, for the adaptive response to non-shivering thermogenesis or the browning of WAT.

2. MATERIALS AND METHODS

2.1. Materials

5-Aminoimidazole-4-carboxamide riboside (AICAR) was purchased from Apollo Scientific (OR1170T; Bredbury, United Kingdom). 991 (5-[[6-chloro-5-(1-methylindol-5-yl)-1H-benzimidazol-2-yl]oxy]-2-methyl-benzoic acid) (CAS#: 129739-36-2) was synthesized by Spirochem (Basel, Switzerland) as previously described [1]. Protein G Sepharose and P81 paper were purchased from GE Healthcare (Chicago, IL, USA). [γ-^{32}P]-ATP was purchased from PerkinElmer (Waltham, MA, USA). The substrate peptide AMARA was synthesized by GL Biochem (Shanghai, China). All other reagents were from MilliporeSigma (Burlington, MA, USA) if not otherwise stated. Lists of primary and secondary antibodies are provided in Supplementary Tables 1 and 2.

2.2. Animal ethics and models

Animal experiments were approved by the internal and local ethics committee and conducted in accordance with the European Convention for the Protection of Vertebrate Animals used for Experimental and Other Scientific Purposes. Protocols used were approved by the Service Vétérinaire Cantonal (Lausanne, Switzerland) under licenses VD3332 and VD3465, and by an ethical committee (Com'Eth, CE17) registered at the French Ministry of Research (Reference #: 10261), and also by the Danish Animal Experiments Inspectorate (Reference #: 2017-15-0202-00058), and were in accordance with McMaster

Animal Care Committee guidelines (AUP #: 16-12-41, Hamilton, ON). Protocols used were also approved by the Ethics Committees at Nanjing University with involved personnel having personal licenses from the regional authority. The generation of a constitutive *Prkag3*$^{-/-}$ (AMPKγ3$^{-/-}$) mice was performed by Taconic Biosciences as described in Supplementary Figure 1. The AMPKα1f/f and AMPKα2f/f mice were as previously described [38], and obtained from the Jackson Laboratory (Bar Harbor, ME, USA). These two strains were used to derive AMPKα1f/f/α2f/f mice that were then bred with the Mlc1f-Cre mice to obtain the AMPKα1f/f/α2f/f - Mlc1f-Cre mice. The resultant AMPKα1f/f/α2f/f - Mlc1f-Cre mice were the AMPKα1/α2 skeletal muscle-specific KO mice. All these lines were on C57BL6 background. The animals were kept and maintained according to local regulations under a light—dark cycle of 12 h and had free access to a standard chow diet. Male mice ranging 10—16 weeks of age were used for experiments otherwise stated. High-fat diet (HFD) (60 kcal% fat) was obtained from Research Diet (RD 12492).

2.3. Analysis of body composition and plasma hormone levels

Body composition (fat content, lean tissues and free body fluid) was assessed using the Minispec analyzer (Bruker) by Nuclear Magnetic Resonance (NMR) technology. The test was conducted on conscious fed mice. Blood was collected at the indicated age by retro orbital puncture under isoflurane anesthesia at noon on mice fasted for 4 h. Plasma insulin and leptin levels were measured on a BioPlex analyzer (BioRad) using the Mouse Metabolic Magnetic Hormone Magnetic Bead panel kit (MilliporeSigma).

2.4. Oral glucose tolerance test

Mice were fasted overnight (16 h) and a bolus of glucose solution (2 g/kg body weight) was administered via oral gavage. Blood glucose collected from the tail vein was measured at different time points over 120 min using blood glucose monitor and glucose test strips (Roche Diagnostics, Accu-Chek).

2.5. Preparation of mouse tissue extracts for protein analysis

Mouse tissue were dissected and immediately frozen in liquid nitrogen. The tissues were homogenized in ice-cold lysis buffer (270 mM sucrose, 50 mM Tris·HCl (pH 7.5), 1 mM EDTA, 1 mM EGTA, 1% (w/v) Triton X-100, 20 mM glycerol-2-phosphate, 50 mM NaF, 5 mM Na$_4$P$_2$O$_7$, 1 mM DTT, 0.1 mM PMSF, 1 mM benzamidine, 1 μg/mL microcystin-LR, 2 μg/mL leupeptin, and 2 μg/mL pepstatin A) using a tissue lyser (Tissue Lyser II; Qiagen). Lysates were centrifuged at 21,300 *g* for 15 min and protein concentration from the supernatant was determined using Bradford reagent (23200, Thermo Fisher) and bovine serum albumin (BSA) as standard. The supernatants were stored in aliquots in a −80 °C freezer until subsequent analysis.

2.6. Immunoblotting

Protein extracts were denatured in Laemmli buffer at 95 °C for 5 min. Twenty micrograms of protein was separated by SDS-PAGE on 4—12% gradient gels (NW04127, Thermo Fisher) and transferred onto nitrocellulose membranes (#926-31090, LiCOR). Membranes were blocked for 1 h at room temperature in LiCOR blocking buffer (#927-60001, LiCOR). The membranes were subsequently incubated in TBST (10 mM Tris (pH 7.6), 137 mM NaCl, and 0.1% (v/v) Tween-20) containing 5% (w/v) BSA and the primary antibody overnight at 4 °C. After extensive washing, the membranes were incubated for 1 h in either HRP-conjugated or LiCOR secondary antibodies diluted 1:10,000. Signal imaging was performed either using enhanced chemiluminescence (ECL) reagent (GE Healthcare) or a LiCOR Odyssey CLx imaging system. Densitometry for ECL blots was performed using Image J Software (NIH). Because of sample limitation (from the incubated muscle tissue samples), we also utilized automated capillary Western Blot system Sally Sue (ProteinSimple, San Jose, CA, USA). Experiments were performed according to the manufacturer's protocol using the indicated standard reagents for the Sally Sue system (SM-S001, ProteinSimple). Briefly, all samples were first diluted to 2 mg/mL in lysis buffer and then further diluted to 0.5 mg/mL in 0.1% SDS. Following the manufacturer's instructions for sample preparation, this resulted in an assay protein concentration of 0.4 mg/mL.

2.7. Immunoprecipitation and in vitro AMPK activity assay

Lysates of muscle (200 μg) or BAT (1,000 μg) were incubated on a rotating platform at 4 °C overnight with a mix of 5 μL packed protein G-Sepharose and the indicated antibodies. The Sepharose beads were pelleted at 500 *g* for 1 min and initially washed twice with 0.5 mL lysis buffer containing 150 mM NaCl and subsequently washed twice with the same amount of buffer A [50 mM HEPES (pH 7.4), 150 mM NaCl, 1 mM EGTA, and 1 mM DTT]. The immunoprecipitated AMPK complexes were either eluted with Laemmli buffer for immunoblot analysis or used for *in vitro* AMPK activity assay. The AMPK activity assay was performed by incubating the beads (i.e. immune-complexes) for 30 min at 30 °C on a heated shaker in buffer A with additional 10 mM Mg^{2+} and 100 μM ATP in presence of 200 μM AMARA peptide (AMARAASAAALARRR) and 1 μCi of [γ-^{32}P] ATP [22]. Reactions were stopped by spotting the reaction mix onto P81 filter papers and washing in 75 mM phosphoric acid. The P81 papers were dried after three washes and the ^{32}P incorporation into the substrate peptide measured by Cherenkov counting (5 min) using a scintillation counter (Tri-Carb 2810TR, PerkinElmer).

2.8. Citrate synthase activity assay

Protein extracts (10 μg) (using the same lysis buffer described above) was assayed in duplicates using a citrate synthase assay kit (CS0720, MilliporeSigma) according to the manufacturer's instruction using recombinant citrate synthase as positive control.

2.9. Analysis of gene expression and mitochondrial DNA copy number using quantitative real-time PCR (qPCR)

To perform a relative quantification of mRNA levels of the AMPK subunit isoforms in mouse skeletal muscle tissues, reverse transcription and qPCR was performed as described [14]. All the primers and sequences are listed in Supplementary Table 3. Relative mRNA quantities were calculated for triplicate muscle samples from four to five animals and normalized using the three reference genes *Hprt1* (hypoxanthine ribosyltransferase, HPRT), *GusB* (beta-glucuronidase) and *Pgk1* (Phosphoglycerate Kinase 1). Real-time qPCR in BAT was performed separately as described [36]. Relative gene expression was calculated using the comparative Ct (2−ΔCt) method, where values were normalized to a reference gene (*Ppia*).

To relatively quantify the amount of mtDNA present per nuclear genome by qPCR, mtDNA (16S, ND4) and nuclear DNA (PMP22, Titin) primers and probes were used, the sequences of which are shown in Supplementary Table 3. The relative mt copy number was determined based on the relative abundance of nuclear and mtDNA, calculated as average of the two targets respectively. The relative abundance was then expressed by ΔCT or CT(nDNA) - CT(mtDNA) and displayed as fold change of copy number of mtDNA per nuclear genome compared to the WT muscle.

Original Article

2.10. Immunofluorescence for fiber type determination and fiber size

For immunostaining against Myh4, Myh2, Myh7 and Laminin, mouse hindlimbs (no skin) without fixation were embedded with Tissue-TEK OCT (Sakura Finetek, Netherlands) and directly frozen in cold isopentane pre-cooled in liquid nitrogen as described [39]. Hindlimb cross sections were prepared using a cryostat (Leica 3050s) with a thickness of 10 μm. The cross sections were washed 3 times for 5 min with PBS and then incubated with blocking solution (PBS and 10% goat serum) for 30 min at room temperature. The sections were incubated overnight with primary antibody diluted in PBS + 10% goat serum solution at 4 °C and washed as described above. The sections were then incubated with secondary antibody, diluted in PBS + 10% goat serum solution for 1 h at room temperature. Sections were further washed and mounted with Mowiol solution and a glass coverslip. Images were collected with a microscope (Olympus BX63F) and a camera (Hamamatsu ORCA-Flash 4.0). Images were analyzed with ImageJ (NIH). Fiber boundaries were defined by the laminin signal and myosin Myh7 (type I), Myh2 (type IIA), and Myh4 (type IIB) heavy chains were quantified. Remaining unlabeled fibers were included for total fiber number and individual proportions of type I, type IIA, and type IIB of that total number calculated. We did not specifically detect and quantify hybrid fibers due to insufficient resolution and lack of established analytical tools.

2.11. Ex vivo skeletal muscle incubation and analysis of glucose uptake

Animals were anesthetized with Avertin [2,2,2-Tribromoehtanol (Sigma-Aldrich #T48402) and 2-Methyl-2-butanol 99% (Sigma-Aldrich #152463)] via an intraperitoneal injection, and EDL or soleus muscles were rapidly dissected and mounted in oxygenated (95% O_2 and 5% CO_2), and warmed (30 °C) Krebs—Ringer buffer in a myograph system (820MS DMT, Denmark). The respective muscles were incubated as described [22,40] in the presence of the indicated drug or vehicle for 50 min. During the last 10 min of the incubation, 2-deoxy-[^{3}H] glucose uptake was measured as described [22,41].

2.12. AICAR and MK-8722 tolerance test

Access of the mice to food was restricted for 3 h (07:00—10:00) prior to the experiment. AICAR (250 mg/kg body weight) or vehicle (water) was injected intraperitoneally and blood glucose levels were monitored for 120 min using the Contour XT glucometer (Bayer, Leverkusen) and single use glucose sensors (Ascensia, Basel). MK-8722 tolerance was tested by oral administration of either MK-8722 (10 or 30 mg/kg body weight) or vehicle (0.25% (w/v) methylcellulose, 5% (v/v) Polysorbate 80, and 0.02% (w/v) sodium lauryl sulfate in deionized water) [24]. Blood glucose measurement was performed as described above for the AICAR tolerance test.

2.13. ZMP and adenine nucleotide measurements

Muscle tissues were lysed in 200 μL cold 0.5 M perchloric acid. Extracts were collected and clarified at 14,000 rpm for 3 min. Subsequently, 100 μL clarified lysate was neutralized with 25 μL cold 2.3 M $KHCO_3$ and incubated on ice for 5 min. Samples were centrifuged at 14,000 rpm for 3 min. ZMP were measured by LC-MS/MS with modifications to our previously described method [42]. Both LC and MS instruments were controlled and managed with the Analyst 1.7.1 software (AB Sciex). The autosampler was set at 4 °C and column oven set at 30 °C, which housed a 150 mm (length) × 0.5 mm (inner diameter) Hypercarb 3 μm porous graphitic carbon column (Thermo Fisher Scientific). The LC solvent system comprised 50 mM triethylammonium bicarbonate buffer (TEAB, MilliporeSigma) pH 8.5 in pump A, and acetonitrile with 0.5% trifluoroacetic acid (TFA; Sigma-Aldrich) in pump B. A flow rate of 400 μl/min was used throughout a gradient program consisting of 0% B (2 min), 0 to 100% B (10 min), 100% B (3 min), 0% B (2 min). Data was analyzed with MultiQuant 3.0.2 software (AB Sciex) using area under the LC curve. Calibration curves were determined by linear regression of the peak area of a ZMP standard curve and were required to have a correlation coefficient (R^2) of >0.98. Adenine nucleotides and adenylate energy charge were measured by LC-MS as described [43].

2.14. Adipose tissue histology

Tissues were fixed in 10% formalin for 24—48 h at 4 °C and processed for paraffin embedding, and hematoxylin and eosin staining by the core histology laboratory at the McMaster Immunology Research Centre (Hamilton, Canada).

2.15. Infrared thermography

UCP1-mediated thermogenesis was assessed in 14-week-old male wild-type (WT) and γ3 KO mice as described [44]. Briefly, mice were anaesthetized with an intraperitoneal injection of 0.5 mg/g body weight Avertin (2,2,2-Tribromoethanol dissolved in 2-methyl-2-butanol; MilliporeSigma) and after 2 min, injected with either saline or the highly selective β3-adrenergic receptor agonist CL 316,243 (Tocris, Bristol, United Kingdom). Mice were subsequently placed dorsal side up onto an enclosed stationary treadmill to measure oxygen consumption (VO_2) with a Comprehensive Laboratory Animal Monitoring System (Columbus Instruments, OH, USA) and 18 min after the second injection a static dorsal thermal image was taken with an infrared camera (FLiR Systems, Wilsonville, OR, USA). Serum samples were collected through tail-nick immediately after the infrared image was taken and non-esterified free fatty acid (NEFA) concentration was determined according to the manufacturer's instructions with a two-step kit (NEFA-HR 2, WAKO).

2.16. Metabolic monitoring

Metabolic monitoring was performed as described [45] in a Comprehensive Laboratory Animal Monitoring System. For the chronic 5-day CL 316,243 challenge, mice were injected intraperitoneally with saline or CL 316,243 (first 4 days 0.5 mg/kg and last day 1.0 mg/kg) at 09:30 h and measurements for VO_2 were calculated 6 h post-injection. Mice were euthanized 24 h after the last injection.

2.17. Statistical analysis

Data are reported as mean ± standard error of the mean (SEM) and statistical analysis was performed using GraphPad Prism software. As indicated in the respective figure legends, differences between only two groups were analyzed using an unpaired two-tailed Student's *t*-test and for multiple comparisons one-way analysis of variance (ANOVA) with Bonferroni *post hoc* test or repeated measures two-way ANOVA was used. Statistical significance was accepted at $P < 0.05$.

3. RESULTS

3.1. A genetic/constitutive loss of the AMPKγ3 reduced AMPKα2 and β2 protein abundance in mouse glycolytic skeletal muscle

We generated constitutive AMPKγ3 KO mice through flanking exons 5—10 of *Prkag3* gene with LoxP sites (Supplementary Figure 1A). This is expected to cause a loss-of-function of the
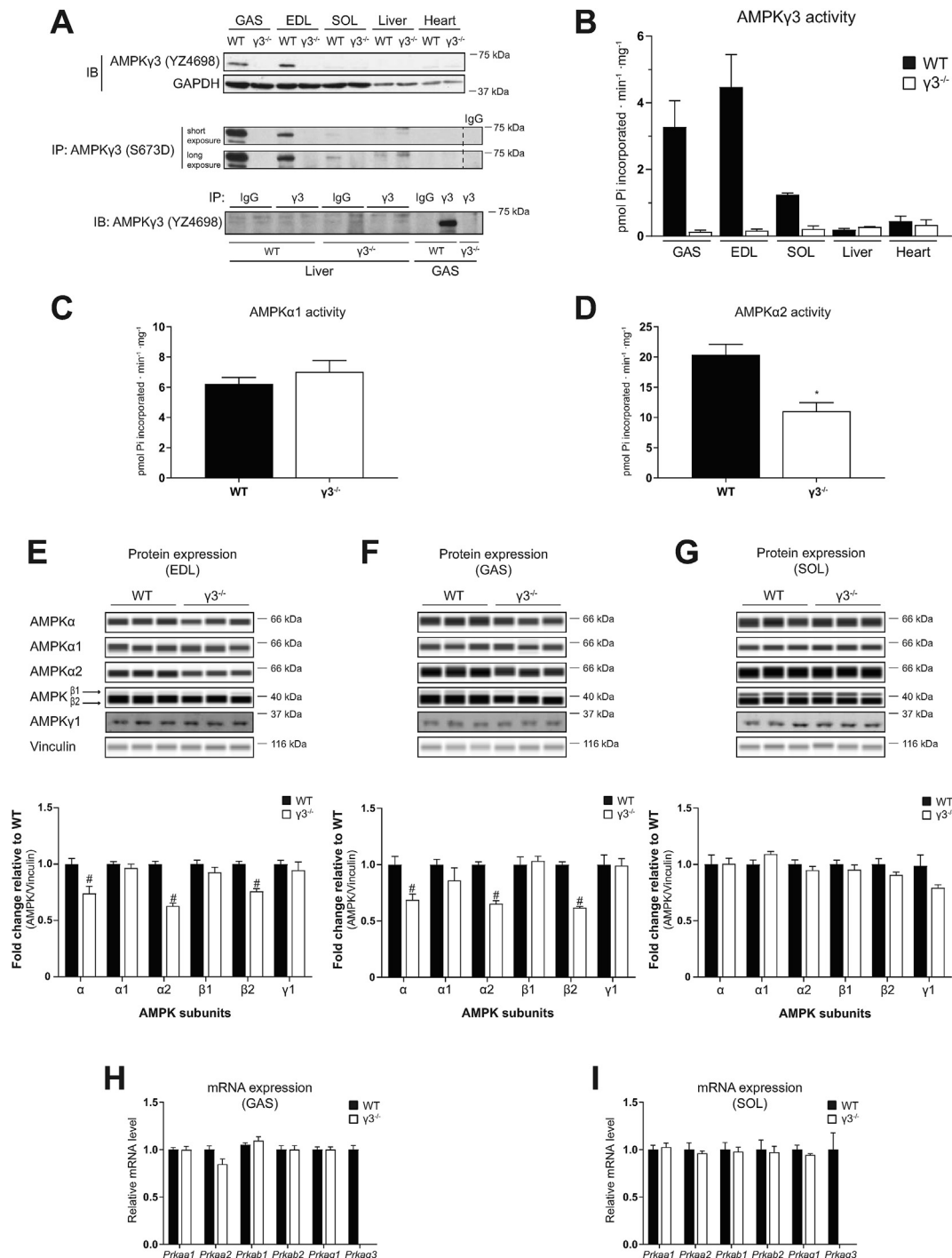
Figure 1: Genetic ablation of the AMPKγ3 causes a significant loss of α2 and β2 expression in mouse glycolytic skeletal muscles. (A) Immunoblot (IB) analysis of γ3 expression in a panel of tissues extracted from wild-type (WT) or AMPKγ3-null (γ3$^{-/-}$) mice (upper panel). γ3 expression was further analyzed by immunoblotting following enrichment of the γ3 proteins via immunoprecipitation (IP) from the indicated tissue extracts (200 μg) (middle panel). Liver and skeletal muscle (GAS) tissue extracts from the indicated genotypes were used for immunoprecipitation with either γ3-specific antibody or species-matched IgG (as negative control) and the immune-complexes were subsequently immunoblotted with γ3 antibody (lower panel). (B) The γ3-containing AMPK complexes were immunoprecipitated from the indicated tissues harvested from the indicated genotypes and an *in vitro* AMPK activity assay was performed in duplicate (n = 3 per tissue/genotype). (C, D) The *in vitro* AMPK activity assay was performed on α1- or α2-containing AMPK complexes immunoprecipitated from GAS extracts (n = 9−10 per tissue/genotype). (E−G) Representative immunoblot images and quantification of the AMPK isoform-specific expression using an automated capillary immunoblotting system (Sally Sue) with the indicated antibodies as described in Materials and Methods. AMPK isoform expressions were normalized by their respective vinculin expression (loading control) and are shown as fold change relative to WT. Note that AMPKγ1 expression was quantified using another immunoblotting system (Li-COR, described in the Materials and Methods) due to antibody compatibility (n = 5−11 per tissue/genotype). (H, I) Relative levels of mRNA of the indicated genes (encoding AMPK isoforms) in the indicated skeletal muscles were assessed by qPCR (n = 5 per tissue/genotype). Results are shown as means ± SEM. Statistical significance was determined using the unpaired, two-tailed Student's t-test and are shown as #$P < 0.05$ (WT vs. γ3$^{-/-}$). GAS; gastrocnemius, EDL; extensor digitorum longus, SOL; soleus, IgG; immunoglobulin G.

Original Article

Prkag3 gene by deleting the nucleotide binding cystathionine β-synthase (CBS)-2 domain and parts of the CBS-1 and -3 domains and by generating a frame shift from exon 4 to exon 11 (premature stop codon in exon 12). In addition, the resulting transcript may be a target for non-sense mediated RNA decay and thereby may not be expressed at a significant level. In support of this, we were unable to detect faster migrating polypeptides using the antibody raised against residues 44—64 (within exon 1—3) of the mouse γ3 (Supplementary Figure 1B). γ3 homozygous KO (γ3$^{-/-}$) mice were born at expected Mendelian frequency (data not shown). Food intake and spontaneous physical activity, as well as oxygen consumption were similar between WT and γ3 KO mice (Supplementary Figure 1C—E).

We first confirmed a complete loss of γ3 protein and its associated AMPK catalytic activity in tissues harvested from γ3 KO mice (Figure 1A, B). Expression of γ3 is restricted to mouse skeletal muscles containing a high proportion of glycolytic/fast-twitch fibers [22,25]. In line with this, we observed that γ3 and its associated AMPK activity were predominantly detected in glycolytic gastrocnemius (GAS) and extensor digitorum longus (EDL) muscles in WT mice. A modest expression of γ3 and its associated AMPK activity were detected in the soleus muscle (which contains a high proportion of oxidative/slow-twitch fibers) from WT mice when γ3 proteins were enriched by immunoprecipitation prior to the immunoblotting (Figure 1A, B). We detected a faint band immuno-reactive to the γ3 antibody in liver lysates from both WT and γ3 KO mice (Figure 1A, middle panel). We confirmed that the observed band was non-specific as it was readily detected in IgG control samples (Figure 1A, lower panel) and only a negligible background γ3-associated AMPK activity was detected in liver (and also heart) lysates in both WT and γ3 KO mice (Figure 1B). Subsequently, we assessed if loss of γ3 affected AMPKα1- and α2-containing complex activity in GAS muscle. As illustrated in Figure 1C and D, we observed that while AMPKα1 activity was unaltered, AMPKα2 activity was reduced (~50%). Because we and other groups have shown that γ3 predominantly interacts with α2 and β2 [21,22] to form a stable trimeric α2β2γ3 complex, we hypothesized that a constitutive loss of γ3 would cause reduced expressions of α2 and β2 due to their destabilization as monomers. To test this hypothesis, we performed an analysis of AMPK subunit/isoform abundance in both glycolytic (EDL and GAS) and oxidative (soleus) muscles in WT and γ3 KO mice (Figure 1E—G). We previously performed an extensive antibody validation for all AMPKαβγ isoforms using individual isoform-specific KO mouse tissues as negative controls and also reported that γ2 proteins (UniProt ID: Q91WG5 isoform A) were not detectable in mouse skeletal muscles [22]. Immunoblot analysis revealed that protein levels of α2, total AMPKα using a pan α1/α2 antibody, and β2 isoforms were selectively reduced (~20—30%) in EDL and GAS (Figure 1E, F), but not in soleus (Figure 1G), of γ3 KO as compared to WT mice. There was no compensatory increase in γ1 isoform in γ3 KO muscles. To examine whether the reduced protein abundance of α2 and β2 was due to decreased mRNA expression of the *Prkaa2* and *Prkab2* (the genes encoding AMPKα2 and β2, respectively) in the γ3 KO mice, we performed qPCR analyses (Figure 1H, I). We confirmed that *Prkag3* mRNA expression was undetectable in skeletal muscle from γ3 KO mice, and observed that there were no differences in mRNA expressions of other AMPK subunit/isoforms in GAS (Figure 1H) or soleus (Figure 1I) between WT and γ3 KO mice. Taken

together, we have demonstrated that a genetic/constitutive loss of AMPKγ3 causes reduction of AMPKα2 and β2 proteins without affecting their mRNA expressions in glycolytic skeletal muscle.

3.2. AMPKγ3 deficiency has no impact on mitochondrial content and components or fiber-type composition in skeletal muscle

A loss-of-function of skeletal muscle AMPK is associated with reduced mitochondrial content and function [45—48]. Interestingly, a transgenic mouse model overexpressing γ3 mutant (R225Q, a gain-of-function mutation), was associated with higher mitochondrial content and increased amount of a marker of the oxidative capacity (succinate dehydrogenase) in individual muscle fibers of the white portion of GAS [49]. Nevertheless, γ3 deficiency did not cause alterations in mitochondrial content or other parameters in GAS muscle [49]. However, the previously generated γ3 deficient mice did not exhibit significantly reduced expression or activity of AMPKα2 [25], the predominant α-catalytic isoform in skeletal muscle. In the current study, we assessed whether γ3 deficiency, coupled to a partial loss of AMPKα2 activity (Figure 1D), had an impact on mitochondrial parameters in both glycolytic (EDL) and oxidative (soleus) skeletal muscle. We observed no differences in mitochondrial DNA copy number (Figure 2A, B), citrate synthase activity (Figure 2C, D), or components of the mitochondrial respiratory chain complex (Figure 2E, F) in soleus or EDL muscles of WT and γ3 mice. Fiber-type analysis of hindlimb cross sections using immunofluorescence revealed no differences in myosin heavy chain isoform composition in EDL or soleus muscles between the genotypes (Figure 2G, H). We also observed no difference in skeletal muscle fiber size (cross sectional area) between the genotypes (Figure 2I). Collectively, we showed that constitutive γ3 deficiency does not affect mitochondrial content, respiratory chain complex expression, or fiber type composition in both glycolytic and oxidative skeletal muscle.

3.3. AMPKγ3 KO mice exhibit normal glucose homeostasis on chow and in response to high-fat diet (HFD) feeding

Transgenic mice overexpressing the γ3 mutant (R225Q) exhibit an increase in muscle lipid oxidation and are protected against HFD-induced insulin resistance in skeletal muscle [25]. In the current study, we examined whether γ3 deficiency affected glucose homeostasis under standard chow and in response to HFD feeding. Body weight and composition were similar between WT and γ3 KO mice during both chow and HFD-feeding periods (Figure 3A, B). We observed similar levels of plasma insulin and leptin on chow diet between WT and γ3 KO mice, with their levels increased in a comparable manner for both genotypes in response to HFD feeding (Figure 3C, D). Consistent with these results, we observed comparable fasted blood glucose levels and no difference in glucose tolerance between the genotypes irrespective of the diets (Figure 3E). To complement these *in vivo* results, we assessed insulin signaling and glucose uptake in isolated EDL muscle *ex vivo*. As shown in Figure 3F, basal glucose uptake and Akt phosphorylation were comparable between WT and γ3 KO mice and insulin equally stimulated both parameters in both genotypes. We also confirmed that there was no difference in the expression of GLUT4 and hexokinase II in EDL muscle between WT and γ3 KO mice (Figure 3F). Taken together, these results suggest that γ3 is dispensable for maintenance of glucose homeostasis on chow and in response to HFD.
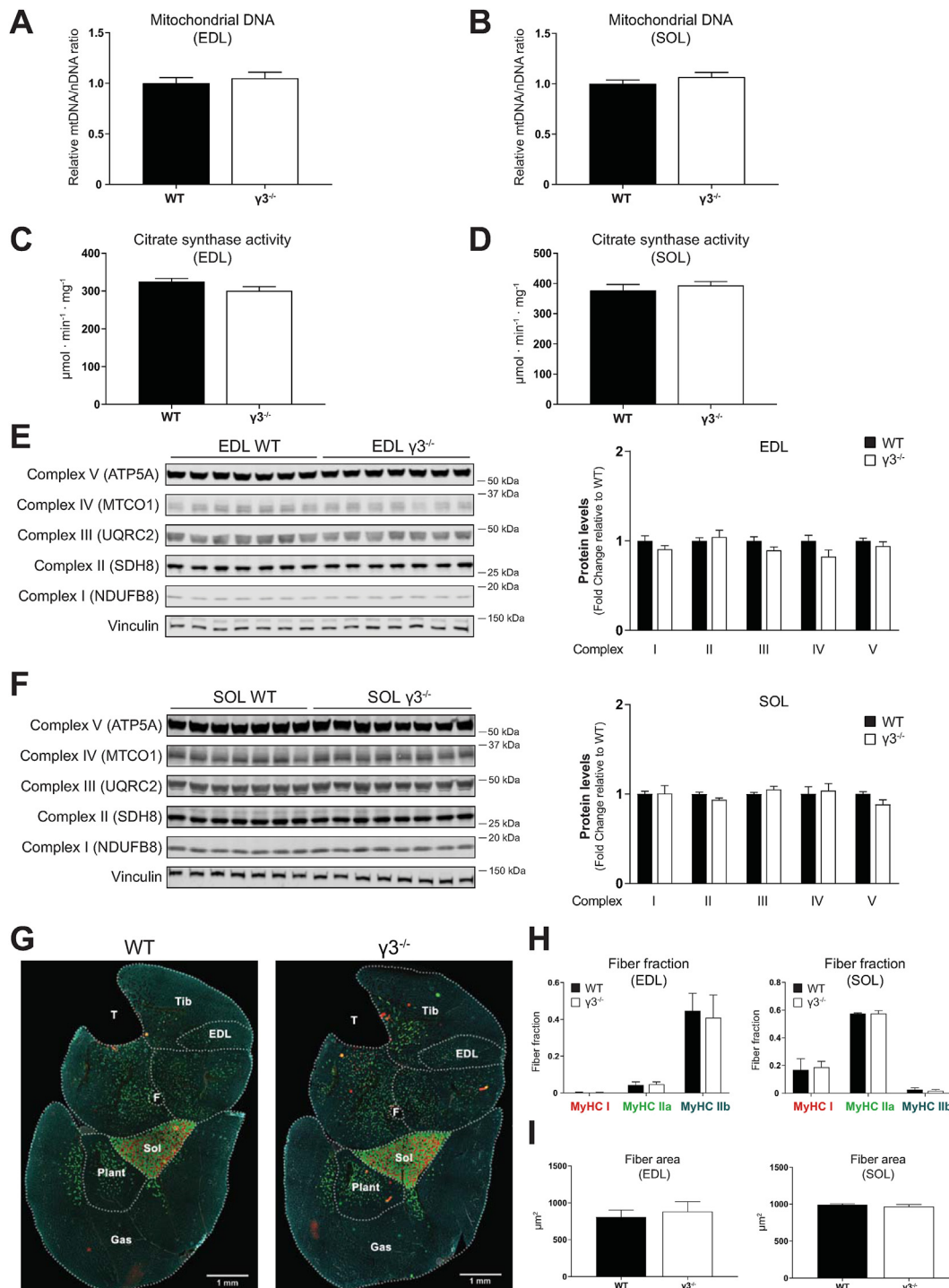
Figure 2: AMPKγ3 deficiency does not affect mitochondrial content and components, or fiber-type composition in skeletal muscles. (A, B) Relative quantification of mitochondrial DNA (mtDNA) was performed using qPCR-based assay as described in the Materials and Methods (n = 5 per tissue/genotype). (C, D) Citrate synthase activity was measured in the indicated muscle extracts (n = 8 per tissue/genotype). (E, F) Immunoblot analysis and quantification of mitochondrial complexes in the indicated muscles (n = 7 per tissue/genotype). (G—I) Representative cross-sectional images (of n = 4 per genotype) of the whole-hindlimb muscle fiber-type analysis of the indicated genotypes using isoform-specific myosin heavy chain (MyHC) and laminin antibodies followed by immunofluorescent signal detection (G). Scale bar = 1 mm. Quantification of relative isoform-specific myosin heavy chain (MyHC) composition/fraction (red: MyHC I, green: MyHC IIa, blue: MyHC IIb, laminin: gray/white) and fiber area in the indicated muscles were performed as described in Materials and Methods. Unstained fibers are not included in the fiber fraction analysis (H, L, n = 3—4 per tissue/genotype). Results are shown as means ± SEM. GAS; gastrocnemius, EDL; extensor digitorum longus; SOL; soleus, Tib; tibialis anterior, Plant; plantaris, F; fibula, T; tibia.

Original Article
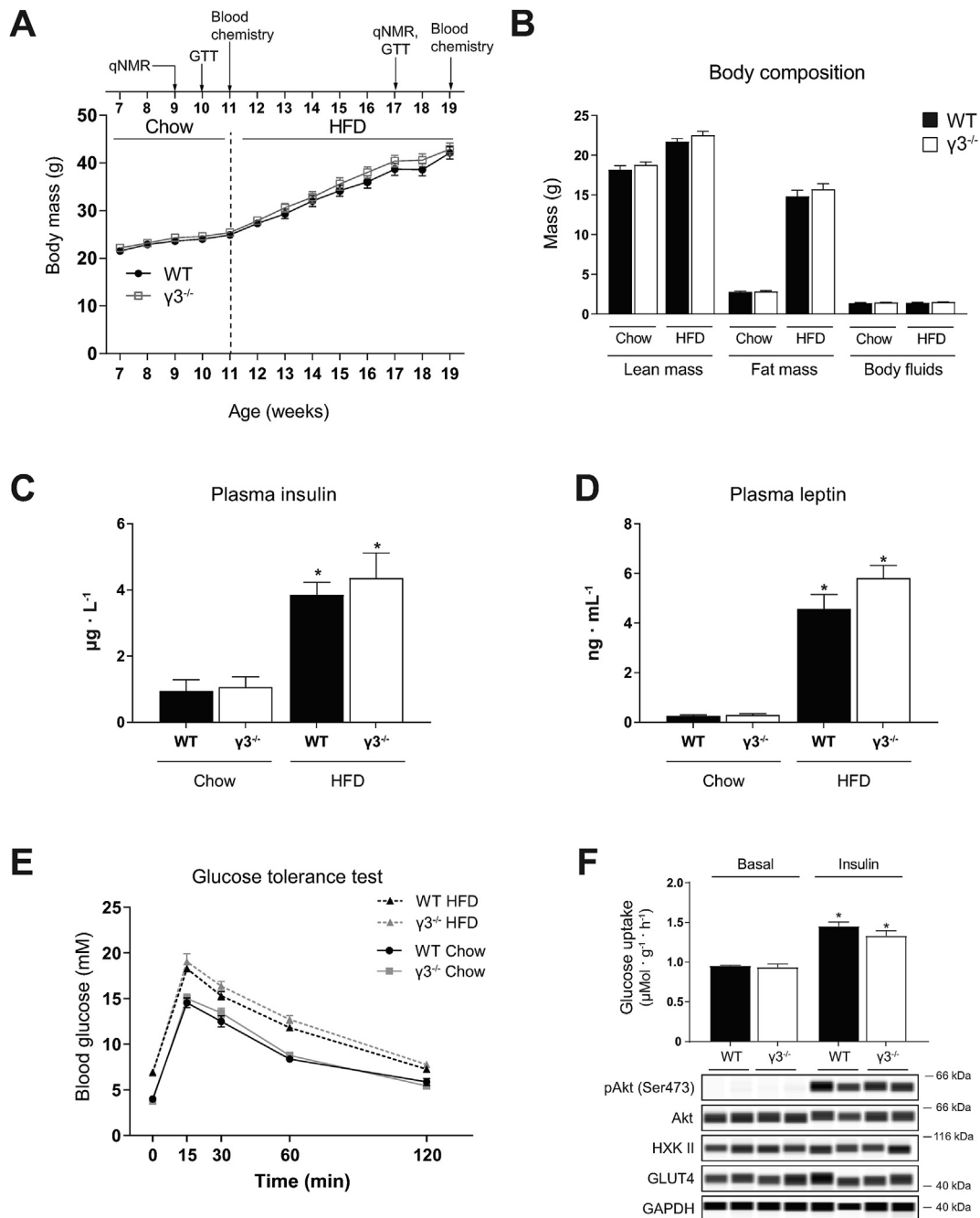
Figure 3: AMPKγ3 is dispensable for maintaining glucose homeostasis under chow and high-fat diet (HFD) feeding. (A) Time sequence of the diet intervention, analysis of body composition (qNMR), oral glucose tolerance test (GTT) and plasma hormone analysis (blood chemistry). Mice were fed chow diet after weaning until 11 weeks of age before switching to HFD (60 kcal% fat). Body weight over time of the indicated genotypes (n = 10 per genotype). (B) Body composition determined by qNMR in the indicated genotypes during the indicated diet treatment. (C, D) Plasma insulin and leptin levels were determined using the commercial enzyme-linked immunosorbent assay kits. (E) Mice were fasted overnight and an oral GTT test was performed during chow (week 10) and HFD (week 17) feeding by monitoring blood glucose kinetics over the indicated duration following an oral administration of a bolus of glucose solution (2 g/kg body weight). (F) Extensor digitorum longus (EDL) muscles from the indicated genotypes on chow diet (10- to 12-week old males from a separate cohort, n = 5−7 per genotype) were isolated in incubated in the presence or absence of insulin (100 nM) for 50 min and were subjected to glucose uptake assay and immunoblot analysis using the indicated antibodies. Results are shown as means ± SEM. Statistical significance was determined using the unpaired/two-tailed Student's t-test or one-way analysis of variance with Bonferroni correction and are shown as *$P < 0.05$ (treatment effect within the same genotype).

3.4. AMPKγ3 deficiency causes attenuated AICAR-stimulated glucose uptake in glycolytic skeletal muscle ex vivo and blood glucose lowering in vivo

AICAR-stimulated glucose uptake in skeletal muscle requires functional AMPK [34]. Consistent with previous studies [30,41], AICAR promoted glucose uptake robustly in EDL ($\sim$2.5-fold) and modestly in soleus ($\sim$1.6-fold) ex vivo in WT mice (Figure 4A, B). Interestingly, we observed that AICAR-stimulated glucose uptake was profoundly reduced in EDL, but not in soleus, in γ3 KO mice (Figure 4A, B). To examine whether a loss of γ3 affected AICAR-induced AMPK activity,
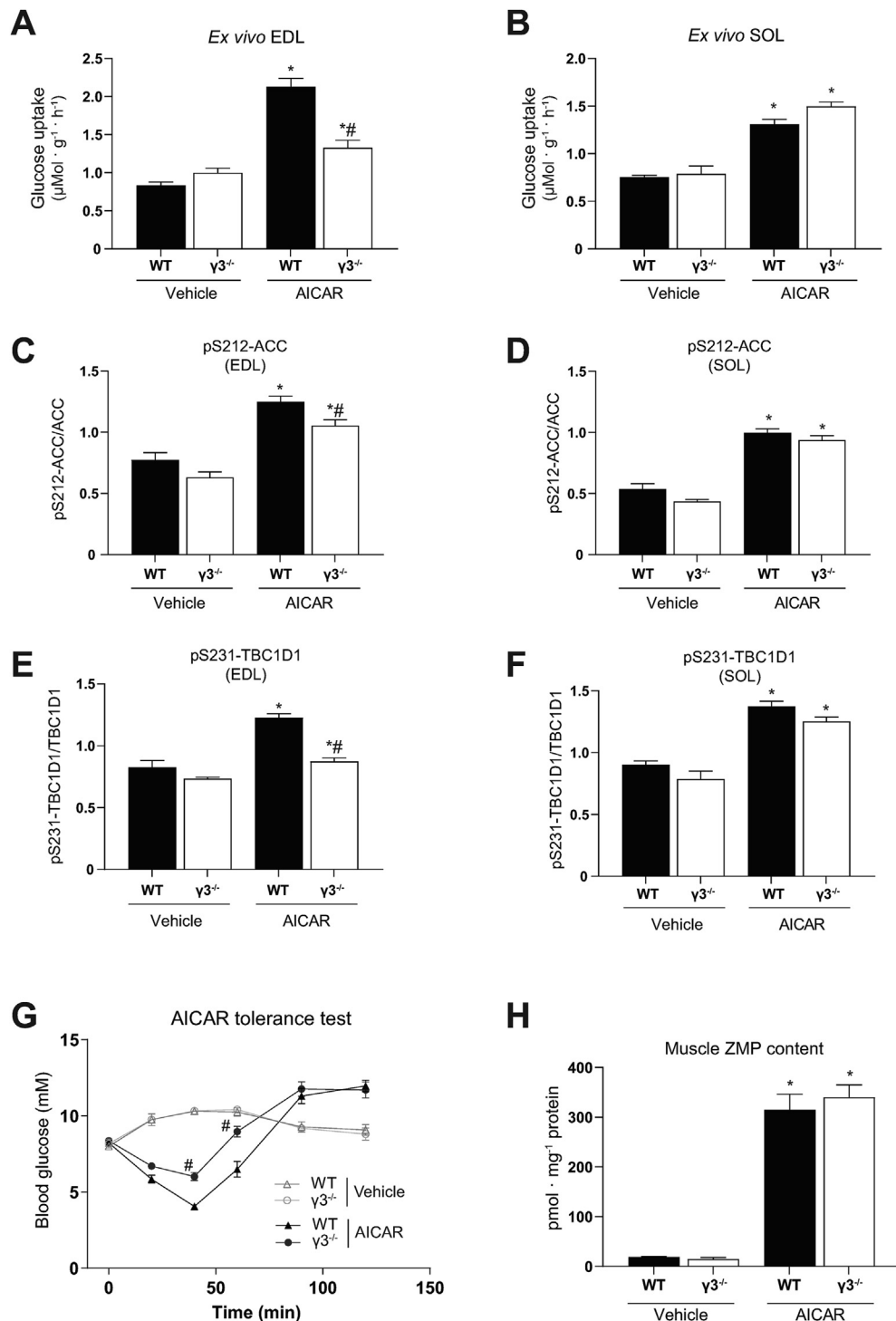
Figure 4: AMPKγ3 is required for AICAR-induced glucose uptake in glycolytic skeletal muscles and hypoglycemia. (A–F) EDL or SOL muscles were isolated from the indicated genotypes and incubated in the absence (vehicle, DMSO) or presence of AICAR (2 mM) for 50 min followed by an additional 10-min incubation with the radioactive 2-deoxy-glucose tracer. One portion of the muscle extracts was subjected to glucose uptake measurement (A, B) and the other was used for immunoblot analysis using the automated capillary immunoblotting system with the indicated antibodies (C–F) (n = 4–7 per treatment/genotype). (G, H) AICAR tolerance test and muscle ZMP analysis. Mice were fasted for 3 h and injected either with vehicle (water) or AICAR (250 mg/kg body weight, i.p.) followed by blood glucose kinetics measurement over the indicated duration (G). Following the AICAR tolerance test, mice were euthanized and GAS muscles were extracted and ZMP levels were determined (H) (n = 5–12 per treatment/genotype). Results are shown as means ± SEM. Statistical significance was determined using the unpaired/two-tailed Student's t-test or one-way analysis of variance (ANOVA) with Bonferroni correction or two-way ANOVA and are shown as *$P < 0.05$ (treatment effect within the same genotype), #$P < 0.05$ (WT vs. γ3$^{-/-}$ within the same treatment). GAS; gastrocnemius, EDL; extensor digitorum longus, SOL; soleus, AICAR; 5-aminoimidazole-4-carboxamide ribonucleoside, ZMP; AICAR monophosphate.

Original Article
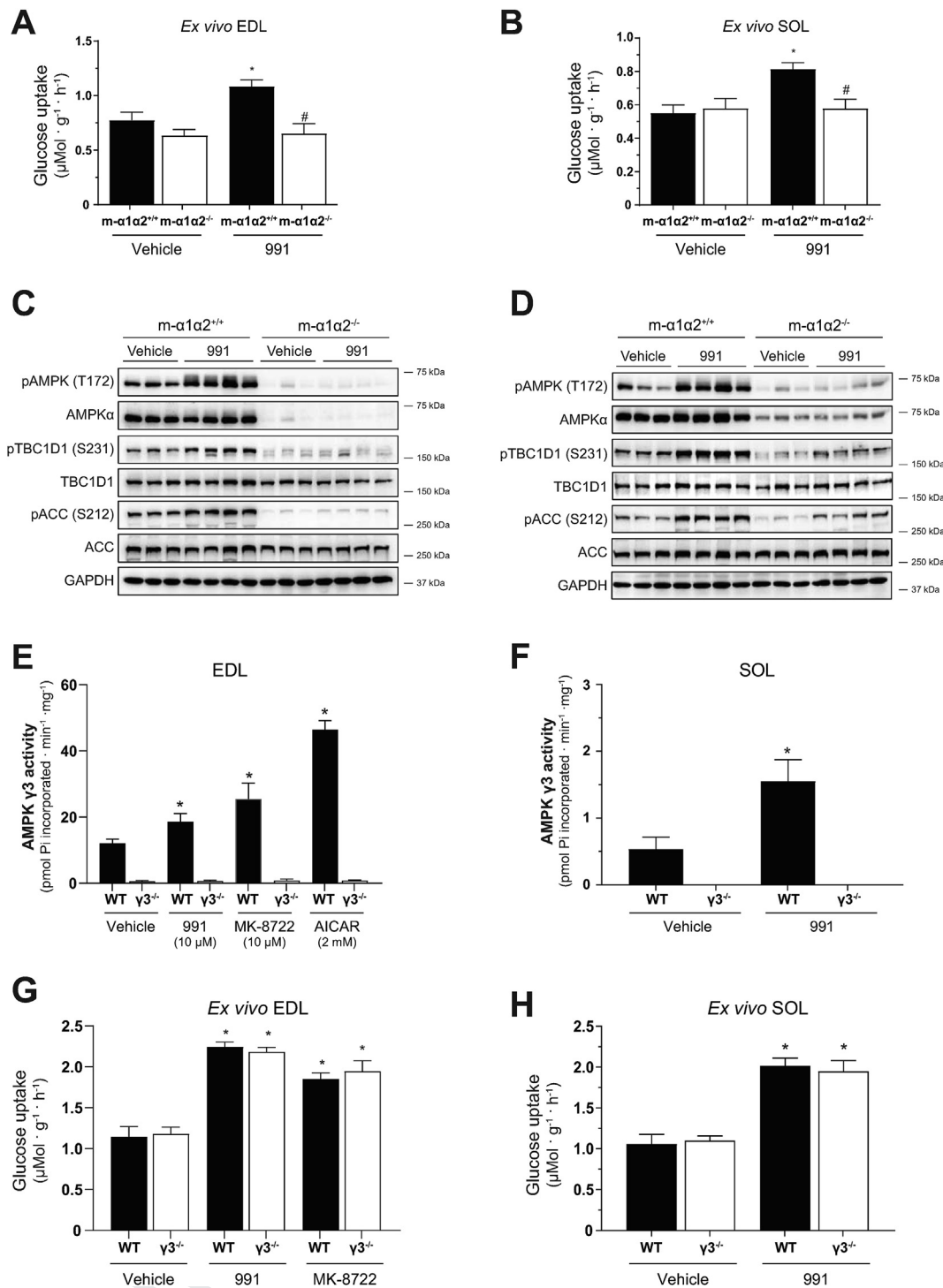
Figure 5: AMPKα1/α2, but not γ3, is required for glucose uptake skeletal muscles and hypoglycemia in response to the ADaM site-targeted activators, 991 and MK-8722. (A–D) EDL or SOL muscles were isolated from the indicated genotypes and incubated in the absence (vehicle, DMSO) or presence of 991 (10 μM) for 50 min followed by an additional 10-min incubation with the radioactive 2-deoxy-glucose tracer. One portion of the muscle extracts was subjected to glucose uptake measurement (A, B) and the other was used for immunoblot analysis using the indicated antibodies (followed by a signal detection using enhanced chemiluminescence) (C, D, n = 3–4 per treatment/genotype). (E–L) EDL or SOL muscles were isolated from the indicated genotypes and incubated in the absence (vehicle, DMSO) or presence of the indicated compounds for 50 min followed by an additional 10-min incubation with the radioactive 2-deoxy-glucose tracer. One portion of the muscle extracts was subjected to immunoprecipitation with the γ3 antibody followed by an *in vitro* AMPK activity assay (E, F, n = 4–14). The other portion was subjected to glucose uptake measurement (G, H, n = 4–9) or immunoblot analysis using the automated capillary immunoblotting system with the indicated antibodies (I–L, n = 4–9). (M) MK-8722 tolerance test. Mice were fasted for 3 h and orally treated either with vehicle or MK-8722 (10 mg/kg body weight) followed by blood glucose kinetics monitoring over the indicated duration. Results are shown as means ± SEM. Statistical significance was determined using the unpaired/two-tailed Student's t-test or one-way analysis of variance (ANOVA) with Bonferroni correction or two-way ANOVA and are shown as *$P < 0.05$ (treatment effect within the same genotype), #$P < 0.05$ (WT vs. γ3$^{-/-}$ within the same treatment). EDL; extensor digitorum longus; SOL; soleus, AICAR; 5-aminoimidazole-4-carboxamide ribonucleoside.

I

pS212-ACC
(EDL)

J

pS212-ACC
(SOL)

K

pS231-TBC1D1
(EDL)

L

pS231-TBC1D1
(SOL)

M

MK-8722 tolerance test
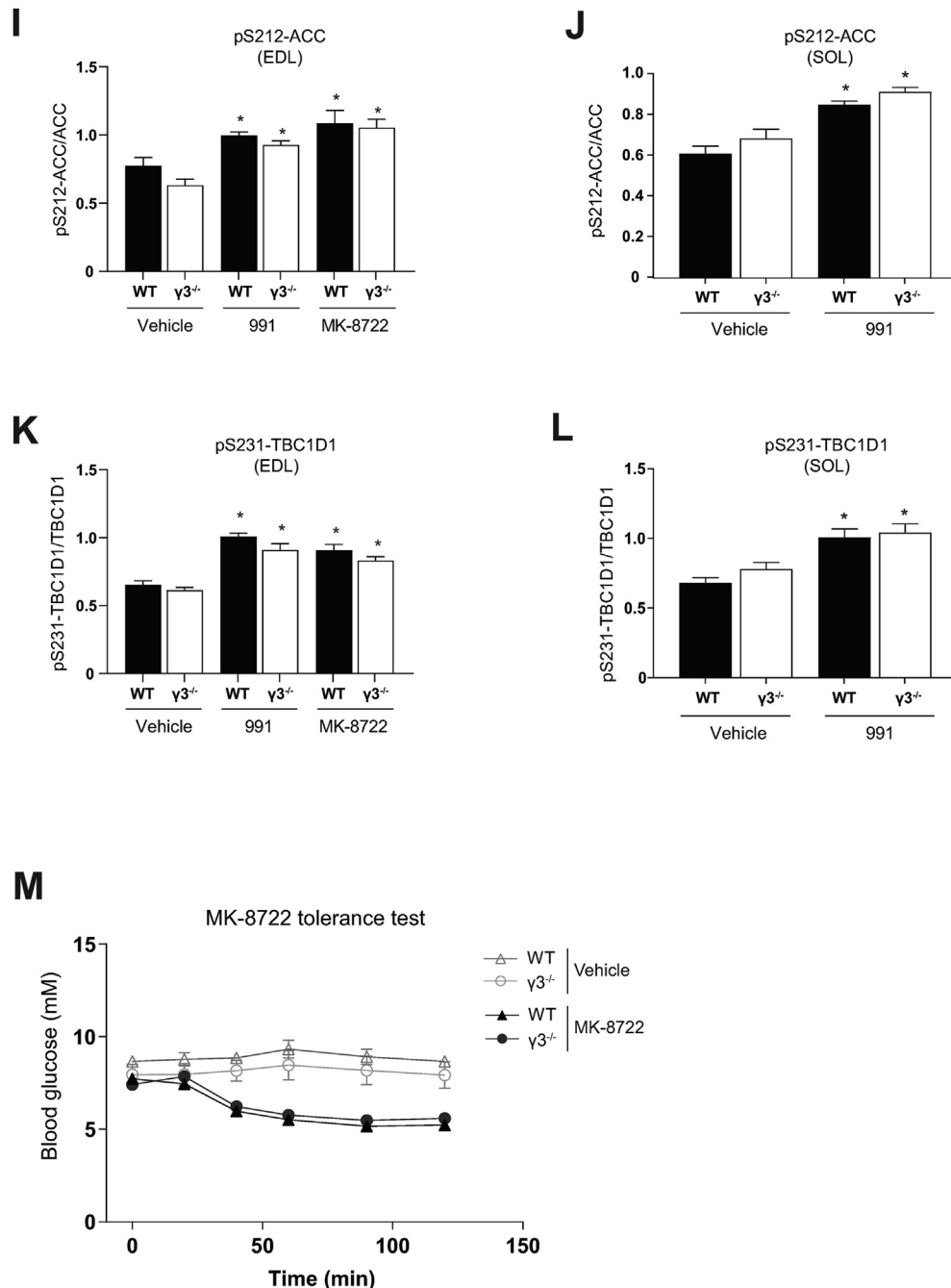
Figure 5: (continued).

we measured the phosphorylation of ACC and TBC1D1, established surrogate markers of *cellular* AMPK activity in muscle. As shown in Figure 4C—F, the phosphorylation of ACC and TBC1D1 was increased in both EDL and soleus in response to AICAR in WT mice. The AICAR-mediated increase in the phosphorylation of ACC and TBC1D1 was reduced in EDL, but not in soleus, in γ3 KO mice (Figure 4C—F). We confirmed that there is no sex-dependent AICAR effect, as AICAR-stimulated glucose uptake was similarly reduced in EDL muscle from female γ3 KO mice (data not shown). We investigated whether a partial loss of γ3 results in a reduction of AICAR-stimulated glucose uptake in EDL. Heterozygous γ3$^{+/-}$ mice had ∼50% reduction in γ3

expression in GAS, but the expression of total AMPKα, α2 and β1/β2 was not reduced (Supplementary Figure 2A and B). Incubation of EDL with AICAR *ex vivo* resulted in similar increases in γ3-associated activity and glucose uptake, as well as phosphorylation of ACC and TBC1D1 in both WT and heterozygous γ3$^{+/-}$ mice (Supplementary Figure 2C—G).

We subsequently wanted to determine whether γ3 deficiency affected the hypoglycemic effects of AICAR *in vivo*. We utilized briefly fasted animals (3-h fast, 07:00—10:00), as the AICAR-induced reduction of blood glucose in overnight fasted (16 h) mice was predominantly caused by the suppression of hepatic glucose output [13]. After

Original Article
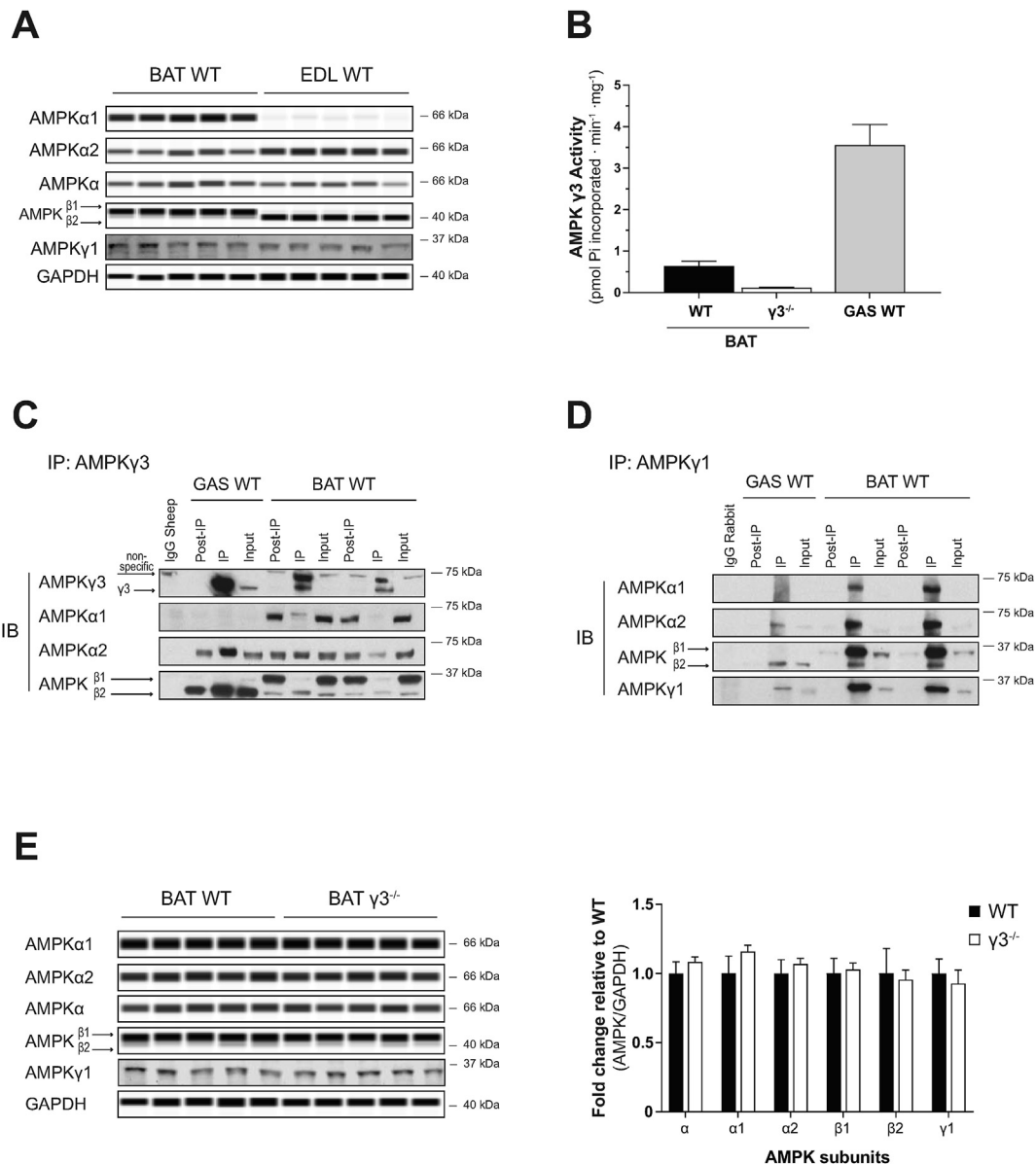
Figure 6: AMPKγ3 is expressed and forms functional trimeric complexes in mouse brown adipose tissue (BAT). (A) Immunoblot (IB) analysis of the skeletal muscle (EDL) and BAT extracts harvested from wild-type (WT) mice using the automated capillary immunoblotting system with the indicated antibodies. Note that γ1 expression was quantified using another immunoblotting system (Li-COR) due to antibody compatibility. (B) Extracts from GAS muscle (100 μg) or BAT (1,000 μg) were subjected to immunoprecipitation (IP) with γ3 antibody and the γ3-containing immune-complexes were assayed for AMPK activity *in vitro*. (C, D) γ3- or γ1-containing AMPK complexes were immunoprecipitated from GAS (100 μg) or BAT (1,000 μg) extracts and subsequently subjected to immunoblot analysis using the indicated antibodies followed by a signal detection using enhanced chemiluminescence. (E) Quantification of the isoform-specific AMPK expression of a panel of tissues (harvested from WT or γ3$^{-/-}$ mice) was performed using the automated capillary immunoblotting system with the indicated antibodies. Results are shown as means ± SEM (n = 5–7). GAS; gastrocnemius, EDL; extensor digitorum longus.

administration of a bolus of AICAR (250 mg/kg body weight, i.p.) or vehicle, we monitored blood glucose kinetics for 2 h in WT and γ3 KO mice. As shown in Figure 4G, we observed that the blood glucose-lowering action of AICAR was blunted (40 and 60 min time points) in γ3 KO compared to that in WT mice. We confirmed that ZMP content in GAS muscle following AICAR administration was comparably increased between the two genotypes (Figure 4H). Additionally, AICAR did not affect adenylate energy charge in GAS from both genotypes (Supplementary Figure 2H). Collectively, these results suggest that γ3 (i.e. γ3-containing AMPK complex(es)) plays an important role in

AICAR-mediated glucose uptake and disposal in glycolytic skeletal muscles.

3.5. ADaM site-targeted activators normally stimulate glucose uptake in skeletal muscle and lower blood glucose levels in AMPKγ3 KO mice

The ADaM site-binding pan AMPK activator, 991, robustly stimulates glucose uptake in isolated mouse skeletal muscle tissues *ex vivo* [22,50]. We initially confirmed that the 991-stimulated glucose uptake was fully dependent on AMPK in both EDL and soleus using skeletal
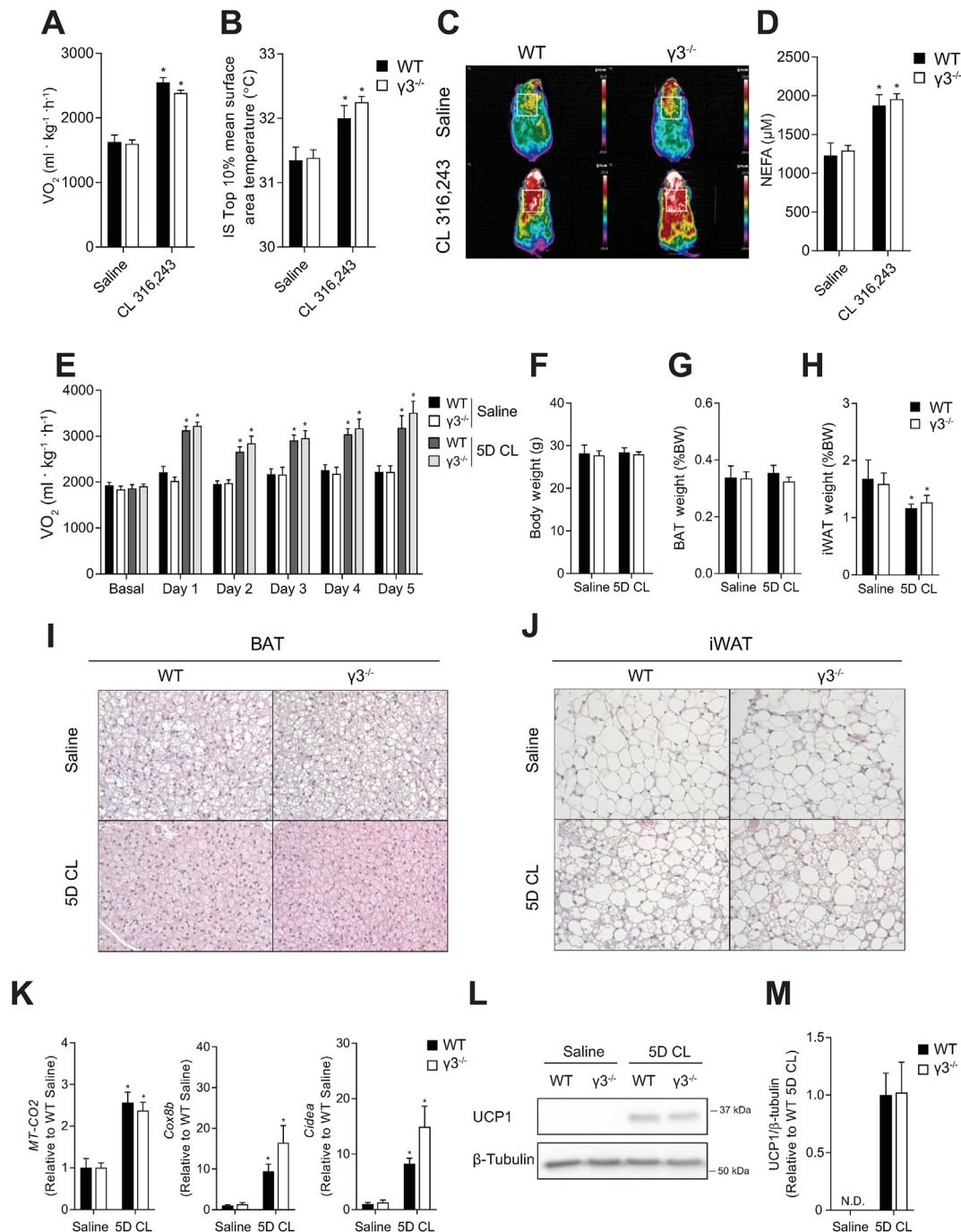
Figure 7: AMPK γ3 is not required for the non-shivering thermogenesis or the browning of inguinal white adipose tissue (WAT) in mice. (A) Oxygen consumption (VO₂), (B, C) Interscapular brown adipose tissue (BAT) surface area temperature with representative thermal images, and (D) serum non-esterified free fatty acid (NEFA) concentration in response to a single injection of saline or CL 316,243 in male WT or γ3$^{-/-}$ mice (0.033 nmol/g, 20 min time-point), n = 9—13 per group. Data are means ± SEM with a CL 316,243 effect shown as *P < 0.05, as determined via repeated measures two-way ANOVA. (E) Oxygen consumption (VO₂) basally and 6-h post-injection of saline or CL 316,243 in male WT or γ3$^{-/-}$ mice on indicated days, n = 5—8 per group. (F) Final body weight (BW), (G) BAT weight, and (H) inguinal WAT (iWAT) depot weight following 5 consecutive days of saline or CL 316,243 (5D CL) injections in male WT or γ3$^{-/-}$ mice, n = 5—8 per group. (I, J) Representative histological images of H&E-stained BAT (I) and iWAT (J) (10× magnification) from male WT or γ3$^{-/-}$ mice treated with saline or 5D CL. K) mRNA expression of genes indicative of iWAT browning, *MT-CO2* (n = 4—8 per group), *Cox8b* (n = 5—8 per group), and *Cidea* (n = 5—7 per group) in male WT or γ3$^{-/-}$ mice treated with saline or 5D CL for 5 days. L) Immunoblot analysis and densitometry quantification (M) of UCP1 in male WT and γ3$^{-/-}$ mice treated with saline or 5D CL for 5 days (n = 6—8 per group). Data are means ± SEM with *P < 0.05 denoting a 5D CL effect, as determined by repeated measures two-way ANOVA (A) and regular two-way ANOVA.

Original Article

muscle-specific AMPKα1/α2 double KO (m-α1/α2 DKO) mice (Figure 5A, B). Immunoblot analysis validated AMPKα deficiency and profound decreases in the phosphorylation of ACC and TBC1D1 in the absence or presence of 991 in both EDL and soleus in the m-α1/α2 DKO mice (Figure 5C, D). We subsequently assessed the effect of 991, MK-8722 (a structural analog of 991 [24]), and AICAR on γ3-associated AMPK activity in isolated muscle from WT and γ3 KO ex vivo. As shown in Figure 5E, γ3-associated activity was increased (∼1.5—2-fold) with 991 or MK-8722 and robustly increased (∼3-fold) with AICAR in EDL from WT mice. Despite minimal γ3-associated activity detectable in soleus, the activity was increased ∼2-fold with 991 in WT mice (Figure 5F). As expected, there was no γ3-associated AMPK activity present in skeletal muscle from γ3 KO mice (Figure 5E, F). In contrast to the effect of AICAR, incubation of EDL with 991 or MK-8722 resulted in comparable increases in glucose uptake in WT and γ3 KO mice (Figure 5G). We also observed that 991-stimulated glucose uptake was similar in soleus between WT and γ3 KO mice (Figure 5H). We noted that 991 and/or MK-8722 increased phosphorylation of ACC and TBC1D1 in EDL and soleus with no differences in the levels of phosphorylation between WT and γ3 KO mice (Figure 5I—L). Consistent with the ex vivo results, oral administration of MK-8722 (10 or 30 mg/kg body weight) resulted in a comparable blood glucose-lowering kinetics in vivo between WT and γ3 KO mice (Figure 5M and Supplementary Fig. 3). Taken together, we demonstrated that γ3 is dispensable for the stimulation of glucose uptake and disposal in skeletal muscle in response to 991 or MK-8722 (ADaM site targeted compounds).

3.6. AMPKγ3 protein and its associated AMPK trimeric complexes are present in mouse BAT

Prkag3 mRNA are expressed in mouse brown adipose precursors [37]; however, whether γ3 proteins are expressed and exist as part of functional AMPK trimeric complexes in BAT is unknown. We initially performed a comparison of AMPK subunit/isoform protein expression profiles between skeletal muscle (EDL) and BAT from WT mice, which revealed distinct profiles between the two tissues (Figure 6A). Compared to skeletal muscle, BAT expresses relatively higher and lower amounts of α1 and α2, respectively. The total AMPKα content (assessed by a pan-AMPKα antibody) was similar between the tissues. However, the efficacy of the isoform-specific detection of α1 and α2 proteins by this antibody is unknown. We observed a divergent expression pattern of the β isoforms between the tissues. While skeletal muscle predominantly expresses β2, BAT predominantly expresses β1 (Fig. 6A). Conversely, γ1 expression is similar between the tissues. We subsequently immunoprecipitated γ3 from BAT (and GAS muscle as control) and performed either γ3-associated AMPK activity assay or immunoblot analysis to identify α and β subunit isoforms interacting with γ3. As shown in Figure 6B, we detected γ3 and its associated AMPK activity in BAT, but not from γ3 KO mice. Interestingly, γ3 preferentially interacts with α2 and β2 (Fig. 6C), whereas γ1 interacts with α1/α2 and preferentially with β1 (Fig. 6D). We also observed that γ3 deficiency in BAT did not affect the abundance of other AMPK subunit isoforms (Fig. 6E). Collectively, we provide evidence that AMPKγ3 protein is expressed in BAT and it forms functional complexes by mainly interacting with α2 and β2.

3.7. AMPKγ3 is not required for the acute induction of UCP1-mediated non-shivering thermogenesis in the BAT

AMPK plays an important role for BAT formation [37] and thermogenesis in response to cold exposure and β3-adrenoreceptor (β3-AR) stimulation in rodents [36]. We probed BAT function using the β3-AR agonist CL-316,243 (CL), which increases thermogenesis through a UCP1-dependent mechanism [44]. A single injection of CL increased oxygen consumption and interscapular BAT surface area temperature in both WT and γ3 KO mice; however, there were no differences between the genotypes (Figure 7A—C). Furthermore, CL increased serum non-esterified free fatty acid concentration to a similar extent in both WT and γ3 KO mice, indicating no major alterations in lipolysis (Fig. 7D).

3.8. AMPKγ3 is not required for the adaptive response to non-shivering thermogenesis or the browning of inguinal white adipose tissue (iWAT)

We subsequently performed injections of CL for five consecutive days to determine whether γ3 is required for the adaptive response to non-shivering thermogenesis or the browning of iWAT. Daily treatment of mice with CL increased oxygen consumption without altering body or BAT weight, but did reduce iWAT weight similarly in both WT and γ3 KO mice (Figure 7E—H). Furthermore, γ3 KO mice treated with CL for five days had similar morphological changes in BAT — with smaller lipid droplets — and the appearance of multilocular adipocytes within iWAT (Figure 7I, J). Finally, CL treatment increased UCP1 expression (at both transcript and protein levels), as well as levels of other thermogenic and mitochondrial genes such as Cox2, Cox8b, and Cidea in both WT and γ3 KO mice (Fig. 7K—M). These results demonstrate that γ3 is dispensable for β-adrenergic-induced remodeling of BAT and iWAT in mice.

4. DISCUSSION

AMPK has been considered as a promising target for the treatment of the metabolic syndrome over the last decades. The identification of new mechanisms for drug targeting on AMPK (i.e. discovery of ADaM site) has advanced the development of more potent and selective AMPK activators with improved bioavailability [9]. Recent proof-of-concept studies in rodents and non-human primates have compellingly demonstrated that oral administration of pan AMPK activators (e.g. MK-8722, PF-739) targeting the ADaM site can promote glucose uptake in skeletal muscle, and ameliorate insulin resistance and reduce hyperglycemia without causing hypoglycemia [23,24]. Since γ3 is exclusively expressed in skeletal muscle, understanding of the physiological roles that γ3 plays in regulating glucose metabolism/homeostasis is important for the development of skeletal muscle-selective AMPK activators. In addition, a recent in vitro study that reported that γ3 plays a role in BAT development [37] prompted us to investigate the role for γ3 in thermogenesis and adipose browning in vivo. In the current study, we found that genetic ablation of γ3 resulted in a selective loss of AICAR-, but not MK-8722-induced blood glucose-lowering in vivo and glucose uptake specifically in glycolytic muscles ex vivo. We also found that γ3 is dispensable for the acute induction of UCP1-mediated non-shivering thermogenesis in BAT or the adaptive response to non-shivering thermogenesis and the browning of WAT.

We observed that the levels of α2 and β2 isoforms were reduced (∼20—30%) in glycolytic (GAS and EDL), but not in oxidative (soleus) muscle in γ3−/− KO compared to WT mice. In soleus, a previous study reported that γ3 was only detectable in a complex with α2 and β2, but relative amount of this complex was shown to be only 2% and >90% of α2 and β2 forms complexes with γ1 [21,34]. Conversely, α2 and β2 form complexes with γ1 (70%) and γ3 (20%), respectively in EDL muscle. Therefore, it is plausible that a constitutive deficiency of γ3 resulted in a partial loss of α2 and β2 proteins due to degradation of

www.molecularmetabolism.com

MOLECULAR METABOLISM

excess monomeric forms of α2 and β2 in GAS/EDL, but not in soleus muscle. Consistent with this notion, a constitutive deletion of γ1, a ubiquitously expressed γ isoform across tissues, resulted in much more profound reductions of all its interacting AMPK isoforms (α1, α2, β1, and β2) in mouse tissues including skeletal muscle [51]. Even though previous work reported that γ3 deficiency did not affect the levels of other AMPK isoforms in GAS muscles, there was a ~25% reduction of α2 protein expression in GAS muscles from γ3 KO compared to WT mice [25]. It might be the case that it did not reach statistical significance due to insufficient power. In line with this assumption, phosphorylation of AMPKα (Thr172) was reduced in EDL from the same γ3 KO mouse model (compared to WT) [52].

A complete loss of functional α2 or β2 was associated with ablated glucose uptake with AICAR in mouse skeletal muscle *ex vivo* [28,30,31]. To our knowledge, whether a partial loss of α2 and/or β2 (e.g. in heterozygous α2$^{+/-}$ or β2$^{+/-}$ mice) reduces glucose uptake in EDL with AICAR *ex vivo* is unknown. However, we previously demonstrated that a profound reduction (>60%) of α2 activity observed in EDL of the LKB1 hypomorphic mice resulted in comparable AICAR-stimulated glucose uptake and ACC phosphorylation compared to WT mice [4]. Moreover, we herein report that 991/MK-8722 stimulates glucose uptake in EDL muscle from the γ3 KO mice. Therefore, a partial reduction of α2/β2 expression (~20–30%) is unlikely to be responsible for the decrease in AICAR-stimulated glucose uptake in γ3-deficient EDL muscle.

One of the major findings of the present study was that γ3-deficiency caused blunted glucose uptake in EDL *ex vivo* and hypoglycemic response *in vivo* with AICAR, but not with ADaM site-targeted compounds (i.e. 991, MK-8722). This was particularly intriguing as both AICAR and 991/MK-8722 require intact AMPK catalytic activity to promote glucose uptake in skeletal muscle tissues/cells [23,24,28–32,45,50], and we report here that both AICAR and 991/MK-8722 increased γ3-associated AMPK activity. The dose of AICAR (2 mM) used had a more potent effects on γ3-associated activity (~3-fold increase) as compared to 10 μM 991/MK-8722 (~1.5–2-fold). However, the results from this assay do not reflect cellular activity, as the *in vitro* kinase assay following immunoprecipitation accounts for covalently-regulated activity (e.g. phosphorylation), but not allosterically-regulated (i.e. by AMP/ZMP, 991/MK-8722) activity. Judging from phosphorylation levels of ACC and TBC1D1, AICAR and 991/MK-8722 comparably increased cellular AMPK activity in skeletal muscle. However, notably, compound-induced phosphorylation of ACC and TBC1D1 *ex vivo* was only reduced in EDL when treated with AICAR, but not with 991/MK-8722, in γ3 KO compared to WT. This raises the possibility that AICAR preferentially activates γ3- over γ1-containing complex(es). Concordantly, AMP appears to have stronger binding affinity to nucleotide binding site 3 (in the CBS domain) of γ3 (~40 μM) than γ1 (~300–600 μM) *in vitro* (using bacterial AMPK-complex preparations) [53]. Conversely, another *in vitro* study reported that while AMP potently (allosterically) activated α2β2γ1 (~3-fold), it barely activated α2β2γ3 (<15%) complex [54]. Thus, how these *in vitro* results can be interpreted and translated into cellular context remain unclear. The γ-isoforms all contain a highly conserved C-terminal region harboring the four CBS domains. Conversely, the γ2 and γ3 isoforms contain long N-terminal extensions that are not present in the γ1 isoform. These N-terminal extensions display no apparent sequence conservation between isoforms. To date, there are no crystal structures available for γ2- or γ3-containing AMPK trimeric complexes and it is unknown whether the N-terminal extensions of γ2 or γ3 play any functional role. A recent study using cell-based assays demonstrated that α2β2γ1 and α2β2γ3 complexes were similarly activated

in response to 991 treatment, whereas α2β2γ2 complexes exhibited a greater activation (compared to α2β2γ1/α2β2γ3 complexes) [55]. The authors proposed that the effect is mediated by the N-terminal region of γ2 and is due to enhanced protection of AMPKα Thr172 from dephosphorylation. Whether N-terminal extension of γ3 has any specific role to play in muscle cells/tissue and in AMP/ZMP-mediated regulation of AMPK and glucose uptake in skeletal muscle is unknown. Even though γ3 deficiency was associated with reduced AICAR-stimulated glucose uptake in EDL muscle *ex vivo*, we provide the first evidence that the AICAR-induced blood glucose lowering effect *in vivo* was robustly reduced in γ3 KO compared to WT mice, which was quite similar to AMPKα2 KO and α2 kinase-dead (KD) expressing transgenic mice [28,30]. Indeed, α2 KO and KD mice still showed decreases in blood glucose in response to an acute injection of AICAR, which is most likely due to the inhibitory effect of AICAR on hepatic glucose production through ZMP-dependent inhibition of fructose 1,6-bisphosphatase 1 [13,56]. MK-8722 has been shown to cause blood glucose-lowering effect through the stimulation of glucose uptake in both glycolytic (GAS) and oxidative (soleus) muscle *in vivo* [24]. In contrast to AICAR, but consistent with *ex vivo* data, we provided evidence that MK-8722-induced skeletal muscle glucose uptake and blood glucose-lowering effects were comparable between γ3 KO and WT mice. This compellingly demonstrates that γ3 is dispensable (in other words γ1 and its containing α2β2γ1 complex is sufficient) in stimulating glucose uptake in skeletal muscle in response to pan-AMPK ADaM site-binding activators. To further test this proposition, it would be of interest to generate and study skeletal muscle-specific and inducible AMPKγ1 KO mouse model.

Evidence suggests that AMPK plays a vital role in regulating the development of BAT, maintenance of BAT mitochondrial function, and browning of WAT [35]. We provided genetic evidence that mice lacking functional AMPK specifically in adipocytes, through an inducible deletion of β1 and β2, were intolerant to cold and resistant to β-adrenergic stimulation of brown and beige adipose tissues [36]. Similar findings were also observed in AMPK α1/α2 KO mice [57]. Detailed protein expression profiles of AMPK subunit isoforms in BAT in comparison to other tissues have not been performed, and to our knowledge, the presence of γ3 protein in BAT has not been demonstrated. RNA sequencing results identified γ3 at intermediate amounts (Reads Per Kilobase of transcript per Million mapped reads, >40) in mouse brown preadipocytes [37]. Strikingly, RNAi-mediated knockdown of either γ1 or γ3 (but not γ2) in brown adipocyte precursors was sufficient to profoundly reduce (>80%) UCP1 protein expression. Using γ3-specific antibodies we developed, we have demonstrated that γ3 protein/activity is present and in complex mainly with α2 and β2 in mouse BAT. Even though we showed that γ3 is dispensable for β-adrenergic-induced thermogenesis and remodeling of BAT and iWAT, future studies are warranted to determine whether the specific activation of the γ3-containing complexes (when such drugs are available) induces adipose browning and subsequent amelioration of insulin resistance and fatty liver disease.

5. CONCLUSIONS

We demonstrated that a genetic loss of γ3 resulted in a selective loss of AICAR-stimulated glucose-lowering *in vivo* and glucose uptake specifically in glycolytic skeletal muscles *ex vivo*. We also showed that γ3 is dispensable for thermogenesis and the browning of WAT. The potent pan-AMPK activators targeting the ADaM site are effective in reversing hyperglycemia in rodents and non-human primates, and this is due to activation of AMPK in skeletal muscle, not in the liver [23,24].

www.molecularmetabolism.com

Original Article

This might make them valuable adjuncts to metformin, which acts primarily on the liver [13,58,59]. However, there are remaining important safety issues that need to be carefully considered and examined, such as the potential for AMPK activation to promote cardiac hypertrophy or the survival of cancer cells (e.g. under hypoxic conditions). To avoid these potential liabilities, the development of AMPK activators that can be targeted to specific tissues (for example, the liver, muscle, and adipose) by taking advantage of isoform-specific selectivity may be beneficial. We and others have shown that selective targeting of specific AMPK isoforms (e.g. α1, β1) by small molecules is possible [9,60,61]. The current study provides key insights that ADaM site binding compounds will not be selective for γ3-containing complex and skeletal muscle-selective AMP-mimetic may provide beneficial effects on glycemia in people with type 2 diabetes. Nevertheless, when a γ3-complex selective activator is available in the future, ascertaining whether it sufficiently promotes skeletal muscle glucose uptake without causing cardiac hypertrophy and glycogen accumulation will be of major interest.

APPENDIX A. SUPPLEMENTARY DATA

Supplementary data to this article can be found online at https://doi.org/10.1016/j.molmet.2021.101228.

REFERENCES

[1] Hardie, D.G., 2011. AMP-activated protein kinase: an energy sensor that regulates all aspects of cell function. Genes & Development 25(18):1895–1908.

[2] Herzig, S., Shaw, R.J., 2018. AMPK: guardian of metabolism and mitochondrial homeostasis. Nature Reviews Molecular Cell Biology 19(2):121–135.

[3] Hawley, S.A., Davison, M., Woods, A., Davies, S.P., Beri, R.K., Carling, D., et al., 1996. Characterization of the AMP-activated protein kinase kinase from rat liver and identification of threonine 172 as the major site at which it phosphorylates AMP-activated protein kinase. Journal of Biological Chemistry 271(44):27879–27887.

[4] Sakamoto, K., McCarthy, A., Smith, D., Green, K.A., Grahame Hardie, D., Ashworth, A., et al., 2005. Deficiency of LKB1 in skeletal muscle prevents AMPK activation and glucose uptake during contraction. The EMBO Journal 24(10):1810–1820.

[5] Shaw, R.J., Lamia, K.A., Vasquez, D., Koo, S.H., Bardeesy, N., Depinho, R.A., et al., 2005. The kinase LKB1 mediates glucose homeostasis in liver and therapeutic effects of metformin. Science 310(5754):1642–1646.

[6] Gowans, G.J., Hawley, S.A., Ross, F.A., Hardie, D.G., 2013. AMP is a true physiological regulator of AMP-activated protein kinase by both allosteric activation and enhancing net phosphorylation. Cell Metabolism 18(4):556–566.

[7] Xiao, B., Sanders, M.J., Underwood, E., Heath, R., Mayer, F.V., Carmena, D., et al., 2011. Structure of mammalian AMPK and its regulation by ADP. Nature 472(7342):230–233.

[8] Oakhill, J.S., Steel, R., Chen, Z.P., Scott, J.W., Ling, N., Tam, S., et al., 2011. AMPK is a direct adenylate charge-regulated protein kinase. Science 332(6036):1433–1435.

[9] Steinberg, G.R., Carling, D., 2019. AMP-activated protein kinase: the current landscape for drug development. Nature Reviews Drug Discovery 18(7):527–551.

[10] Buhl, E.S., Jessen, N., Pold, R., Ledet, T., Flyvbjerg, A., Pedersen, S.B., et al., 2002. Long-term AICAR administration reduces metabolic disturbances and lowers blood pressure in rats displaying features of the insulin resistance syndrome. Diabetes 51(7):2199–2206.

[11] Guigas, B., Sakamoto, K., Taleux, N., Reyna, S.M., Musi, N., Viollet, B., et al., 2009. Beyond AICA riboside: in search of new specific AMP-activated protein kinase activators. IUBMB Life 61(1):18–26.

[12] Foretz, M., Hebrard, S., Leclerc, J., Zarrinpashneh, E., Soty, M., Mithieux, G., et al., 2010. Metformin inhibits hepatic gluconeogenesis in mice independently of the LKB1/AMPK pathway via a decrease in hepatic energy state. Journal of Clinical Investigation 120(7):2355–2369.

[13] Hunter, R.W., Hughey, C.C., Lantier, L., Sundelin, E.I., Peggie, M., Zeqiraj, E., et al., 2018. Metformin reduces liver glucose production by inhibition of fructose-1-6-bisphosphatase. Nature Medicine 24(9):1395–1406.

[14] Collodet, C., Foretz, M., Deak, M., Bultot, L., Metairon, S., Viollet, B., et al., 2019. AMPK promotes induction of the tumor suppressor FLCN through activation of TFEB independently of mTOR. The FASEB Journal 33(11):12374–12391.

MMM

MOLECULAR
METABOLISM

[15] Cool, B., Zinker, B., Chiou, W., Kifle, L., Cao, N., Perham, M., et al., 2006. Identification and characterization of a small molecule AMPK activator that treats key components of type 2 diabetes and the metabolic syndrome. Cell Metabolism 3(6):403–416.

[16] Goransson, O., McBride, A., Hawley, S.A., Ross, F.A., Shpiro, N., Foretz, M., et al., 2007. Mechanism of action of A-769662, a valuable tool for activation of AMP-activated protein kinase. Journal of Biological Chemistry 282(45): 32549–32560.

[17] Scott, J.W., van Denderen, B.J., Jorgensen, S.B., Honeyman, J.E., Steinberg, G.R., Oakhill, J.S., et al., 2008. Thienopyridone drugs are selective activators of AMP-activated protein kinase beta1-containing complexes. Chemistry & Biology 15(11):1220–1230.

[18] Sanders, M.J., Ali, Z.S., Hegarty, B.D., Heath, R., Snowden, M.A., Carling, D., 2007. Defining the mechanism of activation of AMP-activated protein kinase by the small molecule A-769662, a member of the thienopyridone family. Journal of Biological Chemistry 282(45):32539–32548.

[19] Xiao, B., Sanders, M.J., Carmena, D., Bright, N.J., Haire, L.F., Underwood, E., et al., 2013. Structural basis of AMPK regulation by small molecule activators. Nature Communications 4:3017.

[20] Calabrese, M.F., Rajamohan, F., Harris, M.S., Caspers, N.L., Magyar, R., Withka, J.M., et al., 2014. Structural basis for AMPK activation: natural and synthetic ligands regulate kinase activity from opposite poles by different molecular mechanisms. Structure 22(8):1161–1172.

[21] Treebak, J.T., Birk, J.B., Hansen, B.F., Olsen, G.S., Wojtaszewski, J.F., 2009. A-769662 activates AMPK beta1-containing complexes but induces glucose uptake through a PI3-kinase-dependent pathway in mouse skeletal muscle. American Journal of Physiology — Cell Physiology 297(4):C1041–C1052.

[22] Bultot, L., Jensen, T.E., Lai, Y.C., Madsen, A.L., Collodet, C., Kviklyte, S., et al., 2016. Benzimidazole derivative small-molecule 991 enhances AMPK activity and glucose uptake induced by AICAR or contraction in skeletal muscle. American Journal of Physiology. Endocrinology and Metabolism 311(4):E706–E719.

[23] Cokorinos, E.C., Delmore, J., Reyes, A.R., Albuquerque, B., Kjobsted, R., Jorgensen, N.O., et al., 2017. Activation of skeletal muscle AMPK promotes glucose disposal and glucose lowering in non-human primates and mice. Cell Metabolism 25(5), 1147–1159, e1110.

[24] Myers, R.W., Guan, H.P., Ehrhart, J., Petrov, A., Prahalada, S., Tozzo, E., et al., 2017. Systemic pan-AMPK activator MK-8722 improves glucose homeostasis but induces cardiac hypertrophy. Science 357(6350):507–511.

[25] Barnes, B.R., Marklund, S., Steiler, T.L., Walter, M., Hjalm, G., Amarger, V., et al., 2004. The 5′-AMP-activated protein kinase gamma3 isoform has a key role in carbohydrate and lipid metabolism in glycolytic skeletal muscle. Journal of Biological Chemistry 279(37):38441–38447.

[26] Mahlapuu, M., Johansson, C., Lindgren, K., Hjalm, G., Barnes, B.R., Krook, A., et al., 2004. Expression profiling of the gamma-subunit isoforms of AMP-activated protein kinase suggests a major role for gamma3 in white skeletal muscle. American Journal of Physiology. Endocrinology and Metabolism 286(2):E194–E200.

[27] Yu, H., Fujii, N., Hirshman, M.F., Pomerleau, J.M., Goodyear, L.J., 2004. Cloning and characterization of mouse 5′-AMP-activated protein kinase gamma3 subunit. American Journal of Physiology — Cell Physiology 286(2): C283–C292.

[28] Mu, J., Brozinick Jr., J.T., Valladares, O., Bucan, M., Birnbaum, M.J., 2001. A role for AMP-activated protein kinase in contraction- and hypoxia-regulated glucose transport in skeletal muscle. Molecular Cell 7(5):1085–1094.

[29] Fujii, N., Hirshman, M.F., Kane, E.M., Ho, R.C., Peter, L.E., Seifert, M.M., et al., 2005. AMP-activated protein kinase alpha2 activity is not essential for contraction- and hyperosmolarity-induced glucose transport in skeletal muscle. Journal of Biological Chemistry 280(47):39033–39041.

[30] Jorgensen, S.B., Viollet, B., Andreelli, F., Frosig, C., Birk, J.B., Schjerling, P., et al., 2004. Knockout of the alpha2 but not alpha1 5′-AMP-activated protein

kinase isoform abolishes 5-aminoimidazole-4-carboxamide-1-beta-4-ribofuranosidebut not contraction-induced glucose uptake in skeletal muscle. Journal of Biological Chemistry 279(2):1070–1079.

[31] Steinberg, G.R., O'Neill, H.M., Dzamko, N.L., Galic, S., Naim, T., Koopman, R., et al., 2010. Whole body deletion of AMP-activated protein kinase {beta}2 reduces muscle AMPK activity and exercise capacity. Journal of Biological Chemistry 285(48):37198–37209.

[32] Dasgupta, B., Ju, J.S., Sasaki, Y., Liu, X., Jung, S.R., Higashida, K., et al., 2012. The AMPK beta2 subunit is required for energy homeostasis during metabolic stress. Molecular and Cellular Biology 32(14):2837–2848.

[33] Hardie, D.G., Sakamoto, K., 2006. AMPK: a key sensor of fuel and energy status in skeletal muscle. Physiology 21:48–60.

[34] Kjobsted, R., Hingst, J.R., Fentz, J., Foretz, M., Sanz, M.N., Pehmoller, C., et al., 2018. AMPK in skeletal muscle function and metabolism. The FASEB Journal 32(4):1741–1777.

[35] Desjardins, E.M., Steinberg, G.R., 2018. Emerging role of AMPK in Brown and beige adipose tissue (BAT): implications for obesity, insulin resistance, and type 2 diabetes. Current Diabetes Reports 18(10):80.

[36] Mottillo, E.P., Desjardins, E.M., Crane, J.D., Smith, B.K., Green, A.E., Ducommun, S., et al., 2016. Lack of adipocyte AMPK exacerbates insulin resistance and hepatic steatosis through brown and beige adipose tissue function. Cell Metabolism 24(1):118–129.

[37] Perdikari, A., Kulenkampff, E., Rudigier, C., Neubauer, H., Luippold, G., Redemann, N., et al., 2017. A high-throughput, image-based screen to identify kinases involved in brown adipocyte development. Science Signaling 10(466).

[38] Nakada, D., Saunders, T.L., Morrison, S.J., 2010. Lkb1 regulates cell cycle and energy metabolism in haematopoietic stem cells. Nature 468(7324):653–658.

[39] Dos Santos, M., Backer, S., Saintpierre, B., Izac, B., Andrieu, M., Letourneur, F., et al., 2020. Single-nucleus RNA-seq and FISH identify coordinated transcriptional activity in mammalian myofibers. Nature Communications 11(1):5102.

[40] Shi, H., Munk, A., Nielsen, T.S., Daughtry, M.R., Larsson, L., Li, S., et al., 2018. Skeletal muscle O-GlcNAc transferase is important for muscle energy homeostasis and whole-body insulin sensitivity. Molecular Metabolism 11: 160–177.

[41] Chen, Q., Xie, B., Zhu, S., Rong, P., Sheng, Y., Ducommun, S., et al., 2017. A Tbc1d1 (Ser231Ala)-knockin mutation partially impairs AICAR- but not exercise-induced muscle glucose uptake in mice. Diabetologia 60(2):336–345.

[42] Dite, T.A., Langendorf, C.G., Hoque, A., Galic, S., Rebello, R.J., Ovens, A.J., et al., 2018. AMP-activated protein kinase selectively inhibited by the type II inhibitor SBI-0206965. Journal of Biological Chemistry 293(23):8874–8885.

[43] Scott, J.W., Galic, S., Graham, K.L., Foitzik, R., Ling, N.X., Dite, T.A., et al., 2015. Inhibition of AMP-activated protein kinase at the allosteric drug-binding site promotes islet insulin release. Chemistry & Biology 22(6):705–711.

[44] Crane, J.D., Mottillo, E.P., Farncombe, T.H., Morrison, K.M., Steinberg, G.R., 2014. A standardized infrared imaging technique that specifically detects UCP1-mediated thermogenesis in vivo. Molecular Metabolism 3(4):490–494.

[45] O'Neill, H.M., Maarbjerg, S.J., Crane, J.D., Jeppesen, J., Jorgensen, S.B., Schertzer, J.D., et al., 2011. AMP-activated protein kinase (AMPK) beta1beta2 muscle null mice reveal an essential role for AMPK in maintaining mitochondrial content and glucose uptake during exercise. Proceedings of the National Academy of Sciences of the United States of America 108(38): 16092–16097.

[46] Fentz, J., Kjobsted, R., Birk, J.B., Jordy, A.B., Jeppesen, J., Thorsen, K., et al., 2015. AMPKalpha is critical for enhancing skeletal muscle fatty acid utilization during in vivo exercise in mice. The FASEB Journal 29(5):1725–1738.

[47] Lantier, L., Fentz, J., Mounier, R., Leclerc, J., Treebak, J.T., Pehmoller, C., et al., 2014. AMPK controls exercise endurance, mitochondrial oxidative capacity, and skeletal muscle integrity. The FASEB Journal 28(7):3211–3224.

Original Article

[48] Zong, H., Ren, J.M., Young, L.H., Pypaert, M., Mu, J., Birnbaum, M.J., et al., 2002. AMP kinase is required for mitochondrial biogenesis in skeletal muscle in response to chronic energy deprivation. Proceedings of the National Academy of Sciences of the United States of America 99(25):15983–15987.

[49] Garcia-Roves, P.M., Osler, M.E., Holmstrom, M.H., Zierath, J.R., 2008. Gain-of-function R225Q mutation in AMP-activated protein kinase gamma3 subunit increases mitochondrial biogenesis in glycolytic skeletal muscle. Journal of Biological Chemistry 283(51):35724–35734.

[50] Lai, Y.C., Kviklyte, S., Vertommen, D., Lantier, L., Foretz, M., Viollet, B., et al., 2014. A small-molecule benzimidazole derivative that potently activates AMPK to increase glucose transport in skeletal muscle: comparison with effects of contraction and other AMPK activators. Biochemical Journal 460(3):363–375.

[51] Foretz, M., Hebrard, S., Guihard, S., Leclerc, J., Do Cruzeiro, M., Hamard, G., et al., 2011. The AMPKgamma1 subunit plays an essential role in erythrocyte membrane elasticity, and its genetic inactivation induces splenomegaly and anemia. The FASEB Journal 25(1):337–347.

[52] Treebak, J.T., Birk, J.B., Rose, A.J., Kiens, B., Richter, E.A., Wojtaszewski, J.F., 2007. AS160 phosphorylation is associated with activation of alpha2beta2gamma1- but not alpha2beta2gamma3-AMPK trimeric complex in skeletal muscle during exercise in humans. American Journal of Physiology. Endocrinology and Metabolism 292(3):E715–E722.

[53] Rajamohan, F., Reyes, A.R., Frisbie, R.K., Hoth, L.R., Sahasrabudhe, P., Magyar, R., et al., 2016. Probing the enzyme kinetics, allosteric modulation and activation of alpha1- and alpha2-subunit-containing AMP-activated protein kinase (AMPK) heterotrimeric complexes by pharmacological and physiological activators. Biochemical Journal 473(5):581–592.

[54] Ross, F.A., Jensen, T.E., Hardie, D.G., 2016. Differential regulation by AMP and ADP of AMPK complexes containing different gamma subunit isoforms. Biochemical Journal 473(2):189–199.

[55] Willows, R., Navaratnam, N., Lima, A., Read, J., Carling, D., 2017. Effect of different gamma-subunit isoforms on the regulation of AMPK. Biochemical Journal 474(10):1741–1754.

[56] Vincent, M.F., Erion, M.D., Gruber, H.E., Van den Berghe, G., 1996. Hypo-glycaemic effect of AICAriboside in mice. Diabetologia 39(10):1148–1155.

[57] Wu, L., Zhang, L., Li, B., Jiang, H., Duan, Y., Xie, Z., et al., 2018. AMP-activated protein kinase (AMPK) regulates energy metabolism through modulating thermogenesis in adipose tissue. Frontiers in Physiology 9:122.

[58] Fullerton, M.D., Galic, S., Marcinko, K., Sikkema, S., Pulinilkunnil, T., Chen, Z.P., et al., 2013. Single phosphorylation sites in Acc1 and Acc2 regulate lipid homeostasis and the insulin-sensitizing effects of metformin. Nature Medicine 19(12):1649–1654.

[59] Rena, G., Pearson, E.R., Sakamoto, K., 2013. Molecular mechanism of action of metformin: old or new insights? Diabetologia 56(9):1898–1906.

[60] Hunter, R.W., Foretz, M., Bultot, L., Fullerton, M.D., Deak, M., Ross, F.A., et al., 2014. Mechanism of action of compound-13: an alpha1-selective small molecule activator of AMPK. Chemistry & Biology 21(7):866–879.

[61] Langendorf, C.G., Ngoei, K.R.W., Scott, J.W., Ling, N.X.Y., Issa, S.M.A., Gorman, M.A., et al., 2016. Structural basis of allosteric and synergistic activation of AMPK by furan-2-phosphonic derivative C2 binding. Nature Communications 7:10912.

10   Bibliography

1.   WHO, *World Health Statistics 2020*. 2020, World Health Organisation: Geneva.

2.   WHO, *Global report on diabetes*. 2016, World Health Organisation: Geneva.

3.   Federation, I.D., *IDF Diabetes Atlas 2019*. 2019: Brussels.

4.   Egan, B. and J.R. Zierath, *Exercise Metabolism and the Molecular Regulation of Skeletal Muscle Adaptation.* Cell Metabolism, 2013. **17**(2): p. 162-184.

5.   Hallal, P.C., et al., *Global physical activity levels: surveillance progress, pitfalls, and prospects.* The Lancet, 2012. **380**(9838): p. 247-257.

6.   Moller, D.E., *New drug targets for type 2 diabetes and the metabolic syndrome.* Nature, 2001. **414**(6865): p. 821-827.

7.   Hinnen, D., *Glucagon-Like Peptide 1 Receptor Agonists for Type 2 Diabetes.* Diabetes Spectrum, 2017. **30**(3): p. 202-210.

8.   Chao, E.C. and R.R. Henry, *SGLT2 inhibition — a novel strategy for diabetes treatment.* Nature Reviews Drug Discovery, 2010. **9**(7): p. 551-559.

9.   Drucker, D.J., *Biologic actions and therapeutic potential of the proglucagon-derived peptides.* Nature Clinical Practice Endocrinology & Metabolism, 2005. **1**(1): p. 22-31.

10.   Rieg, T. and V. Vallon, *Development of SGLT1 and SGLT2 inhibitors.* Diabetologia, 2018. **61**(10): p. 2079-2086.

11.   Ruderman, N. and M. Prentki, *AMP kinase and malonyl-CoA: targets for therapy of the metabolic syndrome.* Nature Reviews Drug Discovery, 2004. **3**(4): p. 340-351.

12.   Hardie, D.G., D. Carling, and M. Carlson, *The AMP-activated/SNF1 protein kinase subfamily: Metabolic sensors of the eukaryotic cell?* Annual Review of Biochemistry, 1998. **67**: p. 821-855.

13.   Hardie, D.G., *AMP-activated/SNF1 protein kinases: conserved guardians of cellular energy.* Nature Reviews Molecular Cell Biology, 2007. **8**(10): p. 774-785.

14.   Steinberg, G.R. and B.E. Kemp, *AMPK in Health and Disease.* Physiological Reviews, 2009. **89**(3): p. 1025-1078.

15.   Lipmann, F., *Metabolic Generation and Utilization of Phosphate Bond Energy*, in *Advances in Enzymology and Related Areas of Molecular Biology*. 2006. p. 99-162.

16.   Chance, B., H. Lees, and J.R. Postgate, *The Meaning of "Reversed Electron Flow" and "High Energy Electron" in Biochemistry.* Nature, 1972. **238**(5363): p. 330-331.

17.   Kahn, B.B., et al., *AMP-activated protein kinase: Ancient energy gauge provides clues to modern understanding of metabolism.* Cell Metabolism, 2005. **1**(1): p. 15-25.

18.   Hardie, D.G., F.A. Ross, and S.A. Hawley, *AMPK: a nutrient and energy sensor that maintains energy homeostasis.* Nature Reviews Molecular Cell Biology, 2012. **13**(4): p. 251-262.

19.   Hardie, D.G., *AMP-activated protein kinase: a key regulator of energy balance with many roles in human disease.* Journal of Internal Medicine, 2014. **276**(6): p. 543-559.

20.   Musi, N., et al., *AMP-activated protein kinase (AMPK) is activated in muscle of subjects with type 2 diabetes during exercise.* Diabetes, 2001. **50**(5): p. 921-7.

21.   Hardie, D.G., *Energy sensing by the AMP-activated protein kinase and its effects on muscle metabolism.* Proc Nutr Soc, 2011. **70**(1): p. 92-9.

22.   Muise, E.S., et al., *Pharmacological AMPK activation induces transcriptional responses congruent to exercise in skeletal and cardiac muscle, adipose tissues and liver.* PLOS ONE, 2019. **14**(2): p. e0211568.

23.   Cokorinos, E.C., et al., *Activation of Skeletal Muscle AMPK Promotes Glucose Disposal and Glucose Lowering in Non-human Primates and Mice.* Cell Metabolism, 2017. **25**(5): p. 1147-+.

24.   Myers, R.W., et al., *Systemic pan-AMPK activator MK-8722 improves glucose homeostasis but induces cardiac hypertrophy.* Science, 2017. **357**(6350): p. 507-511.

25.   Carling, D., V.A. Zammit, and D.G. Hardie, *A COMMON BICYCLIC PROTEIN-KINASE CASCADE INACTIVATES THE REGULATORY ENZYMES OF FATTY-ACID AND CHOLESTEROL-BIOSYNTHESIS.* Febs Letters, 1987. **223**(2): p. 217-222.

26.   Munday, M.R., et al., *Identification by amino acid sequencing of three major regulatory phosphorylation sites on rat acetyl-CoA carboxylase.* Eur J Biochem, 1988. **175**(2): p. 331-8.

27.   Hardie, D.G., D. Carling, and A.T.R. Sim, *THE AMP-ACTIVATED PROTEIN-KINASE - A MULTISUBSTRATE REGULATOR OF LIPID-METABOLISM.* Trends in Biochemical Sciences, 1989. **14**(1): p. 20-23.

28.   Salt, I., et al., *AMP-activated protein kinase: greater AMP dependence, and preferential nuclear localization, of complexes containing the alpha2 isoform.* Biochem J, 1998. **334 (Pt 1)**: p. 177-87.

29.   Ross, F.A., T.E. Jensen, and D.G. Hardie, *Differential regulation by AMP and ADP of AMPK complexes containing different gamma subunit isoforms.* Biochemical Journal, 2016. **473**: p. 189-199.

30.   Carling, D., et al., *Mammalian AMP-activated protein kinase is homologous to yeast and plant protein kinases involved in the regulation of carbon metabolism.* J Biol Chem, 1994. **269**(15): p. 11442-8.

31.   Hawley, S.A., et al., *Characterization of the AMP-activated protein kinase kinase from rat liver and identification of threonine 172 as the major site at which it phosphorylates AMP-activated protein kinase.* Journal of Biological Chemistry, 1996. **271**(44): p. 27879-27887.

32.   Chen, L., et al., *Conserved regulatory elements in AMPK.* Nature, 2013. **498**(7453): p. E8-E9.

33.   Lizcano, J.M., et al., *LKB1 is a master kinase that activates 13 kinases of the AMPK subfamily, including MARK/PAR-1.* Embo Journal, 2004. **23**(4): p. 833-843.

34.   Shaw, R.J., et al., *The tumor suppressor LKB1 kinase directly activates AMP-activated kinase and regulates apoptosis in response to energy stress.* Proceedings of the National Academy of Sciences of the United States of America, 2004. **101**(10): p. 3329-3335.

35.   Hawley, S.A., et al., *Calmodulin-dependent protein kinase kinase-beta is an alternative upstream kinase for AMP-activated protein kinase.* Cell Metabolism, 2005. **2**(1): p. 9-19.

36.   Woods, A., et al., *Ca2+/calmodulin-dependent protein kinase kinase-beta acts upstream of AMP-activated protein kinase in mammalian cells.* Cell Metabolism, 2005. **2**(1): p. 21-33.

37.   Xiao, B., et al., *Structural basis for AMP binding to mammalian AMP-activated protein kinase.* Nature, 2007. **449**(7161): p. 496-U14.

38.   Sanders, M.J., et al., *Investigating the mechanism for AMP activation of the AMP-activated protein kinase cascade.* Biochemical Journal, 2007. **403**: p. 139-148.

39.   Hardie, D.G., B.E. Schaffer, and A. Brunet, *AMPK: An Energy-Sensing Pathway with Multiple Inputs and Outputs.* Trends in Cell Biology, 2016. **26**(3): p. 190-201.

40.   Li, X.D., et al., *Structural basis of AMPK regulation by adenine nucleotides and glycogen (vol 25, pg 50, 2015).* Cell Research, 2015. **25**(3): p. 398-398.

41.   Xiao, B., et al., *Structural basis of AMPK regulation by small molecule activators.* Nature Communications, 2013. **4**: p. 10.

42.   Xin, F.J., et al., *Coordinated regulation of AMPK activity by multiple elements in the alpha-subunit.* Cell Research, 2013. **23**(10): p. 1237-1240.

43.   Oakhill, J.S., et al., *beta-Subunit myristoylation is the gatekeeper for initiating metabolic stress sensing by AMP-activated protein kinase (AMPK).* Proceedings of the National Academy of Sciences of the United States of America, 2010. **107**(45): p. 19237-19241.

44.   Polekhina, G., et al., *Structural Basis for Glycogen Recognition by AMP-Activated Protein Kinase.* Structure, 2005. **13**(10): p. 1453-1462.

45.   Polekhina, G., et al., *AMPK beta subunit targets metabolic stress sensing to glycogen.* Current Biology, 2003. **13**(10): p. 867-871.

46.   McBride, A., et al., *The Glycogen-Binding Domain on the AMPK beta Subunit Allows the Kinase to Act as a Glycogen Sensor.* Cell Metabolism, 2009. **9**(1): p. 23-34.

47.   Oligschlaeger, Y., et al., *The Recruitment of AMP-activated Protein Kinase to Glycogen Is Regulated by Autophosphorylation.* Journal of Biological Chemistry, 2015. **290**(18): p. 11715-11728.

48.   Hoffman, N.J., et al., *Genetic loss of AMPK-glycogen binding destabilises AMPK and disrupts metabolism.* Mol Metab, 2020. **41**: p. 101048.

49.   Pinkosky, S.L., et al., *Long-chain fatty acyl-CoA esters regulate metabolism via allosteric control of AMPK β1 isoforms.* Nature Metabolism, 2020.

50.   Cool, B., et al., *Identification and characterization of a small molecule AMPK activator that treats key components of type 2 diabetes and the metabolic syndrome.* Cell Metabolism, 2006. **3**(6): p. 403-416.

51.   Ngoei, K.R.W., et al., *Structural Determinants for Small-Molecule Activation of Skeletal Muscle AMPK α2β2γ1 by the Glucose Importagog SC4.* Cell Chem Biol, 2018. **25**(6): p. 728-737.e9.

52.   Kemp, B.E., *Bateman domains and adenosine derivatives form a binding contract.* Journal of Clinical Investigation, 2004. **113**(2): p. 182-184.

53.   Xiao, B., et al., *Structure of mammalian AMPK and its regulation by ADP.* Nature, 2011. **472**(7342): p. 230-233.

54.   Rajamohan, F., et al., *Probing the enzyme kinetics, allosteric modulation and activation of alpha 1-and alpha 2-subunit-containing AMP-activated protein kinase (AMPK) heterotrimeric complexes by pharmacological and physiological activators.* Biochemical Journal, 2016. **473**: p. 581-592.

55.   Pinter, K., et al., *Localisation of AMPK gamma subunits in cardiac and skeletal muscles.* J Muscle Res Cell Motil, 2013. **34**(5-6): p. 369-78.

56.   Stephenne, X., et al., *Metformin activates AMP-activated protein kinase in primary human hepatocytes by decreasing cellular energy status.* Diabetologia, 2011. **54**(12): p. 3101-10.

57.   Carling, D., *AMPK signalling in health and disease.* Curr Opin Cell Biol, 2017. **45**: p. 31-37.

58.   Niesler, C.U., K.H. Myburgh, and F. Moore, *The changing AMPK expression profile in differentiating mouse skeletal muscle myoblast cells helps confer increasing resistance to apoptosis.* Exp Physiol, 2007. **92**(1): p. 207-17.

59.   Jensen, T.E., et al., *EMG-Normalised Kinase Activation during Exercise Is Higher in Human Gastrocnemius Compared to Soleus Muscle.* PLOS ONE, 2012. **7**(2): p. e31054.

60.   Richter, E.A. and M. Hargreaves, *EXERCISE, GLUT4, AND SKELETAL MUSCLE GLUCOSE UPTAKE.* Physiological Reviews, 2013. **93**(3): p. 993-1017.

61.   Hargreaves, M. and L.L. Spriet, *Skeletal muscle energy metabolism during exercise.* Nature Metabolism, 2020.

62.   Kjobsted, R., et al., *Enhanced Muscle Insulin Sensitivity After Contraction/Exercise Is Mediated by AMPK.* Diabetes, 2017. **66**(3): p. 598-612.

63.   Winder, W.W. and D.G. Hardie, *Inactivation of acetyl-CoA carboxylase and activation of AMP-activated protein kinase in muscle during exercise.* Am J Physiol, 1996. **270**(2 Pt 1): p. E299-304.

64.   Chen, Z.P., et al., *AMPK signaling in contracting human skeletal muscle: acetyl-CoA carboxylase and NO synthase phosphorylation.* Am J Physiol Endocrinol Metab, 2000. **279**(5): p. E1202-6.

65.   Wojtaszewski, J.F.P., et al., *Isoform-specific and exercise intensity-dependent activation of 5 '-AMP-activated protein kinase in human skeletal muscle.* Journal of Physiology-London, 2000. **528**(1): p. 221-226.

66.   Birk, J.B. and J.F.P. Wojtaszewski, *Predominant alpha 2/beta 2/gamma 3 AMPK activation during exercise in human skeletal muscle.* Journal of Physiology-London, 2006. **577**(3): p. 1021-1032.

67.   Wojtaszewski, J.F.P., et al., *5 ' AMP activated protein kinase expression in human skeletal muscle: effects of strength training and type 2 diabetes.* Journal of Physiology-London, 2005. **564**(2): p. 563-573.

68.   Jorgensen, S.B., et al., *Knockout of the alpha(2) but not alpha(1) 5 '-AMP-activated protein kinase isoform abolishes 5-aminoimidazole-4-carboxamide-1-beta-4-ribofuranoside- but not contraction-induced glucose uptake in skeletal muscle.* Journal of Biological Chemistry, 2004. **279**(2): p. 1070-1079.

69.   Steinberg, G.R., et al., *Whole Body Deletion of AMP-activated Protein Kinase beta 2 Reduces Muscle AMPK Activity and Exercise Capacity.* Journal of Biological Chemistry, 2010. **285**(48): p. 37198-37209.

70.   Barnes, B.R., et al., *The 5 '-AMP-activated protein kinase gamma 3 isoform has a key role in carbohydrate and lipid metabolism in glycolytic skeletal muscle.* Journal of Biological Chemistry, 2004. **279**(37): p. 38441-38447.

71.   Mu, J., et al., *A role for AMP-activated protein kinase in contraction- and hypoxia-regulated glucose transport in skeletal muscle.* Mol Cell, 2001. **7**(5): p. 1085-94.

72.   O'Neill, H.M., et al., *AMP-activated protein kinase (AMPK) beta 1 beta 2 muscle null mice reveal an essential role for AMPK in maintaining mitochondrial content and glucose uptake during exercise.* Proceedings of the National Academy of Sciences of the United States of America, 2011. **108**(38): p. 16092-16097.

73.   Bultot, L., et al., *Benzimidazole derivative small-molecule 991 enhances AMPK activity and glucose uptake induced by AICAR or contraction in skeletal muscle.* American Journal of Physiology-Endocrinology and Metabolism, 2016. **311**(4): p. E706-E719.

74.   Ducommun, S., et al., *Enhanced activation of cellular AMPK by dual-small molecule treatment: AICAR and A769662.* American Journal of Physiology-Endocrinology and Metabolism, 2014. **306**(6): p. E688-E696.

75.   Thornton, C., M.A. Snowden, and D. Carling, *Identification of a novel AMP-activated protein kinase beta subunit isoform that is highly expressed in skeletal muscle.* Journal of Biological Chemistry, 1998. **273**(20): p. 12443-12450.

76.   Lai, Y.C., et al., *A small-molecule benzimidazole derivative that potently activates AMPK to increase glucose transport in skeletal muscle: comparison with effects of contraction and other AMPK activators.* Biochemical Journal, 2014. **460**: p. 363-375.

77.   Perdikari, A., et al., *A high-throughput, image-based screen to identify kinases involved in brown adipocyte development.* Science Signaling, 2017. **10**(466): p. 11.

78.   ANAND, R., et al., *NOVEL CYCLIC AZABENZIMIDAZOLE DERIVATIVES USEFUL AS ANTI-DIABETIC AGENTS*. 2012.

79.   Wu, L., et al., *AMP-Activated Protein Kinase (AMPK) Regulates Energy Metabolism through Modulating Thermogenesis in Adipose Tissue.* Frontiers in physiology, 2018. **9**: p. 122-122.

80.   Mottillo, E.P., et al., *Lack of Adipocyte AMPK Exacerbates Insulin Resistance and Hepatic Steatosis through Brown and Beige Adipose Tissue Function.* Cell Metab, 2016. **24**(1): p. 118-29.

81.   Mulligan, J.D., et al., *Upregulation of AMPK during cold exposure occurs via distinct mechanisms in brown and white adipose tissue of the mouse.* J Physiol, 2007. **580**(Pt. 2): p. 677-84.

82.   Hanssen, M.J.W., et al., *Short-term cold acclimation improves insulin sensitivity in patients with type 2 diabetes mellitus.* Nature Medicine, 2015. **21**(8): p. 863-865.

83.   Seale, P., et al., *Transcriptional control of brown fat determination by PRDM16.* Cell Metab, 2007. **6**(1): p. 38-54.

84.   Yang, Q., et al., *AMPK/α-Ketoglutarate Axis Dynamically Mediates DNA Demethylation in the Prdm16 Promoter and Brown Adipogenesis.* Cell Metab, 2016. **24**(4): p. 542-554.

85.   Ortega-Molina, A., et al., *Pten positively regulates brown adipose function, energy expenditure, and longevity.* Cell Metab, 2012. **15**(3): p. 382-94.

86.   Lin, S.C. and D.G. Hardie, *AMPK: Sensing Glucose as well as Cellular Energy Status.* Cell Metab, 2018. **27**(2): p. 299-313.

87.   Hawley, S.A., et al., *Complexes between the LKB1 tumor suppressor, STRAD alpha/beta and MO25 alpha/beta are upstream kinases in the AMP-activated protein kinase cascade.* J Biol, 2003. **2**(4): p. 28.

88.   Sakamoto, K., et al., *Activity of LKB1 and AMPK-related kinases in skeletal muscle: effects of contraction, phenformin, and AICAR.* Am J Physiol Endocrinol Metab, 2004. **287**(2): p. E310-7.

89.   Hurley, R.L., et al., *The Ca2+/calmodulin-dependent protein kinase kinases are AMP-activated protein kinase kinases.* Journal of Biological Chemistry, 2005. **280**(32): p. 29060-29066.

90.   Clapham, D.E., *Calcium Signaling.* Cell, 2007. **131**(6): p. 1047-1058.

91.   Suter, M., et al., *Dissecting the role of 5 '-AMP for allosteric stimulation, activation, and deactivation of AMP-activated protein kinase.* Journal of Biological Chemistry, 2006. **281**(43): p. 32207-32216.

92.   Gowans, G.J., et al., *AMP Is a True Physiological Regulator of AMP-Activated Protein Kinase by Both Allosteric Activation and Enhancing Net Phosphorylation.* Cell Metabolism, 2013. **18**(4): p. 556-566.

93.   Scott, J.W., et al., *CBS domains form energy-sensing modules whose binding of adenosine ligands is disrupted by disease mutations.* Journal of Clinical Investigation, 2004. **113**(2): p. 274-284.

94.   Storer, A.C. and A. Cornishbowden, *CONCENTRATION OF MGATP2- AND OTHER IONS IN SOLUTION - CALCULATION OF TRUE CONCENTRATIONS OF SPECIES PRESENT IN MIXTURES OF ASSOCIATING IONS.* Biochemical Journal, 1976. **159**(1): p. 1-5.

95.   Chen, L., et al., *Structural insight into the autoinhibition mechanism of AMP-activated protein kinase.* Nature, 2009. **459**(7250): p. 1146-U139.

96.   Langendorf, C.G. and B.E. Kemp, *Choreography of AMPK activation.* Cell Research, 2015. **25**(1): p. 5-6.

97.   Jenkins, Y., et al., *AMPK activation through mitochondrial regulation results in increased substrate oxidation and improved metabolic parameters in models of diabetes.* PLoS One, 2013. **8**(12): p. e81870.

98.   Jensen, T.E., et al., *PT-1 selectively activates AMPK-gamma 1 complexes in mouse skeletal muscle, but activates all three gamma subunit complexes in cultured human cells by inhibiting the respiratory chain.* Biochemical Journal, 2015. **467**: p. 461-472.

99.   Steinberg, G.R. and D. Carling, *AMP-activated protein kinase: the current landscape for drug development.* Nat Rev Drug Discov, 2019. **18**(7): p. 527-551.

100.   Marcinko, K., et al., *The AMPK activator R419 improves exercise capacity and skeletal muscle insulin sensitivity in obese mice.* Mol Metab, 2015. **4**(9): p. 643-51.

101.   Hawley, S.A., et al., *Use of cells expressing gamma subunit variants to identify diverse mechanisms of AMPK activation.* Cell Metab, 2010. **11**(6): p. 554-65.

102.   Baur, J.A., et al., *Resveratrol improves health and survival of mice on a high-calorie diet.* Nature, 2006. **444**(7117): p. 337-42.

103.   de Ligt, M., et al., *No effect of resveratrol supplementation after 6 months on insulin sensitivity in overweight adults: a randomized trial.* Am J Clin Nutr, 2020. **112**(4): p. 1029-1038.

104.   Hardie, D.G., *AMPK--sensing energy while talking to other signaling pathways.* Cell Metab, 2014. **20**(6): p. 939-52.

105.   Steneberg, P., et al., *PAN-AMPK activator O304 improves glucose homeostasis and microvascular perfusion in mice and type 2 diabetes patients.* JCI insight, 2018. **3**(12): p. e99114.

106.   Hawley, S.A., et al., *The Ancient Drug Salicylate Directly Activates AMP-Activated Protein Kinase.* Science, 2012. **336**(6083): p. 918-922.

107. Willows, R., et al., *Effect of different gamma-subunit isoforms on the regulation of AMPK.* Biochemical Journal, 2017. **474**(10): p. 1741-1754.

108. Rana, S., E.C. Blowers, and A. Natarajan, *Small molecule adenosine 5'-monophosphate activated protein kinase (AMPK) modulators and human diseases.* J Med Chem, 2015. **58**(1): p. 2-29.

109. Salatto, C.T., et al., *Selective Activation of AMPK β1-Containing Isoforms Improves Kidney Function in a Rat Model of Diabetic Nephropathy.* J Pharmacol Exp Ther, 2017. **361**(2): p. 303-311.

110. Dengler, F., *Activation of AMPK under Hypoxia: Many Roads Leading to Rome.* International journal of molecular sciences, 2020. **21**(7): p. 2428.

111. Kudo, N., et al., *High rates of fatty acid oxidation during reperfusion of ischemic hearts are associated with a decrease in malonyl-CoA levels due to an increase in 5'-AMP-activated protein kinase inhibition of acetyl-CoA carboxylase.* J Biol Chem, 1995. **270**(29): p. 17513-20.

112. Salt, I.P., et al., *AMP-activated protein kinase is activated by low glucose in cell lines derived from pancreatic beta cells, and may regulate insulin release.* The Biochemical journal, 1998. **335 (Pt 3)**(Pt 3): p. 533-539.

113. Hutber, C.A., D.G. Hardie, and W.W. Winder, *Electrical stimulation inactivates muscle acetyl-CoA carboxylase and increases AMP-activated protein kinase.* Am J Physiol, 1997. **272**(2 Pt 1): p. E262-6.

114. Vavvas, D., et al., *Contraction-induced changes in acetyl-CoA carboxylase and 5'-AMP-activated kinase in skeletal muscle.* J Biol Chem, 1997. **272**(20): p. 13255-61.

115. Hardie, D.G., *AMP-Activated Protein Kinase: Maintaining Energy Homeostasis at the Cellular and Whole-Body Levels.* Annual Review of Nutrition, 2014. **34**(1): p. 31-55.

116. Schwartz, M.W., et al., *Central nervous system control of food intake.* Nature, 2000. **404**(6778): p. 661-671.

117. Minokoshi, Y., et al., *AMP-kinase regulates food intake by responding to hormonal and nutrient signals in the hypothalamus.* Nature, 2004. **428**(6982): p. 569-74.

118. Kola, B., et al., *The orexigenic effect of ghrelin is mediated through central activation of the endogenous cannabinoid system.* PLoS One, 2008. **3**(3): p. e1797.

119. Steinberg, G.R., J.W.E. Rush, and D.J. Dyck, *AMPK expression and phosphorylation are increased in rodent muscle after chronic leptin treatment.* American Journal of Physiology-Endocrinology and Metabolism, 2003. **284**(3): p. E648-E654.

120. Yang, Y., et al., *Hunger States Switch a Flip-Flop Memory Circuit via a Synaptic AMPK-Dependent Positive Feedback Loop.* Cell, 2011. **146**(6): p. 992-1003.

121. Yamauchi, T., et al., *Adiponectin stimulates glucose utilization and fatty-acid oxidation by activating AMP-activated protein kinase.* Nature Medicine, 2002. **8**(11): p. 1288-1295.

122. Lihn, A.S., S.B. Pedersen, and B. Richelsen, *Adiponectin: action, regulation and association to insulin sensitivity.* Obesity Reviews, 2005. **6**(1): p. 13-21.

123. Iwabu, M., et al., *Adiponectin and AdipoR1 regulate PGC-1alpha and mitochondria by Ca(2+) and AMPK/SIRT1.* Nature, 2010. **464**(7293): p. 1313-9.

124. Civitarese, A.E., et al., *Role of adiponectin in human skeletal muscle bioenergetics.* Cell Metab, 2006. **4**(1): p. 75-87.

125. Morton, G.J., et al., *Central nervous system control of food intake and body weight.* Nature, 2006. **443**(7109): p. 289-295.

126. Hayashi, T., et al., *Evidence for 5' AMP-activated protein kinase mediation of the effect of muscle contraction on glucose transport.* Diabetes, 1998. **47**(8): p. 1369-73.

127. Bergeron, R., et al., *Effect of AMPK activation on muscle glucose metabolism in conscious rats.* Am J Physiol, 1999. **276**(5): p. E938-44.

128. Thiebaud, D., et al., *The Effect of Graded Doses of Insulin on Total Glucose Uptake, Glucose Oxidation, and Glucose Storage in Man.* Diabetes, 1982. **31**(11): p. 957-963.

129. Ferrannini, E., et al., *The Disposal of an Oral Glucose Load in Healthy Subjects: A Quantitative Study.* Diabetes, 1985. **34**(6): p. 580-588.

130. James, D.E., M. Strube, and M. Mueckler, *Molecular cloning and characterization of an insulin-regulatable glucose transporter.* Nature, 1989. **338**(6210): p. 83-7.

131. Rowland, A.F., D.J. Fazakerley, and D.E. James, *Mapping Insulin/GLUT4 Circuitry.* Traffic, 2011. **12**(6): p. 672-681.

132. Kane, S., et al., *A method to identify serine kinase substrates. Akt phosphorylates a novel adipocyte protein with a Rab GTPase-activating protein (GAP) domain.* J Biol Chem, 2002. **277**(25): p. 22115-8.

133. Bruss, M.D., et al., *Increased phosphorylation of Akt substrate of 160 kDa (AS160) in rat skeletal muscle in response to insulin or contractile activity.* Diabetes, 2005. **54**(1): p. 41-50.

134. Ryder, J.W., et al., *Postexercise glucose uptake and glycogen synthesis in skeletal muscle from GLUT4-deficient mice.* Faseb j, 1999. **13**(15): p. 2246-56.

135. Merrill, G.F., et al., *AICA riboside increases AMP-activated protein kinase, fatty acid oxidation, and glucose uptake in rat muscle.* American Journal of Physiology-Endocrinology and Metabolism, 1997. **273**(6): p. E1107-E1112.

136. Sakamoto, K., et al., *Deficiency of LKB1 in skeletal muscle prevents AMPK activation and glucose uptake during contraction.* Embo Journal, 2005. **24**(10): p. 1810-1820.

137. Lantier, L., et al., *AMPK controls exercise endurance, mitochondrial oxidative capacity, and skeletal muscle integrity.* Faseb j, 2014. **28**(7): p. 3211-24.

138. Hingst, J.R., et al., *Inducible deletion of skeletal muscle AMPKα reveals that AMPK is required for nucleotide balance but dispensable for muscle glucose uptake and fat oxidation during exercise.* Mol Metab, 2020. **40**: p. 101028.

139. Kjøbsted, R., et al., *AMPK and TBC1D1 Regulate Muscle Glucose Uptake After, but Not During, Exercise and Contraction.* Diabetes, 2019. **68**(7): p. 1427-1440.

140. Henríquez-Olguin, C., et al., *Cytosolic ROS production by NADPH oxidase 2 regulates muscle glucose uptake during exercise.* Nat Commun, 2019. **10**(1): p. 4623.

141. Sylow, L., et al., *Rac1 and AMPK Account for the Majority of Muscle Glucose Uptake Stimulated by Ex Vivo Contraction but Not In Vivo Exercise.* Diabetes, 2017. **66**(6): p. 1548-1559.

142. Bedard, K. and K.H. Krause, *The NOX family of ROS-generating NADPH oxidases: physiology and pathophysiology.* Physiol Rev, 2007. **87**(1): p. 245-313.

143. Zerial, M. and H. McBride, *Rab proteins as membrane organizers.* Nat Rev Mol Cell Biol, 2001. **2**(2): p. 107-17.

144. Kramer, H.F., et al., *Distinct signals regulate AS160 phosphorylation in response to insulin, AICAR, and contraction in mouse skeletal muscle.* Diabetes, 2006. **55**(7): p. 2067-76.

145. Geraghty, K.M., et al., *Regulation of multisite phosphorylation and 14-3-3 binding of AS160 in response to IGF-1, EGF, PMA and AICAR.* Biochem J, 2007. **407**(2): p. 231-41.

146. Sakamoto, K. and G.D. Holman, *Emerging role for AS160/TBC1D4 and TBC1D1 in the regulation of GLUT4 traffic.* Am J Physiol Endocrinol Metab, 2008. **295**(1): p. E29-37.

147. Treebak, J.T., et al., *AMPK-mediated AS160 phosphorylation in skeletal muscle is dependent on AMPK catalytic and regulatory subunits.* Diabetes, 2006. **55**(7): p. 2051-8.

148. Taylor, E.B., et al., *Discovery of TBC1D1 as an insulin-, AICAR-, and contraction-stimulated signaling nexus in mouse skeletal muscle.* J Biol Chem, 2008. **283**(15): p. 9787-96.

149. Castorena, C.M., et al., *Clustering of GLUT4, TUG, and RUVBL2 protein levels correlate with myosin heavy chain isoform pattern in skeletal muscles, but AS160 and TBC1D1 levels do not.* J Appl Physiol (1985), 2011. **111**(4): p. 1106-17.

150. Sano, H., et al., *Insulin-stimulated phosphorylation of a Rab GTPase-activating protein regulates GLUT4 translocation.* J Biol Chem, 2003. **278**(17): p. 14599-602.

151. Ducommun, S., et al., *Thr649Ala-AS160 knock-in mutation does not impair contraction/AICAR-induced glucose transport in mouse muscle.* American Journal of Physiology-Endocrinology and Metabolism, 2012. **302**(9): p. E1036-E1043.

152. Treebak, J.T., et al., *Identification of a novel phosphorylation site on TBC1D4 regulated by AMP-activated protein kinase in skeletal muscle.* American Journal of Physiology - Cell Physiology, 2010. **298**(2): p. C377-C385.

153. Kjøbsted, R., et al., *Prior AICAR Stimulation Increases Insulin Sensitivity in Mouse Skeletal Muscle in an AMPK-Dependent Manner.* Diabetes, 2015. **64**(6): p. 2042-2055.

154. Roach, W.G., et al., *Substrate specificity and effect on GLUT4 translocation of the Rab GTPase-activating protein Tbc1d1.* Biochem J, 2007. **403**(2): p. 353-8.

155. Frøsig, C., et al., *Exercise-induced TBC1D1 Ser237 phosphorylation and 14-3-3 protein binding capacity in human skeletal muscle.* J Physiol, 2010. **588**(Pt 22): p. 4539-48.

156. Pehmøller, C., et al., *Genetic disruption of AMPK signaling abolishes both contraction- and insulin-stimulated TBC1D1 phosphorylation and 14-3-3 binding in mouse skeletal muscle.* American journal of physiology. Endocrinology and metabolism, 2009. **297**(3): p. E665-E675.

157. Chavez, J.A., et al., *Inhibition of GLUT4 translocation by Tbc1d1, a Rab GTPase-activating protein abundant in skeletal muscle, is partially relieved by AMP-activated protein kinase activation.* J Biol Chem, 2008. **283**(14): p. 9187-95.

158. Pehmoller, C., et al., *Exercise alleviates lipid-induced insulin resistance in human skeletal muscle-signaling interaction at the level of TBC1 domain family member 4.* Diabetes, 2012. **61**(11): p. 2743-52.

159. Vichaiwong, K., et al., *Contraction regulates site-specific phosphorylation of TBC1D1 in skeletal muscle.* Biochem J, 2010. **431**(2): p. 311-20.

160.   Treebak, J.T., et al., *Acute exercise and physiological insulin induce distinct phosphorylation signatures on TBC1D1 and TBC1D4 proteins in human skeletal muscle.* J Physiol, 2014. **592**(2): p. 351-75.

161.   Dale, S., et al., *SIMILAR SUBSTRATE RECOGNITION MOTIFS FOR MAMMALIAN AMP-ACTIVATED PROTEIN-KINASE, HIGHER-PLANT HMG-COA REDUCTASE KINASE-A, YEAST SNF1, AND MAMMALIAN CALMODULIN-DEPENDENT PROTEIN-KINASE-I.* Febs Letters, 1995. **361**(2-3): p. 191-195.

162.   Szekeres, F., et al., *The Rab-GTPase-activating protein TBC1D1 regulates skeletal muscle glucose metabolism.* Am J Physiol Endocrinol Metab, 2012. **303**(4): p. E524-33.

163.   Dokas, J., et al., *Conventional Knockout of Tbc1d1 in Mice Impairs Insulin- and AICAR-Stimulated Glucose Uptake in Skeletal Muscle.* Endocrinology, 2013. **154**(10): p. 3502-3514.

164.   Chen, Q., et al., *A Tbc1d1 (Ser231Ala)-knockin mutation partially impairs AICAR- but not exercise-induced muscle glucose uptake in mice.* Diabetologia, 2017. **60**(2): p. 336-345.

165.   Chen, L., et al., *Disruption of the AMPK–TBC1D1 nexus increases lipogenic gene expression and causes obesity in mice via promoting IGF1 secretion.* Proceedings of the National Academy of Sciences, 2016: p. 201600581.

166.   Liu, Y., et al., *Phosphatidylinositol 3-phosphate 5-kinase (PIKfyve) is an AMPK target participating in contraction-stimulated glucose uptake in skeletal muscle.* Biochem J, 2013. **455**(2): p. 195-206.

167.   Ikonomov, O.C., et al., *ArPIKfyve-PIKfyve interaction and role in insulin-regulated GLUT4 translocation and glucose transport in 3T3-L1 adipocytes.* Exp Cell Res, 2007. **313**(11): p. 2404-16.

168.   Ikonomov, O.C., et al., *Muscle-specific Pikfyve gene disruption causes glucose intolerance, insulin resistance, adiposity, and hyperinsulinemia but not muscle fiber-type switching.* Am J Physiol Endocrinol Metab, 2013. **305**(1): p. E119-31.

169.   Berwick, D.C., et al., *Protein kinase B phosphorylation of PIKfyve regulates the trafficking of GLUT4 vesicles.* J Cell Sci, 2004. **117**(Pt 25): p. 5985-93.

170.   Roach, P.J., et al., *Glycogen and its metabolism: some new developments and old themes.* Biochem J, 2012. **441**(3): p. 763-87.

171.   Skurat, A.V., Y. Wang, and P.J. Roach, *Rabbit skeletal muscle glycogen synthase expressed in COS cells. Identification of regulatory phosphorylation sites.* J Biol Chem, 1994. **269**(41): p. 25534-42.

172.   Skurat, A.V. and P.J. Roach, *Multiple mechanisms for the phosphorylation of C-terminal regulatory sites in rabbit muscle glycogen synthase expressed in COS cells.* Biochem J, 1996. **313 (Pt 1)**(Pt 1): p. 45-50.

173.   Carling, D. and D.G. Hardie, *The substrate and sequence specificity of the AMP-activated protein kinase. Phosphorylation of glycogen synthase and phosphorylase kinase.* Biochim Biophys Acta, 1989. **1012**(1): p. 81-6.

174.   Buhl, E.S., et al., *Chronic Treatment With 5-Aminoimidazole-4-Carboxamide-1-β-D-Ribofuranoside Increases Insulin-Stimulated Glucose Uptake and GLUT4 Translocation in Rat Skeletal Muscles in a Fiber Type—Specific Manner.* Diabetes, 2001. **50**(1): p. 12-17.

175.   Hunter, R.W., et al., *Molecular mechanism by which AMP-activated protein kinase activation promotes glycogen accumulation in muscle.* Diabetes, 2011. **60**(3): p. 766-74.

176. Hingst, J.R., et al., *Exercise-induced molecular mechanisms promoting glycogen supercompensation in human skeletal muscle.* Molecular Metabolism, 2018. **16**: p. 24-34.

177. Pederson, B.A., et al., *Glucose metabolism in mice lacking muscle glycogen synthase.* Diabetes, 2005. **54**(12): p. 3466-73.

178. Bultot, L., et al., *AMP-activated protein kinase phosphorylates and inactivates liver glycogen synthase.* Biochem J, 2012. **443**(1): p. 193-203.

179. Nielsen, J.N., et al., *Role of 5'AMP-activated protein kinase in glycogen synthase activity and glucose utilization: insights from patients with McArdle's disease.* J Physiol, 2002. **541**(Pt 3): p. 979-89.

180. Blair, E., et al., *Mutations in the gamma(2) subunit of AMP-activated protein kinase cause familial hypertrophic cardiomyopathy: evidence for the central role of energy compromise in disease pathogenesis.* Human Molecular Genetics, 2001. **10**(11): p. 1215-1220.

181. Milan, D., et al., *A mutation in PRKAG3 associated with excess glycogen content in pig skeletal muscle.* Science, 2000. **288**(5469): p. 1248-1251.

182. Costford, S.R., et al., *Gain-of-function R225W mutation in human AMPKgamma(3) causing increased glycogen and decreased triglyceride in skeletal muscle.* PLoS One, 2007. **2**(9): p. e903.

183. Barre, L., et al., *Genetic model for the chronic activation of skeletal muscle AMP-activated protein kinase leads to glycogen accumulation.* American Journal of Physiology-Endocrinology and Metabolism, 2007. **292**(3): p. E802-E811.

184. Barnes, B.R., et al., *5'-AMP-activated protein kinase regulates skeletal muscle glycogen content and ergogenics.* Faseb j, 2005. **19**(7): p. 773-9.

185. Cannon, B. and J. Nedergaard, *Brown adipose tissue: function and physiological significance.* Physiol Rev, 2004. **84**(1): p. 277-359.

186. Klingenberg, M., *Uncoupling protein - A useful energy dissipator.* Journal of Bioenergetics and Biomembranes, 1999. **31**(5): p. 419-430.

187. Klingenberg, M. and S.G. Huang, *Structure and function of the uncoupling protein from brown adipose tissue.* Biochimica Et Biophysica Acta-Biomembranes, 1999. **1415**(2): p. 271-296.

188. Cypess, A.M., et al., *Identification and Importance of Brown Adipose Tissue in Adult Humans.* New England Journal of Medicine, 2009. **360**(15): p. 1509-1517.

189. Kajimura, S., P. Seale, and B.M. Spiegelman, *Transcriptional Control of Brown Fat Development.* Cell metabolism, 2010. **11**(4): p. 257-262.

190. Desjardins, E.M. and G.R. Steinberg, *Emerging Role of AMPK in Brown and Beige Adipose Tissue (BAT): Implications for Obesity, Insulin Resistance, and Type 2 Diabetes.* Current Diabetes Reports, 2018. **18**(10): p. 80.

191. Pollard, A.E. and D. Carling, *Thermogenic adipocytes: lineage, function and therapeutic potential.* Biochem J, 2020. **477**(11): p. 2071-2093.

192. Zhao, J., et al., *AMPKα1 deficiency suppresses brown adipogenesis in favor of fibrogenesis during brown adipose tissue development.* Biochem Biophys Res Commun, 2017. **491**(2): p. 508-514.

193. Than, A., et al., *Apelin Enhances Brown Adipogenesis and Browning of White Adipocytes.* J Biol Chem, 2015. **290**(23): p. 14679-91.

194. Son, J.S., et al., *Maternal exercise via exerkine apelin enhances brown adipogenesis and prevents metabolic dysfunction in offspring mice.* Science Advances, 2020. **6**(16): p. eaaz0359.

195. Zhang, H., et al., *MicroRNA-455 regulates brown adipogenesis via a novel HIF1an-AMPK-PGC1α signaling network.* EMBO Rep, 2015. **16**(10): p. 1378-93.

196. Wang, S., et al., *Resveratrol enhances brown adipocyte formation and function by activating AMP-activated protein kinase (AMPK) α1 in mice fed high-fat diet.* Mol Nutr Food Res, 2017. **61**(4).

197. Woods, A., et al., *Liver-Specific Activation of AMPK Prevents Steatosis on a High-Fructose Diet.* Cell Rep, 2017. **18**(13): p. 3043-3051.

198. Pollard, A.E., et al., *AMPK activation protects against diet induced obesity through Ucp1-independent thermogenesis in subcutaneous white adipose tissue.* Nat Metab, 2019. **1**(3): p. 340-349.

199. Kazak, L., et al., *A Creatine-Driven Substrate Cycle Enhances Energy Expenditure and Thermogenesis in Beige Fat.* Cell, 2015. **163**(3): p. 643-655.

200. Ukropec, J., et al., *UCP1-independent thermogenesis in white adipose tissue of cold-acclimated Ucp1-/- mice.* J Biol Chem, 2006. **281**(42): p. 31894-908.

201. Ikeda, K., et al., *UCP1-independent signaling involving SERCA2b-mediated calcium cycling regulates beige fat thermogenesis and systemic glucose homeostasis.* Nature Medicine, 2017. **23**(12): p. 1454-1465.

202. Cheung, P.C.F., et al., *Characterization of AMP-activated protein kinase gamma-subunit isoforms and their role in AMP binding.* Biochemical Journal, 2000. **346**: p. 659-669.

203. Pinter, K., et al., *Embryonic expression of AMPK γ subunits and the identification of a novel γ2 transcript variant in adult heart.* J Mol Cell Cardiol, 2012. **53**(3): p. 342-9.

204. Yu, H., et al., *Cloning and characterization of mouse 5'-AMP-activated protein kinase γ3 subunit.* American Journal of Physiology-Cell Physiology, 2004. **286**(2): p. C283-C292.

205. Mahlapuu, M., et al., *Expression profiling of the gamma-subunit isoforms of AMP-activated protein kinase suggests a major role for gamma 3 in white skeletal muscle.* American Journal of Physiology-Endocrinology and Metabolism, 2004. **286**(2): p. E194-E200.

206. Gollob, M.H., et al., *Identification of a gene responsible for familial Wolff-Parkinson-White syndrome.* N Engl J Med, 2001. **344**(24): p. 1823-31.

207. Arad, M., et al., *Constitutively active AMP kinase mutations cause glycogen storage disease mimicking hypertrophic cardiomyopathy.* J Clin Invest, 2002. **109**(3): p. 357-62.

208. Davies, J.K., et al., *Characterization of the role of γ2 R531G mutation in AMP-activated protein kinase in cardiac hypertrophy and Wolff-Parkinson-White syndrome.* American Journal of Physiology-Heart and Circulatory Physiology, 2006. **290**(5): p. H1942-H1951.

209. Yavari, A., et al., *Mammalian γ2 AMPK regulates intrinsic heart rate.* Nat Commun, 2017. **8**(1): p. 1258.

210. Hamilton, D.N., et al., *The effect of the Halothane and Rendement Napole genes on carcass and meat quality characteristics of pigs.* J Anim Sci, 2000. **78**(11): p. 2862-7.

211. Garcia-Roves, P.M., et al., *Gain-of-function R225Q mutation in AMP-activated protein kinase gamma3 subunit increases mitochondrial biogenesis in glycolytic skeletal muscle.* J Biol Chem, 2008. **283**(51): p. 35724-34.

212. Nilsson, E.C., et al., *Opposite transcriptional regulation in skeletal muscle of AMP-activated protein kinase gamma3 R225Q transgenic versus knock-out mice.* J Biol Chem, 2006. **281**(11): p. 7244-52.

213. Hamilton, S.R., et al., *An activating mutation in the γ1 subunit of the AMP-activated protein kinase.* FEBS Letters, 2001. **500**(3): p. 163-168.

214. Schönke, M., et al., *Skeletal muscle AMP-activated protein kinase γ1(H151R) overexpression enhances whole body energy homeostasis and insulin sensitivity.* Am J Physiol Endocrinol Metab, 2015. **309**(7): p. E679-90.

215. Aoi, W., et al., *Secreted protein acidic and rich in cysteine (SPARC) improves glucose tolerance via AMP-activated protein kinase activation.* The FASEB Journal, 2019. **33**(9): p. 10551-10562.

216. Kim, J., et al., *AMPK activators: mechanisms of action and physiological activities.* Experimental and Molecular Medicine, 2016. **48**: p. 12.

217. Ducommun, S., et al., *Motif affinity and mass spectrometry proteomic approach for the discovery of cellular AMPK targets: Identification of mitochondrial fission factor as a new AMPK substrate.* Cell Signal, 2015. **27**(5): p. 978-88.

218. Sakamoto, K., et al., *Deficiency of LKB1 in heart prevents ischemia-mediated activation of AMPKα2 but not AMPKα1.* American Journal of Physiology-Endocrinology and Metabolism, 2006. **290**(5): p. E780-E788.

219. Hellemans, J. and J. Vandesompele, *Selection of Reliable Reference Genes for RT-qPCR Analysis*, in *Quantitative Real-Time PCR: Methods and Protocols*, R. Biassoni and A. Raso, Editors. 2014, Springer New York: New York, NY. p. 19-26.

220. Vandesompele, J., et al., *Accurate normalization of real-time quantitative RT-PCR data by geometric averaging of multiple internal control genes.* Genome Biology, 2002. **3**(7): p. research0034.1.

221. Bouskila, M., et al., *Insulin promotes glycogen synthesis in the absence of GSK3 phosphorylation in skeletal muscle.* Am J Physiol Endocrinol Metab, 2008. **294**(1): p. E28-35.

222. Fujii, N., et al., *AMP-activated protein kinase alpha 2 activity is not essential for contraction- and hyperosmolarity-induced glucose transport in skeletal muscle.* Journal of Biological Chemistry, 2005. **280**(47): p. 39033-39041.

223. Crane, J.D., et al., *A standardized infrared imaging technique that specifically detects UCP1-mediated thermogenesis in vivo.* Molecular Metabolism, 2014. **3**(4): p. 490-494.

224. Treebak, J.T., et al., *A-769662 activates AMPK beta1-containing complexes but induces glucose uptake through a PI3-kinase-dependent pathway in mouse skeletal muscle.* Am J Physiol Cell Physiol, 2009. **297**(4): p. C1041-52.

225. Kjøbsted, R., et al., *AMPK in skeletal muscle function and metabolism.* The FASEB Journal, 2018. **32**(4): p. 1741-1777.

226. Wasserman, D.H., et al., *The physiological regulation of glucose flux into muscle in vivo.* J Exp Biol, 2011. **214**(Pt 2): p. 254-62.

227. Kimber, N.E., et al., *Skeletal muscle fat and carbohydrate metabolism during recovery from glycogen-depleting exercise in humans.* J Physiol, 2003. **548**(Pt 3): p. 919-27.

228. Fritzen, A.M., et al., *5'-AMP activated protein kinase α2 controls substrate metabolism during post-exercise recovery via regulation of pyruvate dehydrogenase kinase 4.* J Physiol, 2015. **593**(21): p. 4765-80.

229. Ducommun, S., et al., *Chemical genetic screen identifies Gapex-5/GAPVD1 and STBD1 as novel AMPK substrates.* Cellular Signalling, 2019. **57**: p. 45-57.

230. Lytridou, A.A., et al., *Stbd1 promotes glycogen clustering during endoplasmic reticulum stress and supports survival of mouse myoblasts.* Journal of Cell Science, 2020. **133**(20): p. jcs244855.

231. Jiang, S., et al., *Starch binding domain-containing protein 1/genethonin 1 is a novel participant in glycogen metabolism.* J Biol Chem, 2010. **285**(45): p. 34960-71.

232. Foretz, M., et al., *The AMPKγ1 subunit plays an essential role in erythrocyte membrane elasticity, and its genetic inactivation induces splenomegaly and anemia.* Faseb j, 2011. **25**(1): p. 337-47.

233. Pillai-Kastoori, L., A.R. Schutz-Geschwender, and J.A. Harford, *A systematic approach to quantitative Western blot analysis.* Analytical Biochemistry, 2020. **593**: p. 113608.

234. Viollet, B., et al., *The AMP-activated protein kinase alpha2 catalytic subunit controls whole-body insulin sensitivity.* J Clin Invest, 2003. **111**(1): p. 91-8.

235. Day, P., et al., *Structure of a CBS-domain pair from the regulatory gamma1 subunit of human AMPK in complex with AMP and ZMP.* Acta Crystallogr D Biol Crystallogr, 2007. **63**(Pt 5): p. 587-96.

236. Corton, J.M., et al., *5-aminoimidazole-4-carboxamide ribonucleoside. A specific method for activating AMP-activated protein kinase in intact cells?* Eur J Biochem, 1995. **229**(2): p. 558-65.

237. Grahame Hardie, D., *Regulation of AMP-activated protein kinase by natural and synthetic activators.* Acta Pharm Sin B, 2016. **6**(1): p. 1-19.

238. Langendorf, C.G., et al., *Structural basis of allosteric and synergistic activation of AMPK by furan-2-phosphonic derivative C2 binding.* Nature Communications, 2016. **7**: p. 8.

239. Jørgensen, S.B., et al., *The α2–5'AMP-Activated Protein Kinase Is a Site 2 Glycogen Synthase Kinase in Skeletal Muscle and Is Responsive to Glucose Loading.* Diabetes, 2004. **53**(12): p. 3074-3081.

240. Lassiter, D.G., et al., *AMPK activation negatively regulates GDAP1, which influences metabolic processes and circadian gene expression in skeletal muscle.* Mol Metab, 2018. **16**: p. 12-23.

241. Scheffler, T.L., et al., *Gain of function AMP-activated protein kinase γ3 mutation (AMPKγ3R200Q) in pig muscle increases glycogen storage regardless of AMPK activation.* Physiol Rep, 2016. **4**(11).

242. Hedegaard, J., et al., *UDP-Glucose pyrophosphorylase is upregulated in carriers of the porcine RN– mutation in the AMP-activated protein kinase.* PROTEOMICS, 2004. **4**(8): p. 2448-2454.

243. Luptak, I., et al., *Aberrant activation of AMP-activated protein kinase remodels metabolic network in favor of cardiac glycogen storage.* J Clin Invest, 2007. **117**(5): p. 1432-9.

244. Zhu, Y., et al., *The carbohydrate-binding domain of overexpressed STBD1 is important for its stability and protein-protein interactions.* Biosci Rep, 2014. **34**(4).

245. Jiang, S., C.D. Wells, and P.J. Roach, *Starch-binding domain-containing protein 1 (Stbd1) and glycogen metabolism: Identification of the Atg8 family interacting motif (AIM) in Stbd1 required for interaction with GABARAPL1.* Biochem Biophys Res Commun, 2011. **413**(3): p. 420-5.

246. von Wilamowitz-Moellendorff, A., et al., *Glucose-6-phosphate-mediated activation of liver glycogen synthase plays a key role in hepatic glycogen synthesis.* Diabetes, 2013. **62**(12): p. 4070-82.

247. Reaven, G.M., *Banting Lecture 1988. Role of insulin resistance in human disease. 1988.* Nutrition, 1997. **13**(1): p. 65; discussion 64, 66.

248. Pold, R., et al., *Long-term AICAR administration and exercise prevents diabetes in ZDF rats.* Diabetes, 2005. **54**(4): p. 928-34.

249. Buhl, E.S., et al., *Long-term AICAR administration reduces metabolic disturbances and lowers blood pressure in rats displaying features of the insulin resistance syndrome.* Diabetes, 2002. **51**(7): p. 2199-206.

250. Iglesias, M.A., et al., *AICAR administration causes an apparent enhancement of muscle and liver insulin action in insulin-resistant high-fat-fed rats.* Diabetes, 2002. **51**(10): p. 2886-94.

251. Bosselaar, M., et al., *Intravenous AICAR during hyperinsulinemia induces systemic hemodynamic changes but has no local metabolic effect.* J Clin Pharmacol, 2011. **51**(10): p. 1449-58.

252. Cuthbertson, D.J., et al., *5-aminoimidazole-4-carboxamide 1-beta-D-ribofuranoside acutely stimulates skeletal muscle 2-deoxyglucose uptake in healthy men.* Diabetes, 2007. **56**(8): p. 2078-84.

253. Boon, H., et al., *Intravenous AICAR administration reduces hepatic glucose output and inhibits whole body lipolysis in type 2 diabetic patients.* Diabetologia, 2008. **51**(10): p. 1893-900.

254. Collodet, C., et al., *AMPK promotes induction of the tumor suppressor FLCN through activation of TFEB independently of mTOR.* The FASEB Journal, 2019. **33**(11): p. 12374-12391.

255. Daignan-Fornier, B. and B. Pinson, *5-Aminoimidazole-4-carboxamide-1-beta-D-ribofuranosyl 5'-Monophosphate (AICAR), a Highly Conserved Purine Intermediate with Multiple Effects.* Metabolites, 2012. **2**(2): p. 292-302.

256. Rajamohan, F., et al., *Escherichia coli expression, purification and characterization of functional full-length recombinant alpha 2 beta 2 gamma 3 heterotrimeric complex of human AMP-activated protein kinase.* Protein Expression and Purification, 2010. **73**(2): p. 189-197.

257. Hunter, R.W., et al., *Mechanism of Action of Compound-13: An alpha 1-Selective Small Molecule Activator of AMPK.* Chemistry & Biology, 2014. **21**(7): p. 866-879.

258. Barnes, B.R., et al., *Changes in exercise-induced gene expression in 5'-AMP-activated protein kinase gamma3-null and gamma3 R225Q transgenic mice.* Diabetes, 2005. **54**(12): p. 3484-9.

259. Witney, T.H., et al., *A Novel Radiotracer to Image Glycogen Metabolism in Tumors by Positron Emission Tomography.* Cancer Research, 2014. **74**(5): p. 1319-1328.

260. M. Roden, M. and M. G. I. Shulman, PhD, *Applications of NMR Spectroscopy to Study Muscle Glycogen Metabolism in Man.* Annual Review of Medicine, 1999. **50**(1): p. 277-290.

11   Curriculum Vitae

PHILIPP RHEIN

📍 Chemin des Triaudes 4B, 1024 Ecublens, CH
📞 +41 7989 36260
✉ philipp.rhein@icloud.com

EDUCATION

11/2016 - current	**PhD Student at the Nestlé Institute of Health Sciences (NIHS)/EPFL** Doctoral programme of Molecular Life Sciences (EDMS) under supervision of Prof Kei Sakamoto Thesis topic: Investigating physiological roles of the AMPKγ3 subunit isoform
10/2015-10/2016	**MRes Chemical Biology in Health & Disease at Imperial College London, final mark: distinction (best of class, awarded with Sir Alan Fersht prize for excellence)** Thesis topic: Elucidation the Mode of Action of Polysiphenol as PTP1B inhibitor towards Anti-Diabetes drugs Activities: Referee in the Imperial College Football Society
09/2011-09/2015	**BSc Chemistry & Biochemistry at Ludwig-Maximilians University Munich, final mark: 1.53 (3.5/4.0 GPA, top 10 % of the year)** Focused subjects: Inorganic Chemistry and Biochemistry Thesis topic: Genomic tagging in fruit flies using CRISPR-technology Activities: Mentor for potential exchange students, guidance and advice during application process, successful acceptance of 2 mentees to City University of Hong Kong
08/2013-05/2014	**BSc Biochemistry at City University of Hong Kong, final mark: 3.3/4.0 GPA** Activities: Organisation of the introduction week for incoming exchange students, coaching the hall football team and finishing 3rd (out of 11) in the inter-hall football competition
06/2011	**Abitur (equivalent to A level), final mark: 1.0 (4.0/4.0 GPA)** Focused subjects: Mathematics, Chemistry and Geography

PROFESSIONAL EXPERIENCE

01/2009-09/2015	**Football Referee in the German Football association (DFB)** • Taking charge of correct play by application and communication of known rules • Patient and professional conflict management with multiple parties • Self-organisation and time management

EXTRACURRICULAR ACTIVITIES

09/2019 - current	**President of shARE EPFL** • Lead of education programme and recruitment of newcoming shARE student cohort
02/2019 - 08/2019	**Junior Member of shARE EPFL** • Project lead of a team of 5 people to conduct market research analysis for a local food & beverage start-up. Setting tasks and frameworks which were used to conduct the research. Results were presented to the client and were used for fundraising pitches by them

| 01/2018 - current | **Treasurer & Event Coordinator in the Nestlé Research Young Scientists Association** |

- Financial supervision of all association activities
- Vice Coordinator and Financial Officer of the Faces of Industrial Research (FIR)2019 symposium (fir2019.com)
- Lead Organiser of Faces of Industrial Research (FIR)2020 symposium (fir2020.com)

| 03/2015 | **National Finalist of the "Henkel Innovation Challenge 8"** |

- Development of a product suitable for the Henkel portfolio and the needs of a typical consumer in the year 2050

| 10/2011 – 10/2016 | **Scholarship Student of the Friedrich-Naumann-Foundation for Liberty (FNF)** |

- Organising the national German inter-foundation football tournament (StipCup) in Berlin in 2016
- Coaching and playing in the football team of the FNF foundation, two consecutive wins (2013, 2014) of the national German inter-foundation football tournament (StipCup)

| 03/2012-08/2013 | **Board Member for Referee Cases at my Football Club TSV "Eiche" Neu St. Jurgen** |

- Communication with the local football association
- Education and recruitment of new young referees

Co-organisation of referees for and during annual regional youth football tournament with teams from all over Northern Germany

LANGUAGE SKILLS

German	Native proficiency
English	Professional proficiency (IELTS Overall 8.0)
French	Good proficiency (DELF B1)
Russian	Bilingual proficiency
Spanish	Basic proficiency
Mandarin	Elementary proficiency

TECHNICAL SKILLS

Microsoft Office	Very good
Adobe Illustrator	Good